A role for microRNA-21 in the regulation of gastrointestinal health and disease.

Thesis submitted to the

University of Dublin

For the Degree of Doctor of Philosophy

By Daniel Johnston

March 2017

Supervised by Dr. Sinéad Corr and Prof. Luke O' Neill

Declaration

This thesis is submitted by the undersigned to the Univeristy of Dublin for the examination of Doctor of Philosophy. I declare that the work herein is entirely my own, with the exception of the following figures:

Experiments for Figures 3.5, 4.1 and 4.7 were performed by Michelle Williams.
Experiments for Figures 3.12 and 3.13 were performed in collaboration with Christoph Thaiss.
Analysis of Figure 3.15 was carried out in collaboration with Meirav Pevsner-Fischer.
Analysis of Figures 3.17-3.19 was carried out in collaboration with Raul Carbrerra-Bello.
Analysis of histological sections for Figure 3.7A, B and C was performed in collaboration with Mathilde Raverdeu.
Experiments for Figure 3.21 were performed in collaboration with Craig McEntee.
Experiments for Figure 4.23A were performed in collaboration with Jay Kearney.

I declare that this thesis has not been submitted as an exercise for a degree to any other university. I agree to deposit this thesis in the University's open access institutional repository or allow the library to do so on my behalf, subject to Irish Copyright Legislation and Trinity College Library conditions of use and acknowledgement.

Acknowledgments

There are so many people to thank it's not even funny.

First thanks must go to Sinéad! Thank you for having the faith to take me on as your student, thank you for supporting me throughout these four short years, and thank you for teaching me so, so much over that time. It wasn't always easy, there were bumps along the road, but we've gotten there in the end! I've enjoyed the experience from start to finish and I wouldn't change it for the world.

Sincere thanks as well to Luke, for so generously hosting me in the lab, making me feel included and at home, and for giving me a helpful steer whenever it was needed. It was a comfort to know your door was always open, and your persistent optimism really helped get this over the line. I appreciate the opportunities you've afforded me and for all these things I am very grateful.

Thanks to the O'Neill lab, past and present, and to the burgeoning Corr lab. Thanks to Alex, Anne, Annie, Becca, Beth, Caio, Cait, Ciara, Deepthi, Dylan, Eva, Evanna, Gillian, Jamie, Jay, Kathy, Mark, Moritz, Michelle, Mirjam, Mustafa, Niamh, Nick, Paulina, Raquel, Sarah, Sarah G, Silvia, Siobhan, Stefano, Sue, Z and the wonderful people whom I've managed to forget. Without you, these four years would have been immeasurably less craic, and I would have melted without your advice and support. At this point I must single out some people for special gratitude, particularly Beth and Moritz who's kindness, wisdom and endless patience with my myriad stupid molecular biology questions borders on divine. And to my old undergrad friends among you; your Evannas, your Sarahs, your Jays of this world: thank you. Without you guys to celebrate the small wins with, and to commiserate the big fails with, God knows where I'd be. A gutter most likely. And thanks to Jamie, 'cos I know you'd hate to be left out.

To my friends from school and from college, thank you for being there for all this time. Thank you for all the memories over eight years in Trinity; cherry-blossomed summer evenings in the Pav, putting in the miles rowing on frozen lakes in Blessington, long days and nights in the Hamilton library, and everything in between. It's been very special.

Thanks also to my friends and collaborators in TBSI and beyond, your input scientifically and personably has been of huge importance to this project. Brian, Kaisia, Craig and Mathilde especially. I also must acknowledge the wonderful people of the Elinav lab in the Weizmann Institute of Science. Thank you for taking me in, teaching me and making a daunting process a bit easier through your kindness and humour. Thanks to David Wallach who made the whole thing possible, to Eran for hosting so generously, to Hagit, Meriav, Claudia, Maayan and Niv for all your help that summer, and thanks especially to Christoph for taking time out of your days to help me examine mouse colons. I never thought I would spend so many of my waking hours worrying about mouse colons. And special thanks to Marina Lynch who gave me my first go at science in 2011, and to Eric Downer who guided me through it.

To Maeve, Chris and Annie, my indomitable flatmates over the years, thank you. Especially to Maeve, thank you for being such a reliable presence over the last few years, ready to chop down any of the day's issues with charming sarcasm and faux outrage at the temerity of whatever it was that wasn't doing what it was supposed to do. It really made a difference.

To my family, I just can't imagine having gotten this far without you. Thank you for never having any doubt, for always being on my side, for putting up with me, and for everything else I don't have the space or the words to articulate. Thank you Mum, and Dad, and Tom, you mean the world to me. And thank you to my inspirational grandparents who always set the example, and whom I know were, and are, proud of me always.

And finally, to Niamh. I simply would not have been able to do this without you, no question about it. You always slag me for my way with words, and now I find that can't find any sufficient to get across just how much your support has meant to me. All the hours on the phone, all the problems to be solved, all the things you've put up with and you've worn it all with a smile. You're the best, and I'm blessed to have had you to share this with for the last four years. Thank you so much.

Thank you all so much.

Danny

Abbreviations

α-diversity	intra-sample richness
ABX	antibiotics
AGO	Argonaute
A/E	Attaching/effacing
AIM2	Absent in melanoma 2
ALR	Aim2-like receptor
AOM	1 Azoxymethan
AP1	Activator protein 1
APS	Adenosine-5'-phosphosulfate
ASC	Apoptosis speck-like protein containing a CARD
ATG16L1	Autophagy related 16-like 1
ATP	Adenosine-triphosphate
β-diversity	inter-samples richness
B cell	Hematopoietic stem cells that matured in the bone-marrow
BCA	Bicinchoninic acid assay
BHI	Brain heart infusion
BIR	Baculoviral inhibitory repeat
BMDCs	Bone marrow derived dendritic cells
BMDMs	Bone marrow derived macrophages
BSA	Bovine serum albumin
BTK	Brutons tyrosine kinase
C/EBP	CCAAT-enhancer-binding protein
CAC	Colitis-associated cancer
CARD	Caspase recruitment domain
CCR6	Chemokine (C-C motif) receptor 6
CD	Crohn's disease
CD14	Cluster of differentiation 14
cDNA	complentary DNA
CFU	colony forming unit
CH	co-housed
CLR	C-type lectin receptor
CLP	Cecal ligation puncture
COX-2	Cyclo-oxygenase-2
CRC	Colorectal cancer
Da	Dalton
DAI	Disease activity index
DAMP	Danger-associated molecular pattern
dH2O	Distilled Water
DMEM	Dulbecco's modified eagle medium
DNA	Deoxyribonucleic acid
DSS	Dextran sodium sulfate
DTT	Dithiothreitol
EAE	Experimental autoimmune encephalomyeliti
ECL	Enhanced chemiluminescence

EDA-ID	ectodermal dyplasia with immunodeficiency
EDTA	Ethylenediaminetetraacetic acid
EEA1	Early endosome antigen 1
EHEC	Enterohaemorrhagic Escherichia coli
ELISA	Enzyme-linked immunosorbent assay
EMT	epithelial-mesenchymal transition
ER	Endoplasmic reticulum
EtOH	ethanol
Ex-GF	formerly germ-free mice subsequently collonised
FCS	Fetal calf serum
FITC-dextran	Fluorescein isothiocyanate–dextran
GAPDH	Glyceraldehyde 3-phosphate dehydrogenase
GF	germ free
GM-CSF	granulocyte macrophage colony stimulaition factor
GTP	Guanisine triphosphate
GWAS	Genome-wide association studies
H&E	Hematoxylin and eosin
HCV	Hepatitis C virus
HRP	Horseradish peroxidase
i.p	Intraperitoneal
IBD	Inflammatory Bowel Disease
IEC	Intestinal epithelial cells
IgA	Immunoglobulin A
IKK	inhibitor of NF-κB (IκB) kinases
IL-	Interleukin-
IRAK	interleukin-1 associated kinases
IRF3	Interferon regulatory factor 3
JAK	Janus kinase
JNK	C-Jun-N-terminal kinase
L929	Cell type used to generate M-CSF enriched media
LB	Luria broth
LDH	lactate dehydrogenase
LLO	listeriolysin
LLR	Leucine-rich repeat
lncRNA	long non-coding RNA
LPS	lipopollysaccharide
M cell	Microfold cells
MAL	MyD88 adaptor-like protein
MAMP	Microbe associated molecular pattern
MAPK	Mitogen activated protein kinase
MCSF	Macrophage colony-stimulating factor
MD2	lymphocyte antigen 96
MeOH	Methanol
miR	microRNA
miRNA	microRNA
MMP	Matrix metalloproteinases
MOI	multiplicity of infection
MPO	myeloperoxidase
Mw	Molecular weight
Myc	Myelocytomatosis oncogene

MyD88	Myeloid differentiation factor 88
NaCl	Sodium chloride
NF-κB	Nuclear factor kappa-light-chain-enhancer of activated B cells
NFIB	Nuclear factor 1 B type
NK	Natural killer
NLR	NOD-like receptor
NLRC4	NLR family CARD domain-containing 4
NLRP	NACHT, LRR and PYD domains-containing protein
NLRP3	NLR family, pyrin domain-containing 3
NLRP6	NLR family, pyrin domain-containing 6
NO	Nitric oxide
NO-	nitrite
NOD	Nucleotide-binding oligomerization domain
nt	Nucleotide
NSAID	Non-steroidal anti-inflammatory
P/S	Penicilin/streptomycin
PAGE	Polyacrylamide gel electrophoresis
PAMP	Pathogen-associated molecular pattern
PBS	Phosphate buffered saline
PCR	Polymerase chain reaction
PDCD4	programmed cell death 4
PEC	peritoneal exudate cell
PMA	phorbol-12-myristate-13-acetate
Poly I:C	Polyinosinic:polycytidylic acid
Pri-miR	Primary microRNA transcript
PRR	Pattern recognition receptor
PTEN	Phosphatase and tensin homologue
PVDF	Polyvinylidene fluoride
PYD	Pyrin domain
QIIME	Quantitative Insights Into Microbial Ecology
RISC	RNA induced silencing complex
RLR	RIG-like receptor
RLR	Sterol Regulatory Element Binding Protein
RNA	Ribonucleic acid
STAT	Signal transducer and activator of transcription
RNA Pol	RNA polymerase
RNAi	RNA interference
ROS	Reactive oxygen species
RPM	Revolutions per minute
RPMI	Roswell Park Memorial Institute medium
rRNA	ribosomal RNA
RT	Reverse transcription
RT	Room temperature
RT-PCR	Reverse transcription polymerase chain reaction
SARM	Sterile-α and armadillo repeat containing molecule
SD	Standard deviation
SDS	Sodium-dodecyl sulphate
SEM	standard error of the mean
siRNA	small interfering RNA
SLE	systemic lupus erythematosis

SMAD6	Mothers against decapentaplegic homolog 6
SNP	Single-nucleotide polymorphism
SPF	Specific pathogen free
SPI	*Salmonella* pathogenicity island
STAT3	signal transducer and activator of transcription 3
T cells	Hematopoietic stem cells that matured in the thymus
TAB2	TAK1-binding protein 2
TAE	Tris base, acetic acid and EDTA
TBS-Tween	Tris-buffered saline with Tween
TEMED	Tetramethylethylenediamine
TGF-β	Transforming growth factor beta 1
Th	T helper cells
TICAM	Toll-IL-1-homology domain-containing adaptor molecule
TIR	Toll/Interleukin-1 receptor
TIRAP	TIR domain containing adaptor protein
TJ	Tight junction
TLR	Toll-like receptor
TMB	3,3',5,5'-Tetramethylbenzidine
TNBS	Trinitrobenzene sulfonic acid
TNF	Tumour necrosis factor
TNF-α	Tumour necrosis factor alpha
TRAF6	TNFR-associated factor 6
TRAM	TRIF-related adaptor molecule
TRIF	TIR domain containing adaptor inducing interferon-β
TRIS	Tris(hydroxymethyl)aminomethane
UC	Ulcerative colitis
UTR	untranslated region
V	Volts
v/v	Volume per volume
VEGF	Vascular endothelial growth factor Volume/volume
w/v	Weight per volume
WT	Wild-type

Table of Contents

Table of Figures

List of Tables

Abstract

The gastrointestinal (GI) tract is a crucial site of innate and adaptive immune regulation, balancing tolerance of beneficial commensal microorganisms and reaction to invading pathgens. Pattern recognition receptors (PRRs), including Toll-like receptors (TLRs), are vital sensors in the orchestration of these immune responses to maintain intestinal homeostasis. Furthermore, these responses must be tightly regulated to ensure an appropriate level of response. There are multiple classes of regulators including non-coding RNA microRNAs which regulate mRNA expression.

In this project, we sought to explore the role of microRNA-21 (miR-21) in intestinal health and disease. miR-21 is considered to be an anti-inflammatory regulator in various contexts in immunity, with the negative regulation of TLR4 signalling being of particular interest. However, it has also been shown to be deleterious in cancer and its expression is elevated in patients with several inflammatory disease including inflammatory bowel disease (IBD).

Using specifically generated transgenic mice, we investigated the role of miR-21 in IBD and infection. First, we have shown that miR-21 is pathological in chemically induced models of IBD, with miR-21$^{-/-}$ mice protected from the disease relative to wild-type controls. This protection appeared to be in part mediated by the intestinal microbiota of the miR-21$^{-/-}$ mice, as determined by co-housing and germ-free recolonization experiments. 16S sequencing confirmed differences between wild-type and miR-21$^{-/-}$ microbiotas and antibiotic depletion experiments demonstrated that the microbiota is essential for the miR-21$^{-/-}$ protective phenotype. We postulate that miR-21's negative regulation of the tight junction integrity protein RhoB and the mucin secreting protein MARCKS alter the microbiota through modulation of the intestinal microenvironment. We also sought to characterise miR-21's role in infection, and demonstrated that miR-21 limits macrophages invasion the gram-positive pathogen *Listeria monocytogenes*, again possibly through modulation of RhoB and MARCKS and their role in phagocytosis.

These results have uncovered novel roles for miR-21 in modulation of the host response to commensal and infectious bacteria.

Chapter 1
-
Introduction

1. Introduction

1.1. The innate immune system

1.1.1. General introduction

Animals and plants have evolved over time to protect themselves against harmful invading microbes which cause disease. These adaptations form the immune system, which in vertebrate organisms comprises many cells and organs that can recognize and eliminate pathogens in a variety of ways causing minimal damage to the host in the process when functioning correctly. The immune system of many higher organisms is generally thought of as having two arms: the innate immune system and the adaptive immune system. The innate immune system is the point of first contact with invading pathogenic microorganisms which includes bacteria, fungi and viruses. It senses potentially infectious agents in a more general manner than the adaptive arm, meaning it has the capacity to recognize and attack multiple types of invading pathogen quickly and robustly. The adaptive immune system on the other hand provides the later part of the organism's response, is highly specific involving the generation of immune memory and requires activation by the innate response to occur.

The innate immune system is comprised of several components that act in tandem to prevent and manage infection. The first of these components are the body's barriers: the epithelia and mucosal linings, which possess non-specific anti-microbial properties (e.g. anti-microbial peptides, cilia etc) to prevent infectious agents entering the body (the skin) or staying in the body once they have made their entry (gut and lung epithelia etc) [1]. Beyond these barriers, the innate immune system possesses several cell types and other mechanisms to control and destroy any pathogens which do make it through the initial defence and try to establish themselves. These include white blood cells such as macrophages, neutrophils and other granulocytes, which are broadly termed leukocytes and can either be tissue-resident or circulating through the body's vasculature [2]. There are also biochemical pathways, such as the complement and coagulation pathways among others. These cells and biochemical processes

combine to stall invading pathogens, label them for destruction, destroy them via several killing mechanisms and instigate mobilisation of the more specific adaptive immune system to the danger presented so that the host may mount a fully fledged immune response.

1.1.2. The innate immune response and inflammation

As the innate arm of the immune system is the first point of contact for invading pathogens it must be generated rapidly in response to infection. During this response the site of infection becomes inflamed due to the infiltration of immune cells and chemical mediators. During inflammation, the blood vessels become dilated leading to increased local blood flow and the leakage of fluid that accounts for the heat, redness, and swelling. This response has evolved to allow the rapid accumulation of immune cells and mediators to help clear the infection. Macrophages encountering pathogens in the tissues are triggered to release secreted protein messengers termed cytokines that influence the behaviour of the body's cells in response to infection: in this case, they increase the permeability of blood vessels, allowing fluid and proteins to pass into the affected tissue. They also produce specialised cytokines termed chemokines that direct the migration of neutrophils to the site of infection [2]. As this process continues, the adaptive immune system becomes involved upon activation by antigens released from destroyed pathogens and presented to T lymphocytes by professional antigen-presenting cells (APCs) such as macrophages and dendritic cells (DCs) amongst other processes. Inflammation is therefore a key part of the defence against infection. Macrophages are a crucial cell type in this context with many important roles including bacterial recognition, phagocytosis, cytokine release, and antigen-presentation. While inflammation is an important process for clearing infection, excessive inflammation causes enormous tissue damage and is detrimental to the body. As such, tight controls are required to ensure that resolution and tissue repair begins once the need for inflammation has been eradicated. Serious inflammatory disease results from a breakdown in these controls.

1.1.3. Macrophages

Macrophages are professional phagocytic cells of the innate immune system, which encounter and engulf invading pathogens, cellular debris and other potential deleterious substances in order to protect the body from infection and maintain normal homeostatic conditions[3]. Discovered by Élie Metchnikoff in 1884, the term phagocyte was coined and is derived from Greek for "big eater" in keeping with their role as professional phagocytes. Macrophages are present throughout the body's tissues, and can be either derived from monocyte precursors or, as is the case with most tissue-resident macrophages, from embryonic precursors seeded before birth and can maintain themselves by self-renewal [4]. There is an increasing recognition of the variety of roles they play in maintaining homeostasis and resolving inflammation [5]. Macrophages in different environments display altered gene expression and immune phenotypes as a result. In addition, macrophage-like populations in different compartments (e.g. microglia in the brain, Kuppfer cells in the liver) add to this heterogeneity. For instance, a lung-resident alveolar macrophage is required to react to far more exogenous pathogens and particulate matter than the brain resident microglia whose primary role is the clearance of dying neurons and maintenance of brain homeostasis [6]. A model of differentiation between functionally distinct macrophages arose during the late 20th century, which describes "classically activated" (or M1) pro-inflammatory macrophages and "alternatively activated" (or M2) anti-inflammatory macrophages. Whilst this paradigm is now outdated, and it is apparent that macrophages in fact fall somewhere along the spectrum between these two poles, it is still a useful means of describing macrophage function [7]. One of the most important functions of macrophages of all types is phagocytosis.

1.1.4. Phagocytosis

Phagocytosis is the process by which cells "eat" objects and is associated once again with Élie Metchnikoff's work in the late 1800s [8]. This process is employed physiologically for a variety of reasons by a variety of organisms, but in the immune system it is used both to destroy invading organisms and to clear dead cells or parts of

dead cells in the resolution of inflammation to restore homeostasis. The former process is generally regarded as being pro-inflammatory, and the latter anti-inflammatory [9-12]. Following recognition of invading bacteria, actin polymerisation is initiated through signals from phagocytic receptors and RhoGTPase activity [12]. This actin restructruring forms a phagocytic cup which subsequently encloses around the bacterium to form the early phagosome. The early phagosome is associated with a number of markers such as Early Endosome Antigen 1 (EEA1) and Rab5 which localise to the phagosome and aid its subsequent maturation. The maturation steps which follow involve fusion with endosomal vesicles and fission vesicles, moving through early, intermediate and late stages (characterized by Rab7 localisation) culminating in formation of the mature phagolysosome which has acquired a full bactericidal repertoire [13]. This maturation is demonstrated in Figure 1.1. This repertoire includes an increased acidicity than the early phagosome (pH 4.5 over pH 6.2), the ability to generate reactive nitrogen intermediates such as nitric oxide (NO) and production of reactive oxygen species (ROS) [14]. In this way, macrophages can clear infectious agents, but also during the process of degrading them they can process antigen for presentation to cells of the adaptive immune system via the surface major histocompatibility complex (MHC) class I and II molecules. Several pathogens have evolved strategies for evading and manipulating the phagocytic response, using it to their advantage to gain an intracellular niche. These niches can be formed by inhibiting the maturation of the phagolysosome, as is the case in *Mycobacterium tuberculosis* infection, or by escaping the early phagosome completely, a strategy employed by the Gram-positive bacteria *Listeria monocytogenes* [15,16].

These functions of the macrophage are crucial for the swift response to infection and the maintenance of tissue homeostasis. In order to achieve this, the cell must first recognize the offending pathogen and this is achieved through the expression of Pattern Recognition Receptors (PRR). Indeed, so important are these receptors that the M1 macrophage is defined by the polarization that results in the sensing of bacterial lipopolysaccharide (LPS) using the PRR Toll-like receptor (TLR) 4 [7].

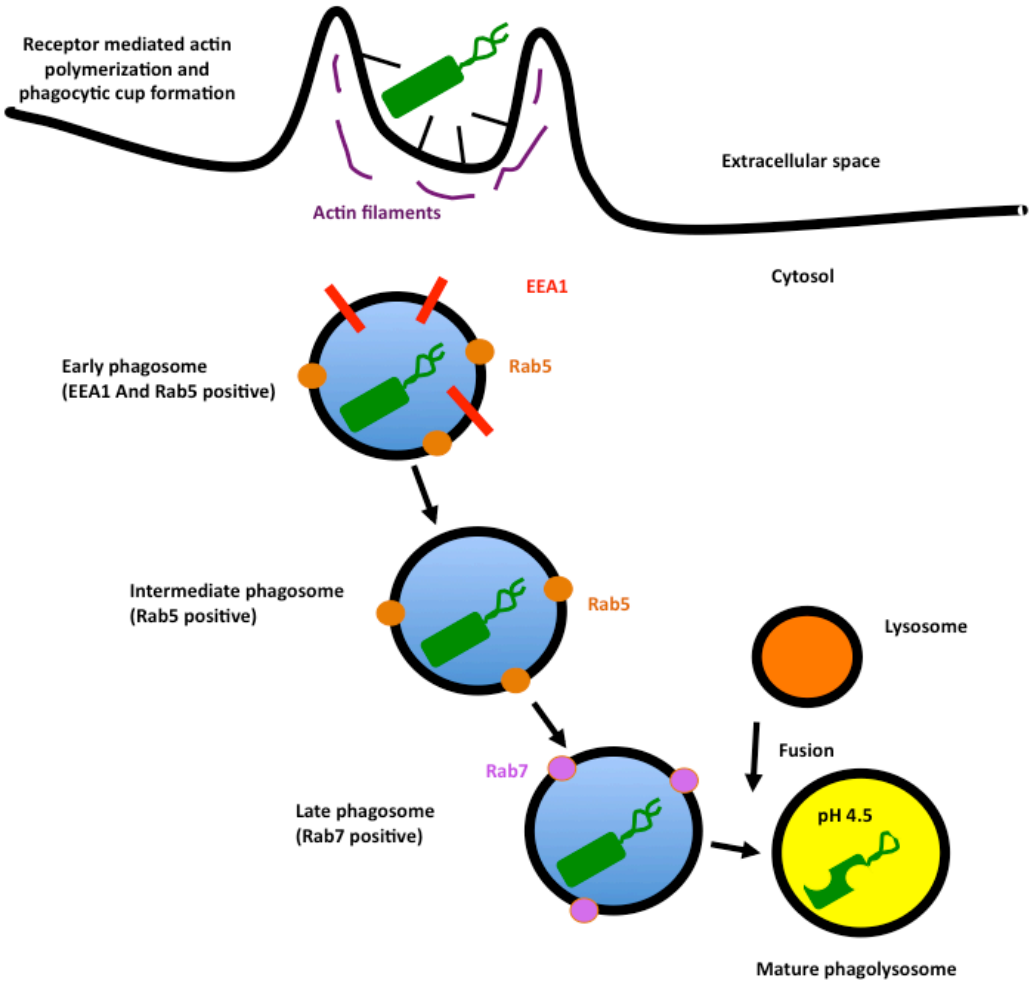

Figure 1.1 Phagocytosis of bacteria and maturation of the phagosome

Bacteria are initially sensed by phagocytic receptors on the surface of the plasma membrane which initiate actin filament polymerization to form a phagocytic cup. This phagocytic cup encloses the bacteria and is pinched off the forms a phagosome vacule, where the bacteria is contained inside an endosomal compartment formed from the plasma membrane. This phagosome gradually matures to through early (EEA1 and Rab5 positive), intermediate (Rab5 positive) and late stages (Rab 7 positive) before fusion with the lysosome generates a mature acidic phagolysosome capable of degrading the ingested pathogen.

1.2. Pattern recognition receptors

Several innate immune cells recognize invading pathogens or components of damaged host cells using what have been termed PRRs that sense parts of the invading pathogen broadly termed Pathogen Associated Molecular Patterns (PAMPs) or in the case of damaged host cells Damage Associated Molecular Patterns (DAMPs). In more recent years the term Microbe-associated molecular pattern (MAMPs) has also been coined to account for the sensing of microbes which are not inherently pathogenic such as those in the commensal microflora. Cells that possess these PRRs are vital in triggering both inflammation and other innate responses, and in triggering the adaptive response. These PRRs have led to a change in the conventional perception of innate immunity as being "non-specific" as they in fact recognize these conserved PAMPs with very high levels of specificity. The adaptive system however recognizes the specific strain of pathogen exactly. Several PRRs have been identified over the last 15 years or so, beginning with the discovery of TLR4 as a human homologue of the Toll-protein from *Drosophila melanogaster*[17]. Since then, different types of PRR have been described and characterized which appear in the plasma membrane, endosomes and cytosolically. These include the Nucleotide Oligomerization domain (NOD)-like receptors (NLRs), Toll-like receptors (TLRs), Retinoic-acid inducible (RIG)-like receptors (RLRs) and Absent in myeloma 2 (AIM2)-like receptors (ALRs)[17,18]. There are a huge variety of receptors present, and this allows the cells of the innate immune system to respond to many different PAMPs in order to mount an effective response against any pathogen it encounters.

1.2.1. Toll-Like Receptors

The discovery of Toll-like receptors and their crucial role in the immune response was fully recognized in 2011 as one of the most important scientific discoveries of recent times when the Nobel Prize for Physiology or Medicine was awarded to Bruce Beutler and Jules Hoffman (along with the late Ralph Steinman who characterized the dendritic cell) for their work in the area [19-21]. The Toll protein was initially discovered in the mid-1980s [22] and then implicated in host defence by Hoffman in 1996 [20] before a human homologue was found shortly afterwards by Beutler *et al* [21]. Charles Janeway played a crucial role in their characterization as functional receptors in mammals, and was the first to propose the existence of such a set of receptors [23].

The first TLR found, later renamed TLR4, responds to the gram-negative bacterial PAMP LPS via an LPS binding protein (LBP), Cluster of Differentiation 14 (CD14) interaction and MD2 (also known as lymphocyte antigen 96) [24]. TLRs are type-1 transmembrane glycoproteins which belong to the Interleukin-1/Toll-like receptor Superfamily due to a conserved domain, shared by all members of this family, called a Toll/IL-1R homology (TIR) domain [25]. This TIR domain is in the cytosolic part of proteins in this family and is a crucial domain for downstream signalling by these receptors. The extracellular domain (or extra-vesicular in the case of the cytosolic TLRs 3, 7, 8 and 9) of TLRs is made up of several leucine-rich repeats with which it binds PAMPs using its unique horseshoe conformation. PAMPs that are sensed by TLRs are hugely varied and include products from bacteria, viruses, fungi and protozoa. There are currently 10 known human TLRs (12 in the mouse) that fall into two types. Cytosolic TLRs (TLR 3, 7, 8 and 9) recognize nucleic acid in different forms and cell surface TLRs (TLR 1, 2, 4, 5, 6 and 10) recognize proteins, lipids, phospholipids, carbohydrates and other pathogen-derived molecules [17]. TLRs (and other PRRs) are highly conserved and many homologues can be found in a huge number of organisms, from recently evolved to ancient, many of which use them as their sole defence against pathogens [26,27]. PRRs and TLRs sense pathogens or danger signals in the form of ligands and respond by activating different transcription factors [28,29]. These enable the transcription of a huge multitude of different genes that function in immunity. Originally TLRs were most commonly thought of as sensors that induce pro-inflammatory signals such as regulation cell-surface receptor expression, secretion of pro-inflammatory cytokines, ROS, NO etc. However, it is now evident that they also induce anti-inflammatory signals [30-32]. They achieve this by signalling through complex networks of signalling molecules, which are often organized into discrete pathways for ease of understanding, though there is often crossover between these networks.

1.2.2. TLR signalling

Research into the mechanisms by which TLRs signal to induce changes in the cell has been a huge area ever since they were discovered to have a key role in innate immunity. As previously stated, TLRs belong to the Interleukin-1/Toll-like receptor

Superfamily and contain a cytosolic TIR domain[33]. Upon ligand binding to the extra-cellular domain, TLRs dimerize (mainly forming homodimers, apart from TLR2 which forms heterodimers with TLR 1 or 6) and recruit TIR containing adaptor proteins to their own TIR domains. There are currently 5 known adaptors; Myeloid differentiation primary response gene 88 (MyD88), MyD88-adaptor like protein (Mal, also known as TIR-containing adaptor protein [TIRAP]), TIR-containing adaptor protein inducing interferon-β(IFN-β) (TRIF), TRIF-related adaptor molecule (TRAM, also known as TIR-containing adaptor molecule [TICAM-2]) and sterile α- and armadillo-motif containing protein (SARM) [34]. These adaptors associate with different combinations of TLRs and activate various different downstream effecter molecules that eventually lead to transcription factor activation. Examples of these effecter molecules include the Mitogen-activated protein (MAP) kinases, the Interleukin-1 associated kinases (IRAKs), the I-κB kinases (IKKs) etc [17]. The signal is often transferred through kinase activity of each molecule, leading to a phosphorylation cascade effect. This phosphorylation can also target proteins for ubiquitination by E3 ligases and subsequent degradation by the proteosome.

The diversity of receptors, adaptors and downstream signalling molecules allows for the generation of very specific responses and also allows the immune system to compensate if one sensing mechanism is defective or blocked by a pathogen. These signals eventually lead to induction of genes specific to the immune response via different transcription factors such as nuclear factor κB (NF-κB) via IKKs or Akt, activator protein-1 (AP-1) via MAPKs, interferon regulatory factor (IRF3) via TRIF or signal transducer and activator of transcription 3 (STAT3) via the Janus associated kinase (JAK)/STAT pathway. These pathways lead to the transcription of highly potent immune mediators such as pro-inflammatory cytokines, and as such they must be tightly controlled. A summary of these pathways is illustrated in Figure 1.2. Numerous heritable conditions exist where aberrant activation of TLRs or elements of their signalling pathways leads to disease, including anhidrotic ectodermal dysplasia (EDA-ID) [35].

It is clear that the loss or loss of function of these key molecules could lead to severe infection, but overactivation or excessive functionality could be equally deleterious,

as excessive inflammation would lead to tissue damage. The correct function of PRR's is particularly crucial at the body's barriers, where reacting appropriately to clear invading pathogens and tolerate beneficial commensal microbes is crucial for the health of the host. The main barrier of interest to this thesis is the intestinal barrier.

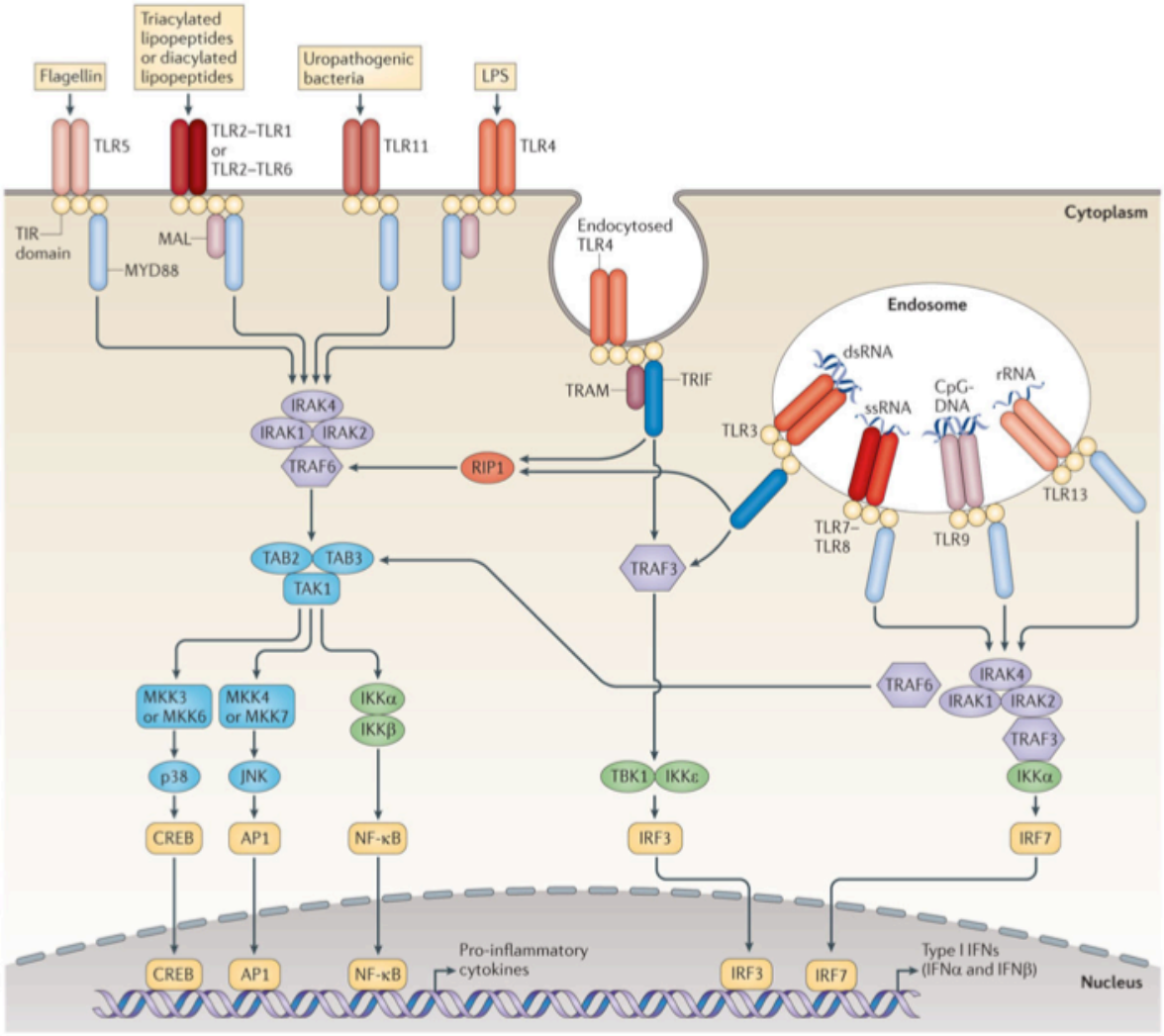

Figure 1.2 A summary of TLR signaling pathways

TLR signalling is initiated by ligand-induced dimerization of receptors. Following this, the Toll–IL-1-resistence (TIR) domains of TLRs engage TIR domain-containing adaptor proteins (either myeloid differentiation primary-response protein 88 (MYD88) and MYD88-adaptor-like protein (MAL), or TIR domain-containing adaptor protein inducing IFNβ (TRIF) and TRIF-related adaptor molecule (TRAM)). Engagement of the signalling adaptor molecules stimulates downstream signalling pathways that involve interactions between IL-1R-associated kinases (IRAKs) and the adaptor molecules TNF receptor-associated factors (TRAFs), and that lead to the activation of the mitogen-activated protein kinases (MAPKs) JUN N-terminal kinase (JNK) and p38, and to the activation of transcription factors. Multiple transcription factors are activated by TLR signalling the most important of which are nuclear factor-κB (NF-κB) and the interferon-regulatory factors (IRFs). Other transcription factors, such as cyclic AMP-responsive element-binding protein (CREB) and activator protein 1 (AP1), are also important. A major consequence of TLR signalling is the induction of pro-inflammatory cytokines, and in the case of the endosomal TLRs, the induction of type I interferon (IFN). dsRNA, double-stranded RNA; IKK, inhibitor of NF-κB kinase; LPS, lipopolysaccharide; MKK, MAP kinase kinase; RIP1, receptor-interacting protein 1; rRNA, ribosomal RNA; ssRNA, single-stranded RNA; TAB, TAK1-binding protein; TAK, TGFβ-activated kinase; TBK1, TANK-binding kinase 1. Adapted from O' Neill *et al* 2013 [29]

1.3. Intestinal Immunity

1.3.1. Barrier immunity

As previously mentioned in section 1.1.1, the mucosal sites of mammalian hosts are the first point of contact for the majority of antigens and potential pathogens, and as such they are sites for immunity and immune tolerance to the commensal organisms which reside there. The physical barriers of the respiratory, gastrointestinal and urogenital tracts are sites of intense immune activity, where resident immune cells sample the environment and potentially dangerous foreign bodies or pathogens are distinguished from harmless material or commensal microflora [36]. The barriers also must often serve multiple roles simultaneously, with enough flexibility to allow in nutrients, gases and other essential materials while also remaining impregnable to pathogenic foreign bodies [1,37].

1.3.2. The gastrointestinal barrier

The gastrointestinal (GI) barrier is a site with a very large surface area of approximately ~32m^2 that encounters the majority of the foreign antigens that enter the body [38]. The environment of the GI barrier is composed of four interconnected elements: the commensal microbiota, a two-part mucus layer, a single layer thick epithelial cell layer, and finally various populations of immune cells in compartments known as the gut associated lymphoid tissue (GALT) and spread through the underlying lamina propria. These four elements regulate one another to ensure homeostasis, and if one element is compromised disease is likely to follow.

The two-part mucus barrier is the first host layer of the homeostatic intestinal immune system. The mucus layer of the intestine consists of an inner glycocalyx of membrane-anchored mucin proteins, covered by an outer layer of secreted mucins, which, in addition to being a viscous barrier to microbes, forms a matrix loaded with high concentrations of intestinal epithelial cell (IEC)-derived antimicrobial peptides and secretary IgA (sIgA) which physically separates the intestinal microflora from

aberrant contact with epithelium itself [39]. This outer layer of mucus is inhabited by the commensal bacteria residing in the intestinal lumen, whereas in the denser inner layer there are no bacteria present [40]. Mucin proteins contain a proline-threonine–serine domain which allows the proteins to be glycoslyated. This *O*-glycosylation amounts for the 80% carbohydrate composition of the mucous mass, and provides glycans and other nutrients for commensal bacteria [41]. This layered regulation allows commensal microorganisms to occupy the outer niche and provides a source of nutrients for microbes that are beneficial to the host. The maintenance of this mucus barrier relies on both intestinal IECs to secrete mucins, mostly Muc2, but also the presence of a resident microflora population to provide signals to the IECs via PAMP release. This is evidenced by the finding that the reduced mucus layer present in germ-free mice can be restored by the administration of TLR ligands [42].

This brings us to the second element of the host's GI tract innate immune system. The epithelial barrier is composed of a combination of absorptive IECs, specialized IECs with diverse regulatory functions such as goblet cells and Paneth cells, and resident immune cells of various lineages [43]. It consists of a single layer of columnar epithelial cells that provide an effective physical barrier separating the vast bacterial load of the intestinal flora from cells of the host immune system beneath. The continuous crypts and villi that make up the intestinal epithelium possess several physical, biochemical and immunological mechanisms ensuring intestinal immune homeostasis. In the context of the gut, immune homeostasis entails mutualistic interactions with commensal microbes contrasted by protective immunity to invasive pathogens. Actin-rich microvillar protrusions from the apical IEC surface form a mechanical brush border, which, in combination with goblet cell-secreted mucins, comprise a sterile barrier that is impermeable to most intestinal microbes. IECs are permanently in contact with the intestinal lumen contents and, therefore, ideally located to undertake immunosurveillance of commensal and pathogenic populations within the intestinal microbiota in collaboration with the underlying *bona fide* innate immune cells. MAMPs triggering of PRRs classically drives a nuclear factor-κB (NF-κB)-dependent pro-inflammatory response and initiation of both innate and adaptive immune responses to the invading microbe. Importantly, triggering of PRR signalling within IEC is critical for a broad spectrum of host- protective responses to pathogenic species in the intestine [44]. IECs express PRRs at a low level, and their

function is crucial for intact barrier function as has been shown through mouse models deficient in TLR signalling components [45]. Along with this direct sensing, IECs are involved in the sampling of the luminal contents via specialized microfold cells (M cells) and the delivery of these contents to innate immune cells. One of the most important modulatory functions of the IEC layer is the maintenance of a flexible physical barrier via tight junctions (TJs) to stop invading pathogens gaining entry, but to allow uptake of nutrients and other material across via paracellular uptake [37]. Material can also be taken up via direct entry in to the cell, termed transcellular uptake. The same is true for antigen and other immune stimulating materials such as PAMPs or DAMPs, which can then be taken for processing by the resident cells of the innate and adaptive immune system. This process must be tightly regulated to ensure that the TJs do not allow in harmful material or excessive amounts of immunomodulatory molecules from commensals that reside in the lumen. Control of TJs is regulated by many different proteins and requires paracrine signalling from cell to cell. Host health can be severely compromised if there is a breakdown in the capacity of the gastrointestinal barrier to monitor the luminal contents, regulate TJ integrity during nutrient uptake or maintain an effective mucus layer to localize commensal bacteria. This is summarized in Figure 1.3.

The final element of the host immune system in the gut is the immune cells themselves. As the IEC barrier must be somewhat permeable, these cells are crucial for ensuring homeostasis. The immune cells present are varied, and appear within different locations along the GI tract. For instance, there are aggregated lymphoid follicles (also called Peyer's patches) in the small intestine which contain a high proportion of B and T lyphocytes and smaller populations of mononuclear leukocytes such as DCs, macrophages and neutrophils [46]. There are similar follicles present in the colon, termed isolated lymphoid follicles, which contain similar distributions of immune cells of both innate and adaptive immune cells. These are sites of immune surveillance, and feature the specialised M cells mentioned previously to sample the contents of the lumen [47]. As well as these concentrated areas of organised immune activity, there are also cells distributed throughout the lamina propria which can sense the luminal contents. These include DCs and macrophages, the former of which can migrate to the mesenteric lymph nodes to present antigen to adaptive immune cells and initiate a robust immune response to pathogens. The macrophages on the other

hand do not migrate, and it is thought that they are more responsible for eliciting immune responses through coordinating with IECs and local adaptive immune cells, as well as phagocytosing and destroying pathogens or commensal microbes which have traversed the epithelial barrier [43,48]. Much of this functionality is dependant on PRR signalling and cytokine secretion and signalling. This allows a complex interplay between commensal bacteria, IECs and immune cells to occur to maintain a homeostatic balance. There are many examples of knockout mice deficient in one of these elements which display a breakdown in this homeostasis. For instance, mice deficient in the anti-inflammatory cytokine IL-10 develop spontaneous intestinal inflammation [49]. Similarly, loss of important PRRs like TLR4 also increases the severity of intestinal inflammation in a mouse model [50]. The ability of the various elements to sense the intestinal microflora and communicate with one another to act appropriately is therefore important, but the microflora itself also has a role in maintaining this delicate homeostatic balance.

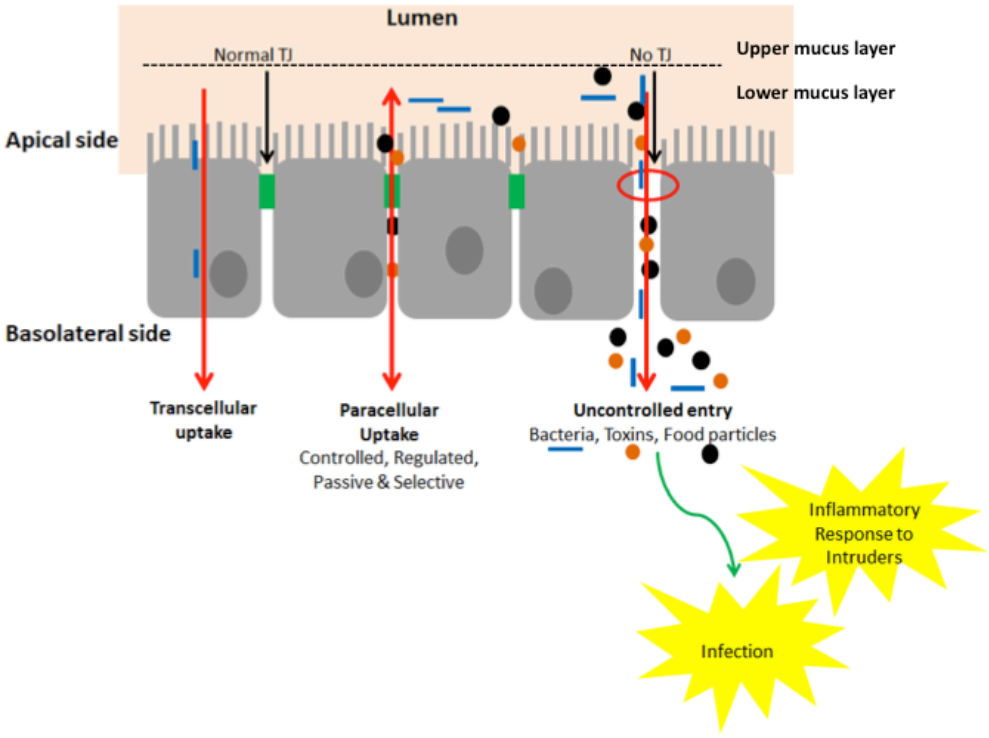

Figure 1.3 The gastrointestinal barrier, function and dysfunction.

The gastrointestinal barrier is a highly versatile collection of cells which mediates the homeostasis of the host in a number of ways. Nutrients and other essential materials are taken up either across the intestinal epithelial cell (IEC) (shown in grey) membranes (transcellular) or by opening the tight junctions (TJs) between the cells to allow movement from the apical (or luminal) side of the gut to the basolateral side (paracellular) where they can be absorbed in the blood stream. The same is true for antigen and other immune stimulating materials such as PAMPs or DAMPs, which can then be taken for processing by the resident cells of the innate and adaptive immune system. This process must be tightly regulated to ensure that the TJs do not allow deleterious material or commensals that reside in the lumen to reach the basolateral side of the IEC layer. The latter event can lead to severe infection and inflammatory disease, so there is an additional mode of protection mediated by the mucus layers on the apical surface that serve to keep commensal microbes correctly localized.

Adapted from Johnston and Corr (Methods in Molecular Biology 2016)[37]

1.3.3. The gut microbiota and intestinal pathogens

As mentioned previously, the human body houses a highly significant population of commensal organisms that exist in several niches mediated by the innate and adaptive immune system [51]. These organisms are collectively termed the microbiota or microflora, with the term microbiome used to refer to the collective genomes of said microorganisms. The term microbiome was first coined by Lederberg in 2001, and research in this area has exploded in recent years [52]. The first recorded scientific study of the microbiota dates back to Van Leeuwenhoek who compared his oral and fecal microbial populations (which he called his "little animals") [53,54]. The total number of cells that make up the microbiota was previously thought to outnumber the human cells by 10:1, though these figures have recently been called in to question and the ratio has been estimated to be closer to the region of 1.3:1 [55,56]. The microbiota is composed of bacteria, fungi, archea and viruses with the proportions of these changing throughout the various anatomical compartments. These microbes have enormous potential to impact human physiology, both in health and in disease. The most abundant and diverse microbes present as part of the human microbiota are bacteria and they will be the focus of this section. However, whilst the other members are not present in the same volume (though it is proposed phages outnumber bacteria) they still contribute significantly to host homeostasis [57-59]

Commensal bacteria contribute to host metabolic function, protect against pathogens, educate the immune system, and, through these basic functions, directly or indirectly affect most of our physiological functions [55]. Humans harbour quite a diverse bacterial microflora with over 1000 species represented from a few well known bacterial phyla, with populations belonging to the phyla *Bacteriodetes* and *Firmicutes* being the best represented [60]. The gut microflora is particularly diverse compared to the various other colonized anatomical sites (and indeed compared to other free-living microbial communities in most other environments) [61]. In order to understand fluxuations in the microbiota over time, a cohort study was performed that found 70% of the bacterial species present in the feces of an individual were stable over the course of 1 year. The study found few changes to the structure of the microbiome

over 5 years and it is so estimated that the microbiota is likely to be relatively stable over the course of an individual's life time [62].

The mouse microbiota is comparable to that of the human at a phylogenetic level, with Firmicutes, Bacteriodetes and Proteobacteria making up over 70% of the bacteria present. However, different phylogeny levels this similarity is not as evident, but a study has estimated that of the 20 most abundant "core" genera in humans, 13 are shared by mice though not always in the same proportions [63]. The shared human and mouse genera are as follows, listed in order of decreasing abundance in humans: *Bacteriodes, Clostridium, Butyrivibrio, Prevotella, Alistipes, Lactobacillus, Roseburia, Ruminococcus, Eubacterium, Blautia, Parabacteriodes, Coprococcus, Enterococcus, Odoribacter* and *Faecalibactierum*. The same study demonstrated substantial difference between mouse and human at gene level, but high overlap at the functional level [63]. The presence of the microbiota is vital for the proper function of the mammalian GI tract. This is evidenced by the numerous abnormalities displayed by mice bred in sterile conditions which will be discussed in a subsequent section. The microbiota is regulated by host factors such as anti-microbial peptides in order to shape its composition to suit the host. However, this composition can be altered leading to a deleterious makeup called a "dysbiosis" [64]. Several diseases correlate a dysbiotic microbiota, and so analysis of these microbial alterations and the functional consequences this may entail has become a key research avenue.

1.3.4. Analysing the microbiota

These studies of the commensal microbiome have been made possible in recent years thanks to the advent of revolutionary new culture-independent analysis and phylogenetic methods to organize microbial diversity [61]. Chief among the former is the next generation genetic sequencing of the bacterial 16S ribosomal rRNA gene (16S). This technology allows a culture free analysis of all the bacterial species present by sequencing the 16S gene and comparing variation to known bacterial databases [65]. Other adjunct technologies have allowed for an even deeper understanding of microbial physiology. These include the integration of microbial proteomics, transcriptomics and metabolomics among others [66]. These developments

are enabling the study of the relationship between the microbiota and the host and how that impacts on health and disease [65]. Several major projects have been undertaken in this vein, including the Human Microbiome Project (HMP) and the European Metagenomics of the Human Intestinal Tract (MetaHIT) [67,68]. These studies both sought to characterize the microbial composition of a healthy human microbiota so as to understand what alterations are occurring in diseased individuals.

As mentioned above, to understand the vast population data now being generated using high throughput DNA sequencing technologies, bioinformatics and microbial ecology tools have also been created, including various influential online platforms such as QIIME (Quantitative Insights Into Microbial Ecology) [69]. With this, ecological terminology has entered the lexicon of various biomedical science disciplines. Microbial communities are now described in a plethora of ways, but among the most important to understand are Operational taxonomic units (OTUs), alpha (α) and beta (β) diversity and relative abundance. OTUs refers to clusters of microorganisms grouped by DNA sequence similarity of a specific taxonomic marker gene[70]. In practice, OTUs are pragmatic proxies for microbial "species" at different taxonomic levels, which is particularly useful as it allows for the classification of hitherto uncultured microorganisms. α diversity refers to the microbial diversity within a sample whereas β diversity compares levels of diversity between samples. More specifically, according to Ursell *et al,* β diversity refers to "the measurement of the degree of difference in community membership or structure between two samples" [61]. One of the most common and robust methods for assessing β diversity is UniFrac, which measures the proportion of shared branch lengths on a phylogenetic tree between samples. UniFrac scores communities for similarity, with a score of 0 indicating identical structure, and a score of 1 indicating completely independent popultations. Principal coordinates analysis (PCoA), a method of data conversion, can then visualize the Unifrac distances between samples in two or three dimensions, allowing for easy visualization of the clustering of similar communities or separation of distinct communities [61,70]. Relative abundance is simply the abundance of one taxonomic group compared to another, but it can reveal many important biological distinctions between communities and samples.

The technological and methodological advances of recent years have given the field a much greater understanding of the make up of the human microbiome and its dynamics, but there are still many issues and unanswered questions to be resolved. One particular issue that requires addressing is moving beyond descriptive studies of the microbiome into more functional work to allow the translation of the advances in this field into therapies [65].

1.3.5. Homestatic functions of the gut microbiota

The gut microbiota has a number of important functions in maintaining host homeostasis. A number of these functions overlap with one another, and their disruption can lead to adverse effects on the health of the host. The first, and best characterized, function of the gut microbiota is augmenting host digestion and nutrient acquisition. A particularly important example of this function is the breakdown of ingested dietary fibre by commensal microbes to release short chain fatty acids (SCFAs) which have multiple benefits for the host including aiding in glucose homeostasis and insulin sensitivity [71,72]. In particular, the SCFAs butyrate, acetate and propionate have been shown to be important for host health, with deficiencies in each being linked to various disease states. There are multiple SCFA producing biochemical pathways employed by a variety of bacterial species present in the normal gut microflora, but interestingly only a few have the capacity to produce multiple SCFAs (e.g. *Roseburia inulinivorans* and *Coprococcus catu*s can produce both buyrate and propionate [73]). The importance of this metabolic function to human health is underlined by the observation that reduction in SCFA levels, and the abundance of SCFA producing bacteria, correlates with several diseases including ulcerative colitis and asthma [74-76]. Additional metabolic functions include synthesis of vitamins B12 and K which are important for a variety of host physiological functions[77]. The next key function of the gut microbiota is repression of harmful microorganisms which may attempt to colonize the gut [78]. By outcompeting potential invaders, the microbiota may act as a screen to deflect invaders before they reach the host and cause infection. The archetypal example of this role in action is the remarkable efficacy of fecal transplant in patients with chronic *Clostridium difficle* (*C. difficle*) infection. The supplementation or repletion of these patients' microflora

with that of a healthy donor has proved an extremely efficacious treatment for an infection where common antibiotics therapies have proved relatively ineffective [79].

One of the most interesting and important roles for the human gut microbiota is the maintenance of immune homeostasis. This is interesting in the context of the "hygiene hypothesis" which infers that reduced microbial exposures (particularly in early life) lead to an increased risk of allergic disease. The hypothesis centres on the idea that the immune system must be exposed to pathogens to learn and generate memory against viable threats rather than becoming sensitized to innocuous antigens. It is now thought that this process might be the responsibility of the microbiota, and that behaviours which alter its composition may be detrimental to the host [80]. In addition, studies in germ-free animals have shown that a gut microbiota is necessary for a fully developed immune system. The intestinal immune system of these animals is quite different to that of a mouse bred in specific pathogen-free (SPF) conditions, with notable alterations to the development of gut-associated lymphoid tissue, impaired antibody production and altered IEC turnover and microvilli structure [55,81-86]. As a result of these immune deficiencies, germ-free animals are also more susceptible to infection than colonized mice, as evidenced by reduced clearance of *Listeria monocytogenes* and increased mortality upon infection with *Shigella flexinari* [87,88]. Some of these effects can be reduced with the addition of microbes that would ordinarily colonize the gut, and indeed germ-free mice can have their developmental anomalies returned to normal by the introduction of commensals [88,89]. More relevant evidence for the importance of this role of the microbiota comes from evidence of disease correlating with dysbiosis (a deleterious change to the composition of the microbiota). Microbiome alterations have been associated with myriad immunological disease states including IBD, asthma, metabolic syndrome, obesity and type 1 and 2 diabetes [65,75,78,90-96]. Interestingly, whilst some of these diseases are largely due to aberrant immune function, some link the immune system to metabolism, and indeed there have been very interesting studies done, in the context of obesity and metabolic syndrome, which show that the microbiota's composition can be a predictor of glycemic response, and demonstrate that both parameters can be nutritionally altered [97]. This linking of the roles of the gut microbiota in human homeostasis truly serves to underline its importance to human health.

1.3.6. GI tract infection

The capacity of the immune system to cooperate with the intestinal microbiota and not react to its presence is an interesting aspect of mucosal immunology, particularly given the requirement to respond to pathogenic microorganisms by mounting robust immune response. Food-borne pathogens are a major cause of disease in both the developed and, to a greater extent, the developing world [98]. Of interest to this thesis are the common food-borne bacterial pathogens *Listeria monocytogenes* and *Salmonella* Typhimurium. These pathogens are causative agents of infectious disease but are also widely used model organisms for the study of immune cells and their function [99,100].

Listeria monocytogenes (*L. monocytogenes or Listeria*) is the causative agent of the group of systemic infections known as listeriosis, associated with a fatality rate of 20% or more and the third leading cause of death among food-borne bacteria [101]. *Listeria*'s ability to establish itself intracellularly where it can avoid host responses creates a more favourable environment that ensures their pathogenesis. Indeed, *L. monocytogenes* have evolved to escape from the phagolysosome through the expression of a hemolysin, LLO, and subsequently grow and replicate within the cytosol of macrophages and in other non-phagocytic cell types. Indeed LLO is one of many mechanisms employed by *Listeria* to The ability of *Listeria* to establish an intracellular niche and evade immune surveillance typifies the struggle between infectious agents and the host immunity and is critical to the outcome of infection [99,102].

Salmonella enterica is a species of *Salmonella* comprising over 2,500 serovars, many of which cause various forms of infectious disease in a broad array of vertebrate hosts. These serovars are broken down in to typhoid and non-typhoid strains, the former of group causing typhoid fever and abdominal pain and the latter group causing a range of diseases upon ingestion by humans and common livestock [100]. These disease generally fall under the category of temporary gastroenteritis but can be more serious in immuno-compromised individuals where infection may lead to systemic infection and bacteraemia [100]. *Salmonella enterica* serovar Typhimurium (*S.* Typhimurium or *Salmonella*) is a commonly used model organism for studying

infection. Like *Listeria,* this bacterium is a facultative intracellular pathogen which can invade non-phagocytic cells as well as escaping destruction in the phagolysosome of phagocytic cells of the immune system [103]. *Salmonella* appears to have developed the capacity to survive inside epithelial cells and macrophages in order to evade killing by neutrophils which are very effective at clearing it [104]. . *Salmonella* has evolved many strategies to avoid destruction by host cells, and like *Listeria* several of these involve phagosomal escape or neutralisation of the phagosome [105].

Actin modification and mobilization is a crucial host pathway for infection by both *Listeria* and *Salmonella*. Both organisms encode several effector molecules to modulate actin in the host to allow initial invasion of the cell and also subsequent infection. For instance, after replication in the host cytosol, *Listeria* employs the ActA protein to mobilize actin to its end and form "comet tails". These actin filaments allows the bacterium to burst from the cell into neighbouring cells (termed cell-cell spread) and propagate infection [106]. Similarly, *Salmonella* encodes a variety of actin modulating proteins to facilitate entry in to the cell and survival within it. For example, encoded on *Salmonella* pathogenicity island (SPI)-1 is the effector protein SopB which activates Rho-GTPases to allow actin filament rearrangement for cell entry and subsequently prevents acidification of the phagosome [100]. These are just a few examples of the complex interations that GI tract pathogens have with host cells networks and pathways to facilitate infection. When considering the normal function of these networks and pathways, and their alteration upon stimulation, it is important to consider the host's regulatory machinery which maintains this normal function. One class of regulatory molecules employed by host cells is microRNAs which post-transcriptionally regulate a variety of cellular processes. Their function and relevance in immunity, inflammation and infection are discussed in the following sections.

1.4. microRNA

MicroRNA (miRNA) are ~22 nucleotide (nt) long endogenous non-coding RNA molecules that serve as post-transcriptional regulators of target mRNA by binding to complementary sites in their 3' untranslated region (UTR) [107,108].

MiRNAs were first described in the *Caenorhabiditis elegans*, a model organ organism commonly used in developmental studies, where two short non-coding RNAs (*Lin-4* and *let-7*) were found to regulate the timing of larval development[109]. Soon after, it was realized that the RNA interference pathway (RNAi), which had been observed in plants and other species, might involve miRNA[110,111]. Eventually it became clear that miRNA are endogenous substrates for the same mRNA regulatory machinery employed by the RNAi pathway to target mRNA using small interfering RNA (siRNA) [112]. The next major leap in the field was the discovery that miRNA were highly conserved across species and had the potential to regulate a plethora of targets in mammalian cells [113,114]. This discovery led to an intense period of research in to finding miRNA in mammalian genomes and the miRNA pathway itself. Multiple novel miRNAs were uncovered in this period and their functions implicated in a vast array of biological processes including maintenance of the cell cycle and apoptosis [115].

MiRNA transcription can occur in a number of ways. RNA polymerase (RNA Pol) II is often responsible for the transcription of miRNAs from their own promoters whilst RNA Pol III is the operative enzyme for miRNA located downstream of Alu elements [116,117]. MiRNA can also be located in clusters that are transcribed simultaneously, or, as is very commonly the case, they can be embedded in an intronic region of a protein-coding gene [118]. Regardless of the circumstances of their transcription, miRNAs are initially produced as primary miRNA (pri-miRNA) transcripts containing hairpin structures[115]. These structures form the basis for the mature miRNA. The first stage of processing towards this mature RNA occurs in the nucleus, where the pri-miRNA is cleaved at the hairpin's base by DGCR8 and Drosha, two proteins that together form the Microprocessor complex. The resulting

pre-cursor miRNA (pre-miRNA) is ~70 nt in length and is translocated from the nucleus to the cytoplasm via Exportin 5 and RAN GTP [115,118]. Once in the cytosol, the pre-miRNA is further processed by the endonuclease Dicer to generate a mature miRNA duplex. The two strands of the duplex stem from either side of the hairpin and it is now understood that both strands can be expressed equally and that their expression is independently regulated. This is summarised in Figure 1.4.

MiRNAs exert their regulatory function by acting as a targeting molecule within the RNA-induced silencing complex (RISC) [119]. The Argonaute family proteins (AGO1-4) anchor the complex by the binding a lone miRNA strand and several accessory proteins [118]. These proteins serve to link the complex to the cellular machinery necessary for mRNA translation inhibition, including the translation machinery itself. This process also leads to recruitment of target mRNAs to cytoplasmic processing bodies (P bodies). Here translation repression can occur upon interaction of the target mRNA with the AGO1 protein part of the RISC complex [120] (Fig. 1.4). This repression can take the form of mRNA degradation, which requires deadenlyation and decapping, or interference with the initiation and elongation steps of translation [121]. The relative importance of one form of repression versus the other is debatable, but it is likely that both repression of mRNA level and mRNA translation occur to broadly similar degrees given that they are tightly linked processes [122].

In this mRNA silencing process, the miRNA's role is critical to the specificity as well as the effectiveness of the RISC complex's function. For the majority of miRNAs, mRNA binding is mediated by binding of a sequence of perfect complimentary base pairing, known as a seed sequence, followed by a sequence of non-complimentary bases. This second region forms a bulge that is often important in determining the fate of the mRNA [123]. The Argonaute proteins are more readily able to interact and perform their endonuclease activity on mRNA that is bound with a longer complimentary sequence. This implies that the bigger the miRNA bulge, the more less likely the mRNA is to be cleaved and the more likely is to be repressed by deadenylation and translation inhibition[124]. This process is summarized in Figure 1.4.

The short seed sequence required for miRNA binding to mRNA means that predicting true target mRNAs for individual miRNAs is very difficult as the number of potential

candidates is huge [123]. Several predictive algorithms have been developed based on known miRNA-mRNA interactions as well as evolutionary conservation, but these approaches still generate numerous false positive results [124,125]. Experimental validation is essential for effective characterization of a target mRNA for any given miRNA, and this is commonly done by immunoprecipitation using ever more sophisticated methodologies [126,127]. With each passing year the number of miRNAs identified, as well as the number of potential mRNA targets, grows for each species. Given the potentially enormous number of potential target mRNAs, miRNAs can exert their regulatory effects at several stages of any given pathway and they can also connect different pathways. Hence it is not surprising that dysregulation of miRNAs is evident in cancer, and in fact the miRNA status of cells is now used to classify various forms of the disease [128]. Unsurprising too is the growing body of evidence which links miRNA expression to modulation of highly interconnected immune signalling pathways [33,129,130]. These miRNAs can form regulatory loops, limiting their own expression after a given response has been elicited, or modulating the expression of another miRNA involved in the pathway in various ways [130]. An illustration of some of the elements of the TLR signalling pathway, as well as some of the post-translational modifications employed to regulate TLR signalling, is presented in Figure 1.5. Of particular interest to this project is the microRNA-21 (miR-21) which was first shown in the O' Neill lab to modulate the function of innate immune signalling by negative regulation of the tumor suppressor PDCD4 in order to allow translation of IL-10 mRNA [129].

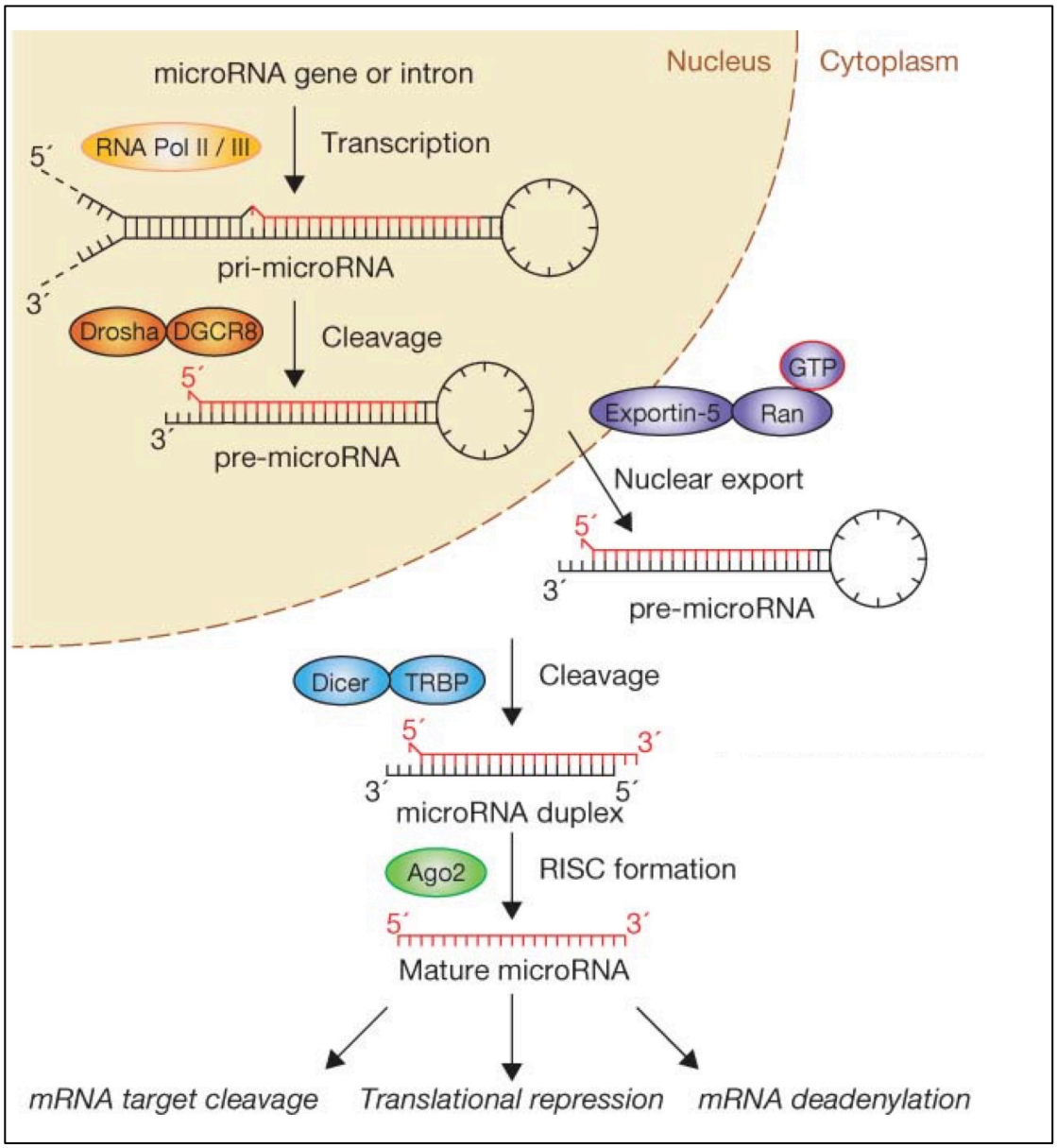

Figure 1.4 Processing of miRNA

miRNAs are transcribed as pri-miRNAs and processed in the nucleus by Drosha as part of the microproccesor complex. The pre-miRNA formed then reaches the cytoplasm, via the Exportin-5 transporter, where it is cleaved by Dicer to form the mature miRNA duplex. From here, either strand can then be incorporated in to the RISC where it performs targeting functions leading to repression of mRNA translation. Adapted from Winter *et al* 2009 [118]

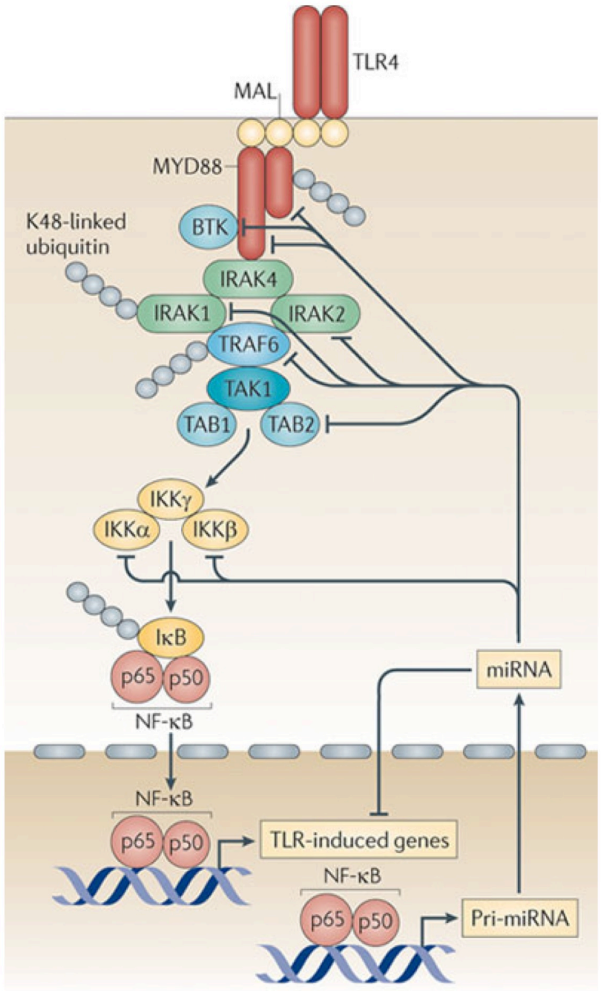

Figure 1.5 TLR4 signalling and regulation by miRNAs

TLR4 uses a variety of adaptor molecules and downstream signalling proteins to activate gene transcription in response to the sensing of the bacterial ligand lipopolysaccharide (LPS) or other danger signals such as low-density lipoprotein. Adaptors such MyD88 and MAL are used by TLRs to recruit downstream signalling molecules that can propagate the signal to activate pro-inflammatory genes. In order to maintain control of the signal and prevent excessive inflammation occurring, several regulatory mechanisms must exist. K48-linked ubiquitylation of various signalling components provides one level of regulation by labelling proteins for proteosomal degradation. At the mRNA level, miRNA provide a post-transcriptional level of regulation by preventing the translation of mRNA. This is achieved by the targeting of the 3'UTR of these mRNAs, preventing their translation into functional proteins. TLRs themselves activate this regulatory mechanism by induceing the expression of pri-miRNA After processing to mature miRNA, many elements of the TLR signalling pathway are targeted for repression to regulate the signal. These include the adaptors MyD88 and MAL as well as downstream signalling components such as inhibitor of NF-κB (IκB) kinases (IKKα and IKKβ). This is a powerful regulatory mechanism for TLR signalling regulation. Adapted from O'Neill *et a* 2011 [131].

1.5. miR-21

This project focuses on the miR-21, the expression of which has been shown to be upregulated in human inflammatory bowel disease (IBD) [132,133] as well as in many scenarios in immunity [129,134]. miR-21 is among the most widely expressed miRNAs in many different mammalian cells types. It has been well studied in cancer where it has been shown to be upregulated in many forms of the disease, most strikingly in solid tumors where it is among the most highly expressed miRNAs and indicates a poor prognosis in several forms including breast and early-stage colon cancer [135,136]. For this reason it has been designated an oncomiR.

The *miR-21* gene is strongly conserved throughout evolution and sits in an intronic region of the protein-coding gene *TMEM49* located on chromosome 17q23.2 [137,138]. Despite being located in this region, *miR-21* and *TMEM49* are regulated separately as *miR-21* appears to have its own promoter which features conserved sites for a number of transcription factors related to immune signalling including AP-1, STAT3, NFIB and PU.1 [139,140]. There are several suggested putative promoter sites which are illustrated in Figure 1.6. Two of these sites overlap heavily (−3,403 to −2,395 and −3,565 to −2,415), whereas the other one has minimal overlap (−3,770 to −3,337), which suggests that *miR-21* may have independent promoter elements[138,141,142]. Whilst there have been several studies defining the roles of these transcription factors in miR-21 induction, notably IL-6 mediated induction via STAT3 and phorbal-12-myristate-13-acetate (PMA) mediated induction via AP-1[138,141,143], there is strong evidence to suggest that the regulation of miR-21 transcription and processing into its mature form is multi-layered and complex. Beginning with the promoter itself, the presence of multiple alternative transcription start sites suggests that the regulation of its activity is complex. Once pri-miR-21 has been transcribed, there is an added layer of regulation as miR-21 belongs to a family of miRNA that requires additional co-factors to aid its post-transcriptional processing towards their mature forms [130,144]. These co-factors and enzymes are themselves subject to regulation by extrinsic signalling events. A notable example of this occurs in TGF-β/BMP induced miR-21 expression, where the adaptor Mothers against decapentaplegic homolog 6 (SMAD6)

is activated in response to TGF-β and binds pri-miR-21 to allow recruitment of the RNA helicase p68 (a necessary additional co-factor) and promotion of cleavage by Drosha [145]. As TGFβ/BMP are indirect targets of miR-21, this pathway also provides a feedback loop with which miR-21 can control it's own expression levels. This is one of several apparent feedback loops, both positive and negative, which miR-21 may use to regulate it's own expression and activity [143]. Finally, the additional role of other non-coding RNAs in miR-21 expression adds an additional layer of complexity, with the recently discovered family of long non-coding RNAs (lncRNAs) potentially acting on miR-21 expression at a transcriptional level or by acting as a miRNA sponge to block its activity. miR-21 has been shown to regulate one such lncRNA, GAS5 [146]. In the context of immunity, this level of complexity of regulation has been implicated as a potential mechanism by which miR-21 might be temporally controlled. It has been suggested that miR-21 expression may act as a molecular switch where, in response to cytokine signaling and other inflammatory stimuli, its delayed induction allows the initial inflammatory phase to take it's course before altering the cell towards resolution of this inflammation. This benevolent role of miR-21 in inflammation is juxtaposed with its well-established role in cancer, which has lead to its designation as a *bone fide* oncomiR.

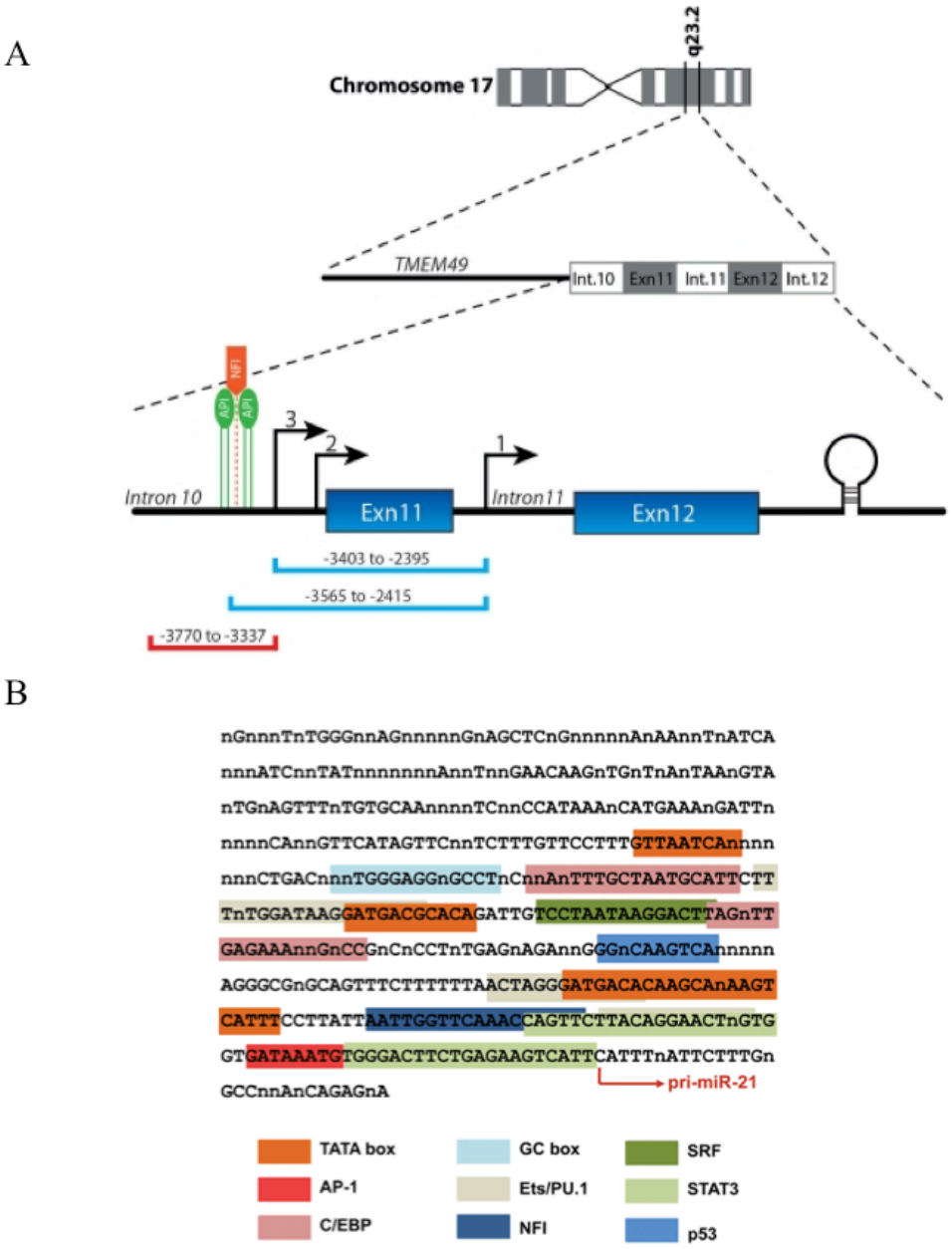

Figure 1.6 Location of the *miR-21* gene, promoter and transcription biding sites

A) The gene coding for pri-miR-21 is located on chromosome 17q23.2 overlapping with the protein coding gene TMEM49. Transcriptional start sites described by Cai et al, Fujita et al and Mudduluru et al are indicated as 1, 2 or 3[137,138,147]. Different proposed promoter regions and their location with respect to miR-21 hair-pin and binding regions for transcriptional activator (AP1) and repressor (NFI) are also shown. As discussed in the text, two promoter regions with a high degree of overlap while the promoter region proposed by Fujita *et al* has minimal overlap suggesting that miR-21 may have independent promoter elements (Adapted from Kumarswamy *et al* [139]). B) Putative transcription factor binding sites in the miR-21 promoter regions (Adapted from Krichevsky *et al* [140]).

1.6. miR-21 in disease and immunity

The role of miR-21 in cancer has been well described over recent years, so it will only be mentioned briefly here. Many targets of miR-21 are tumor suppressor genes, including PDCD4 and phosphatase and tensin homolog (PTEN), and due to its capacity to take these brakes off the cell cycle, it is hardly surprising that it is implicated in so many solid tumors and leukemic cancers [140]. In addition to this, miR-21 has also been shown to mediate the epithelial-mesenchymal transition (EMT) via a variety of mechanisms [143,148-150]. Several of miR-21's pro-oncogenic functions potentially overlap with some of the novel roles for immunity which have been recently uncovered, including regulation of ROS [151,152], NO [153,154] and *in vivo* host responses to infection [155]. The studies regarding ROS and NO, two factors which have key roles as anti-microbial agents in the phagocytosis and subsequent degradation and killing of pathogens, have been carried out in the context of cancer models which must be borne in mind when interpreting their results in the context of the immune system. However, of particular note is a study by Das *et al* showing the miR-21 expression boosts levels of the ROS superoxide via repression of tumour necrosis factor alpha (TNF-α), an important cytokine in innate and adaptive immunity [152].

In recent years, numerous roles have been described for miR-21 in cells of the immune system. As this project focuses on the innate immune system, I will largely limit my description to cells involved in this arm of immunity. miR-21 expression is altered during hematopoietic differentiation. In immature progenitor cells of various lineages, miR-21 expression is moderate until the cells switch to a more functional state whereupon expression is increased [144]. Of particular interest to this thesis, miR-21 upregulation can be seen to mark the activation of several bacteria sensing cells of the innate immune system; PMA–induced monocyte differentiation in to macrophages , retinoic acid induced differentiation, granulocyte/macrophage colony stimulating factor (GM-CSF)/IL-4 induced dendritic cell differentiation and classic macrophage activation in response to LPS [138,144,156,157]. In adaptive immune contexts, elevated miR-21 expression is associated with T cell activation and differentiation in to a

variety of different lineages, which appear to be functionally conflicting in different contexts, with miR-21 deletion shown to skew T cell responses in response to various immune challenges [158-161]. It has also been asserted that miR-21 acts as a break on M2 macrophage polarization, also this does not entirely fit with the general view of miR-21 as a pro-resolution regulator in the immune response [162]. This is another indicator miR-21 function is highly signal and context dependant.

As mentioned above, within activated innate immune cells miR-21 has been proposed to act as a mediator of the resolution phase of inflammation in response to various pro-inflammatory stimuli including LPS [144]. In this model, the mature form of miR-21 is induced by the inflammatory stimulus acting upon it before going on to target various mRNAs to dampen down the response elicited by the same stimulus. This model is strongly supported by data from macrophage studies where, in response to LPS binding to TLR4, miR-21 is upregulated and results in the negative regulation of the pro-inflammatory cytokine IL-12 by direct targeting of its p35 subunit, and indirect induction of the anti-inflammatory (or pro-resolution) cytokine IL-10 via negative regulation of the translation inhibitor PDCD4 [129,163,164]. Indeed, mice-deficient in miR-21 fared worse in a model of LPS-induced sepsis (although this did not correlate with a second model, caecal ligation punction model, performed by the author) [155]. In addition, in macrophages, miR-21 activity has been associated with enhancement of efferocytosis – the process of engulfing dead or dying cells – and the negative regulation of TNF-α levels, once again suggesting that miR-21 is involved in processes which limit inflammation [165]. This aspect of miR-21's apparent role in the immune response would appear to tally well with its established role in oncogenesis; the promotion of an anti-inflammatory state in the site of tumor growth, allied with miR-21's direct role in the cancerous cells, is likely to benefit the tumor progression due to the reduced access of anti-tumor immune effector cells [144]. MiR-21 has recently also been implicated in resolution of damage caused during rheumatoid arthritis [166]. However, miRNAs often affect multiple pathways due to their capacity to disrupt expression of many multiple target mRNAs. Therefore, it is reasonable to assume that miR-21 may not solely act to dampen down immune responses and may in some cases augment them.

miR-21 expression has been shown to be upregulated in several inflammatory diseases, several of which can be linked to the possible promotion of an anti-inflammatory environment by the miRNA, such as cancer and chronic bacterial or viral infections [163,167,168]. There is also a cohort of diseases where miR-21 expression is elevated where miR-21's role may in fact be pathological. These include IBD, systemic lupus erythematosus (SLE) and psoriasis [132,133,169-172]. It has also been experimentally demonstrated that miR-21 promotes a form of inflammatory cell death termed necroptosis in mouse models of pancreatitis [173]. In these more complex systems, there are several cell types in play and multiple pathways that miR-21 may impact on at any given time. This is particularly notable in SLE which is a heavily T cell influenced disease. In this context, miR-21 has been put forward as a therapeutic target [174], and in several case antisense miR-21 has already been therapeutically employed to block diseases like SLE and psoriasis [144]. A summary of some of miR-21's roles in immunity and disease is presented in Figure 1.7. Given miR-21's role in the innate immune response via TLR regulation, the disease of particular interest to this thesis is IBD. This disease, and the role miRNA and intestinal immunity play in its pathogenesis are discussed in the next section.

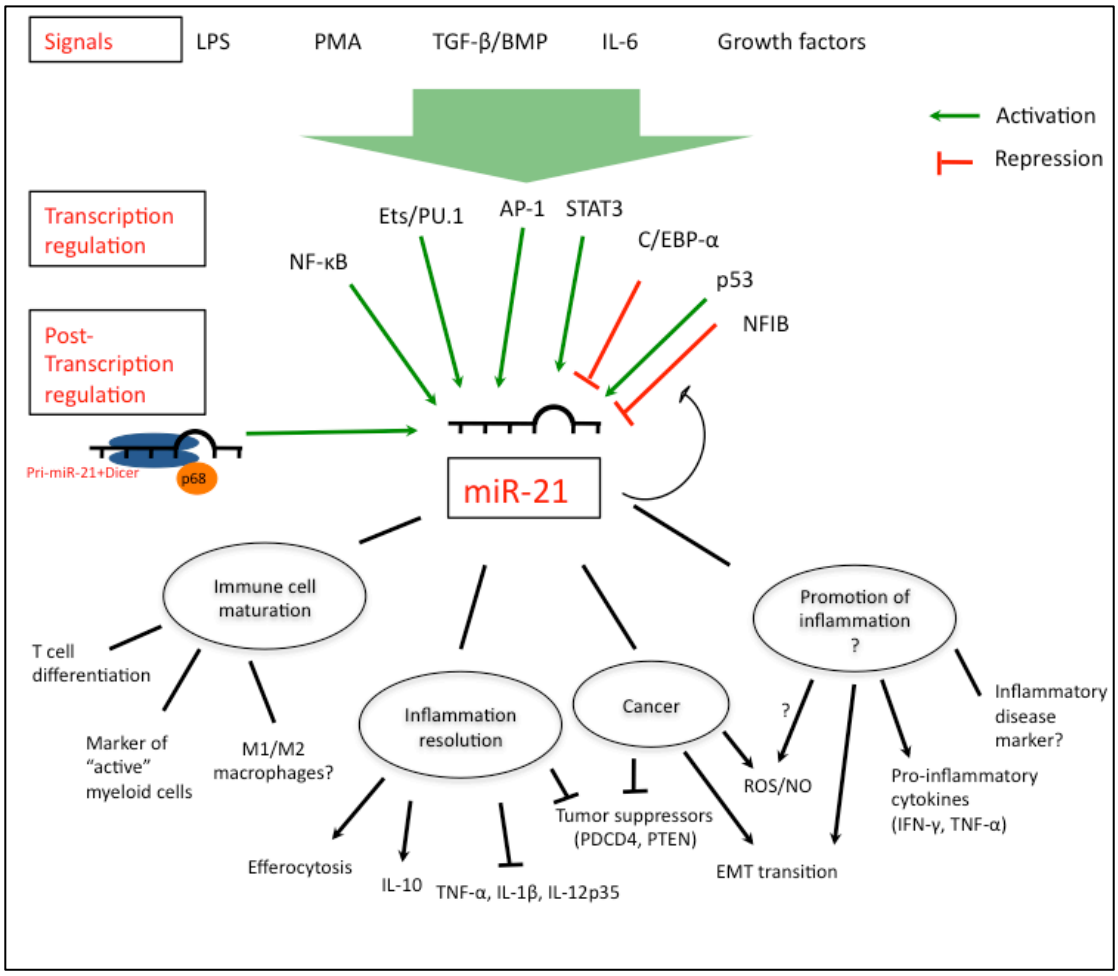

Figure 1.7 miR-21 in immunity

miR-21 is induced following cellular sensing of a number of different external stimuli, including the pro-inflammatory signals lipopolysaccharide (LPS) and interleukin (IL-)6 as well as other signalling molecules and growth factors as is the case in cancer. Its induction is mediated at the transcriptional level by a number of transcription factors, including nuclear factor-κB (NF-κB) and signal transducer and activator of transcription 3 (STAT3), and repressors such as Ccaat enhancer binding protein-α (C/EBP-α) and nuclear factor 1 B (NFIB). The repressor sits on the promoter but can be degraded following to allow transcription. miR-21 regulates its own expression at this level by targeting different effecter molecules. There is also an element of post-transcriptional regulation, for example the recruitment of p68 to the Dicer complex to all processing of pre-miR-21 in to mature miR-21, induced by transforming growth factor (TGF)-β/ bone morphogenic protein (BMP) signaling. miR-21 itself regulates a number of processes involved in immune function and disease, both anti-inflammatory but also potentially pro-inflammatory, including its well described role in cancer.

1.7. Inflammatory bowel disease

1.7.1. Intestinal inflammation & IBD

Today, the innate immune system is recognised as the major contributor to acute inflammation induced by microbial infection or tissue damage [175,176]. It is well accepted that physiological inflammation is beneficial in the intestine and diverse innate immune compartments in the gut encompass many innate leukocyte populations, as well as several types of IEC which act together to maintain a balanced immune response to the microbiota [177]. As previously stated, the intestinal epithelium seems to play a crucial role in regulation of intestinal homeostasis. However, the inflammatory response must be well regulated as excessive inflammation can lead to the development of highly debilitating chronic diseases such as IBD.

IBD refers to a spectrum of inflammatory disorders that affect the gastrointestinal tract and is most often diagnosed between the ages of 15 and 30 when its peak onset occurs [178]. The instances of IBD have risen dramatically over the second half of the 20th century in both developed and developing countries [55,179]. IBD is more prevalent in Caucasians and in those living in northern hemisphere-industrialized countries. However, rates are also on the rise in non-whites and in southern, non-industrialized nations. IBD is estimated to affect between 2.5-3 million people in Europe, with Ireland having a particularly high prevalence [119] with an estimated 20,000 IBD sufferers present in the country in 2015 [180]. Patients diagnosed with IBD typically suffer from a variety of symptoms including recurrent intestinal inflammation, diarrhea, abdominal pain, rectal bleeding, weight loss and anaemia. These symptoms dramatically impact on the patients quality of life and are associated with increased risk for additional diseases such as colitis-associated cancer (CAC) [181]. IBD has two main clinical forms – Crohn's disease (CD) and Ulcerative colitis (UC). CD presents as patchy inflammation that can affect any part of the GI tract but often begins at the terminal ileum. The pathological lesions characteristic with CD feature trans-mural inflammation (inflammation present in all layers of the intestinal wall) and granulomas, high infiltration of macrophages and T cells with a pro-inflammatory Th1/Th17 profile. UC, by contrast, is generally localised to the rectum and colon

where mucosal inflammation and high infiltration of neutrophils and T cells with an atypical Th2 phenotype being observed [182]. IBD is generally thought of as being a multifactorial disease. The exact aetiology is still unclear despite a heavy research focus in recent years. However, several factors have been identified which play an important role in the disease's pathology and progression. These include the host's genetic disposition, lifestyle factors including diet alteration and antibiotic use, the composition of the intestinal microbiota and alterations to the immune profile of the patient [178]. These overlapping factors and their interaction with one another are key in the development of the disease [182]. The importance of the immune system, both innate and adaptive arms, in intestinal homeostasis is made evident by a variety of genome-wide association studies (GWAS) that have identified polymorphisms in several genes involved in immune pathways which correlate with susceptibility to IBD. These studies have helped identify over 160 unique loci associated to IBD, with some loci specific for CD or UC and the remainder shared between both diseases [183-185]. However, these loci represent only a small fraction of the overall disease variance of 13.6% for CD, 7.5% for UC, which in turn only accounts for a small fraction of heritability observed in twin studies (50% for CD and 19& for UC) [132,186]. As such, it is unclear whether the IBD phenotype is a result of a wide range of relatively insignificant SNPs interacting with one another, or a few rarer variants with a more significant impact, or indeed both [187]. Several of the loci identified are involved in immune signalling (IL-23R, IL-10, STAT, JAK2), regulation of inflammation (CCR6, MST1) and regulation of endoplasmic reticulum (ER) stress and autophagy (XBP1, ATG16L1, IRGM). These pathways are all involved in the immune system and its interaction with the intestinal barrier and luminal bacteria. Interestingly, despite these pathways sharing similar functions at a macro level, there are distinctions between the two main forms of IBD in some pathways. For instance, autophagy genes (e.g. ATG16L1), NOD-like receptors (e.g. NOD2/CARD15) and intelectins have been related to CD whereas loci related to regulatory pathways (e.g. IL-10, ARPC2) and intestinal epithelial cell function (e.g. ECM1) are more specific for UC [188]. In addition, it is now widely recognized that alteration in the recognition of the commensal microbiota by PRRs of the mucosal immune system plays a large role in the pathogenesis of IBD [189,190]. Current IBD treatment usually involves either drug therapy or surgery with the aim of reducing the inflammation that causes disease symptoms. This approach is intended to alleviate symptoms in the short term and

induce remission in the longer term in some cases. IBD is currently treated with a pyramid approach, depending on severity, beginning with antibiotics and topical aminosalicates at the pyramid base. The next stage of the pyramid is made up of a variety of steroids as well as azathioprine, methotrexate, tacrolimus. These agents suppress the inflammatory response in the gut by largely unknown mechanisms. However, they are all accompanied by several potentially serious side effects, including opportunistic infections which arise due to this immunosupression [191]. The current third tier of the pyramid come in the form of biological agents (e.g, monoclonal antibodies, recombinant proteins or peptides, antisense oligonucleotides) targeted at neutralizing specific pro-inflammatory proteins. Monoclonal antibodies targeting TNF-α (such as infliximab, adalimumab or certolizumab pegol) have proven to be highly effective in patients with moderate to severe Crohn's disease and Ulcerative colitis [192-194]. Several other biological agents targeting other pro-inflammatory proteins have been trialled for use in IBD with mixed results. Several of these agents have been shown to be efficacious in other inflammatory diseases like rheumatoid arthritis and psoriasis, but this has been demonstrated to be a poor indicator of their effectiveness in IBD. For instance, the anti-IL-17 antibody secukinumab is effective in the treatment of psoriasis but is deleterious in CD patients [195]. This points to the complexity of IBD pathogeneis, and this fact is reinforced by the observation that the anti-IL-12p40 antibody ustekinumab is efficacious in both psoriasis and IBD and works upstream of IL-17 [195]. The point of the pyramid is often a combination of the aforementioned therapies as well as surgery, which is employed in severe instances.

1.7.2. Mouse models of IBD

In the past few decades, the need to understand the pathology of IBD and develop effective treatments has led to the development of several mouse models of the disease. These models can be categorized into six groups: chemically induced, bacterially induced, cell-transfer, spontaneous, congenital (spontaneous gene mutation), and genetically engineered models [196]. These models have led to significant insights into the mechanisms that govern IBD, although, as with all experimental models, they do not fully mirror the human disease presentation.

Despite their drawbacks, these models have led to the generation of several novel therapeutics for IBD [196,197]. Each model has its strengths and limitations; ease and length of experiments, type of inflammation induced (acute or chronic), spontaneous versus chemically induced onset and subtle versus severe phenotypes [196]. Chemically induced murine models of IBD are the most prevalent models for a number of reasons including their simplicity, relatively low cost and wide applicability. Currently, the most commonly used chemical models are the dextran sodium sulfate (DSS) and trinitrobenzene sulfonic acid (TNBS) induced colitis. A variation of the DSS model of colitis which includes azoxymethane (AOM) pre-treatment with multiple cycles of DSS administration is also routinely employed as a model of colitis-associated-cancer [198]. In the DSS model, colitis is induced by the *ad libitim* oral administration of heparin-like polysaccharide DSS in drinking water. It is still unknown precisely how DSS administration initiates colitis, but the literature suggests multiple possible contributory mechanisms including direct epithelial cell toxicity, increased intestinal permeability and macrophage activation [93,199,200]. It is also suggested that the characteristic increased apoptosis and decreased proliferation causes the epithelial barrier to become leaky and allows the mucosal invasion of intraluminal microorganisms during the acute phase of DSS colitis [201]. The typical onset of DSS-induced colitis presents symptoms such as diarrhea, bloody faeces, cachexia and the histological features of colonic inflammation. The acute inflammatory response to DSS is considered independent of T- and B-cells, and so the model is considered to be ideal studying the role of innate immune mechanisms in intestinal inflammation, although recent evidence indicates that antigen-specific T cell responses can be induced [202]. This model is simple to perform; the onset, duration, and severity of inflammation are immediate and controllable. Importantly, the acute DSS-induced colitis model mimics the clinical and histological features of IBD, that have characteristics of UC [203,204]. Moreover, it has also been validated as a model using multiple current efficacious therapies for human IBD, making this model highly relevant for study of this disease [205]. To date, the murine IBD DSS-induced model has been widely used to understand immune signalling pathways employing mice deficient in various components including PRRs, inflammasome components and cytokines [50,206-208].

One of the most commonly used bacterial infection models of IBD is the *Citrobacter rodentium* infection model. This bacterium is a gram negative attaching and effacing pathogen which, in mice, closely resembles human infection with the attaching effacing (A/E) pathogens enteropathogenic *Escherichia coli* and enterohemorrhagic *E. coli* which are an important cause of morbidity and mortality worldwide [209]. *Citrobacter* has been used as a model to study these infectious pathogens, but due to its mechanism of action it is also a useful tool for studying colitis. *Citrobacter* regulates epithelia barrier integrity, inflammation, mucosal healing and also the composition of the commensal microbiota [210]. The mechanism of action by which *Citrobacter* induces these responses involves activation of cytokine production in the epithelium upon bacterial attachment, and stimulation of the immune system by bacterial antigens. Both the innate and adaptive arms of the immune system are critical for controlling *Citrobacter* as demonstrated by the wide variety of knockout mice that display increased susceptibility to the infection, including group 3 innate lymphoid cells (ILCs) deficient and Rag deficient mice respectively [211]. The *Citrobacter rodentium* model and the DSS induced colitis model are two of the most commonly used in the field. As mentioned in section 1.6, miR-21 is potentially involved in the pathogenesis of colitis. It is expressed in both adaptive and innate immune compartments as well as potentially playing a role in the intestinal epithelial cell wall, and so these models were deemed appropriate to address its possible role.

1.7.3. Role of the innate immune system in the development of IBD

As discussed previously, there is a huge commensal population of bacteria, viruses, and fungi present in the large intestine and this presents a challenge for the mucosal innate immune system [44,212]. The mucosal immune system has evolved to balance the need to respond to pathogens while tolerating and co-existing with commensal microbes and food antigens. In inflammatory bowel disease, this hyporesponsiveness or tolerance breaks down and inflammation supervenes, driven by the intestinal microbiota [132].

As previously described, bacteria contain compounds that are recognized by a variety of receptors, including TLRs and NLRs and are potent stimuli of innate immune

responses. These aforementioned multi-receptors are expressed on epithelial and immune cells in the gastrointestinal tract and various mutations in these receptors have been associated with development of IBD. Numerous PRR gene knockout mice have been generated and have provided important information pertaining to individual PRRs regarding their intestinal phenotypes and susceptibility to colitis, suggesting their important role during intestinal inflammation. In addition, several of these knockout mice exhibit altered gut microbiota composition, which in itself can be a marker for disease.

1.7.4. Role of PRRs and the microbiota in IBD and other inflammatory diseases

In recent years, it has been observed that mice with deficiencies in innate immune signalling have altered microbial populations, and that this can predispose them to certain inflammatory diseases including IBD [132,213,214]. This has led to a shift in the field, where it is now recognized that sensing of the commensal microbiota is a necessary factor for effective mutualism between the host and the microbial passengers [51]. There are several prominent examples of host-microbiota interactions that demonstrate the need for appropriate innate immune sensing. For example, alterations in NOD2, a member of the NLR family, have been shown to lead to an altered shaping of the composition of the intestinal microbiota due to defect antimicrobial secretion [215]. Mice with deficiencies in other NLR receptor components involved in inflammasome formation (e.g. NLRP6) have been shown to have an increased susceptibility to DSS induced IBD with expanded representation from the phyla Bacteriodetes and TM7, which is thought to be at least due in part to the reduced production of IL-18 [216]. Though IL-18 is conventionally considered to be a pro-inflammatory cytokine, it appears to have additional homeostatic roles in the context of mucosal immunity including the maintenance of epithelial barrier integrity [217]. Most interestingly this susceptibility was transmissible to wild-type mice via microbial transfer which illustrates how the intestinal microflora are crucial in maintaining immune homeostasis. TLRs have also been implicated in the process of host-microbiome interactions. Mice-deficient in TLR5 display altered microbial populations and a pre-disposition to metabolic syndrome[94]. As mentioned earlier,

there is still an interesting dichotomy between the responses of the mucosal innate immune response to sensed commensal bacteria and invading pathogenic bacteria, which often display similar PAMP (or perhaps more appropriately MAMPs) [51]. It has been suggested that the innate immune system employs receptor cooperation in order to differentiate between pathogenic and commensal microbes at densely populated mucosal surfaces. This concept is supported by evidence of redundancy between inflammasome receptors in the response to *Salmonella* infection [218], as well as the observation that NLRC4-mediated production of the pro-inflammatory cytokines interleukin (IL)-1β by phagocytes is far higher in response to pathogens than commensal bacteria [219].

Most relevant to this thesis is the body of literature indicating a role for TLR4 in the inflammatory process in IBD and colitis-associated cancer (CAC) [190,220]. TLR4 is expressed on the surface of IECs and various innate immune cells, as well as regulatory T cells of the adaptive immune system [221 222]. Luminal LPS is usually non-immunogenic within the healthy intestine most likely due to low TLR4 expression on IECs. TLR4 up-regulation may alter this balance from tolerance to a proinflammatory state [223]. Indeed, TLR4 has been shown to be upregulated in both CD and UC [224]. A possible "gain of function" hyperactivity mutation has also been described for TLR4, where up-regulation of TLR4 on IECs due to long lasting disease may lead to increased LPS sensitivity and heightened pro- inflammatory response [225]. Notably, the cellular distribution of TLR4 differs between CD and UC, with TLR4 expressing cells localised near the mucosal surface, thereby supporting the superficial inflammation observed in UC [224]. Indeed, dysbiotic alterations in the intestinal microflora have been linked to an increase in intestinal inflammation due to excessive TLR4 stimulation [226,227]. However, TLR4's role in intestinal inflammation is not that straightforward, as impaired responses to LPS are also linked to the disease. For instance, genetic variants of TLR4 appear to contribute to the IBD phenotype. The TLR4 gene is found on chromosome 9, a region containing a CD susceptibility gene [228]. Two main single nucleotide polymorphisms (SNPs) of TLR4 have been observed, namely the co-segregating, missense mutations Asp299Gly and Thr399Ile, with the Asp299Gly mutation resulting in a hypo-responsive phenotype to LPS [229]. Indeed, another report has shown that C3H/HeJ mice strain which have a single point

mutation in TLR4, were more susceptible to developing DSS induced colitis [198]. In addition, studies in knockout mice have demonstrated that TLR4 and TLR2, as well as their common adaptor MyD88 have a protective role in DSS induced colitis, with the homeostatic function of epithelial barrier repair proving particularly important [50,207,213]. This protective function of TLRs is mainly mediated by the epithelial compartment, with ligand binding initiating downstream signalling pathways for repair.

1.7.5. miRNA in IBD

Due to their role as important modulators of a vast array of cellular processes, miRNA have been implicated in the development of disease, with a dysregulated expression of miRNA been associated with disease states including IBD [230]. Several studies have examined the expression of different miRNAs in both UC and CD, showing dysregulation in a number of miRNAs which in term regulate the expression of coding mRNAs implicated in IBD. For instance, miR-106b negatively regulates the autophagy gene ATG16L1, a known IBD linked gene, is upregulated in IBD [231,232]. Given that PRRs and modulators of innate and adaptive immunity (such as cytokines) are shown to be important in maintaining intestinal homeostasis, and that their dysregulation can be linked to IBD, it stands to reason that modulators of their expression and function like miRNAs might also play a role in the disease. Indeed miR-155 has been suggested as a target for antagonistic therapy in IBD as it has many immunomodulatory functions including targeting suppressor of cytokine signalling 1 (SOCS-1) and is upregulated in IBD [233,234]. However, one of the most consistent miRNA alterations observed in these studies is elevated miR-21 expression in IBD (both CD and UC) and IBD-associated colorectal cancer, which arises due to the excessive inflammatory present in the colon [140,233]. MiR-21 regulates many different cellular processes as discussed previously, and given that there are so many delicately balanced processes occurring in IBD it understandable that its dysregulation would be problematic. Given that miR-21 regulates TLR signalling it is interesting to speculate whether this aspect plays a role in IBD, and whether miR-21 has a role in sensing the microbiota and/or GI tract pathogens in this context. In addition, while the role of miR-21 in modulating TLR responses to bacterial ligands such as LPS has been well

studied in vitro, work investigating its role in infection with live bacteria, in particular using *in vivo* models is lacking. Elucidating these functions may help to shed light on miR-21's role in inflammation and inflammatory diseases such as IBD.

1.8. Aims

The overall aim of this project is to examine the effect of miR-21 expression in animal models of IBD and infection.

The specific aims are as follows:

I. Using transgenic mice deficient in miR-21, characterise the role of miR-21 in experimental models of IBD.
    a. Is miR-21 expression beneficial or pathological?
    b. What are the mechanisms by which miR-21 acts in this disease?
    c. Does miR-21 expression impact on the intestinal microbiome in its capacity as a negative regulator of TLR function?

II. Characterise the role of miR-21 in negative regulation of TLR signalling *in vivo*.
    a. How does miR-21 expression affect primary cells and their responses to infection with live bacteria?
    b. Do miR-21$^{-/-}$ mice respond differently to infection and if so why?

A greater understanding of miR-21's role in the inflammatory reponse to infection and in the maintainance of intestinal homeostatis will provide new insights into the pathogenesis of inflammatory disease and elucidate the potential to target miR-21 as a therapeutic strategy for the treatment of these diseases.

Chapter 2
-
Materials and Methods

2. Materials and Methods

2.1. Materials

2.1.1. Buffers

Table 2.1 Buffer compositions

Buffer Name	Buffer Composition
PBS (10X)	1.45M NaCl, 39mM NaH_2PO_4, 22.7 mM Na_2HPO_4
MPO Buffer 1 (pH 4.7)*	NaCl 0.1M – 5.84g/L, Na_3PO_4 0.02M – 3.12g/L, Na_2EDTA 0.015M – 5.58g/L
MPO Buffer 2 (pH 5.4)*	Na_3PO_4 0.05M – 7,8 g/L Hexadecyltrimethylammonium bromide (HTAB) 0.5% - 5 g/L (add after pH is 5.4)
MPO Red blood cell lysis solutions	NaCl 0.2% - 2 g/L NaCl 1.6% + Glucose 5% - 16 g/L of NaCl and 50 g/L of Glucose
MPO Substrate solution	3.845 mg of 3,3',5,5'-Tetramethylbenzidine per mL of Dimethyl sulfoxide (protect from light).
Hydrogen peroxide (for MPO assay)	0.0002% in MPO buffer 2.
ELISA wash buffer	0.05% Tween 20 in PBS, pH 7.2–7.4
Radioimmunoprecipitation assay (RIPA) buffer (2X)	NaCL 300mM, 2% NP40, 1% sodium deoxycholate, 0.2% sodium dodecyl sulfate, 100mM Tris (pH 8). Inhibitors added immediately prior to use: 1mM Na3VO4, mM PMSF, µg/ml Leupeptin, apoprotinin 1:200.
Sample Lysis buffer (5X)	10% (w/v) glycerol, 2% (w/v) sodium dodecyl sulfate (SDS), 200µg/ml bromophenol blue, 215mM Tris pH 6.8. 50µl DTT is added per 1ml 5X sample buffer immediately prior to use.
SDS–PAGE running buffer (10X)	30.3g 25mM Tris, 144g 192mM glycine, 10g 0.1%SDS. Made up to 1L with dH_2O.
SDS–PAGE transfer buffer	0.25M Trizma base, 1.9M Glycine, 35mM SDS.
Tris-buffered saline (TBS) Tween (TBST) 10X	12.11g Tris, 87.6g NaCl, 10ml Tween 20. Made up in 1L dH_2O.

* to reach the correct pH a solution of NaH_2PO_4 was used

2.1.2. Animals

Animals were maintained under specific pathogen-free or germ-free conditions in line with Irish, Israeli and European Union regulations. Experiments were subject to ethical approval by the Animal Research Ethics Committee (AREC), a Level 2 ethics committee responsible for reviewing the proposed use of animals in teaching and research at Trinity College Dublin (TCD), and were carried out in accordance with the recommendations of the Irish Health Products Regulatory Authority, the competent authority responsible for the implementation of Directive 2010/63/EU on the protection of animals used for scientific purposes in accordance with the requirements of the S.I No 543 of 2012. MiR-21 deficient mice were generated by Taconic Artemis using a Cre/lox approach. Briefly, miR21 was modified by the insertion of two loxP sites that enable excision of the floxed miR21 segment through Cre-mediated recombination. Chimeric offspring were backcrossed to C57BL/6 for a total of 8 generations. Homozygous deletion confirmed by PCR genotyping. The mice were bred and maintained in TCD. Mice were maintained as WT or miR-21$^{-/-}$ homozygous pairs for breeding purposes. Germ-Free mice were used in the Weizmann Institute of Sciene, Rehovot Israel and were either C57BL/6 or Swiss-Webster. For *in vivo* experiments, male and female animals between 8 and 12 weeks of age were used. For primary cell culture, male and female animals between 8 and 20 weeks were used.

2.1.3. Cell culture media

DMEM and RPMI were obtained from Gibco Biosciences (Dun Laoghaire, Ireland). Fetal calf serum (FCS) was from Biosera. Penicillin and streptomycin (P/S) were from Sigma (Arklow, Ireland).

2.1.4. Cell lines

L929 cells were obtained from Sigma (Arklow, Ireland). RAW264.7 cells were obtained from the European Collection of Animal Cell Cultures (ECACC).

2.1.5. Bacterial strains

Salmonella enterica subsp Typhimurium UK-1 (*S.* Typhimurium UK-1), *Citrobacter rodentium* ICC180 and *Listeria monocytogenes* EDG-e and EGDeΔLLO were provided by Dr Sinéad Corr.

2.1.6. General laboratory chemicals

All general laboratory chemicals were obtained from Sigma (Ireland and UK) and Thermo Fisher Scientific (Ireland).

2.1.7. TLR ligands

LPS for *in vitro* experiments (ultrapure rough, from *E. Coli* serotype EH100) was purchased from Alexis (Ireland). Pam3Csk4 was obtained from Calbiochem (UK). Poly (I:C) was obtained from Invivogen (Dun Laoghaire, Ireland).

2.1.8. ELISA reagents

Mouse IL-6, IL-10, IL-12p70 and TNF-α ELISA Duoset kits, as well as TMB substrate solution were obtained from R&D systems (UK). Tween-20, Bovine Serum Albumin (BSA) were purchased from Sigma (Ireland).

2.1.9. RNA extraction and PCR reagents

RNaseZap, RNase-free H_20 and RNeasy Plus Mini Kits were from Qiagen (Dun Laoghaire, Ireland). PCR fast plates, 10X RT buffer, dNTPs, RNase inhibitor, Multiscribe reverse transcriptase and 2X Fast PCR buffer were obtained from Applied Biosystems (Dun Laoghaire, Ireland). TRIzol reagent was obtained from Thermo Fisher Scientific (Ireland). Probes for miR-21 and RNU6B were obtained from Applied Biosystems (Dun Laoghaire, Ireland). SYBR Green real time qPCR reagents were purchased from Kapa Biosystems (UK), and primers for SYBR qPCR were generated by MWG Eurofins (Wolverhampton, UK).

Table 2.2 Primer sequences for SYBR qPCR (mouse genes)

Primer pair	Forward (5'-3')	Reverse (5'-3')
MARCKS	CTCCTCCTTGTCGGCGGCCGG	GGCCACGTAAAAGTGAACGGC
RhoB	GACGGCAAGCAGGTGGAG	ATGGGCACATTGGGGCAG
Cdc42	CGACCGCTAAGTTATCCACAG	AGGGCAGAGCACTCCACA
Rps13	GGCCCACAAGCTCTTTCCTT	GACCTTCTTTTTCCCGCAGC
YM-1	TGTGGAGAAAGACATTCCAAG	AAGAGACTGAGACAGTTCAGGG
IL-12p40	GACCATCACTGTCAAAGAGTTTCTAGAT	AGGAAAGTCTTGTTTTTGAAATTTTTTA
TNF-α	GCCTCTTCTCATTCCTGCTT	TGGGAACTTCTCATCCCTTTG
Arg1	GATTATCGGAGCGCCTTTCT	TGGTCTCTCACGTCATACTCT
NOS2	CCAAGCCCTCACCTACTTCC	CTCTGAGGGCTGACACAAGG
MRC	GGCGAGCATCAAGAGTAAAGA	CATAGGTCAGTCCCAACCAAA

2.1.10. Western blotting reagents

Ammonium persulphate (APS), N, N, N', N' Tetramethylethylenediamine (TEMED), sodium dodecyl sulphate (SDS), Tris-HCL and acrylamide:bisacrylamide were all purchased from Sigma (Ireland). WesternBright ECL HRP substrate was from Advansta (Ireland). Polyvinylidene diflouride (PVDF) membranes were from Immobilon, a Millipore company (via ThermoFisherScientific, Ireland). BCA protein quantification kits were obtained from Thermo Fisher Scientific (Ireland).

2.1.11. Antibodies

Endosomal maturation marker antibodies were obtained from Cell Signalling (Dublin, Ireland). Anti-RhoB antibodies (sc-180) were purchased from Santa Cruz (USA). Anti-MARCKS antibodies (ab51100) were obtained from Abcam (Dublin, Ireland). Anti-β-actin Clone AC-74 was purchased from Sigma (Arklow, Ireland). Secondary HRP-conjugated antibodies (anti-mouse IgG, anti-goat IgG, anti-rabbit IgG) were purchased from Jackson ImmunoResearch Inc (US). Alexa Flour 488 confocal

microscopy secondary antibodies were obtained from Invitrogen (Dun Laoghaire, Ireland).

2.1.12. Flow cytometry reagents

CellROX and Aqua Live/Dead stains were obtained from Molecular probes (Dun Laoghaire, Ireland). FITC-dextran particles (Mr 3-5kDa) were obtained from Sigma (Ireland).

2.1.13. Greiss Reaction and LDH assay reagents

Greiss reactions and LDH assays were performed using kits obtained from Promega (via MyBio, Ireland).

2.1.14. Experimental colitis reagents and materials

Dextran sulphate sodium (DSS) was obtained from MP Biomedicals (France) and Fisher (now Thermo Fisher Scientific, Ireland). Hemocult occult blood detection kits were purchased from Sarstedt (Ireland).

2.1.15. Histology and Alcian blue staining reagents

Histoclear, EtOH, acetic acid, Alcian Blue, Nuclear Fast Red, Hemotoxylin and eosin were obtained form Sigma (Ireland). Cytoseal and paraffin wax was obtained from Leica (Ireland).

2.1.16. Bacterial culture and enumeration reagents

Luria broth (LB) and Brain-Heart infusion (BHI) broth and agar were obtained from Sigma (Ireland). Nalidixic acid was obtained from Sigma (Ireland). *Listeria* strains were cultured in BHI broth and plated onto BHI agar. *Salmonella* and *Citrobacter* were cultured in LB broth and plated onto LB agar.

2.1.17. MPO reagents

NaCl, Na_3PO_4, Na_2EDTA, Na_2HPO_4, Na_3PO_4, NaCl, Glucose, 3,3',5,5'-Tetramethylbenzidine and Hydrogen peroxide were purchased from Sigma (Arklow, Ireland).

2.1.18. MiSeq 16S sequencing

DNA extraction kits were purchased from MOBIO (UK). Kapa Hifi hot-start PCR reagent was purchased from Kapa Biosystems (UK). V3/V4 primer sets were custom made for the Eran Elinav lab in the Weizmann Institute of Science. Agencourt AMPure magnetic beads were obtained from Beckman Coulter (Israel). Wizard® SV Gel and PCR Clean-Up system was purchased from Promega (Israel). Reagents used with the Illumina MiSeq 16S sequencing platform were purchased from Illumina (USA).

2.1.19. Miscellaneous reagents

Cytochalasin D was obtained from Sigma (Ireland).

2.2. Methods

2.2.1. Cell culture

2.2.1.1. L929 culture

L929 cells were cultured in RPMI medium containing 10% fetal calf serum (FCS) and 1% penicillin/streptomycin (P/S) and maintained in standard cell culture conditions (humidified 37°C atmosphere with 5% CO_2). Cells were seeded in T175 flasks at $5x10^5$ for 7 days before subculturing. On day 7, the media was removed and filter sterilized before being stored at -20°C for subsequent use in bone marrow cell culture. Cells were then washed with warm PBS before being incubated in Trypsin-EDTA for ~10 mins to remove them from the base of the flask. The cells in Trypsin EDTA were removed from the flask and added to falcon tubes containing cell culture media. Cells were centrifuged for 5 mins at 1500 rpm. The cell pellet was resuspended, counted and seeded in 40mls media/T175 flask.

2.2.1.2. RAW 264.7 culture

Cells were maintained in DMEM supplemented with 10% FCS and P/S. When cells reached confluency they were washed with warm PBS before being incubated in Trypsin-EDTA for ~10 mins to remove them from the base of the flask. The cells in Trypsin EDTA were removed from the flask and added to falcon tubes containing cell culture media. Cells were centrifuged for 5 mins at 1500 rpm to form a pellet. This pellet was resuspended and cells were counted and plated for experiments or split 1/6 and reseeded in T175 flasks.

2.2.1.3. Bone marrow isolation and bone marrow-derived macrophage (BMDM) culture

WT and miR-$21^{-/-}$ mice were euthanized using CO_2 and cervical dislocation. The mice and all instruments were sprayed with 70% EtOH prior to dissection in a laminar flow hood. An incision was made in the middle of the abdomen and the skin was pulled back over the hindlegs. The knee joint was gradually hyperextended

repeatedly to break it, before the top of the femur was held and the lower limb pulled down in order to remove the muscle from around it. The clean femur was then cut just below the hip joint and placed into ice-cold DMEM containing 1% P/S. The foot was then removed from the tibia above the ankle joint, and the latter is placed in the ice-cold DMEM. The bones were then flushed through using DMEM, and the flow through collected in a 50ml falcon tube. The suspension was centrifuged at 1500 rpm for 5 mins. The cell pellet was then resuspended in 3ml red-blood cell lysis buffer for precisely 3 minutes before neutralization by the addition of 3ml DMEM to the tube. The suspension was centrifuged at 1500 rpm for 3 mins and the resulting cell pellet reuspended in 30 ml DMEM containing 20% M-CSF containing L929 media, 10% FCS and 1% P/S. The suspension was evenly split between three non-cell culture coated 10cm dishes (10mls/dish) and the cells were incubated in standard cell culture conditions for 6 days. On day 3, an additional 1ml of L929 was added to each dish. On day 6, cells were scraped, resuspended and counted in order to be plated for experiments in DMEM containing 10% L929, 10% FCS and 1% P/S.

2.2.1.4. Bone marrow-derived dendritic cell (BMDC) culture

Bone marrow was flushed and subjected to red-blood cell lysis as described in section 2.2.1.2. The cells were then counted and seeded in T175 flasks at $5x10^5$ cells/ml (25mls/flask) in DMEM containing 20ng/ml GM-CSF, 10% FCS and 1% P/S. On day 3, cells were fed by the addition of 15mls DMEM containing 20ng/ml GM-CSF, 10% FCS and 1% P/S. On day 6, the loosely adherent cells in the flasks were removed by gentle agitation and repeat pipetting, and counted before being reseeded in T175 flasks at a concentration of $1x10^6$ (35 mls/flask) in DMEM containing 20ng/ml GM-CSF, 10% FCS and 1% P/S. On day 8, cells were fed by addition of 15ml DMEM containing 20ng/ml GM-CSF, 10% FCS and 1% P/S. On day 10, the loosely adherent cells in the flasks were removed by gentle agitation and repeat pipetting. The cells were then resuspended and plated for experiments in DMEM containing 10ng/ml GM-CSF, 10% FCS and 1% P/S.

2.2.2. Enzyme-linked immunosorbant assay (ELISA)

Post-treatment, supernatants were removed from cell culture wells and the cytokine levels present were measured using either Duoset or BD ELISA kits according to the manufacturer's instructions. Optical density was measured using a 96 well plate reader at 450nm and concentrations were determined using a standard curve.

2.2.3. RNA analysis

2.2.3.1. RNA extraction

Cell monolayers were lysed in 350µl of RLT buffer and colon samples were lysed in RNA lysis buffers provided with RNA extraction kits using the TissueLyserII system (Qiagen). Qiagen RNeasy Plus mini kits or Purelink RNA mini kits were used to extract RNA from both cell monolayers and colon samples using a slightly modified version of the manufacturer's instructions (Qiagen or Thermo Fisher Scientific). Briefly, in order to extract microRNAs as well as longer RNAs from the preparations, 500µl of 100% EtOH was used in place of 350µl in the initial precipitation step and the RW-1 wash buffer step was replaced by a second RPE step (for Purelink kits this corresponds to replacing buffer 1 with a second wash of buffer 2). Alternatively, Trizol RNA extraction was performed to extract RNA from samples from the mouse gastrointestinal tract. Up to 1g of tissue was lysed in 1ml TRIzol using the TissuelyserII system. The samples were incubated for 5 min at RT before the addition of 200µl chloroform per tube. The tubes were vigorously shaken for 30s before being incubated at 2-3 min at RT. The tubes were then centrifuged at 12,000 g in a 4°C centrifuge for 15 min. The aqueous phase was then transferred to fresh tubes (~500µl/1ml TRIzol). 1µl Glycoblue was added to each tube and the tubes agitated to mix. 500µl isopropanol was added to each tube, tubes were agitated to mix before being incubated for a minimum of 1 h at -80°C. Without being thawed, the samples were centrifuged at 12,000 g in a 4°C centrifuge for 20 min. The supernatant was then removed from the tube leaving a small pellet at the base of the tube. The pellet was then washed twice by adding 1ml of ice-cold 75% EtOH and centrifuging at 7400 g in a 4°C for 5 min. The EtOH was completely removed and the samples were left to air dry for 10-30 min. The pellet was resuspended in 15-30µl of nuclease-free water and the samples were quantified for cDNA generation or frozen indefinitely at -80°C.

These two methods were also combined, beginning the TRIzol extraction and taking the aqueous phase separated after the chloroform step and placing it in an equal volume of ethanol before placing it on a column from the aforementioned RNA extraction kits. After extraction, RNA concentrations were measured using a Nanodrop 2000 UV visible spectrophotometer and equalized to various concentrations. Equalized RNA was then used for reverse transcription PCR or frozen at -80°C for later use.

2.2.3.2. Reverse transcription-polymerase chain reaction

cDNA was generated by reverse transcription-polymerase chain reaction (RT-PCR) of isolated RNA using a high capacity cDNA reverse transcription kit. 10µl of RNA was added to 10µl of reaction mix as listed in Table 2.3. For microRNA cDNA, an altered reaction mix was used as listed in Table 2.4. The latter reaction mix is scaled down as it uses a reduced volume of 5X miRNA primer/reaction.

Table 2.3 General cDNA reaction mix

Component	Volume (µl)
10X RT buffer	2
10X random primers	2
100mM deoxyribonucleotide triphosphates (dNTPs)	1
RNase inhibitors	0.5
Multiscribe reverse transcriptase enzyme	1
Nuclease-free water	3.5
RNA (30-100ng/µl)	10

Table 2.4 miRNA cDNA reaction mix

Component	Volume (µl)
dNTP	0.125
10X Buffer	1.5
RNase inh	0.18

RT enzyme	0.5
Primer (5X)	0.375 per microRNA target
Nuclease-free water	Make up to 12
RNA (10ng/μl)	3

The following parameters were used for the general cDNA RT-PCR run:

Table 2.5 RT-PCR protocol for general cDNA

Temperature	**Duration (min)**
25°C	10
37°C	120
85°C	15
4°C	hold

The following parameters were used to generate microRNA-specific RT-PCR run:

Table 2.6 RT-PCR protocol for miRNA-specific cDNA

Temperature	Duration (min)
16°C	30
42°C	30
85°C	5
4°C	hold

2.2.3.3. Real-time quantitative PCR

Real time quantitative PCR (qPCR) was performed on cDNA using Taqman probes specific for mouse miR-21 and RNU6B (or U6 SNO). The reaction mix for each sample was as below, and similar to Table 2.4 it is a scaled down reaction as it uses a reduced volume of 20X miRNA probe/reaction:

Table 2.7 Taqman qPCR reaction mix

Component	Volume (µl)
2X Fast master mix	5
Taqman probe	0.33
Nuclease-free water	3.67
cDNA	1

qPCR was performed on cDNA using SYBR Green reagents and primer sets using the following reaction mix:

Table 2.8 SYBR qPCR reaction mix

Component	Volume (µl)
Kapa SYBR mix	5
Primer pair mix (10µM)	0.2
Nuclease-free water	3.8
cDNA	1

2.2.4. Western Blotting

2.2.4.1. SDS lysis for total protein

Media was removed from cell monolayers after treatment and 70µl SDS sample lysis buffer containing DTT (50µl DTT/1 ml sample buffer) was added to the well. The lysates were removed to microfuge tubes and boiled at 95°C for 5 mins. Protein samples were frozen at -20°C. Alternatively, tissues were homogenized in RIPA buffer containing protease inhibitors and the resulting supernatant was quantified and normalized using a BCA kit.

2.2.4.2. SDS polyacrylimide gel electrophoresis (SDS-PAGE)

Protein samples were resolved by loading on to an SDS-PAGE gel composed of an initial 5% stacking gel and a 12% resolving gel. Gel compositions are shown in Table 2.9. Gels were run at a constant current of 25mA per gel. Pre-stained molecular weight standards were also run on the gel to allow determination of the sizes of proteins in the experimental samples.

Table 2.9 PAGE composition for protein seperation

Component	5% stacking gel	12% Resolving gel
Protogel	1 ml	6 ml
dH_2O	4.1 ml	4.9 ml
Tris pH 8.6	–	3.8 ml
Tris pH 6.8	0.75 ml	–
10% SDS	60µl	150µl
10% (APS)	60µl	150µl
TEMED	6µl	6µl

2.2.4.3. Electrophoretic transfer of proteins of membranes

Once resolved, proteins were transferred to PVDF membranes using wet transfer apparatus. The membrane was activated with 100% methanol (MeOH). All the other components of the wet transfer apparatus were soaked in transfer buffer before assembly in the following order, from cathode to anode: sponges, 2 layers filter paper, activated PVDF membrane, gel, 2 layers of filter paper, sponge. Air bubbles were then removed from the sandwich by rolling with a cylinder. The sandwich was placed in the transfer cassette. This cassette was then placed in the transfer tank along with transfer buffer and a glycol cooling pack. Proteins were transferred at 200mA for 2h or at 30 mA overnight.

2.2.4.4. Antibody incubation and visualization

After transfer, the PVDF membrane was removed and blocked with 5% (w/v) milk powder in TBST for 1h at RT to block non-specific binding of proteins to the membranes. The membrane was then incubated in primary antibody diluted in 5 ml 5% milk according to the manufacturer's instruction for 1h at RT or overnight at 4°C. The membrane was then washed three times in TBST for 5 minutes per wash. The membrane was then incubated in HRP-conjugated secondary antibody corresponding to the species of primary antibody used diluted 1:2000 in 5% milk for 1h at RT. Finally, the membrane was washed again 3 times in TBST as before. The

chemiluminescent substrate was then prepared as advised by the manufacturer and added to the surface of the membrane. The protein bands present were visualized using a BioRad GelDoc.
MARCKS and RhoB antibodies were diluted in 3% BSA in TBST instead of milk, and blocked in 3% BSA in TBST instead of milk.

Densitometry was performed using BioRad ImageLab software.

2.2.5. Nitric oxide measurement

To estimate nitric oxide release, the nitrate present in the supernatants was measured using a Griess reaction. Cell monolayers were cultured overnight in 1ml media/500,000 cells. Before treatment, the media was removed and replaced with 500µl media. After treatment, the supernatants were immediately removed and 50µl were placed in a 96 well plate. The reaction was then carried out according to the manufacturer's instructions. Briefly, 50µl sulfanilamide solution was added to each standard (standards were made using cell culture media as a diluent) and incubating for 5-10 min at room temperature protected from light. After this incubation, 50µl N-1-napthylethylenediamine dihydrochloride (NED) solution was added to each well and incubated for a further 5-10 min protected from light. Optical density was then read using a plate reader between 520 and 550nm and the nitrate present in each sample was quantified using the standard curve.

2.2.6. LDH assay

LDH release in response to various treatments was measured in accordance with the manufacturer's instructions. Briefly, 45 min before the end of the treatment 10X lysis solution was added to a control well to act as maximum LDH release marker. At the end of the treatment, 50µl of media from each well was placed in a 96 well plate. This was followed by the addition of 50µl CytoTox 96® reagent and 30 min incubation protected from light. At the end of this incubation the reaction was stopped by the addition of 50µl stop solution to each well. Absorbance was then measured in a plate reader using a filter at 90nm.

2.2.7. Myeloperoxidase (MPO) assay

Colon samples were weighed and homogenised in 1.9ml of buffer 1 per 100mg tissue using the TissueLyserII system (90s at 25Hz). The samples were then centrifuged at 10,000 g for 10 min at 4°C. The supernatants were collected and stored at -20°C for later use. Red blood cell lysis was performed by adding 0.2% w/v NaCl to the samples for 30s before adding 1.6% NaCl+5% glucose w/v in equal volumes (1.5ml per 100mg tissue). The tubes were shaken for 30s at 25Hz the TissueLyserII system and the resulting homogenate was centrifuged at 10,000 g for 10 min at 4°C. The supernatants were discarded and a fresh homogenate was made in buffer 2 using the TissueLyserII system for 30s at 25Hz. After this point samples could be frozen at -20°C and the protocol resumed later. The samples were then freeze/thawed in liquid nitrogen three times before being centrifuged 10,000 g for 15 min at 4°C. The supernatants were collected and diluted 1:3 before being added in duplicate to a 96 well plate (25µl/well). An equal volume of TMB substrate solution was added and the plate incubated in the dark for 5 min. The hydrogen peroxide solution was prepared and added to the plate (100µl per well) before incubation in the dark for 5 min. The reaction was stopped by the addition of 100µl of sulfuric acid 1M to each well. Optical density was measured at 450nm using a plate reader.

2.2.8. Confocal microscopy

Cells were seeded at $5x10^5$/ml in 6 well plates containing sterile coverslips and maintained overnight at 37°C and 5% CO_2. Following treatment, cells were fixed in 3% paraformaldehyde at RT for 10 min. The cells were then washed twice in PBS (15 min per wash) before being permeabilized in 0.15% Triton X-100 in PBS for 15 min at RT. Cells were then blocked in 2% BSA (in PBS) for 30 min at room temperature before being probed with EEA1 primary antibody diluted at 1:100 in 2% BSA for 1h at RT. Cells were then washed three times in PBS/2%BSA/0.15% TritonX-100 before being probed with fluorochrome-coupled secondary antibody diluted at 1:1000 for 45 min at RT in the dark. Cells were then washed 3 times in PBS/2%BSA/0.15% TritonX-100 to remove non-specifically bound antibody. The

cells were then mounted on coverslips using "antifade" reagent containing Hoescht stain and imaged using a Leica SP8 scanning confocal micrscope.

2.2.9. Bacterial infections and LPS-induced sepsis.

2.2.9.1. Bacterial culture and storage

S. Typhimurium UK-1, *C. rodentium* ICC180 and *L. monocytogenes* EDGe were cultured from glycerol stocks and then maintained on agar plates. In a laminar flow hood, 100µl of thawed glycerol stock was added to a 15 ml falcon tube containing 10 ml of LB broth for *Salmonella*, 10 mls of LB broth containing nalidixic acid (50µg/ml) or BHI broth for *Listeria*. 100µl of the culture was spread in a T-streak to separate pure colonies which could be grown overnight at 37°C (LB agar plates for *Citrobacter rodentium* infection containted nalidixic acid at a concetration of 50µg/ml). A single colony was taken and placed in a 15ml falcon tube containing 10ml broth. The falcon tube was then placed in a bacterial shaker and grown overnight at 37°C. For bacterial enumeration, the optical density at 600nm (OD600) value of the culture was measured using a spectrophotometer and 10-fold serial dilutions of the culture were made in sterile PBS. These dilutions were then spread out on appropriate nutrient agar plate, 100µl dilution per plate, and left to incubate at 37°C overnight. The following day, the colonies were formed and used to calculate colony-forming units (CFU) per ml of culture. The bacteria were then spun down at 4000pm for 10 min and resupsended in 1 ml of sterile PBS. The bacterial suspension could then be diluted to an appropriate concentration for subsequent infection. To generate glycerol stocks, 500µl of neat bacterial culture was mixed with 500µl of sterile glycerol and the bacteria were frozen at -80°C.

2.2.9.2. *In vitro* infection with *Salmonella* and *Listeria*

Cells were plated at $5x10^5$ cells/ml in media containing 10% FCS and P/S. The following day, the cells were washed in PBS and the media replaced with media containing 10% FCS but without antibiotics. Bacteria were added at desired multiplicity of infection. After 15 min, the media was removed and replaced with

media containing gentamicin (100μg/ml) to kill extracellular bacteria. After various timepoints, the media was removed, the cells were washed three times with sterile PBS and the monolayers were lysed in 100μl ice-cold sterile H_2O. The lysate was then serially diluted and the dilutions plated on to nutrient agar plates using a spot plate technique (20μl per quarter plate) and incubated overnight. The following day CFUs were counted and converted to Log CFU/ml.

2.2.9.3. *In vivo* infection with *Salmonella* and *Listeria*

Mice were infected either via oral inoculation (oral gavage) or via intraperitoneal infection. For oral gavage, the food was removed from the mice the evening before the inoculation. The following morning, the mice were inoculated with $5x10^7$ CFU of *Salmonella* or *Listeria* in 100-200μl PBS. Six days post-infection, the mice were euthanized with CO_2 and cervical dislocation. Their blood was harvested by terminal bleed, and the liver and spleen were removed and kept on ice in 12-well tissue culture plates. Half the spleen was snap frozen in liquid nitrogen for RNA analysis and stored at -80°C. The remaining spleen and liver were homogenized in 5ml PBS using stomacher bags. The homogenate was then serially diluted ten-fold in PBS and 100μl of each dilution was plated on to appropriate nutrient agar plates. The plates were incubated overnight, and the following morning the CFUs were counted and converted into Log CFU/organ. For intraperitoneal infection, the mice were injected with $1x10^6$ bacteria in 100-200μl of PBS and the organs and blood were harvested in the same manner as for oral gavage three days post-infection.

2.2.9.4. LPS-induced sepsis *in vivo*

Mice were given a sub-lethal dose of 15mg/kg LPS via intraperitoneal injection (100-200μl). After 4 or 24 hours the mice were euthanized with CO_2 and cervical dislocation. Their blood was harvested by terminal bleed and serum obtained by centrifuging for at 4°C for 10 mins at 14,000 g.

2.2.10. Experimental models of colitis

2.2.10.1. DSS-induced colitis

Dextran sodium sulphate (DSS) was prepared to the appropriate concentration (w/v) in dH_2O. Mice aged between 8 and 12 weeks were weighed and administered DSS *ad libitum* on day 0. Over the course of the model, the mice were weighed daily and their stool was measured for consistency and occult blood using Hemocult kits according to the manufacturers' instructions. The scoring system is included in Table 2.10.

Table 2.10 Scoring for DSS colitis

Score	Weight loss	Occult blood	Stool consistency
0	None	No blood – negative	Well-formed pellets
1	1-3%	Trace blood – positive	Changed form (soft)
2	3-6%	Moderate reaction – positive	Loose stool (wet)
3	6-9%	Bleeding (Visible by eye)	Diarrhea/No stool
4	>10%	Gross anal bleeding	

The scores were combined and averaged to generate a Disease Activity Index score (DAI). At the end of the study, the mice were euthanized by CO_2 and cervical dislocation. The serum was taken by terminal bleed and the colon removed. The colon's length was measured before it was divided into sections and stored for subsequent analysis. Proximal and distal sections were placed in 10% formalin and then moved to 70% EtOH for histology analysis. Other sections were snap frozen in liquid nitrogen and stored at -80°C for MPO, protein and RNA analysis.

2.2.10.2. *C. rodentium* induced colitis

C. rodentium ICC180 was grown overnight in 10 ml LB medium at 37°C with nalidixic acid at 50 μg/ml, centrifuged at 3,000g for 10 min, and resuspended in 10 ml of sterile phosphate-buffered saline (PBS) for oral gavage. Each mouse received

200µl (approximately $5x10^9$ bacteria) of the bacterial suspension. Post-gavage, the remainder of the suspension was plated in serial dilutions for retrospective enumeration. For bacterial enumeration in stool samples collected at different time points, serial dilutions of a fecal-PBS suspension (ranging from undiluted to 10^{-7} dilution) were plated on supplemented LB agar by a spot plate technique and incubated overnight at 37°C. Mice were then were monitored for changes in body weight and clinical signs of disease as in Table 2.10

2.2.10.3. Tissue preparation for histology

Distal colon sections were fixed in 10% formalin for 24h before being placed in 70% EtOH for storage. The sections were then dehydrated by being placed in a gradient of solutions with increasing EtOH concentrations before being embedded upright in paraffin wax and left to set on a cooling block overnight. Once set, 5μm transverse sections were cut using an upright microtome and mounted on poly-D-lysine coated microscopy slides. Once air dried, the slides were then further dried overnight in an incubator set at 37°C. The slides were then either stored in this dried state or prepared for staining by removing the surrounding paraffin wax with xylene.

2.2.10.4. Hemotoxylin and Eosin (H&E) staining

Prepared histology slides were stained using the following protocol:

Reagent	**Time**
Xylene	30s x2 (sections dipped in and out)
Ascending Dehydration EtOH gradient (100%, 90%, 70%)	1 min per solution
dH_2O	1 min wash (sections dipped in and out)
Hemotoxylin	5 min
Eosin	30s
dH_2O	1 min wash (sections dipped in and out)
Ascending Dehydration EtOH gradient (70%, 90%, 100%)	1 min per solution

The stained sections were then finished by the addition of a coverslip attached with Cytoseal (Leica) and left to dry overnight. Sections were imaged using an Olympus BX51 upright microscope.

2.2.10.5. Alcian blue staining

Pre-prepared histology slides were stained to detect mucus by treatment using the following protocol:

Reagent	**Time**
Xylene	30s x2 (sections dipped in and out)
3% Acetic Acid	3 min
1% Alcian Blue in 3% acetic acid	30 min
dH_2O	1 min wash (sections dipped in and out)
0.1% Nuclear Fast Red counterstain	5 min
dH_2O	1 min wash (sections dipped in and out)
Ascending Dehydration EtOH gradient (70%, 80%, 90%)	1 min per solution

The stained sections were then finished by the addition of a coverslip attached with Cytoseal (Leica) and left to dry overnight. Sections were imaged using an Olympus BX51 upright microscope.

2.2.10.6. Quantification of mucus area

Mucus area was determined using images of Alcin blue stained colon sections captured using an Olympus BX51 upright microscope magnified 200X. Open access ImageJ software was employed, specifically using the *Threshold_Colour* plugin to convert images to a 24-bit (RGB) format before selecting out areas stained in blue. These sections were converted into an image mask and the mask area was quantified as a percentage of the whole image. 10 frames were quantified per section. This methods was employed to quantify mucus area as performed by Biton *et al* [235].

2.2.10.7. Pathological scoring of histology samples

H&E stained sections of distal colon were blind scored to ascertain the extent of colitis using a previously established protocol [236]. A combined score of inflammatory cell infiltration and tissue damage was determined as follows: cell infiltration: score 0, occasional inflammatory cells in the lamina propria (LP); 1, increased infiltrate in the LP predominantly at the base of crypts; 2, confluence of inflammatory infiltrate extending into the mucosa; 3, transmural extension of infiltrate. Tissue damage: score 0, no mucosal damage; 1, partial (up to 50%) loss of crypts in large areas; 2, partial to total (50–100%) loss of crypts in large areas, epithelium intact; 3, total loss of crypts in large areas and epithelium lost.

2.2.10.8. Colonoscopy

On day 13 of the induction of experimental colitis, mice were taken and anesthetized by injection of a ketamine/xylazine mixture. Colonoscopy was performed using the Mainz COLOVIEW® system and the video recorded. The extent of colitis was assessed by blind scoring (performed by Christoph Thaiss, Weizmann Insitute of Science) according to a number of parameters presented in Table 2.11.

Table 2.11 Scoring for colonoscopy

	Stool	**Translucency**	**Vascularity**	**Granularity**	**Fibrin deposition**
0	Normal+solid	Transparent	Normal	None	None
1	Still shaped	Moderate	Moderate	Moderate	Little
2	Unshaped	Marked	Marked	Marked	Marked
3	Spread	Intransparent	Bleeding	Extreme	Extreme

2.2.10.9. Co-housing experiments

Mice were co-housed to assess the impact of the microbiota on disease. For these experiments, 4-week old wild-type and miR-21$^{-/-}$ mice were mixed for a minimum of 4 weeks before being used in disease models.

2.2.10.10. Antibiotic treatment of mice

Mice were put on an *ad libitum* antibiotic treatment course for two weeks. The course of treatment consisted of vancomycin (0.5 g/l), ampicillin (1 g/l), kanamycin (1 g/l), and metronidazole (1 g/l) in their drinking water.

Recolonization of germ-free mice

A suspension for recolonization of germ free (GF) mice was made by homogenizing frozen feces from wild-type or miR-21$^{-/-}$ mice in sterile PBS in anaerobic conditions so as to preserve and anaerobic bacterial colonies present in the fecal samples. Each suspension was prepared to contain 20mg feces per 100µl innoculum. The appropriate weight of fecal material was added to the PBS in 2ml microcentrifuge tubes and shaken using the Tissue LyserII system. The contents were then filtered through a sterile 70µm strainer to remove soil particles. Each mouse was then administered with 100µl by oral gavage and allowed to rest for 9 days to ensure recolonization. DSS colitis studies were then performed on day 10.

2.2.11. 16S sequencing

2.2.11.1. Faecal DNA extraction

Mouse faeces was collected in 1.5ml epindorf tubes and snap frozen in liquid nitrogen before being stored at -80°C for subsequent DNA extraction. The samples were thawed and DNA extraction performed using MOBIO PowerLyser DNA extraction kit according to the manufacturers' instructions.

2.2.11.2. V3/V4 DNA amplification

16S DNA was amplified on the V3/V4 region using custom primer sets. The forward primer was common to each sample, and the reverse primer was unique to each sample (the latter primers contain individual barcodes for subsequent identification after sequencing) . The reaction mix was prepared as presented in Table 2.12, and each sample reaction mixture was placed in a well of a 96-well PCR plate. The reaction was run in a thermocycler and the conditions used are presented in Table 2.13, and the product is presented in Figure 2.1.

Table 2.12 V3/V4 PCR reaction mix

Component	Volume (µl)
Forward primer (common)	1
Reverse primer (unique)	1
Kapa HIFI Hotstart	12.5
Nuclease-free water	8.5
DNA	2

Table 2.13 V3/V4 PCR reaction protocol

Temperature	Time	Repetition
95°C	5 min	1
98°C 60°C 72°C	20s 30s 1 min	16
98°C 52°C 72°C	20s 30s 1 min	19
72°C	10 min	1
4°C	∞	Hold

2.2.11.3. PCR cleanup

PCR cleanup was performed using the AMPure beads in the 96-well format as described by the manufacturers. Briefly, 45µl of AMPure bead were added to each well containing PCR products (25µl) and titurated to mix. The 96-well plate was then placed on a magnetic plate to separate the magnetic beads. The supernatants were then removed, and the beads washed twice with 200µl EtOH. The plate was then removed from the magnet and the beads were mixed with 40µl elution buffer (Tris-HCL) before being placed on the magnet again for 1 min. 38µl of the eluted DNA is removed to a fresh plate.

2.2.11.4. Library Preparation

The concentration of each DNA sample was assessed using the Nanodrop spectrophotometer. The library was generated by pooling 100ng of DNA from each sample. The whole volume of the library was then run in multiple wells of an agarose gel with loading dye, and the bands were subsequently cut out and the DNA extracted using the Wizard® SV Gel and PCR Clean-Up system (Promega). The concentration of the double stranded DNA present in the library was measured using the Qubit fluorometric dye system. Briefly, 198µl buffer, 1µl dsDNA stain and 1µl DNA were combined in a microcentrifuge tube and the concentration was measured (ideally the concentration would fall between 5-25ng/µl). The library quality was then assessed using the Aligent Tape station system. The desired peak is expected to appear between 450 and 500nm.

2.2.11.5. Sequencing

The library was sequenced using the Illumina MiSeq system according to the manufacturers' protocol. Briefly, the cartridge and HT-1 buffer were thawed in water at RT and on ice respectively. The DNA must be prepared for loading at a concentration of 4nM. The concentration of the library is assessed using the following formula:

Qubit concentration x 1000 / 0.649 x Tape Station peak size

The DNA was diluted in 10mM Tris-HCL as required. The DNA was then denatured from double stranded form to single stranded by diluting 1:1 with 0.2M NaOH (5µl:5µl) and incubating at RT for 5 min. The DNA was then diluted with HT-1 buffer 1:100. This dilution was further diluted 1:3 with HT-1 buffer and spiked with 15% PhiX. The instrument set up was then completed as instructed and 600µl of the final library product was loaded for sequencing. A brief overview of the library design and the sequencing procedure is presented in Figure 2.1.

2.2.11.6. Analysis (performed by Raul Cabrera-Bello, UCC)

Sequences were obtained from the MiSeq filtered on the basis of quality (removal of low quality nucleotides at the 3' end, and remove windows 20 nt with a low average quality) and length (removal of sequences with less than 200nt) with prinseq and joined using fastq-join (https://code.google.com/archive/p/ea-utils/). The sequences were clustered with 97% identity level (calculated at the operational taxonomic unit; OTUs) using closed-reference *usearc*h v7.0 to assign the cluster sequences the RDP's Classifier [237-239]. α and β-diversity were determined using QIIME [240].

2.2.11.7. Statistical analysis

P-values were calculated using GraphPad Prism software. Student's *t*-tests, Chi-squared tests and one-way ANOVA tests were used as appropriate. 16S sequencing data were statistically analyzed using Adonis for beta-diversity analysis. Statistical differences between multiple samples were estimated by Kruskal-Wallis and False discovery rate (FDR, qvalue) control based on the Benjamini-Hochberg procedure was used to correct for multiple testing with the R statistical package (https://www.r-project.org/).

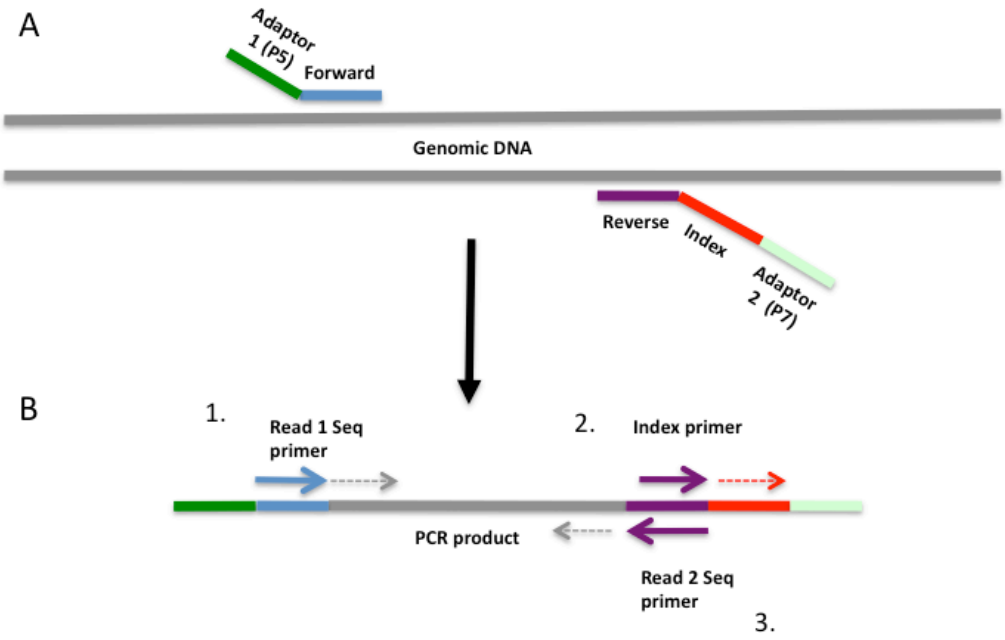

Figure 2.1 16S sequencing of fecal DNA

A) PCR reactions are set up with common forward primers amplify DNA at the V3/V4 16S region and anneal an adaptor to to the end of the synthesized fragment (Adaptor 1 or P5). Each sample reaction uses an individual reverse primer which attaches an index or "barcode" to the region of interest, as well as a second adaptor (Adaptor 2 or P7). B) The PCR product generated is then loaded on the sequencing flow cell, where the adaptors anneal to complimentary oligos on the surface, and undergo cycles of bridge amplification. 1. To begin sequencing, the product is cut at the the P5 adaptor so that remaining fragments are attached at the P7 end and all sequencing occurs in the same direction. Read 1 sequencing primers are introduced to sequence the region of interest (grey arrow). 2. The product is then washed off and the index primers are added to sequence this section to identify the sample later in the analysis (red arrow). 3. The product is washed away once again and the template undergoes bridge amplification once more before being cut at the P7 end. Read 2 primers are then introduced to sequence from the opposite end of the template.

Chapter 3
-
miR-21 in DSS colitis

3. miR-21 in DSS colitis

3.1. Introduction

IBD are multi-factorial disorders which are becoming increasingly prevalent in the 21st century [178,182,241]. It is widely recognised that the innate immune system plays a key role in the development of the disease, and several of the licensed therapies for IBD target mediators of the innate and adaptive immune system such as pro-inflammatory cytokines in particular TNF-α. Recently miRNA have been shown to play a critical role in the regulation of innate immune responses to various inflammatory stimuli, and as a result have been implicated in inflammatory disease. Indeed, several miRNA have been linked to IBD, with their expression either negatively or positively correlating with active disease [230]. As these regulators can be detected in the colonic tissue and the serum they are increasingly being used as diagnostic markers of inflammatory diseases including IBD [230]. However, the role that these miRNAs play in IBD is still very unclear. Of interest to this project, miR-21 is one such miRNA, associated with an elevated expression in ulcerative colitis[133]. miR-21 has been shown to regulate several innate immune responses, enhancing signalling to produce the anti-inflammatory cytokine IL-10 in response to TLR4 sensing of bacterial LPS and promoting inflammation resolution by enhancing the clearance of apoptotic bodies by efferocytosis [129,165] However it has yet to be established whether miR-21 is an anti-inflammatory agent that is overexpressed in an attempt to resolve inflammation in a chronic disease, or whether it is playing a pathological role. Indeed the mechanism underlying its increased expression in IBD and the consequence of this oveexpression has yet to be determined. Thus, the aim of this chapter is to explore the role of miR-21 in IBD by employing the dextran sodium sulfate (DSS)-induced colitis model in a miR-21 knockout mice.

3.2. Investigation into the role of miR-21 in Inflammatory Bowel Disease

3.2.1. Generation of miR-21$^{-/-}$ mice

In order to investigate the role of miR-21 in various contexts, miR-21$^{-/-}$ mice were generated in 2009 by Taconic Artemis using a homologous recombination targeting vector (Fig. 3.1) by prior to the beginning of this project. Briefly, a targeting allele was designed by members of the O' Neill lab in TCD with several important features: a negative selection thymidine kinase (*tk)* gene which induces sensitivity to the drugs gancyclovir or FIAU, a positive selection puromycin resistance cassette flanked by F3 nuclease sites and LoxP3 sites flanking the miR-21 coding sequence. The *tk* gene is placed outside the arms of homology in order that it will be lost during a homologous recombination event and the clone will be resistant to drug selection. However, in a random insertion event the *tk* gene will be incorporated, rendering the clone drug sensitive and allowing for negative selection. The puromycin resistance cassette then allows for positive drug-based selection. This resistance cassette was later removed using the site specific recombinase flippase (FLP) to excise the region at the F3 nuclease sites. ES cells containing the conditional knockout allele were then inserted into the blastocyst and mice containing the allele were recovered and crossed to mice expressing Cre recombinase to knockout the miR-21 gene by excising the region between the Lox P3 sites. Chimeric offspring were backcrossed onto the C57BL/6J background for a total of 8 generations. Homozygous deletion of miR-21 was confirmed by PCR genotyping. Homozygous WT and miR-21$^{-/-}$ breeding pairs were maintained and were used to generate mice for animal studies. The mice were housed in the Comparative Medicine unit in TCD, where they were maintained and genotyped regularly.

3.2.2. Optimization of the DSS colitis model

In order to evaluate the involvement of murine miR-21 in the regulation of intestinal inflammation *in vivo*, the acute dextran sodium sulfate (DSS)-induced colitis mouse model was employed. The DSS model is one of the most widely used mouse models of chemically induced colitis, which mimics symptoms of human ulcerative colitis. Oral administration of DSS in drinking water results in disruption of the murine intestinal epithelial barrier, exposing cells of the lamina propria to commensal bacteria and their products resulting in extensive inflammation [242]. Due to its simplicity and reproducibility this mouse model has been extensively used in many studies involving innate immune regulators such as PRRs and cytokines.

We first began optimisation of this model in our mice, as it is known that there are numerous factors which can affect and influence induction and severity of the DSS colitis in mice including DSS concentration, molecular weight, duration of exposure, manufacturer or intestinal microflora of the animals [242-245]. Based on the preceding reports pertaining to the preferred DSS vendor and optimal *in vivo* concentration to ensure for successful induction of colitis in mice, DSS was incorporated with different molecular weights from two different suppliers; Fisher Scientific [now Thermo Fisher Scientific], Mw = 500 kDa and MP Biomedicals with a range of Mw between 36 – 50 kDa).

In all trials, colitis was induced in age- and sex-matched WT and miR-21$^{-/-}$ mice. Mice were weighed at the start of the trial. Mice were checked daily for morbidity and body weight was recorded. The Disease Activity Index (DAI) was calculated daily for each mouse based upon pathological features (diarrhoea, rectal bleeding, weight loss). The method is described in section 2.2.10.

3.2.2.1. Induction of colitis with 2.5% (w/v) DSS (Fisher Scientific, 50kDa)

The first experiment was conducted using 2.5% (w/v) DSS from Fisher Scientific. The mice were given the DSS in their drinking water *ad libitum* for 5 days before being switched to conventional drinking water for 3 days (Fig. 3.2). Control mice

were given normal drinking water. In this first model, administration of DSS resulted in little weight loss in WT mice and some in the miR-21$^{-/-}$ mice, with the latter losing ~10% and the WT group losing none relative to their initial weight (Fig. 3.2A). There was virtually no occult blood detectable in either group during the experiment, with a mild amount present on day 8 (Fig. 3.2B). Similarly, the diarrhea scores were low in both groups, peaking briefly on day 7 but low overall (Fig. 3.2C). The DAI was reflective of the low scores, with the WT group DAI score on day 8 not reaching 1 and the miR-21$^{-/-}$ being appearing slightly higher due to the difference in weight loss (Fig. 3.2D). The colons were removed at the end of the experiment and measured, with a short and swollen colon being indicative of disease. There was no difference between the lengths of the colons between WT and miR-21$^{-/-}$ mice, and both groups had long colons indicating little inflammation (Fig. 3.2E). Taken together, these data suggested that the dose of 2.5% DSS (Fisher) was too low to effectively induce colitis in the mice and that this required further optimization. At this concentration the solution was quite viscous which posed a number of problems, including cost effective sterile filtration, which may impact on the consistency of future experiments. Given that a higher concentration was likely to exacerbate this issue further, it was decided to trial the 36 - 50 kDa molecular weight obtained from MP Biomedicals for this reason.

3.2.2.2. Induction of colitis with 1.5% (w/v) DSS (MP Biomedicals, 36-50 kDa)

Upon consultation of the literature, an initial dose of 1.5% was chosen and the mice were given this solution for 5 days before being switched to conventional drinking water for 3 days (Fig. 3.3). There was substantial variability in the weight lost by WT mice, whilst miR-21$^{-/-}$ mice lost approximately 18% ± standard error of the mean (SEM) by the end of the experiment (Fig. 3.3A). There was also little detectable fecal occult blood detected until the end of the experiment whereupon the mice reached levels approaching the maximum for this parameter (Fig. 3.3B, days 7 and 8), and this increase was broadly similar between the two groups. The mice in both groups displayed an increased tendency towards diarrhea-like stool as reflected in the increased stool score across the days measured, all contributing to an increase in DAI score in the latter days of the experiment (Fig. 3.3C and D). As another indicator of disease induction, the colon lengths of both groups were very short relative to

previously observed healthyl colons and there was no difference between the groups (Fig. 3.3E). Overall these data indicated that the dose used was sufficient to induce disease, and that there might be a difference between the groups as indicated by the difference in weight loss. However, there were several issues that needed addressing. The first of these was that the mice appeared to suffer few symptoms early in the experiment but they rapidly reach maximum scores in the various parameters towards the end of the experiment which may have caused difficulty in observing any significant changes between the groups.

3.2.2.3. Induction of colitis with 2.5% (w/v) DSS (MP Biomedicals, 36-50 kDa)

We next attempted to induce colitis using a dose of 2.5% (w/v) DSS, which was administered to mice *ad libitum* for 5 days. It was apparent that colitis was being induced compared to water controls, and furthermore, a significant difference in phenotype emerged between WT and miR-21$^{-/-}$. Specifically, there were observed differences in weight loss (days 3 and 4), diarrhea and most strikingly in fecal occult blood (Fig. 3.4A-C) between WT and miR-21$^{-/-}$ mice, with miR-21$^{-/-}$ mice exhibiting reduced weight loss, reduced diarrheal scores and reduced bleeding, indicative of a protective effect against DSS-induced colitis following loss of miR-21. The protection exhibited by mice lacking miR-21 was also clear when presented as a DAI score (Fig. 3.4D). In addition, WT mice suffered more severe colon shortening when compared to their miR-21$^{-/-}$ counterparts (Fig. 3.4E). Levels of myeloperoxidase (MPO) were also measured in the colon as a measure of neutrophil activation, and this was also lower in the miR-21$^{-/-}$ though not to a statistically significant degree (Fig. 3.4F).

Having found an optimal dose of DSS for inducing colitis, we next confirmed that miR-21 is induced in this model as it is in human IBD [133]. miR-21 levels were compared between WT mice given water or a course of DSS and indeed miR-21 expression was markedly higher in the colonic tissue of WT mice administered DSS (Fig. 3.5) indicating that our model was representative of the disease and relevant for its study.

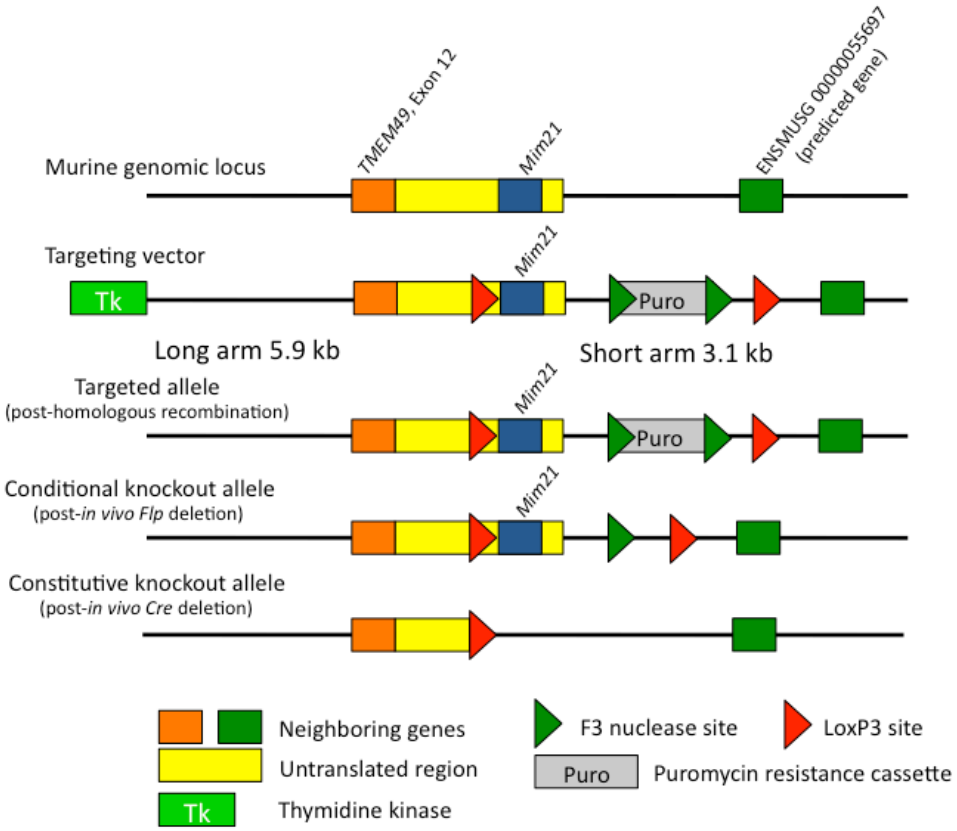

Figure 3.1 Generation of miR-21$^{-/-}$ mice

The murine miR-21 coding sequence (situated at the 3' of exon 12 of Tmem49 gene) was targeted for deletion by homologous recombination. Targeted alleles were selected for using a puromycin resistance cassette, later removed using F3 nuclease sites. Following the implantation of recombinant ES cells and recovery of mice carrying the conditional allele, the mice were crossed to transgenic whole body expressing Cre mice to generate full-body miR-21 knockout mice (miR-21$^{-/-}$) via the loxP sites flanking the miR-21 coding sequence. Wild-type (WT) controls were generated by uncrossing the mice.

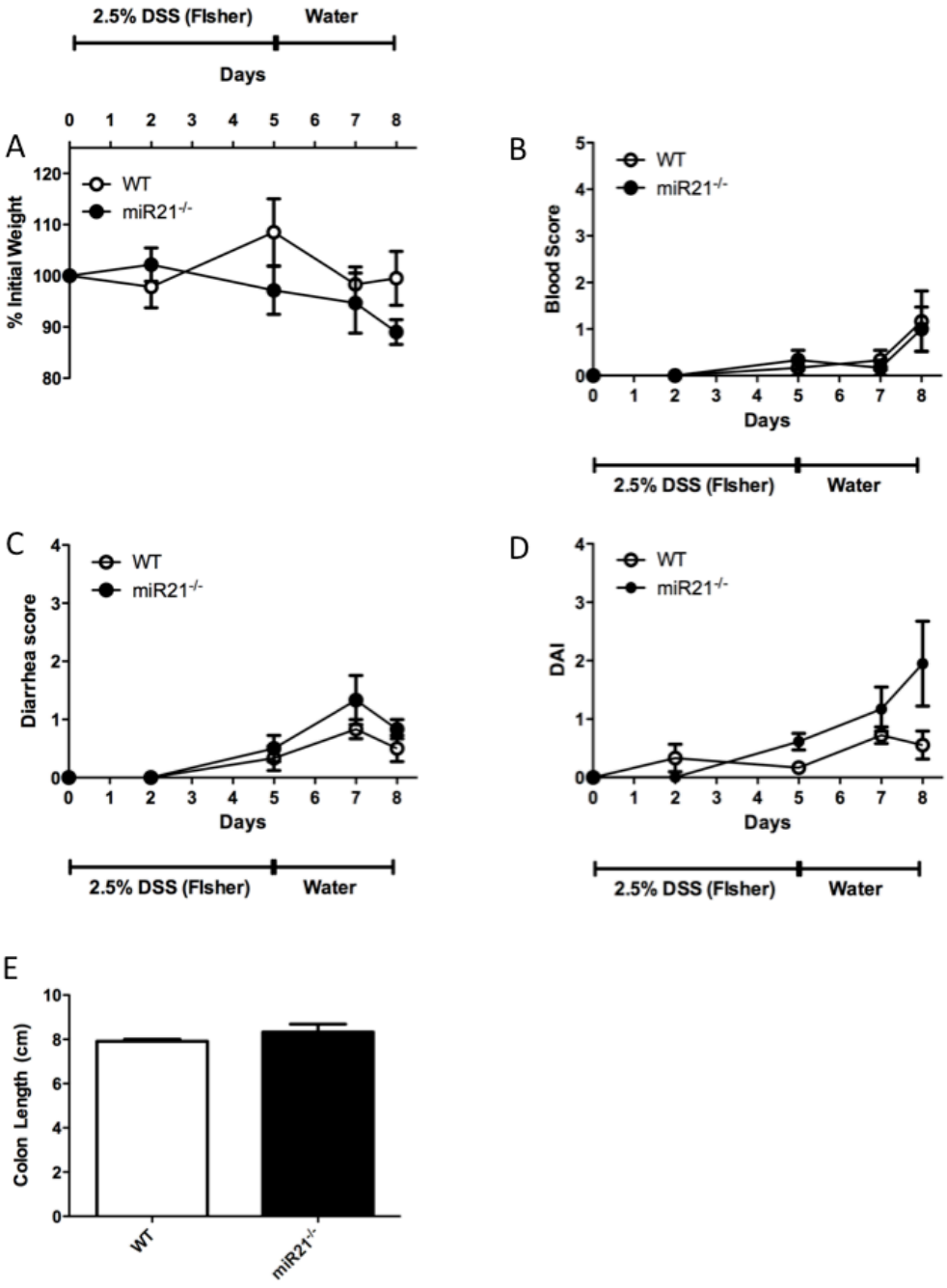

Figure 3.2 Optimization of DSS induced colitis in WT versus miR-21$^{-/-}$ mice: 2.5% DSS (Fisher)

Wild-type (WT) and miR-21$^{-/-}$ mice aged between 8 and 12 weeks were weighed on day 0 and given 2.5% DSS (Fisher) a*d libitum* for 5 days. On day 5 the DSS was replaced by normal drinking water for 3 days. Their weight (A), fecal occult blood (B) and stool consistency (C) were measured daily throughout the experiment and combined to generate a disease activity index score (DAI) [D]. The mice were sacrificed on day 8 and their colons were removed and measured (E) before being treated and stored for subsequent analysis. Data represent mean values ± SEM of n= ≥ 3 mice per group.

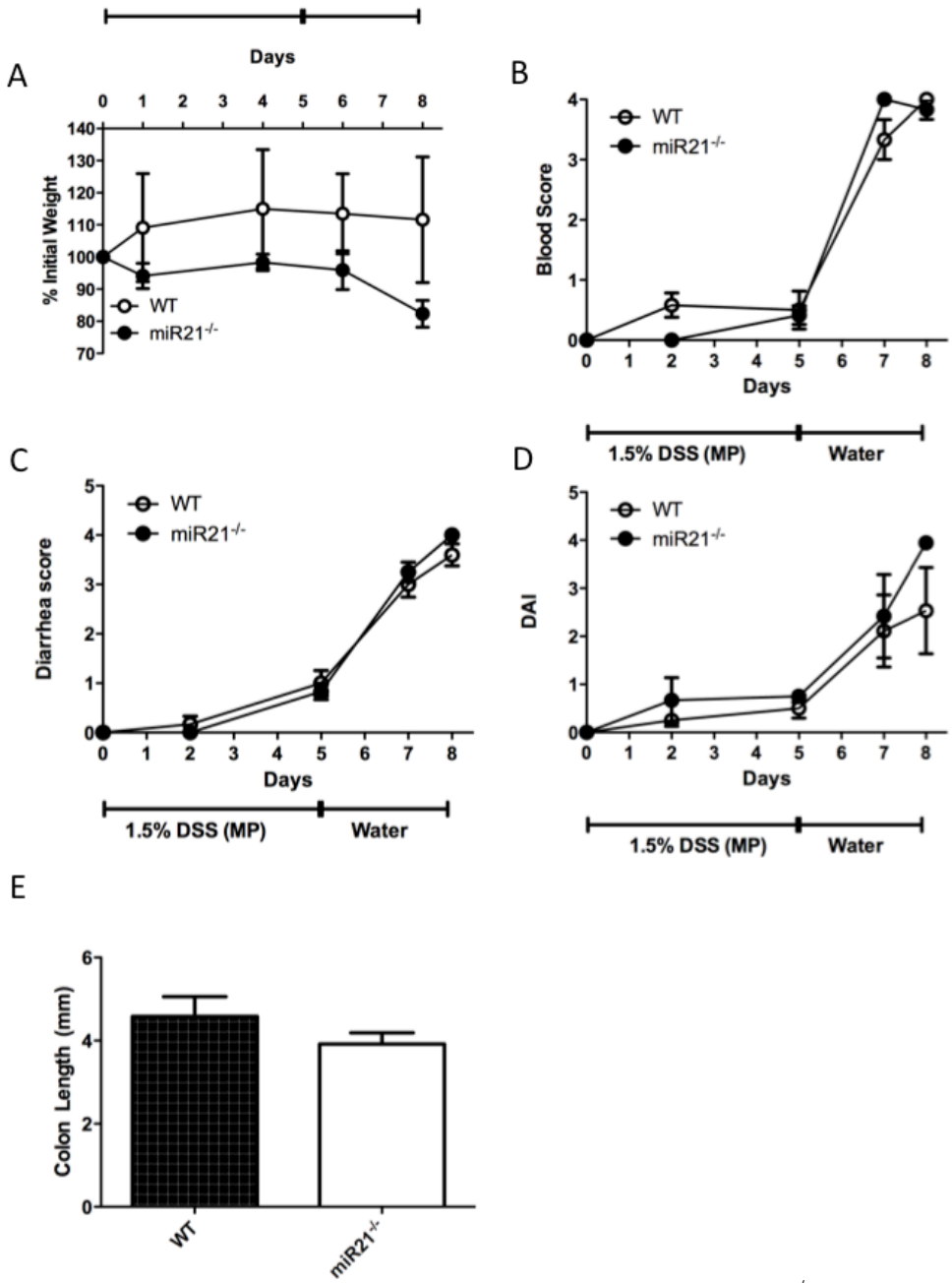

Figure 3.3 Optimization of DSS induced colitis in WT versus miR-21$^{-/-}$ mice: 1.5% DSS (MP Biomedicals)

Wild-type (WT) and miR-21$^{-/-}$ mice aged between 8 and 12 weeks were weighed on day 0 and given 1.5% DSS (MP Biomedicals) a*d libitum* for 5 days. On day 5 the DSS was replaced by normal drinking water for 3 days. Their weight (A), fecal occult blood (B) and stool consistency (C) were measured daily throughout the experiment and combined to generate a disease activity index score (DAI) [D]. The mice were sacrificed on day 8 and their colons were removed and measured (E) before being treated and stored for subsequent analysis. Data represent mean values ± SEM of n= ≥ 3 mice per group.

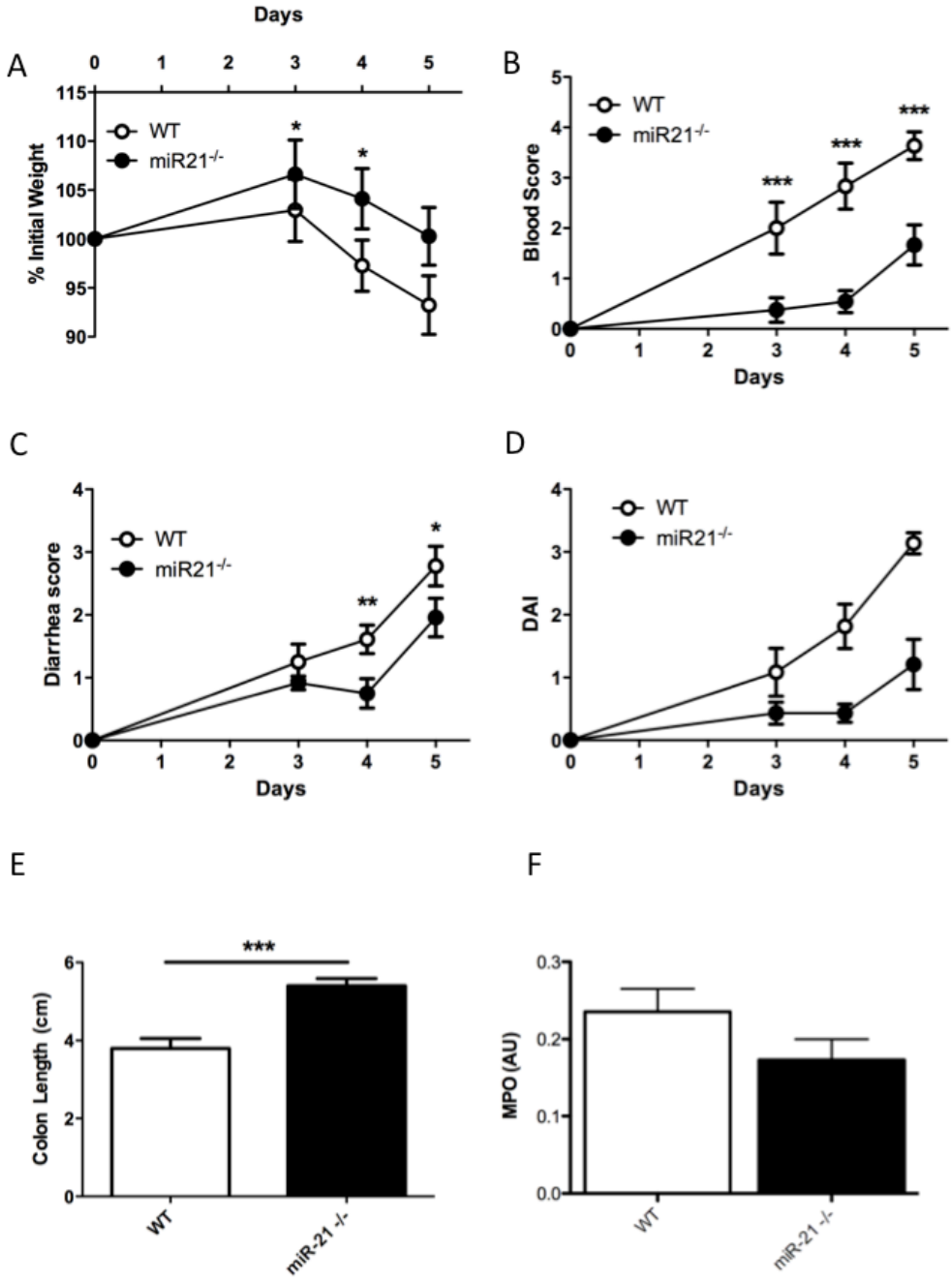

Figure 3.4 miR-21$^{-/-}$ mice are protected in DSS colitis – Optimization of DSS induced colitis in WT versus miR-21$^{-/-}$ mice: 2.5% DSS (MP Biomedicals)

Wild-type (WT) and miR-21$^{-/-}$ mice aged between 8 and 12 weeks were weighed on day 0 and given 2.5% DSS (MP Biomedicals) a*d libitum* for 5 days. Their weight (A), fecal occult blood (B) and stool consistency (C) were measured daily throughout the experiment and combined to generate a disease activity index score (DAI) [D]. The mice were sacrificed on day 5 and their colons were removed and measured (E) before being treated and stored for subsequent analysis. Levels of myelperoxidase (MPO) in equalised colon segments were also measured *F). Data represent mean values ± SEM pooled from two experiments of n= ≥5 mice per group. P values were calculated for A-E using Student's T-test , * p<0.05, ** p< 0.01, ***p< 0.001.

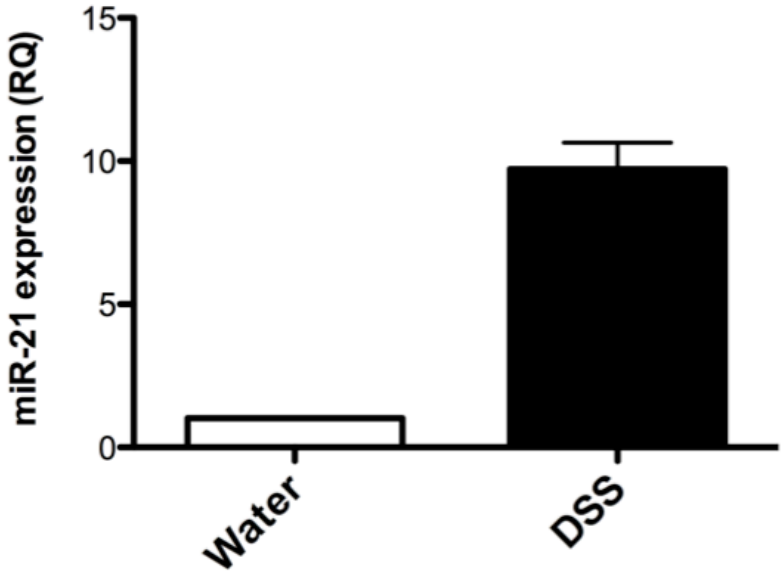

Figure 3.5 miR-21 expression is induced in the colon following DSS administration

C57Bl/6 mice aged between 8 and 12 weeks were given either water or 2.5% DSS (MP Biomediacls) a*d libitum* for 7 days. At the end of the 7 days, the mice were sacrificed and the colons harvested for subsequent analysis. RNA was extracted and used to generate cDNA, and miR-21 expression was assessed by qPCR. Data expressed as mean values ± SD or relative quantification (RQ) relative to water controls. Water group n=2, DSS group n=4.

3.2.3. miR-21$^{-/-}$ mice are protected from DSS-induced colitis

Having observed a protective effect for miR-21$^{-/-}$ mice in an acute model of colitis (2.5% x 5 days) we next assessed the susceptibility of mice in a DSS recovery model. In this model, water is reintroduced to ascertain if the phenotype remained or changed over a longer period of time and with sufficient recovery time. Specifically, mice were given 2.5% w/v DSS (MP Biomedicals) for 5 days before being switched to conventional drinking water for a further 5 days. Water only controls were also included (Fig. 3.6). Overall, a similar protective phenotype was observed in miR21$^{-/-}$ mice, albeit with a different rate of progression. WT mice fed DSS again lost more weight than their miR-21$^{-/-}$ counterpart, though it was not until day 6 that this occurred in a statistically significant manner (Fig. 3.6A, days 6, 7, 8 and 9). The same was apparent in the diarrhea scores of the two groups, with significant differences being observed from day 6 onwards. However WT mice exhibited more exacerbated fecal occult blood from as early as day 3 as observed in previous experiments (Fig. 3.6B and C). In all parameters, both WT and miR-21$^{-/-}$ mice began to recover once DSS was replaced with water. This was apparent at different days for each parameter, with both groups of mice continuing to lose weight until day 7 but beginning to recover towards baseline blood and diarrhea scores immediately. These differences were reflected in the combined DAI score (Fig. 3.6D), but not in the colon lengths as the colons of the miR-21$^{-/-}$ were not significantly longer than those of the WTs. However, they were also not significantly shorter than their water control in contrast to the WT group, indicating that the WT mice did indeed suffer more severe colitis in this model (Fig. 3.6E).

The DSS-induced colitis model is regarded as a useful model for studying IBD partly because of the histopathological changes it induces which resemble those of the human disease [244]. The inflammation induced causes significant infiltration of immune cells and destruction of healthy crypt architecture. In order to assess whether the protected phenotype observed in miR-21$^{-/-}$ mice was also reflected histopathologically, sections were taken from the distal colons of WT and miR-21$^{-/-}$ mice given DSS or regular drinking water and stained with hematoxlyin and eosin. The sections were blind scored to generate a combined histology score (Fig. 3.7A)

comprised of combined crypt damage scores and inflammation scores (Fig. 3.7B and C), revealing significantly less histopathological damage in the miR-21$^{-/-}$ colon sections. Representative images show normal crypt architecture in both WT and miR-21$^{-/-}$ control mice, and a marked influx of inflammatory cells with corresponding crypt loss in the WT mice treated with DSS. The miR-21$^{-/-}$ mice also display a degree of crypt loss and inflammatory cell infiltration foci, but it is markedly less than that of the WT (Fig. 3.7D). As miR-21 has been reported to influence the expression of different pro- and anti- inflammatory cytokines, colon homogenates were assessed for their expression. Surprisingly, miR-21$^{-/-}$ displayed a cytokine profile which would indicate higher inflammation than that of the WT mice (Fig. 3.8). The levels of the anti-inflammatory cytokine IL-10 were significantly reduced in the miR-21$^{-/-}$ relative to the WT (Fig. 3.8A), and there was no difference in the levels of the pro-inflammatory cytokine IL-6 (Fig. 3.8B).

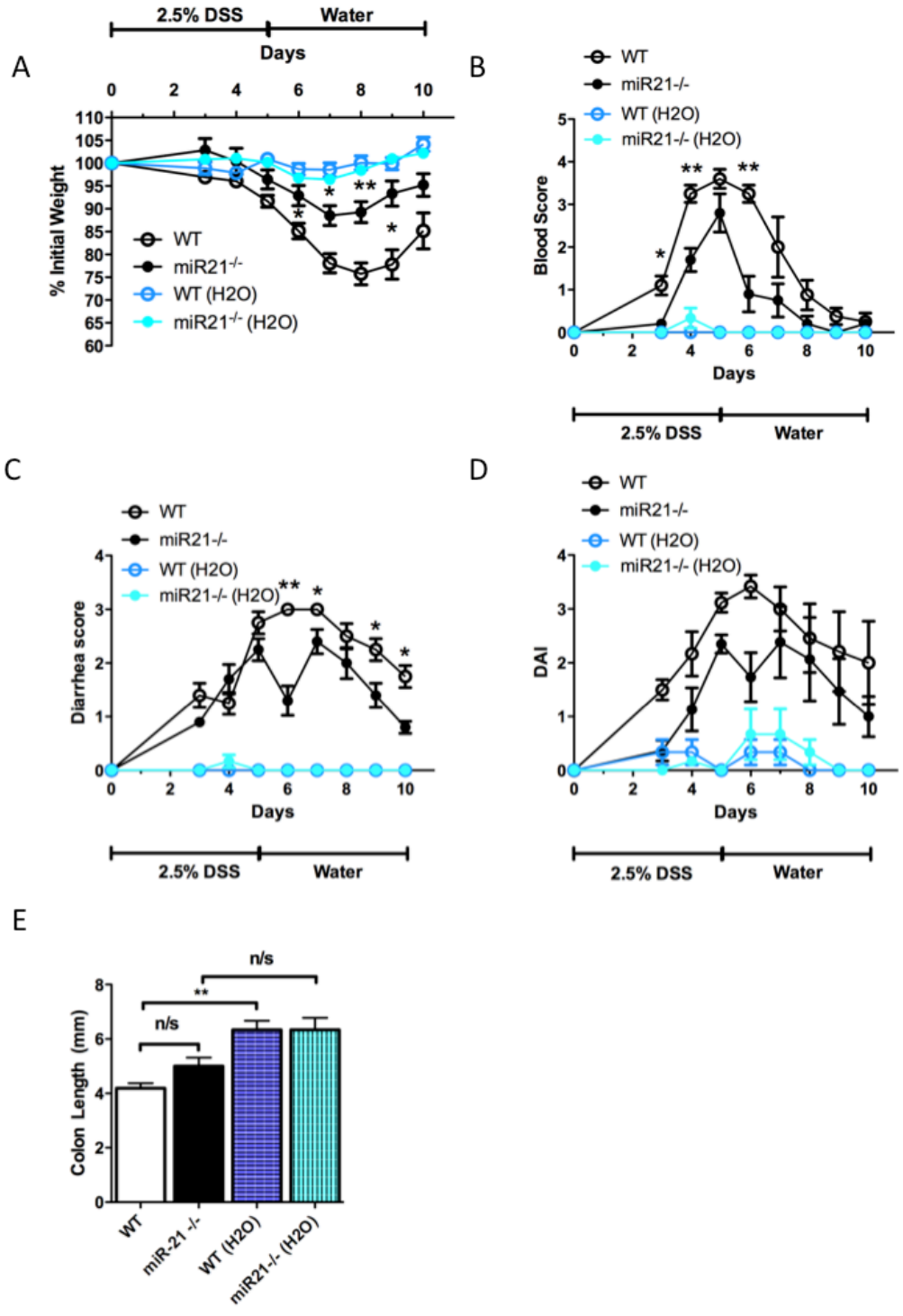

Figure 3.6 MiR-21 deficient mice are protected compared to wild-type mice in an extended DSS colitis model.

Wild-type (WT) and miR-21$^{-/-}$ mice aged between 8 and 12 weeks were weighed on day 0 and given 2.5% DSS a*d libitum* for 5 days before being switched to normal drinking water. Control mice were given conventional drinking water throughout. Their weight (A), occult blood (B) and stool consistency (C) were measured daily throughout the experiment and combined to generate a disease activity index score (D). On day 10, the mice were sacrificed and their colons were removed and measured (E) before being stored for subsequent analysis. Data represent mean values ± SEM pooled of n= ≥5 mice per group. P values were calculated for A-E using Student's T-test , * $p<0.05$, ** $p< 0.01$.

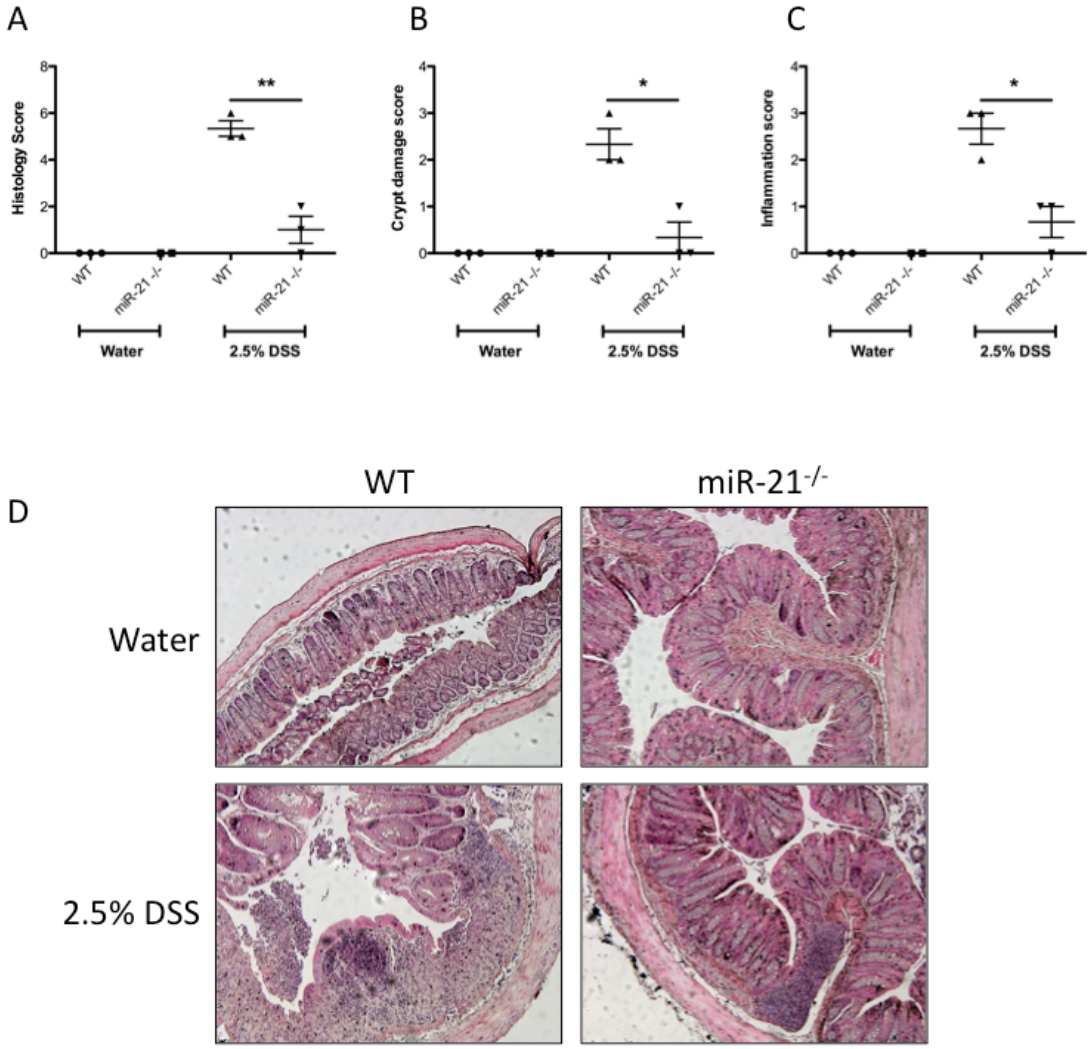

Figure 3.7 Histological comparison of WT and miR-21$^{-/-}$ mice post colitis

Distal colons of of wild-type (WT) and miR-21$^{-/-}$ mice treated for 5 days with 2.5% DSS a*d libitum* , followed by 5 days with regular drinking water and control group (water only) were harvested and analyzed using hematoxylin and eosin (H&E) staining. Colitis severity of H&E stained colonic tissues was assessed by: (A) combined histological score of (B) tissue disruption (crypt damage score; 0–3, according to the severity of mucosal and crypts damages) and (C) colon cellular infiltration (inflammation score; 0–3, according to the extent of inflammation throughout the intestinal wall). (D) Representative microscopic pictures of (H&E) stained colon sections of water and 2.5% DSS treated of WT and miR-21$^{-/-}$ mice on the last day of the experiment (100x magnification). Data represent mean values ± SEM of n= ≥3 mice per group (n=2 in the miR-21$^{-/-}$ water control group) . P values were calculated for A-C using Student's T-test , * $p<0.05$, ** $p< 0.01$.

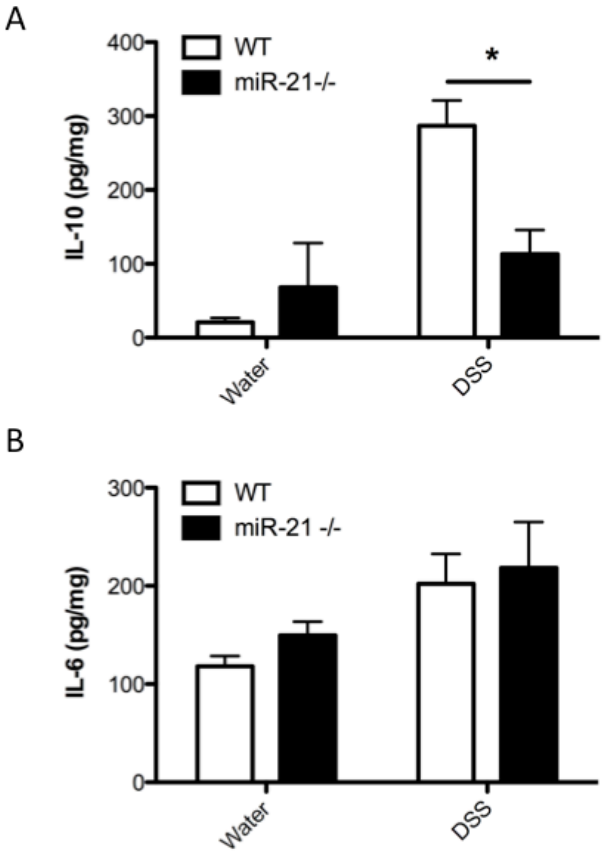

Figure 3.8 Cytokine analysis of WT and miR-21$^{-/-}$ colons post colitis

Wild-type (WT) and miR-21$^{-/-}$ mice were treated for 5 days with 2.5% DSS a*d libitum,* followed by 5 days with regular drinking water and control group mice were given conventional drinking water only throughout. On day 10, colons were harvested and segments were taken for homogenization and protein extraction. The protein was quantified and equalized before cytokine levels were assessed using ELISA. Data represent mean values ± SEM of n= ≥3 mice per group. P values were calculated using Student's T-test , * $p<0.05$.

3.2.4. Attempted optimization of the *C. rodentium* bacterially induced colitis model

In addition to the chemically-induced DSS colitis model, an infectious model of colitis was sought as an alternative model in which to further explore the role of miR-21 in IBD. *Citrobacter rodentium* was employed to induce colitis in mice. Specifically, WT and miR-21$^{-/-}$ mice had their food withdrawn overnight prior to inoculation with *Citrobacter* by oral gavage ($5x10^9$ CFU/mouse). Weight loss, fecal occult blood and diarrhea were monitored every second day over the course of 21 days to assess colitis progression. Neither WT nor miR-21$^{-/-}$ mice lost weight over the course of the experiment, and no fecal occult blood was detected in either group at any stage (Fig. 3.9A and B). The WT mice displayed a significantly increased diarrhea score on days 8 and 10, but this was not reflected in the composite DAI score which depicted the more accurate lack of induction of colitis during the course of infection (Fig. 3.9C and D). The colon lengths of WT and miR-21$^{-/-}$ mice were not different to one another and were a healthy length when compared to previous experiments where colitis was induced chemically (Fig. 3.9E). Subsequently, various modified protocols were used to try to induce colitis including varying inoculums however to no success (data not shown). To ascertain if bacterial colonisation occurred, fecal pellets were taken, homogenized and dilutions were grown overnight to enumerate the levels of bacteria shed. Bacteria were detectable in the feces of both WT and miR-21$^{-/-}$ mice, with the peak shedding appearing at day 6 before gradually shedding reduced until bacteria were no longer present in the feces on day 16 (Fig. 3.10). This pattern of shedding is consistent with that observed in published papers using this model [211]. There was a significantly higher level of bacteria present in the stool of miR-21$^{-/-}$ mice on day 12, but this was deemed not to be biologically relevant given that the bacteria failed to induce colitis. Given this failure to induce colitis across multiple experiments, coupled with discussions with members of the Prof Fiona Powrie lab (Oxford), it was decided that this model was not suitable for use in the TCD facility. However, it is possible that there are differences between WT and miR-21$^{-/-}$ reponses to infection that may be revealed at these earlier times (e.g. day

12) which may be revealed by analysing gene expression and other non-symptomatic readouts.

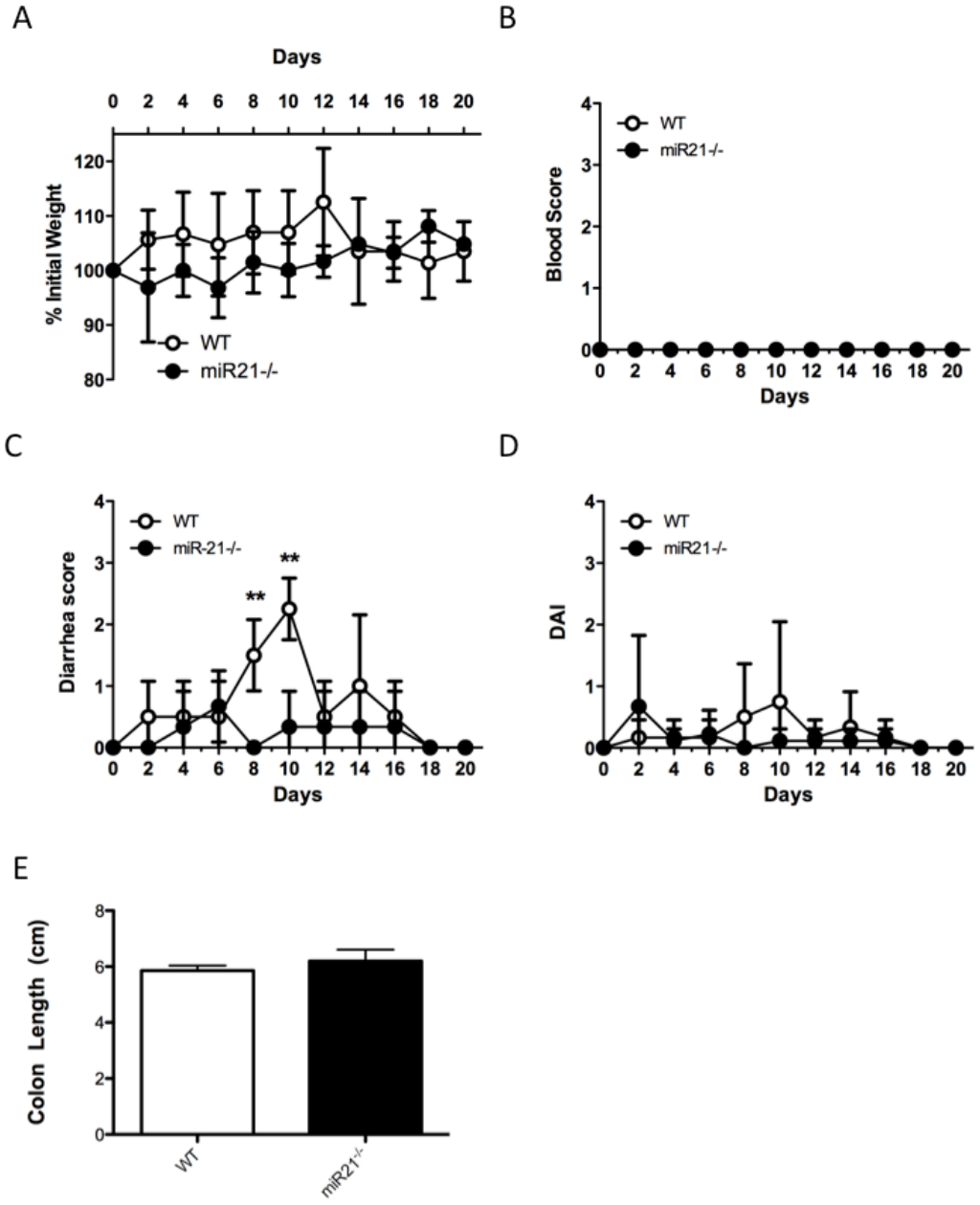

Figure 3.9 Optimisation of *Citrobacter rodentium* model in wild-type and miR-21$^{-/-}$ mice.

Wild-type (WT) and miR-21$^{-/-}$ mice aged between 8 and 12 weeks were weighed on day 0 and orally innoculated with 5x10^{9} *Citrobacter rodentium* (their food was removed on day -1 and replaced on day 0). Their weight (A), fecal occult blood (B) and stool consistency (C) were measured every second day throughout the experiment and combined to generate a disease activity index score (D). On day 21, the mice were sacrificed and their colons were removed and measured (E) before being stored for subsequent analysis. Data represent mean values ± SEM of n= ≥4 mice per group. P values were calculated for A-E using Student's T-test , ** $p<0.01$.

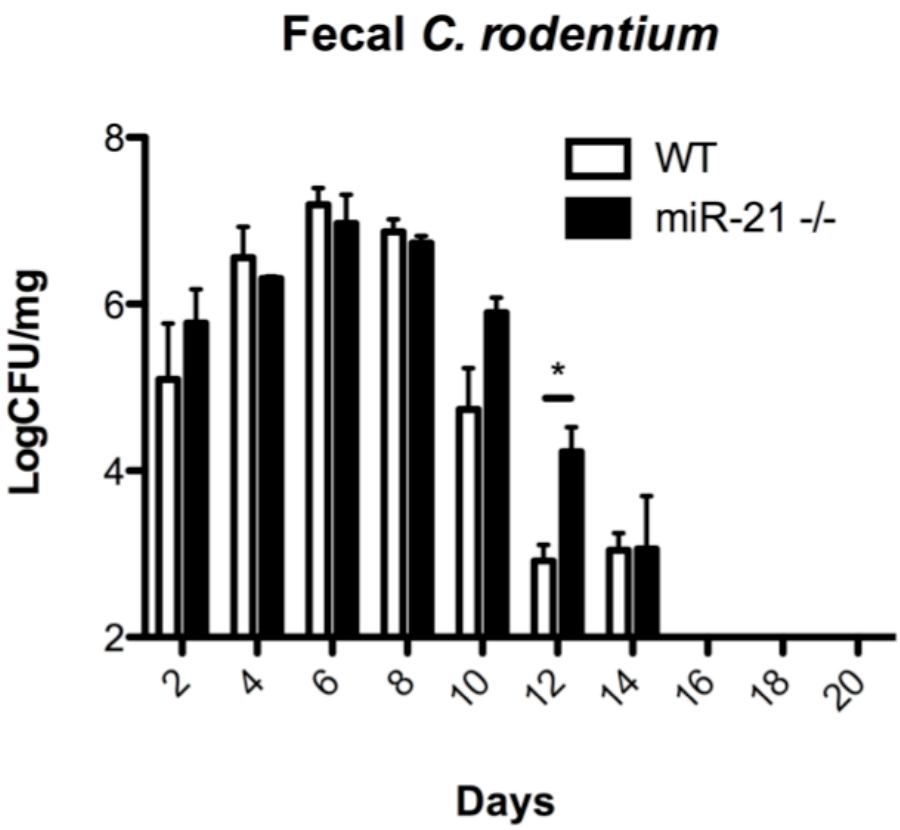

Figure 3.10 *Citrobacter rodentium* shedding in a model of infection induced colitis in wild-type and miR-21$^{-/-}$ mice.

Wild-type (WT) and miR-21$^{-/-}$ mice aged between 8 and 12 weeks were weighed on day 0 and orally innoculated with 5x10^{9} *Citrobacter rodentium* (their food was removed on day -1 and replaced on day 0). Fecal pellets were taken every second day throughout, weighed, homogenized in PBS, diluted and plated before being incubated overnight at 37°C. The following day the bacterial colonies were enumerated and converted in to LogCFU/mg feces. Data represent mean values ± SEM of n= ≥4 mice per group. P values were calculated for A-E using Student's T-test , * $p<0.05$.

3.2.5. Co-housing confers protection on WT mice, indicating a protective role for the microbiota in miR-21$^{-/-}$ mice.

The gut microbiota plays an important role in the homeostasis of the host organism, and it has also been shown to have an impact on the development of diseases such as IBD [90,179]. In order to assess whether or not the microbiota was having an effect on the observed disease phenotype in our mice we co-housed WT and miR-21$^{-/-}$ mice for four weeks prior to treatment with DSS. At this point in our investigations, a new order of DSS was purchased with a lesser potency than that used in the previous experiments. Accordingly, the dose used in these experiments was raised to 3.5%. In this model, WT mice co-housed with miR-21$^{-/-}$ mice were annotated CH-WT, and miR-21$^{-/-}$ mice that were co-housed with WT were annotated CH-miR-21$^{-/-}$. These test groups were compared to control mice that were co-housed with mice of the same genotype and so annotated simply WT or miR-21$^{-/-}$. The disease progression was followed over the course of 7 days and the DAI is presented here (Fig. 3.11A). The control mice displayed the same phenotype as previously seen, with the miR-21$^{-/-}$ showing protection from the disease, particularly at day 4 (Fig. 3.11B). Interestingly, there was also a suggestion, although subtle, that WT mice which had been co-housed with miR-21$^{-/-}$ mice may also be protected, once again day 4 being the strongest indicator (Fig. 3.11C). When the individual disease parameters are considered, it is clear there is no difference in weight loss between WT and CH-WT animals, however there were significant differences in diarrhea score at day 4 and in detectable occult blood at days 4 and 6 (Fig. 3.11D-F) which indicated that the co-housed WT mice were indeed gaining partial protection via exposure to the miR-21$^{-/-}$ microflora. Colon lengths were once again measured as a mark of disease severity, and once again control mice demonstrated that mice lacking miR-21 had significant longer colons that WT mice. In addition, the colons of the CH-WT mice were longer than WT controls although not to a statistically significant level (Fig. 3.11G). This transfer of microbes between mice appeared to only impact disease in the CH-WT group as the CH-miR-21$^{-/-}$ mice disease course followed that of the miR-21$^{-/-}$ controls and their colon length was virtually unchanged relative to the miR-21$^{-/-}$ controls (Fig. 3.11A

and G). Taken together, these results suggest that upon loss of miR-21, the microbiota undergoes a shift towards a less colitogenic one, which is transferrable.

3.2.6. Colonisation of germ-free WT mice with the fecal microbiota of miR21$^{-/-}$ miceconfers protection to DSS-induced colitis.

At this point in my studies, an opportunity arose to carry out experiments in the laboratory of Dr Eran Elinav at the Weizmann Insitute of Science (Israel). This provided the necessary germ-free facilities to further investigate the intestinal microbiota of WT and miR-21$^{-/-}$ mice. Germ-free mice have been used to explore the impact of different microbial populations on different diseases for several years and have been regularly employed by the Elinav lab for this purpose [51,246,247]. Thus, we next performed colonization of GF mice with the fecal microbiota of either our WT or miR-21$^{-/-}$ mouse. Specifically, fecal pellets were collected from WT and miR-21$^{-/-}$ mice, flash frozen in liquid nitrogen and shipped on dry ice to the Weizmann Institute. Upon receipt, fecal samples were subsequently thawed, homogenised in PBS (100mg/ml) and filtered in anaerobic conditions to form a bacterial suspension. This suspension was delivered to germ-free mice by oral gavage (200µl/mouse) and they were left for 9 days to allow the microbial communities to establish in the gut. After 9 days, the mice were given a dose of 3% DSS (MP Biomedicals) for 13 days (based on the model used by the Elinav group within their facility) and monitored throughout the course of the disease. There were significant differences in weight loss between mice inoculated with the WT fecal microbiota [Ex-GF(WT)] vs mice inoculated with the miR-21$^{-/-}$ fecal microbiota [Ex-GF(miR-21$^{-/-}$)] early in the course of the disease, with the former group gaining weight steadily as the latter remained the same (Fig. 3.12A, days 4 and 5). However this difference was lost as the disease progressed and the two groups began to gain weight on day 7. The other disease parameters measured showed a striking similarity to those seen in previous experiments comparing WT and miR-21$^{-/-}$ mice, with higher fecal blood observed throughout, most significantly at days 7 and 9, and higher diarrhea scores from day 6 onwards though these were not statistically significant (Fig. 3.12B and C). There was no difference in disease severity as measured by DAI, though this was likely due to the lack of weight lost by the mice over the course of the disease which likely skewed the overall score (Fig. 3.12D) and in addition there was no difference between Ex-

GF(WT) vs Ex-GF(miR-21$^{-/-}$) in colon length (Fig. 3.12E). Whilst the full colitis phenotype observed in previous experiments was not fully apparent, there did seem to be some correlation between the blood scores elicited by the different microbiota and the blood scores of the mice they originated from as seen in previous experiments. A second tool was employed to further investigate this model, , namely endoscopic analysis of the colon post-DSS colitis and clinical scoring of the inflammation present. At the end of the experiment, the mice were sedated with a ketamine/xylazine cocktail and colon inflammation was assessed using the Mainz COLOVIEW® system. Videos were recorded and scored for various clinical parameters which were combined to generate a colitis severity score. This showed that mice inoculated with the miR-21$^{-/-}$ microbiota had a significantly lower score than that of mice inoculated with the WT microbiota (Fig. 3.13A). Representative images show increased visible bleeding, fibrin deposition and granularity (bumpy surface) in the Ex-GF(WT) when compared to Ex-GF(miR-21$^{-/-}$) (Fig. 3.13B). These data indicated that the microbiota composition of the miR-21$^{-/-}$ mouse was indeed altered and appeared to at least partially impact on the course of DSS-induced colitis. In order to assess if an intact microbiota is required for induction of miR-21 in IBD, germ-free mice were given DSS and the expression of miR-21 in the colon was compared to water controls. Interestingly, miR-21 is still induced in the colons of germ-free mice after treatment with DSS (Fig. 3.14) implying that the microbiota or microbial signals are not required for DSS-induced miR-21 induction.

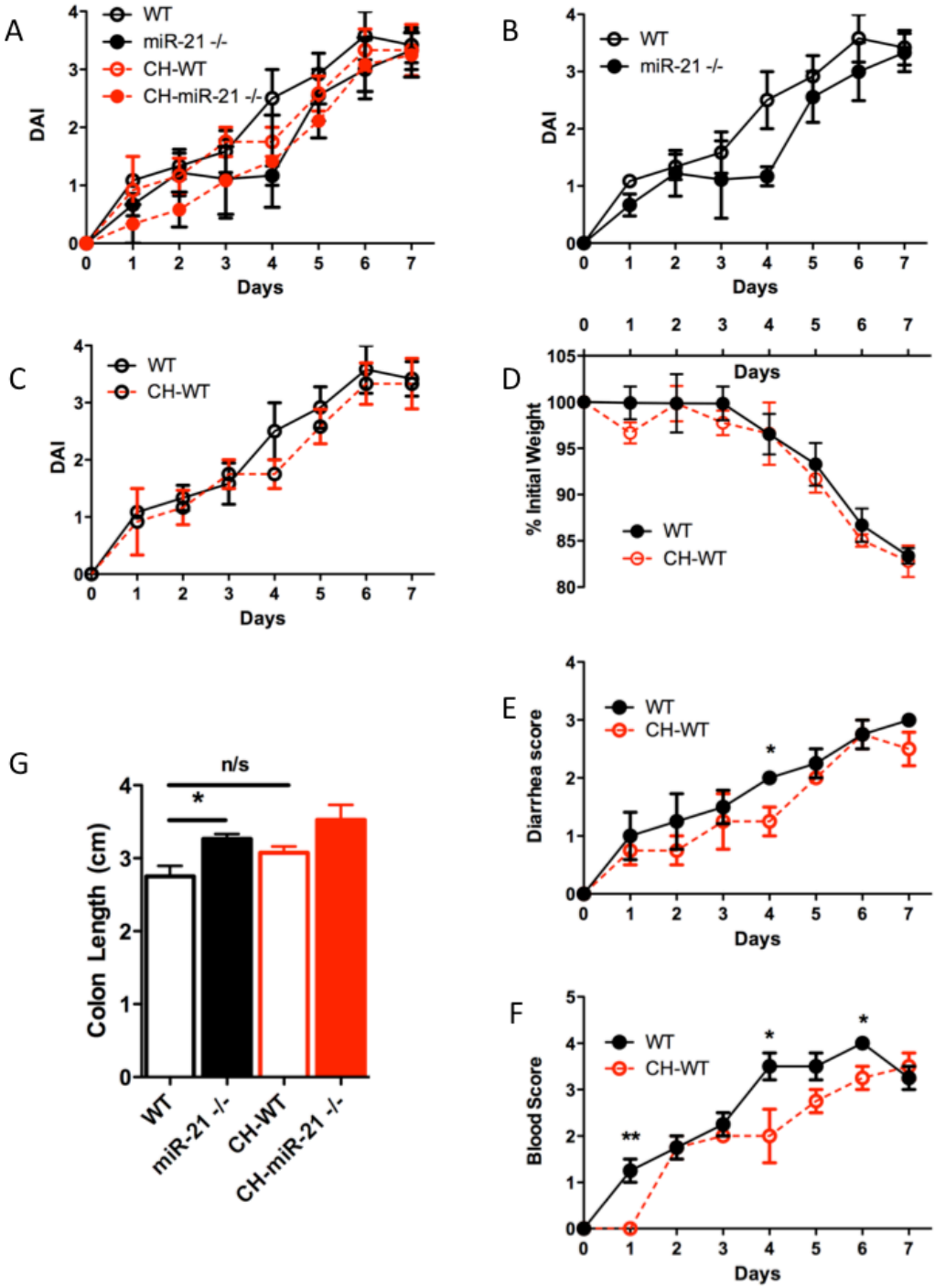

Figure 3.11 Wild-type mice cohoused with miR-21$^{-/-}$ mice are protected from DSS colitis compared to wild-type controls.

Wild-type (WT) and miR-21$^{-/-}$ mice aged between 4-6 weeks were cohoused for 4 weeks with either mice of the opposite genotype (e.g WT mouse co-housed with miR-21$^{-/-}$ = CH-WT) or other mice of the same genotype (e.g WT mouse co-housed with another WT = WT) before being weighed on day 0 and given 3.5% DSS *ad libitum* for 7 days, with fresh DSS being provided on day 3. Their weight, stool consistency and occult blood were measured daily throughout the experiment and combined to generate a disease activity index score (A). Individual plots of selected groups DAI, weight loss, stool score and blood score are shown (B-F). On day 7, the mice were sacrificed and their colons were removed and measured (G) before being stored for subsequent analysis. . Data represent mean values ± SEM of n= ≥3 mice per group. P values were calculated for A-G using Student's T-test , * $p<0.05$, ** $p<0.01$.

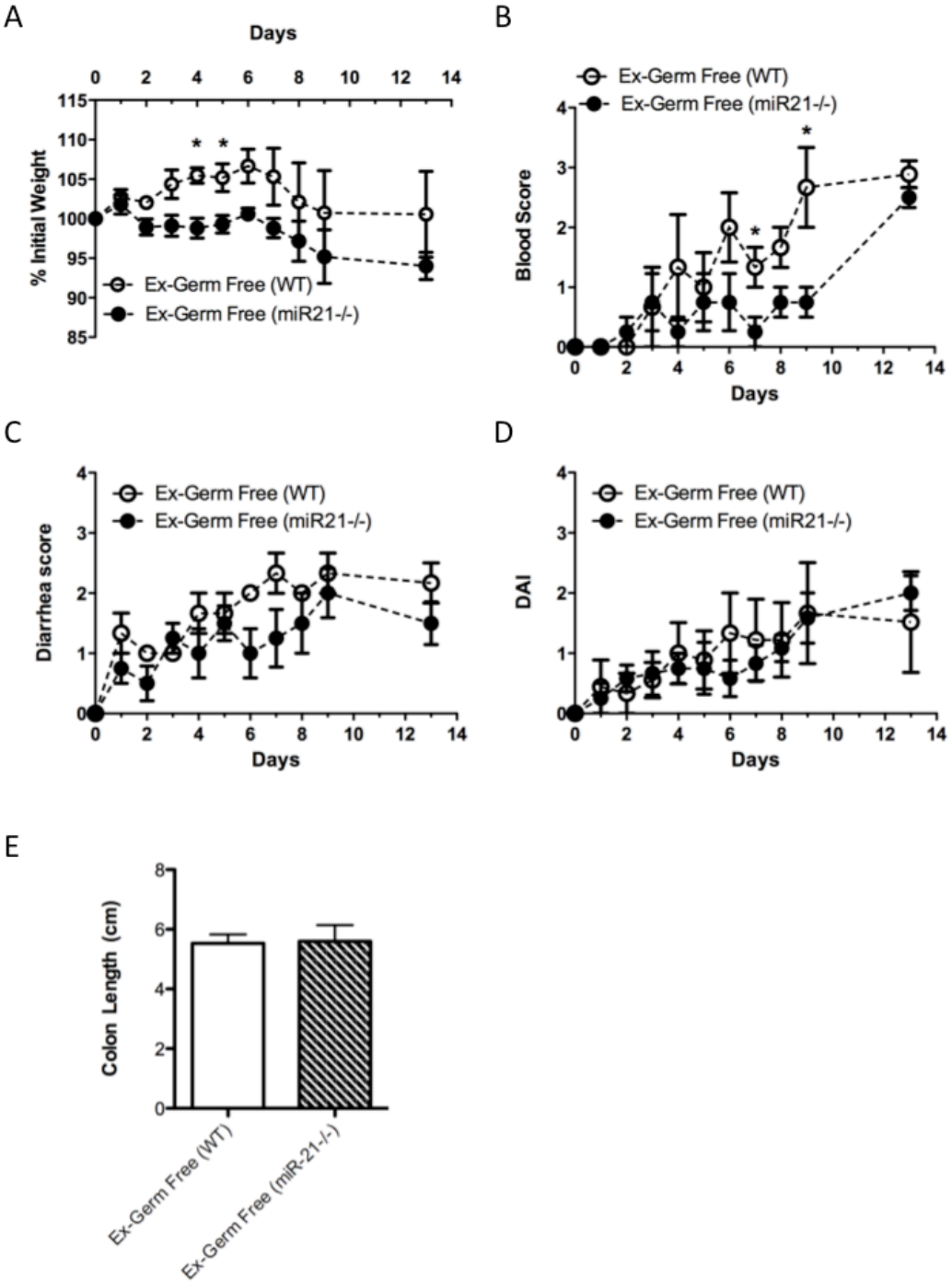

Figure 3.12 Comparison of wild type and miR-21$^{-/-}$ microbiota in a germ-free colonization model

Germ-free Swiss-Webster mice were colonized with fecal preparations from wild-type (WT) or miR-21$^{-/-}$ mice by oral gavage. After 9 days the mice were given 3% DSS *ad libitum* in their drinking water for 13 days, with fresh DSS being administered as required. Body weight (A), fecal occult blood (B) and stool consistency (C) were measured daily and combined to give a disease activity index score (D). On day 13, mice were subsequently sacrificed and the colon was removed and measured (E) before being stored for subsequent analysis. . Data represent mean values ± SEM of n=3 mice per group. P values were calculated for A-E using Student's T-test , * $p<0.05$.

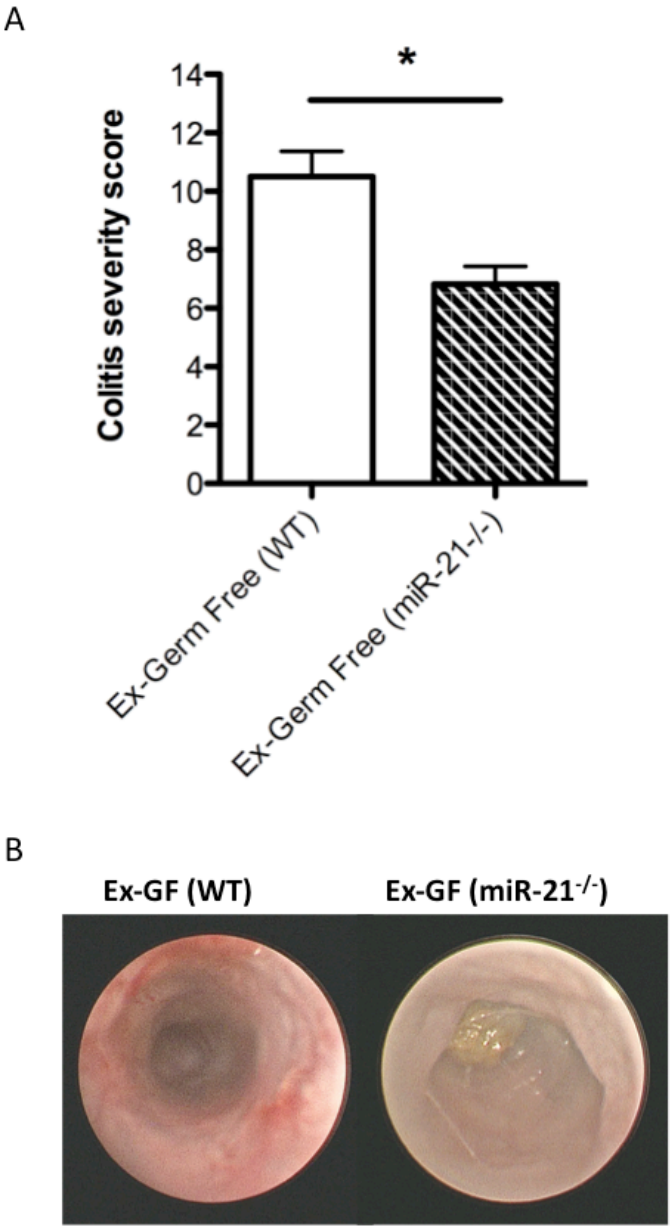

Figure 3.13 The miR-21$^{-/-}$ intestinal microbiota is protective in DSS colitis compared to wild-type.

Germ free Swiss-Webster mice were colonized with fecal preparations from wild-type (WT) or miR-21$^{-/-}$ mice by oral gavage (Ex-GF (WT) or Ex-GF (miR-21$^{-/-}$) . After 9 days the mice were given 3% DSS *ad libitum* in their drinking water for 13 days, with fresh DSS being administered as required. On day 13, mice were anesthetized and underwent a colonoscopy using the ColoView system. Colons were blind scored for a number of clinical parametrs which were combined to give a colitis severity score (A). Representative images are shown (B). Data represent mean values ± SEM of n=3 mice per group. P values were calculated for A-E using Student's T-test , * $p<0.05$..

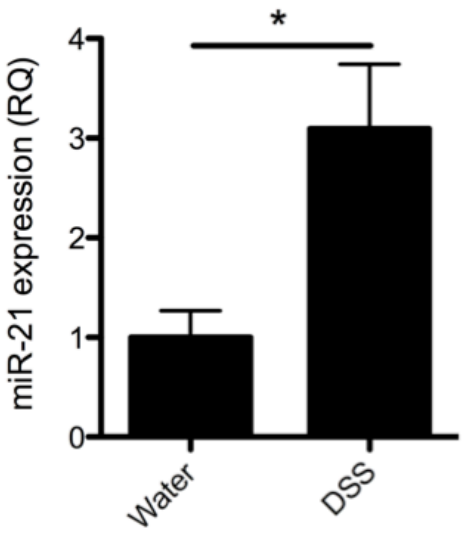

Figure 3.14 Intestinal miR-21 expression is increased in germ-free mice following DSS treatment

Germ free mice were were given 1.5% DSS *ad libitum* in their drinking water for 10 days, with fresh DSS being administered as required. On day 10, mice sacrificed and the colon was removed. RNA was extracted using TriZOL reagent and miR-21 expression was analyzed by qPCR using the Applied Biosystems ViiA 7 Real-Time PCR system and Taqman reagents. . Data represent mean values ± SD of n= ≥4 mice per group, relative quantification (RQ) relative to water group. P values were calculated using Student's T-test , * $p<0.05$

3.2.7. 16S rRNA Analysis of the fecal microbiota revealed differences following loss of miR-21$^{-/-}$

16S sequencing of the fecal DNA is a widely used tool for analysis of the intestinal microbiome. We performed an initial analysis which indicated that significant differences did exist. Specifically, DNA was extracted from fecal pellets from male WT and miR-21$^{-/-}$ mice and prepared in to a sequencing library to compare the composition of the bacterial populations present in each. The sequencing data was obtained using the Illumina MiSeq system and analysed using the QIIME (Quantitative Insights Into Microbial Ecology, http://www.qiime.org) analysis pipeline. There were several differences between the WT and miR-21 microbiota using Principle co-ordinate (PCoA) statistical analysis to measure and visualize relatedness of samples (β diversity) and OTU analysis was used to compare abundances of individual species (OTU) between the groups. The PCoA plot presented is an analysis based on UniFrac distances, where greater distance between dots indicates greater dissimilarity, and shows a clustering of the WT samples (represented by blue dots) in a quadrant separate from those of the miR-21$^{-/-}$ samples (represented by red dots) (Fig. 3.15A). This distance was statistically significant as measured by ANOVA, but was considered worthy of further investigation. Similarly, OTU analysis indicated that there was a significantly higher number of OTUs detected of the genus *Rikenellaceae* present in the miR-21$^{-/-}$ mice compared to the WT (4.833333 vs 0) as determined by a false discovery rate (FDR) corrected p value of 0.028386686 and a Bonferroni post-test value of 0.028386686 (Fig. 3.15B). These data indicated that there is a difference in the composition of the miR-21$^{-/-}$ fecal microbiota, but that this preliminary study could not sufficiently confirm that. It was determined that a full analysis would be carried out with enhanced n numbers and samples from both male and female mice.

Subsequently a larger analysis was performed and sequenced commercially by Novogene (China). Stool samples were collected from WT and miR-21$^{-/-}$ mice from which DNA was extracted and sent to Novogene for 16S sequencing. The resulting 16S sequencing data was generated by Novogene and subsequently analyzed by

collaborators, Dr Paul Cotter and Dr Raul Cabrerra-Bello, at the sequencing facility at Teagasc, Moorepark, Co. Cork, as described in Materials and Methods (2.2.11.6). The α diversity of the fecal microbiota bacteria (a measure of species diversity within a sample) was assessed and compared between WT and miR-21$^{-/-}$ sample data (Fig. 3.16). As is common practice, a number of different diversity indices were used to ensure any findings are robust and these included observed species, Chao1, ACE, Shannon, Simpson, inverse Simpson and Fisher. There were no significant differences between the groups in male or female mice across any of the above indices as assessed by two-sample T-test as is standard using the QIIME pipeline. These results indicate that the species composition of WT and miR-21$^{-/-}$ are equally diverse. Having established that the two groups had equally diverse bacterial populations, the next comparison to be made was were the populations made up of the same constituents or were they independently diverse. This was assessed using the QIIME pipeline to compare β diversity between samples. As described previously, a PCoA plot was generated to visualize UniFrac distances, where greater distance between dots indicates greater dissimilarity (Fig. 3.17). This data was statistically analyzed using Adonis and revealed a significant difference between WT and miR-21$^{-/-}$ mice. This data indicated that whilst there were equally diverse bacterial populations, the populations were likely to be made up of significantly different types of bacteria.

Several approaches were taken to analyze the composition of the miR-21$^{-/-}$ bacterial microbiota versus that of the WT controls. The QIIME pipeline allows the comparison of 16S sequences to established databases and assign the sequences to a known OTU. The top 25 most abundant OTUs were compared between the two groups and the results are presented in Figure 3.18 with each OTU being given its phylum name followed by its genus name (e.g A*ctinobacterium*; *Bifidobacterium*). It was apparent that there were considerable differences between the two groups, with the miR-21$^{-/-}$ group displaying a higher proportion of A*ctinobacterium*; *Bifidobacterium*, *Firmicutes*; *Coprococcus*, *Firmicutes*; *Lactonifactor*, *Firmicutes*; *Oscilibacter*, *Firmicutes*; *Clostridium sensu stricto*, *Firmicutes*; *anaerosporobacter* and *Firmicutes*; *Catonella*, and a lower proportion of *Firmicutes*; *Clostridium XIVa*, *Firmicutes*; *Tannerella*, *Firmicutes*; *Dorea*, *Bacteroidetes*; *Barnesiella* and *Bacteroidetes*; *Prevotella*, relative to WT mice (Fig. 3.18). Further analysis was

performed to compare the relative proportions at various taxa levels, from phyla through to genus level, so that we could establish whether wider groups of bacteria were present in different proportions between the two groups as distinct from changes to individual OTUs. A number of significant differences were apparent across several taxa. At the phylum level, *Proteobacteria* (q=0.00079935) were present in higher proportions in the miR-21$^{-/-}$ microbiota (Fig. 3.19A). At the family level, the miR-21$^{-/-}$ samples contained higher proportions of *Bifidobacteriaceae* (q=0.01181564) and *Peptostreptococcaceae* (q=0.14586726), and reduced proportions of *Verrucomicrobiaceae* (q=0.07853655) and *Bacteroidaceae* (q=0.05746273) Fig. 3.19B). At the genus level, the WT samples group contains higher proportions of *Enterorhabdus* (q=0.00036569), and reduced proportions of *Odoribacter* (q=7.896e-05) and *Bifidobacterium* (q=0.00143734) (Fig. 3.19C). These differences (summarised in Fig 3.19D) further indicated to us that mice deficient in miR-21 had an altered microbiota, and we wished to further confirm that this altered microbiota was protective in disease.

A

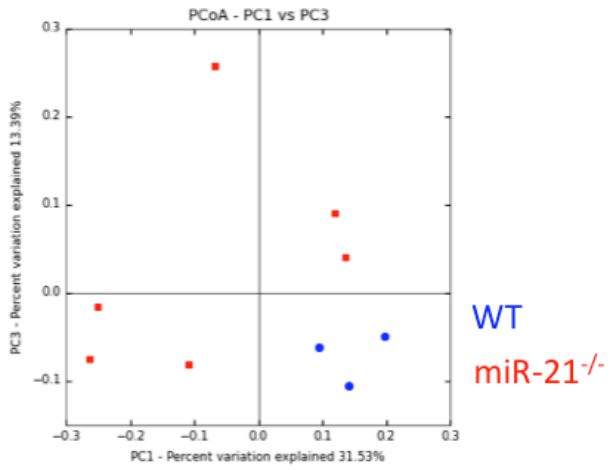

B

FDR_P	Bonferroni_P	Mir21KO_mea	Mir21WT_mean	taxonomy
0.02838669	0.02838669	4.83333333	0	k__Bacteria;p__Bacteroidetes;c__Bacteroidia;o__Bacteroidales;f__Rikenellaceae;g__;s__

Figure 3.15 Preliminary 16S sequencing of the wild-type and miR-21$^{-/-}$ fecal microbiota.

Fecal samples were taken from male wild-type (WT) and miR-21$^{-/-}$ mice aged between 8-12 weeks and immediately snap frozen in liquid nitrogen and stored at -80°C. DNA was extracted using the MOBIO fecal soil extraction kit and the V3/V4 bacterial rRNA gene segment was amplified and a library preparation was made for use in the Illumina MiSeq 16S sequencing system. Principle coordinate analysis was employed to assess the relatedness of WT and miR-21$^{-/-}$ fecal microbiota, individual samples represented by blue or red dots based on unwieghted UniFrac distances (A). ANOVA analysis identified a significantly increased abundance of the genus *Rikenellaceae* in the miR-21$^{-/-}$ microbiota (B). Data representative of n=≥3/group. Analysis was performed by Meirav Pevsner-Fischer (WIS).

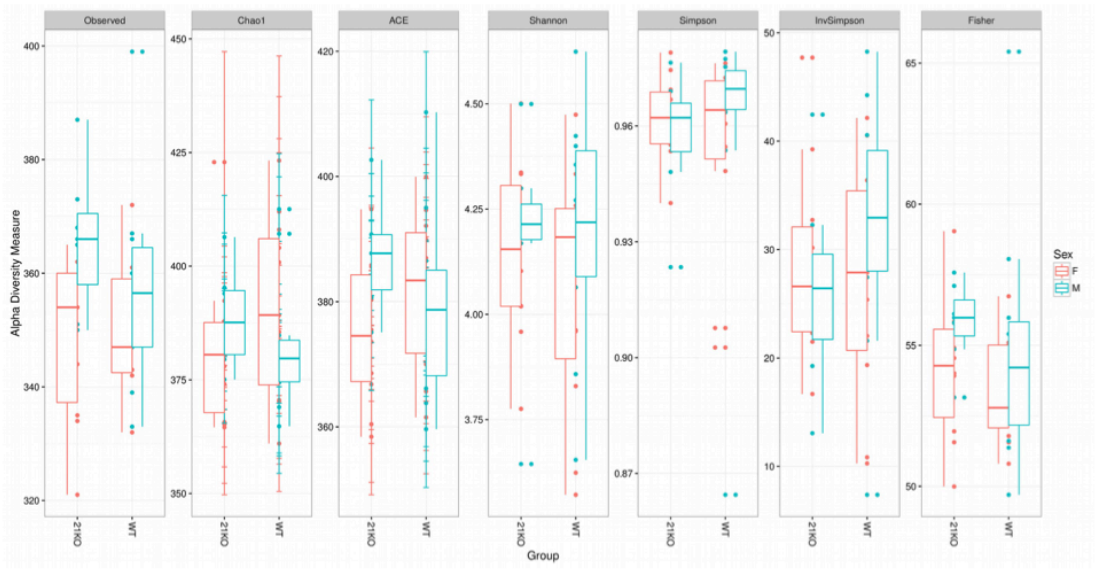

Figure 3.16 16S sequencing analysis: WT and miR-21$^{-/-}$ fecal microbiota do not differ in α-diversity.

Fecal samples were taken from wild-type (WT) and miR-21$^{-/-}$ mice aged between 8-12 weeks and immediately snap frozen in liquid nitrogen and stored at -80°C. DNA was extracted using the MOBIO fecal soil extraction kit and the V3/V4 bacterial rRNA gene segment was amplified and a library preparation was made for use in the Illumina MiSeq 16S sequencing system by Novogene (China). The 16S rRNA reads were compared to the RDP database, and WT and miR-21$^{-/-}$ microbiota samples were compared for intra-sample richness (α) diversity as descibed using OTU, Choa1, ACE, Shannon, Simpson, invSimpson and Fisher indices (A). Kruskal-Wallis and False discovery rate (FDR, qvalue) control based on the Benjamini-Hochberg procedure was used to correct for multiple testing with the R statistical package. Data is representative of n=≥9. Analysis was performed by Raul Cabrerra-Bello (Teagasc)

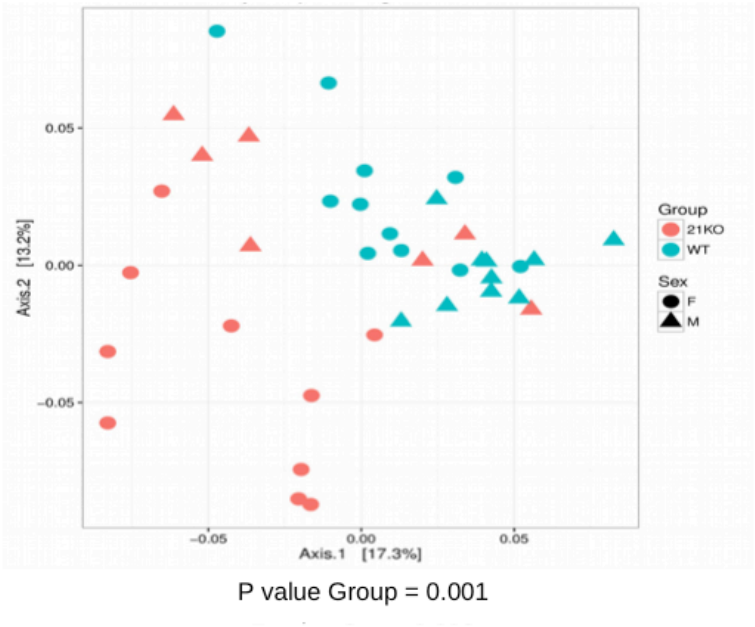

Figure 3.17 16S sequencing analysis: WT and miR-21$^{-/-}$ fecal microbiota differ in β diversity.

Fecal samples were taken from wild-type (WT) and miR-21$^{-/-}$ mice aged between 8-12 weeks and immediately snap frozen in liquid nitrogen and stored at -80°C. DNA was extracted using the MOBIO fecal soil extraction kit and the V3/V4 bacterial rRNA gene segment was amplified and a library preparation was made for use in the Illumina MiSeq 16S sequencing system by Novogene (China). The 16S rRNA reads were compared to the RDP database, and WT and miR-21$^{-/-}$ microbiota samples were compared for inter-sample (β) diversity. β diversity is represented by a Principal Coordinates Analysis (PCoA), performed using all 16S rRNA reads clustered at 97% similarity. (Anosim Pvalue = 0.001). Analysis was performed by Raul Cabrerra-Bello (Teagasc).

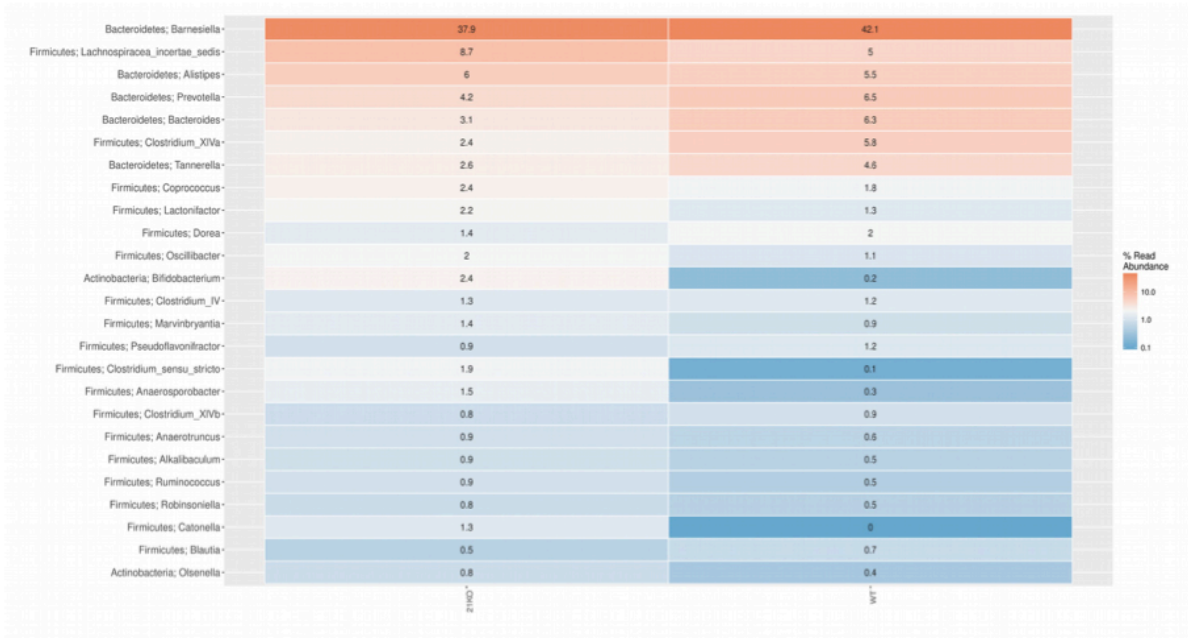

Figure 3.18 16S sequencing analysis: Comparing the top 25 most abundant observable taxonomic units in the WT and miR-21$^{-/-}$ microbiota.

Fecal samples were taken from wild-type (WT) and miR-21$^{-/-}$ mice aged between 8-12 weeks and immediately snap frozen in liquid nitrogen and stored at -80°C. DNA was extracted using the MOBIO fecal soil extraction kit and the V3/V4 bacterial rRNA gene segment was amplified and a library preparation was made for use in the Illumina MiSeq 16S sequencing system by Novogene (China). The 16S rRNA reads were compared to the RDP database, and WT and miR-21$^{-/-}$ microbiota samples were compared for the proportions of the 25 most abundant OTUs . Data is representative of n=≥22. Analysis was performed by Raul Cabrerra-Bello (Teagasc)

Phylum

A

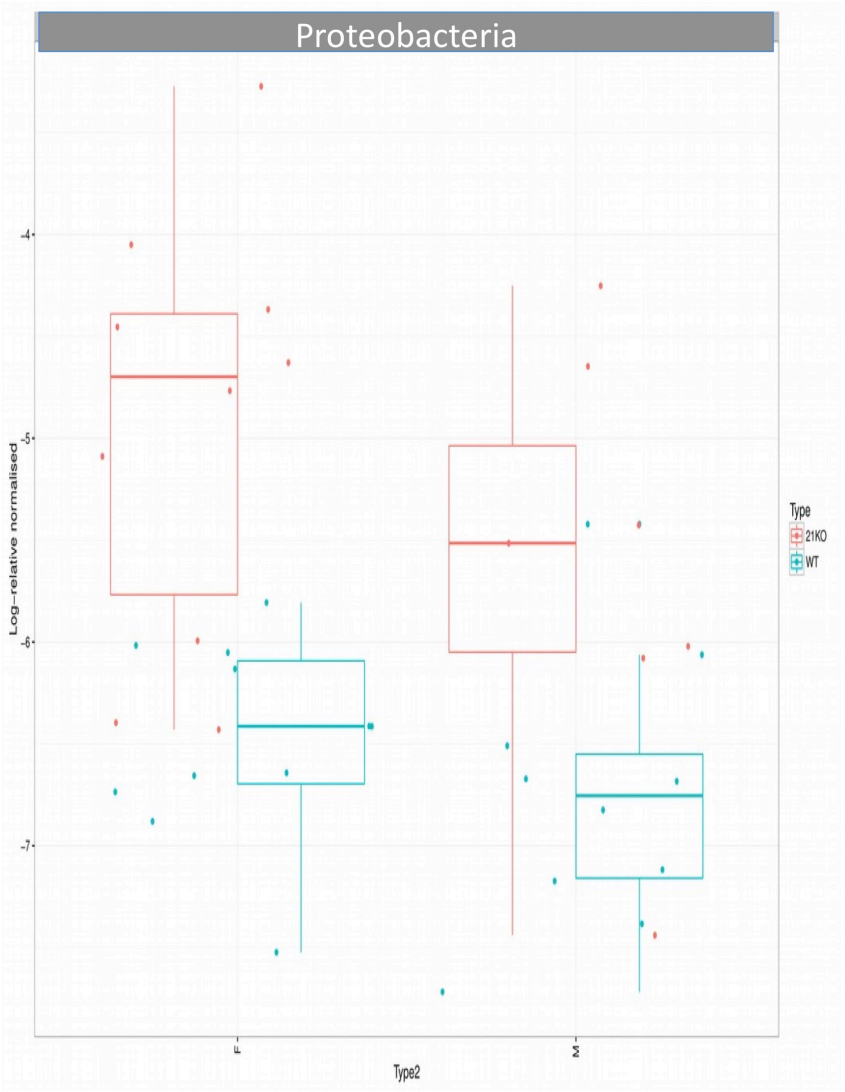
Proteobacteria
Log−relative normalised
-4
-5
-6
-7
F
M
Type2
Type
21KO
WT

Family

B

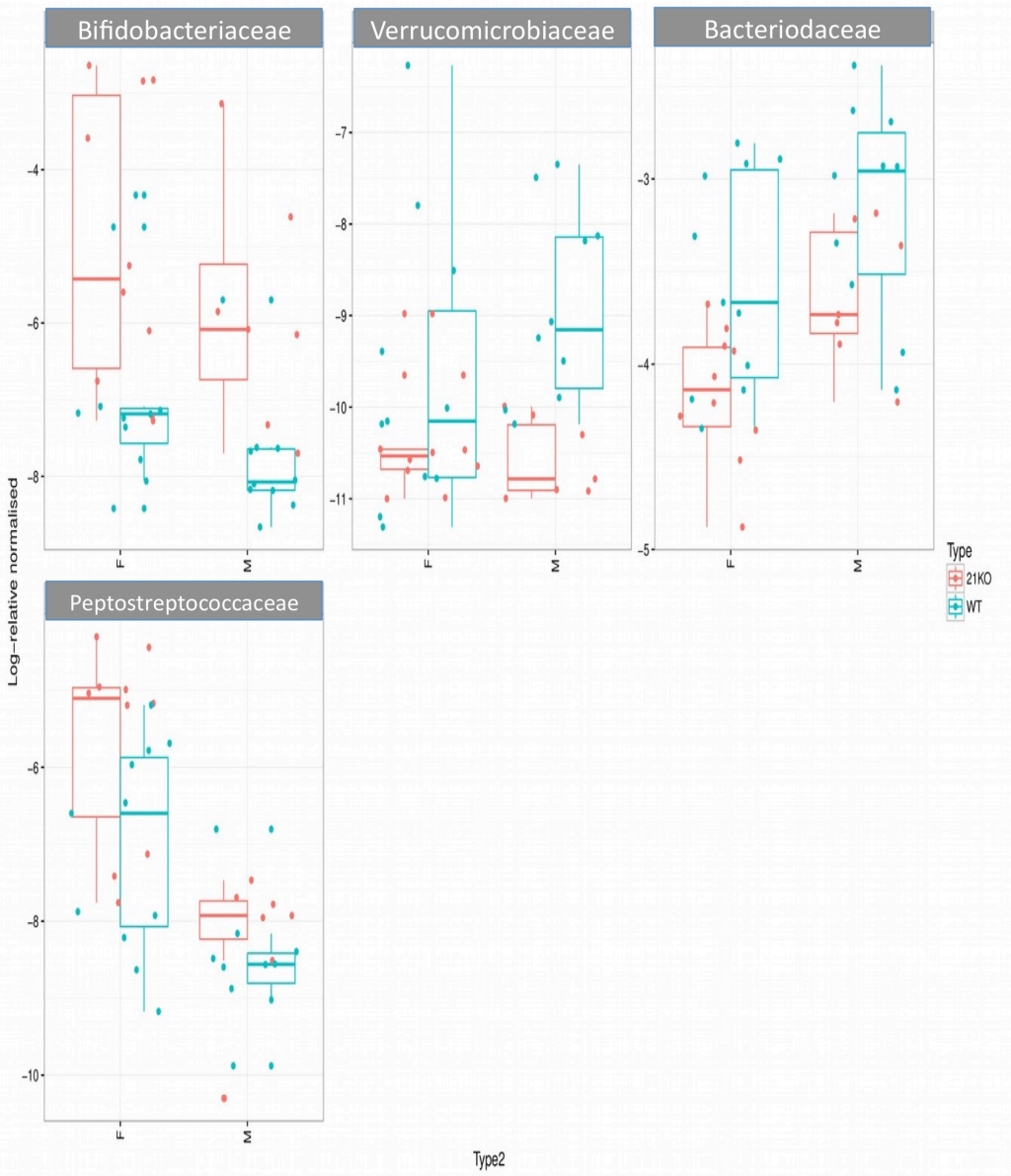
Bifidobacteriaceae
Verrucomicrobiaceae
Bacteriodaceae
Peptostreptococcaceae
Log−relative normalised
Type2
F
M
Type
21KO
WT

C

Genus

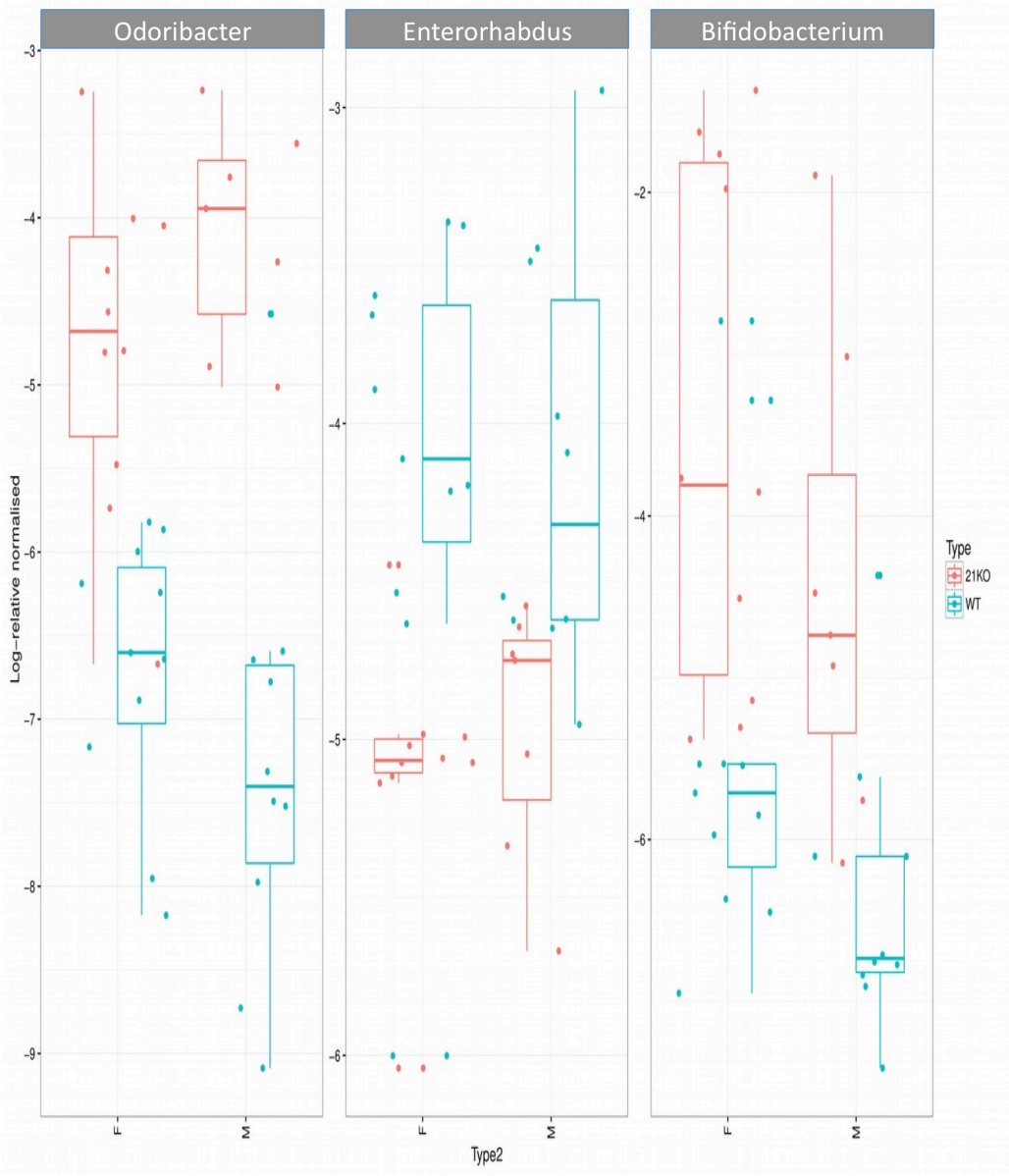
Odoribacter
Enterorhabdus
Bifidobacterium
Log−relative normalised
Type2
F
M
Type
21KO
WT

D

Phylum	Alteration in miR-21$^{-/-}$	IBD association
Proteobacteria	↑	Disease

Family	Alteration in miR-21$^{-/-}$	IBD association
Bifidobacteriaceae	↑	Health
Peptostreptococcaceae	↑	Health
Bacteroidadeae	↓	Disease

Genus	Alteration in miR-21$^{-/-}$	IBD association
Bifidobacterium	↑	Health
Odoribacter	↑	Health

↑ Increased Abundance vs WT ↓ Decreased Abundance vs WT

Figure 3.19 16S sequencing analysis: WT and miR-21$^{-/-}$ fecal microbiota differ in relative abundance of bacterial taxa at several levels.

Fecal samples were taken from wild-type (WT) and miR-21$^{-/-}$ mice aged between 8-12 weeks and immediately snap frozen in liquid nitrogen and stored at -80°C. DNA was extracted using the MOBIO fecal soil extraction kit and the V3/V4 bacterial rRNA gene segment was amplified and a library preparation was made for use in the Illumina MiSeq 16S sequencing system by Novogene (China). The 16S rRNA reads were compared to the RDP database, and WT and miR-21$^{-/-}$ microbiota samples were compared for abundance of different bacterial taxa at phylum level (A), family level (B) and genus level (C). These results are summarised in a table (D).

3.2.8. The miR-21$^{-/-}$ protective phenotype is lost after treatment of mice with antibiotics.

We next wanted to establish whether miR-21$^{-/-}$ mice would remain protected from DSS-induced colitis compared to WT mice following depletion of their microbiota. To ascertain this, a cocktail of antibiotics was administered orally to mice to deplete the microbiota before induction of colitis with DSS (Fig. 3.20). The mice were fed a mix of four antibiotics (ABX) for two weeks prior to being given 3% (w/v) DSS for seven days, and compared to control mice who were given conventional drinking water only prior to DSS treatment. The differences in weight loss observed were consistent with previous experiments, with WT mice losing more weight than miR-21$^{-/-}$ mice. Both WT and miR-21$^{-/-}$ mice treated with antibiotics suffered more severe weight loss than their respective controls (Fig. 3.20A). Interestingly, there was a striking difference between the antibiotics-treated groups (ABX) and the controls with regards to the presence of occult blood in stools, with both WT and miR-21$^{-/-}$ ABX groups displaying detectable levels of blood in stool after a single days treatment with DSS, which was in contrast to the slower progression of the control animals (Fig. 3.20B). The diarrhea scores also demonstrated that the presence of antibiotics prior to DSS treatment caused a slight exacerbation of disease, though it was not as pronounced as in the blood scores. The control groups behaved as seen in previous experiments with WT mice displaying higher scores and the overall disease scores indicating protection in the miR-21$^{-/-}$ mice at the latter days of the experiment, which was lost following antibiotic pre-treatment (Fig. 3.20C and D). Interestingly, the control groups displayed the same colon length phenotype as seen in previous experiments, while the antibiotic treated groups had marginally longer colons, although not a statistically significant difference (Fig. 3.20E). However, the most striking feature of these data was the increased sickness behaviour as indicated by loss of mobility and increased morbidity in miR-21$^{-/-}$ mice following antibiotic treatment (miR-21 ABX) (Fig. 3.20F and G). This measure was taken alongside the colitis-specific parameters mentioned in previous experiments, to ensure correct animal welfare practice is maintained. When mice reach a maximum score for loss of

mobility, or a maximum composite score made up from the various other parameters, they must be humanely sacrificed. Treatment with antibiotics led miR-21$^{-/-}$ mice to lose mobility at a significantly higher rate compared to WT mice that had also be given antibiotics (Fig. 3.20F, days 5 and 6). This was indicative of significantly impaired health and resulted in death of mice either spontaneously or following humane sacrifice. This lead to a pronounced impairment in survival in miR-21 ABX mice (Fig. 3.20G). Taken together, these data demonstrate that the miR-21$^{-/-}$ protective phenotype is dependant on the presence of the intestinal microbiota.

3.2.9. Investigations into the underlying mechanism by which miR-21$^{-/-}$ may modulate the microbiota

Having established that mice lacking miR-21 expression have an altered microbiota which impacts on the course of DSS-induced colitis, the possible mechanisms by which this miRNA might shape the composition of intestinal bacteria populations were preliminarily explored. The intestinal microenvironment coordinates with the microbiota in numerous ways including secretion of immunoglobulins, the most important of which sIgA that bind bacterial surface antigens and tethers the bacteria to the outer mucus layer amongst other mechanisms [248]. In order to assess if miR-21 deletion led to altered levels sIgA in the feces, pellets were collected and homogenised. This homogenate was then analysed by ELISA and though overall there was a reduction in sIgA levels in the feces obtained from miR-21$^{-/-}$ mice relative to the WT samples, it was not statistically significant (Fig. 3.21).

As mentioned previously, the mucous layers themselves are a critical determinant in the correct localisation and composition of the microbiota, with this layer forming a physical barrier which limits interaction of the microbiota with epithelial cells while mucins are an important source of nutrition for members of the microbiota thereby influencing its composition. To determine whether there are altered production of mucins following loss of miR-21, we first performed an Alcian blue staining to analyse distal colon sections from WT and miR-21$^{-/-}$ mice. Images were used to estimate the amount of mucous present throughout the epithelial layer, which was expressed as percentage area (Fig. 3.22). There was no statistical difference in mucous present, though there were reduced levels observed in both WT and miR-21$^{-/-}$

DSS-treated mice compared to water controls (Fig. 3.22B). The outer mucous layer is primarily composed of the secretary mucin Muc2, so we deduced that this mucin was unlikely to be affected by miR-21 expression according to this staining. However, there are other mucins present in this layer that may be influenced by miR-21 expression that may have been lost in this analysis. Using the miRNA target databases miR-WALK 2.0 and miR-Base, it became apparent that miR-21 targets a protein named Myristoylated alanine-rich C-kinase substrate (MARCKS) which has a number of cellular functions including regulation of mucin secretion [249,250]. Thus, colon explants were analysed to determine whether the expression of this protein may be altered by deletion of miR-21. In addition, miR-21 has previously been shown to target the RhoGTPase RhoB which has an impact on barrier integrity, so this target was also investigated (Fig. 3.23) [133]. Colon segments were cultured overnight in media alone or media containing 3% DSS or LPS before being lysed in RIPA buffer to generate protein lysates. Western blot analysis showed that there was altered expression of MARCKS in colon explants lacking miR-21 (Fig. 3.23A). Densitometry revealed that there was less MARCKS present in miR-21$^{-/-}$ colon explants basally (Fig. 3.23A lanes 1 and 2), but that upon treatment with DSS or LPS there was a marked enhancement of MARCKS expression relative to WT explants (Fig. 3.23A lanes 5 and 6 versus 3 and 4, B). Similarly, RhoB was expressed at very similar levels in both WT and miR-21$^{-/-}$ colon explants basally (Fig. 3.23A lanes 1 and 2) but demonstrated an 3-fold increase in expression in miR-21$^{-/-}$ explants upon DSS treatment (Fig. 3.23A lanes 5 versus 3, C). These data indicate that miR-21 expression impacts on several important barrier factors which may play a role in shaping the microbiota and thus intestinal homeostasis, in particular in the face of inflammatory stimuli such as DSS.

Taken together, these data demonstrate that deletion of miR-21 in mice is protective in the DSS-induced model of colitis, and that this protection is at least in part mediated by the presence of an altered intestinal microbiota. This confirms that the increase in miR-21 expression seen in human IBD is deleterious in this disease.

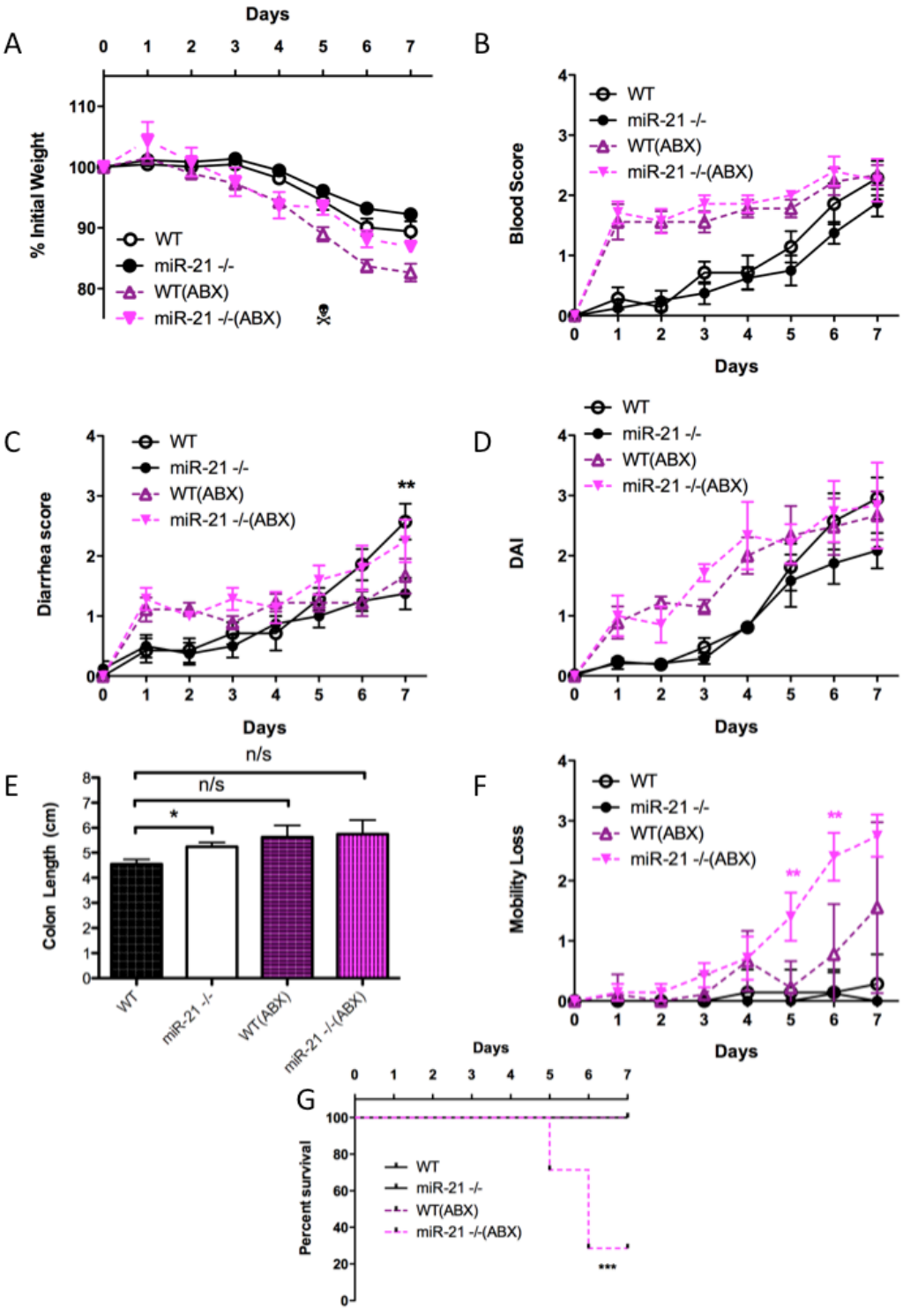
A
Days
% Initial Weight
WT
miR-21 -/-
WT(ABX)
miR-21 -/-(ABX)
B
Blood Score
Days
C
Diarrhea score
**
Days
D
DAI
Days
E
n/s
n/s
*
Colon Length (cm)
WT
miR-21 -/-
WT(ABX)
miR-21 -/-(ABX)
F
Mobility Loss
**
**
Days
G
Days
Percent survival
***

Figure 3.20 The microbiota of miR-21$^{-/-}$ mice is protective in DSS-induced colitis.

Wild-type (WT) and miR-21$^{-/-}$ mice aged between 8 and 12 weeks were given a 4-way antibiotics mix a*d libitum* for 2 weeks. The mice were then weighed on day 0 and given 3% DSS (MP Biomedicals) a*d libitum* for 7 days. Their weight (A), fecal occult blood (B) and stool consistency (C) were measured daily throughout the experiment and combined to generate a disease activity index score (DAI) [D]. The mice were sacrificed on day 8 and their colons were removed and measured (E) before being treated and stored for subsequent analysis. In addition, the mice were scored for mobility loss (F) and morbidity (G). Data represent mean values ± SEM pooled from two experiments of n= ≥5 mice per group. P values were calculated for A-E using Student's T-test and Chi squared test for Kaplan-Meier survival curve , * $p<0.05$, ** $p< 0.01$, *** $p=<0.001$. Black asterisks compare WT vs miR-21$^{-/-}$, magenta asterisks compare WT (ABX) vs miR-21$^{-/-}$ (ABX) except in panel G.

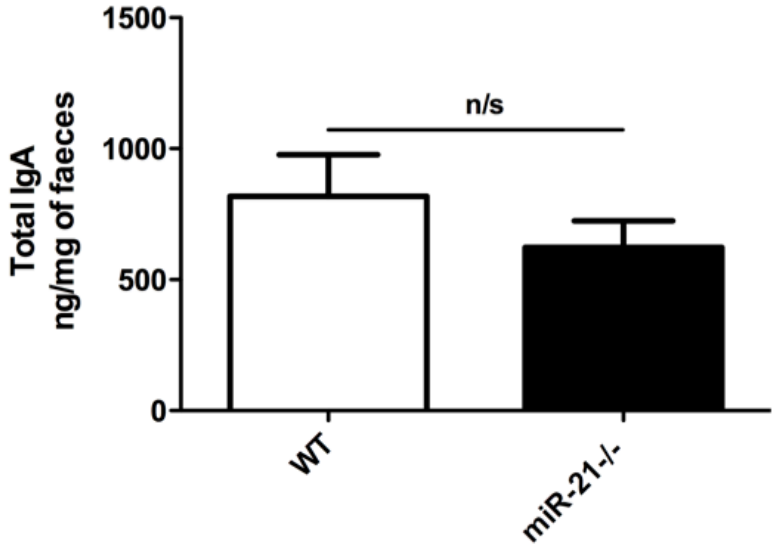

Figure 3.21 Fecal IgA levels do not differ between WT and miR-21$^{-/-}$ mice.

Fecal pellets were taken from wild-type (WT) and miR-21$^{-/-}$ mice and placed in pre-weighed tubes of homogenization buffer. The pellets were weighed, then mashed manually in their tubes before the homogenate was centrifuged at 10,000g for 10 min at 4°C. The supernatant was removed and the IgA content present was assessed by ELISA, with the values obtained being normalized by weight. Data presented representative of data pooled from two experiments, n=15. Statistical significance was assessed using Student's T test.

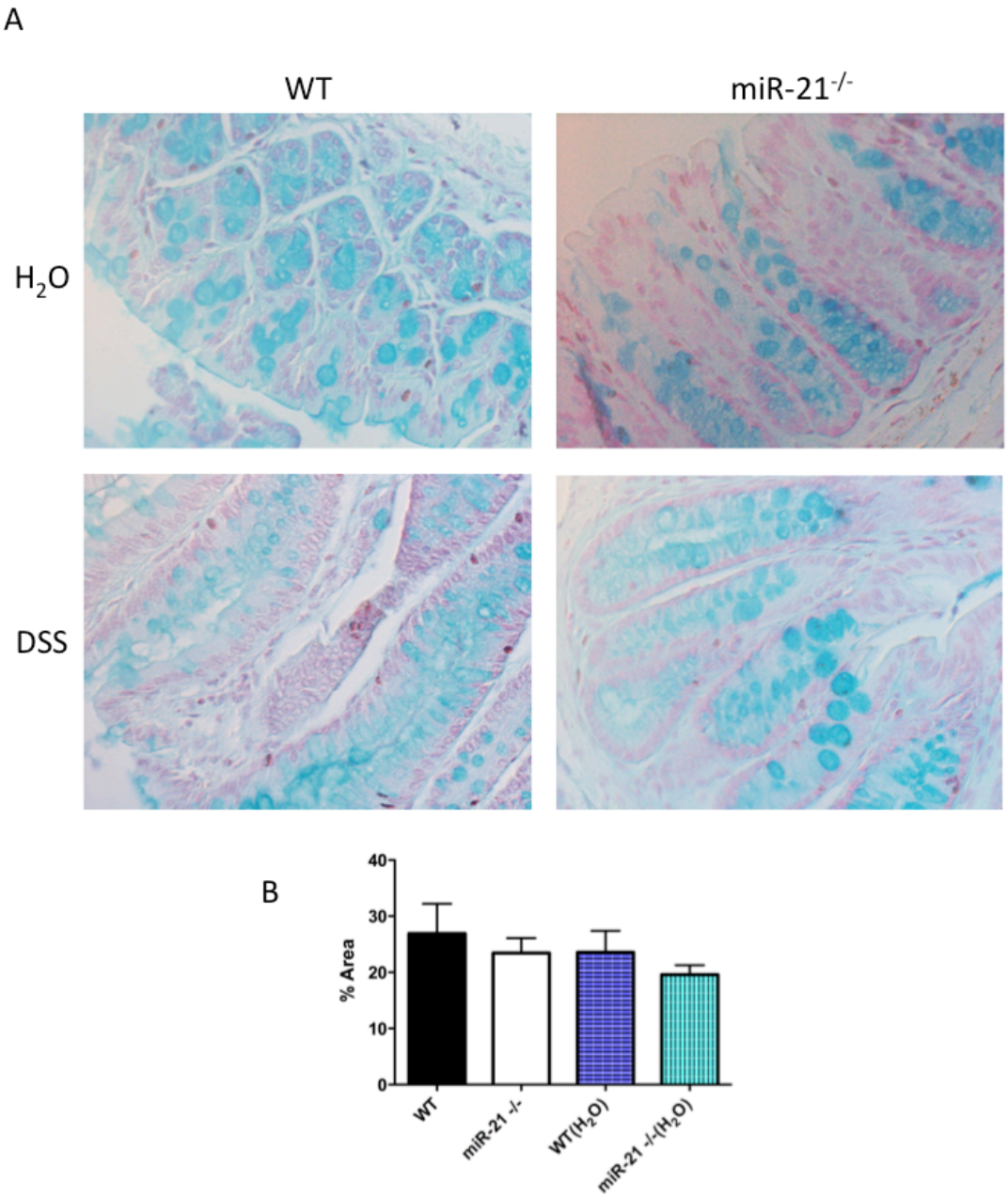

Figure 3.22 Comparison of mucus production between wild-type and miR-21$^{-/-}$ mice post-DSS colitis.

Wild-type (WT) and miR-21$^{-/-}$ mice aged between 8 and 12 weeks were weighed on day 0 and given 2.5% DSS a*d libitum* for 5 days before being switched to normal drinking water. Their weight, stool consistency and occult blood were measured daily throughout the experiment and combined to generate a disease activity index score (C). On day 7, the mice were sacrificed and sections of the colon were taken for histology and stained with Alcian blue and nuclear fast red (A). The percentage area stained with Alcian blue was quantified using ImageJ (B). n= ≥5 per group.

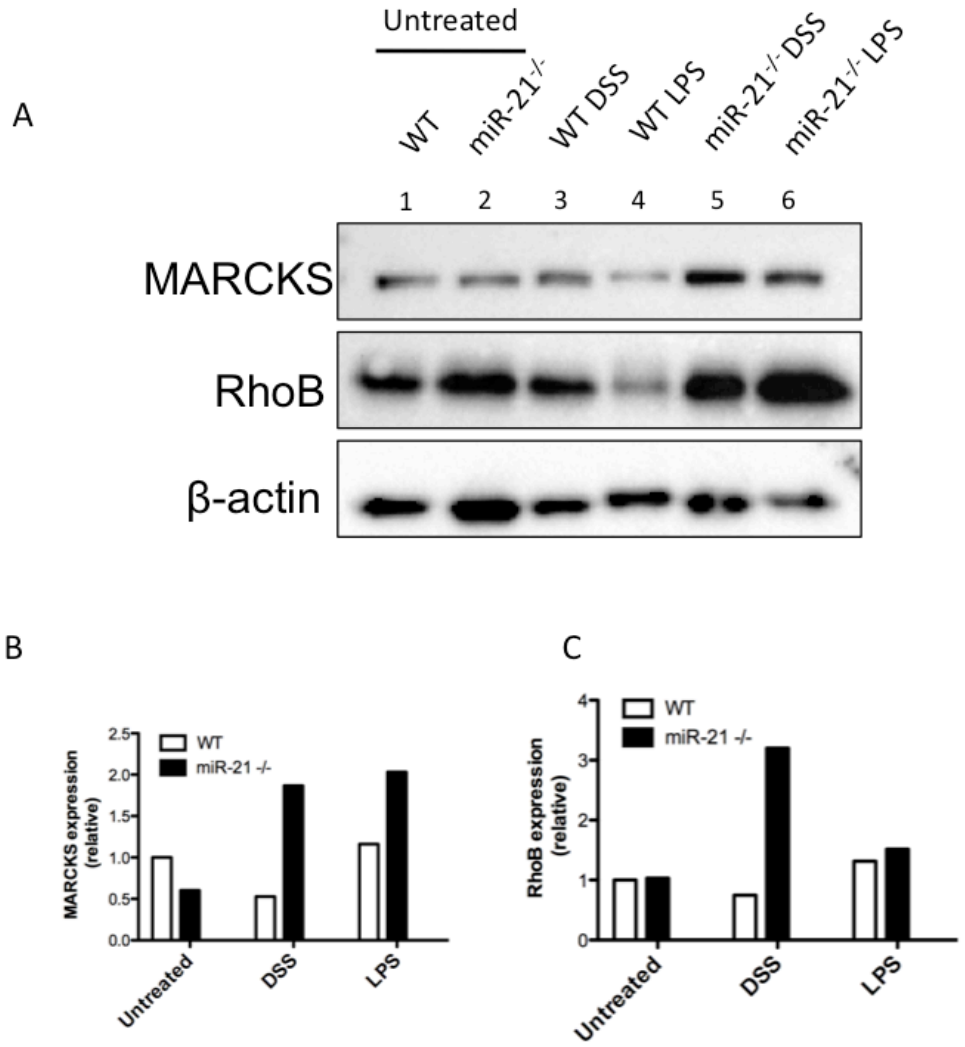

Figure 3.23 Comparison of colonic expression of miR-21 targets MARCKS and RhoB between WT and miR-21$^{-/-}$ mice.

Colon segments of approximately 0.5cm from wild-type (WT) and miR-21$^{-/-}$ mice were cultured overnight in DMEM alone or DMEM containing 3% DSS or 100ng/ml LPS. The following day the explants were weighed and split for proteins and RNA analysis. For protein analysis, the colon segments were homogenised and lysates were resolved by SDS-PAGE, transferred on to a PVDF membrane and probed for MARCKS, RhoB and β-actin (A). Densitometry analysis was performed, normalizing MARCKS (B) and RhoB (C) to actin and expressed relative to WT Untreated. Data shown is representative of two independent experiments.

3.3. Discussion

The role of miRNAs in various aspects of health and disease has received much interest in recent years due to their capacity to regulate a wide variety of biological processes. The miRNA of interest in this project, miR-21, has been thoroughly researched in cancer, where it is an almost ubiquitous marker of disease, but less well studied and characterized in inflammatory diseases [140,144]. In the macrophage, miR-21 has been shown to be an anti-inflammatory mediator including during TLR4 signalling in response to bacterial LPS and during resolution of inflammation by efferocytosis [129,165]. With this in mind, the observation that miR-21 expression is elevated in several chronic inflammatory diseases such as psoriasis and IBD, where resolution of inflammation is inhibited, is intriguing. Interestingly, the data generated in this chapter demonstrates that loss of miR-21 is protective in a mouse model of IBD, which correlates with its increased expression in IBD patients. Furthermore, we show for the first time that this protection is due to modulation of the gut microbiota by miR-21, with loss of miR-21 leading to a less colitogenic microbial community.

Using mice in which miR-21 was deleted, we investigated the influence of miR-21 on development of colitis, and furthermore, we investigated the molecular mechanisms underlying its disease association. Using the chemically-induced DSS colitis model, a marked protection was observed in the miR-21$^{-/-}$ relative to WT controls. miR-21 is induced in colonic tissue of mice in response to DSS, mimicking its elevated expression seen in human IBD and validating this model as relevant for exploring the role of this miRNA in this disease [133]. In a recovery model, in which mice were administered 2.5% DSS for 5 days followed by normal drinking water, we observed that mice lacking miR-21 recover more quickly than their WT counterparts. These results were initially surprising to us, as we had hypothesized that miR-21 would have a beneficial effect in models of colitis due to its previously ascribed role in IL-10 production in macrophages and the well established finding that IL-10-deficient mice develop spontaneous colitis [49,251]. However, at the time of our studies, a research paper was subsequently published which also demonstrated that mice lacking miR-21 are protected from DSS-induced colitis and furthermore, from colitis-associated

colorectal cancer [252,253]. Similar to our own findings, this publication also described a significant protection from the histological features of DSS-induced colitis. Combined, our study and this paper provide evidence that miR-21 plays a pathological role in the development of intestinal inflammation. Indeed, in a subsequent study by Shi *et al*, miR-21 expression is upregulated in IL-10$^{-/-}$ mice, which are susceptible to DSS-induced colitis, indicating that perhaps without an anti-inflammatory signal to repress miR-21 its expression goes unchecked and further propagates disease [252]. To investigate the role of IL-10 in our model, control and DSS-treated colon homogenates were homogenised and analysed for the presence of IL-10 and also the pro-inflammatory cytokine IL-6. IL-10 was inducible upon DSS treatment, and there were significantly lower levels present in the miR-21$^{-/-}$ colon homogenates. This result concurs with the aforementioned studies in macrophages, which demonstrated the miR-21 induction allowed increased IL-10 translation in response to LPS stimulation of TLR4, but is puzzling in the context of a protective colitis phenotype. In contrast to IL-10, IL-6 levels were similar between WT and miR-21$^{-/-}$ mice and did not appear to be particularly inducible with DSS which was also surprising given that IL-6 has been previously implicated in IBD while the monoclonal antibody tocilizumab which targets IL-6, has been approved for treatment of the disease [254].

We wished to further explore the mouse phenotype by testing another colitis model with a different mechanism of action. The infectious attaching-effacing bacterium *Citrobacter rodentium* model of colitis was employed to this end, however despite multiple experiments were performed in an attempts to establish colitis, this model ultimately proved to be ineffective in our animal facility. Indeed, the mice never suffered the weight loss associated with functioning models of IBD, nor did they exhibit any signs of intestinal bleeding, while the diarrhea scores were also inconclusive. The bacterium displayed the normal fecal shedding pattern seen in a functioning colitis-inducing experiment, suggesting that the infection was established in the mice. However, it was cleared from the animals without any symptoms of the disease developing. At this point, it was decided to continue our investigations using the validated DSS-induced colitis model.

Multiple mechanisms are implicated in the development of IBD, and current opinion is that an interaction of host genetic susceptibilities, environmental factors, and the gut microbiota leads to a dysregulation of the mucosal immune system and subsequent development of chronic inflammation [179,216]. Indeed, microbial dysbiosis has been found to play a significant contribution in a number of DSS-induced colitis phenotypes exhibited by transgenic mice with alterations in immune function. One such study demonstrated that the inflammasome component NLRP6 was required for intact host-microbe interaction, and that the exacerbated colitis phenotype exhibited by NLRP6$^{-/-}$ mice in response to treatment with DSS could be transferred to wild-type mice by co-housing [216,255]. As miR-21 is a known regulator of the immunological activity of the bacterial sensor TLR4, we sought to ascertain the significance of the gut microbiota in our mice. Firstly, we observed that following co-housing of mice, WT mice cohoused with miR-21$^{-/-}$ mice displayed a reduced colitis phenotype when compared to the WT control group, which was evident in fecal occult blood and in the diarrhea score. This indicated that mice lacking miR-21 have an altered microbiota compared to their WT counterparts, which offers protection against development of colitis and furthermore, that this protection is transferable. The literature is sparse regarding the potential of miRNAs to modulate the gut microbiota, but given the variety of roles in regulating bacterial sensing it is likely that miRNA may play an indirect role. In one interesting study conducted by Lui *et al*, the authors demonstrated that host miRNA, including miR-21, are present in mouse feces and that they can be taken up by commensal bacteria to alter their gene expression. In addition, this study showed a significant microbial dysbiosis was present in *Dicer* knockout mice which lack all functional miRNAs, and that this dysbiosis could be rescued by re-introducing synthetic miRNA to the mice [256].

To further explore the protective microbiota observed in the miR-21$^{-/-}$ mice, we recolonised germ-free mice with the fecal microbiota of WT or miR-21$^{-/-}$ mice prior to DSS challenge. In this experiment, mice colonised with a miR-21$^{-/-}$ fecal microbiota exhibited protection from DSS-induced colitis relative to the mice colonized with the WT microbiota. A colonoscopy confirmed that the miR-21$^{-/-}$ colonized mice displayed fewer signs of inflammation. Colonoscopy is the current gold standard in IBD diagnosis, and it is becoming increasingly utilised in studies modelling the disease [257]. Surprisingly, weight loss was the one parameter which did not show at

least some degree of protection in these experiments. It had previously been reported that miR-21 expression was downregulated in the caecum of germ-free mice relative to conventional controls, implying that the caecal microbiota impacts on its expression [258]. In order to establish if miR-21 is induced in the DSS colitis model due to increased penetration of the epithelium by commensal bacteria and subsequently enhanced immune activation, miR-21 expression levels were compared in germ-free mice given DSS or water. It was observed that miR-21 expression remains enhanced in these mice upon DSS treatment. This was interesting and points to a mechanism of induction more related to the epithelial damage caused by DSS administration [244]. The mechanisms by which DSS induce this damage are still not well understood, but it is clear that it is one of the primary modes by which it induces disease.

Having shown that the microbiota of the miR-21$^{-/-}$ mouse determines the outcome of DSS-induced colitis, we wished to confirm any differences in the composition of this microbial population compared to that of WT mice. Microbial communities can be assessed in a number of ways, with α diversity referring to the number and distribution of taxa within a given sample and β diversity referring to the number of shared taxa between samples. In order to measure these parameters, we employed 16S rRNA sequencing which allows amplification of DNA from all bacterial species present by amplifying ribosomal RNA along the conserved V3/V4 region and then differentiating between species using the genes variable regions. A preliminary study performed at the Weizmann Institute of Science showed that there are differences between the taxa present in the microbiotas of WT and miR-21$^{-/-}$ mice, however unfortunately, these results were not statistically significant. Despite this, it was interesting to see that miR-21$^{-/-}$ mice display a significantly higher abundance of the family *Rikenellaceae* compared to WT mice. This family has been associated with protection in IBD as well as correlating with increased IL-18 and reduced severity in DSS-induced colitis models [91,259,260]. With these preliminary results as a starting point, 16S rRNA sequencing analysis was carried out commercially (Novogene, China) on a larger number of mice. In depth data analysis was subsequently performed in collaboration with Dr Paul Cotter and Dr Raul Cabrerra-Bello based in Teagasc, Co. Cork. From this subsequent study, we compared loss of α diversity in our mice, as this is often associated with a deleterious dysbiosis in various disease states. α diversity was compared using a number of statistical models and found to be

of a similar level in both WT and miR-21$^{-/-}$ mice, indicating that there was a similar level of species richness in both populations. In order to assess whether or not these populations shared similar species, β diversity was assessed as in the preliminary study and found to be significantly different between WT and miR-21$^{-/-}$ fecal bacterial populations. This supported the case for an altered, protective microbiota being present in the miR-21$^{-/-}$ intestinal compartment. In order to explore the composition of the WT and miR-21$^{-/-}$ microbiota further, the 16S sequences obtained were compared to the Green Genes database (standard with the QIIME pipeline) and these sequences were matched with existing OTUs. The top 25 most abundant OTUs in WT and miR-21$^{-/-}$ mice were compared and there was several significant differences noted. Several of the observed differences pointed towards a potentially protective microbial signature in the miR-21$^{-/-}$ mouse, including a generally higher abundance of genera within the *Firmicute* phylum which correlates with protection against IBD while there was a lesser abundance of *Bacteroidetes* and *Prevotella* which correlates with development of IBD [261,262]. The higher abundance in the gram positive probiotic genus A*ctinobacterium* and *Bifidobacterium* can also be interpreted as evidence of a protective microbiota as several studies have indicated a reduction in the severity of DSS-induced disease in mice treated with members of these genus [263-265]. We next performed a taxa analysis to compare the relative proportions of different bacterial groupings at various taxonomic levels. Surprisingly, at the phylum level there was an increased presence of *Proteobacteira* in the miR-21$^{-/-}$ mice which would run counter to the idea of a protective microbiota. This phylum of gram-negative bacteria generally increase in proportion in IBD with a commensurate decrease in *Firmicutes* [266,267]. Further down the taxa, at family level the fecal microbiota of the mice lacking miR-21 display an increased proportion of *Bifidobacteriaceae* and *Peptostreptococcaceae* relative to the WT microbiota, and at genus level an increase in *Bifidobacterium* and *Odoribacter,* all of which correlate with a healthy microbiota in various studies [268,269]. Overall, these data confirm that there is an altered microbiota in the miR-21$^{-/-}$ knockout mouse, with some of these alterations correlating with studies that indicate protective associations with IBD and mouse models of colitis.

As a final confirmation that the microbiota of miR-21$^{-/-}$ mice confers protection against DSS-induced colitis, we determined the consequence of depleting this

microbiota by administering antibiotics to mice prior to challenged with DSS. Both WT-depleted and miR-21$^{-/-}$-depleted mice displayed increased detectable fecal occult blood and higher diarrhea scores earlier in the experiment. However interestingly, the protective phenotype previously observed in the miR-21$^{-/-}$ mouse was lost following antibiotic treatment, as demonstrated in each of disease scores and overall DAI score. The increase in intestinal haemorrhage in antibiotic-treated mice has been observed in other studies, and may contribute to the enhanced fecal occult blood scores noted in this experiment [270]. Most striking of all the observations in this experiment was the highly significant increase in sickness behaviour (measured by loss of mobility) and associated mortality displayed in the miR-21$^{-/-}$ mice treated with antibiotics. This finding confirms that the microbiota of miR-21$^{-/-}$ mice is protective in DSS-induced colitis. However, to seek further confirmation of this finding it would be interesting to generate germ-free miR-21$^{-/-}$ mice and to challenge them with the DSS model of colitis. This would rule out any influence from PAMPs aberrantly released due to antibiotic killing of the microbiota which may trigger inflammation.

The final step of this study sought to elucidate how miR-21 expression might influence the microbiota. Firstly we assessed any role for sIgA, which is a major player in the shaping of the composition of bacteria communities in the gut albeit through relatively poorly understood mechanisms [271]. Certain IgA clones have been shown to selectively bind harmful pathogenic bacteria in models of IBD and act in a protective manner by promoting restoration of a correct microbial balance [272]. To determine whether miR-21 might affect secretion of IgA in to the gut lumen, sIgA levels in the stools of WT and miR-21$^{-/-}$ mice were assessed, however there was no significant difference between the groups of mice. Next we assessed whether miR-21 might regulate the production of mucins from the epithelium, as the composition of the mucous layer and effective mucus secretion are crucial for maintaining a homeostatic balance of gut bacteria [41,255,273]. In order to assess whether or not the mucus barrier in miR-21$^{-/-}$ mice was different to that of WT mice, colonic sections from control WT and miR-21$^{-/-}$ mice and WT and miR-21$^{-/-}$ mice treated with antibiotics were stained with the broad mucus stain Alcian blue and the mucus present was quantified using ImageJ software. This analysis demonstrated that there was no significant difference between WT and miR-21$^{-/-}$ in the mucus layer. There was more mucus observed in water controls compared to DSS treated mice, although this

difference was not statistically significant. Alcian blue is a broad glycan stain that will dye all mucins present in the tissue. In the gut, Muc2 is the most abundant mucin and so, whilst our experiments indicate that the secretion of this mucin is likely unchanged, other mucins might be lost by broad staining in this manner [274]. With this in mind, the miR-21 target, MARCKS, which is involved in regulation of mucin secretion, was identified from comparative database searches. MARCKS has been shown to regulate secretion of the mucin Muc5AC in airways [249]. We hypothesized that miR-21 deletion may allow increased MARCKS expression and ultimately allow for favourable mucin secretion as an available nutrient to support an altered microbiota. Using a colon explant model, it was demonstrated that miR-21 deletion does indeed allow for enhanced MARCKS expression in response to both DSS and LPS, but that basally its expression is actually lessened. Previous studies have also identified a role for the miR-21 target RhoB in regulating epithelial barrier permeability. Of course, intestinal barrier permeability has been well established to be associated with microbial dysbiosis. In a study of miR-21$^{-/-}$ mice, enhanced RhoB expression was associated with heightened barrier integrity and reduced colitis severity [133,252]. In our analysis using colon explants, we have also demonstrated an increase in RhoB expression in miR-21$^{-/-}$ mice in response to DSS treatment. This would lead to an enhanced epithelial barrier needed to maintain a healthy microbiota, as it has been shown that a "leaky" gut leads to deleterious alterations in the intestinal microbiota [275,276].

In summary, our findings demonstrate that miR-21 expression is deleterious in the DSS model of IBD, and that the intestinal microbiota is crucial to the course of this disease progression. Our findings identify a novel role for miR-21 in regulating the composition of the intestinal microbiota.

Chapter 4
-
miR-21 limits infection by *Listeria monocytogenes*

4. miR-21 limits infection by *Listeria monocytogenes*

4.1. Introduction

Macrophages form a crucial part of our body's defence, with the ability of macrophages to engulf and digest invading pathogens, termed phagocytosis, being fundamental to the control of infection [277]. Bacterial pathogens are sensed through the expression of PRRs on phagocytes, including TLRs expressed on the phagocyte cell surface and membranes of vesicular compartments that recognize PAMPs, [29,278]. The sensing of these PAMPs leads to the activation of multiple signalling pathways which result in the production of cytokines to alert nearby immune cells as well as phagocytosis and intracellular killing of the ingested microbe [279].

The initial stage of phagocytosis involves triggering of intracellular signalling pathways leading to actin polymerization, cytoskeleton rearrangements which causes remodelling of the cell surface to form plasma membrane extensions. These extensions referred to as pseudopods lead to formation of a phagocytic cup which subsequently encloses around the bacterium so that it becomes engulfed into the cell in an enclosed structure referred to as the phagosome. The phagosome subsequently undergoes a series of maturation steps which involves fusion with endosomal vesicles and fission vesicles, moving through early, intermediate and late stages culminating in formation of the mature phagolysosome which has acquired the full bactericidal repertoire, including acidification and ability to generate bacteriocidal free radicals [13]. In this way, macrophages play a critical role in host responses to intracellular pathogens and the clearance of infections which significantly contribute to the high morbidity and mortality rates associated with infectious diseases worldwide. However, certain intracellular bacteria have evolved strategies which allow them to exploit these intracellular niches. *Listeria* is a gram-positive pathogen responsible for the group of systemic infections known as listeriosis, associated with a fatality rate of 30% or more and the second leading cause of death due to food-borne infection[101]. *Listeria* have evolved to escape from the phagolysosome through the expression of a hemolysin, LLO, and subsequently grow and replicate within the cytosol of

macrophages. The ability of bacteria like *Listeria* to establish an intracellular niche and evade immune surveillance typifies the struggle between infectious agents and the host immunity and is critical to the outcome of infection [102].

As previously mentioned in this thesis, miRNA have emerged as critical regulators of host immune responses [109,111,114] and have been implicated in the regulation of immune cell function including the fine-tuning of PRR signalling [116,130,131]. Although, there is growing understanding that regulation of miRNA expression is a crucial part of the host response to bacterial infection, knowledge of their cellular expression in response to bacteria and the impact of this on the outcome of infections is limited. Furthermore, modulation of miRNAs has emerged as a novel strategy employed by bacterial pathogens to manipulate host cell pathways and survive within host cells. MiR-21 was shown to regulate expression of the anti-inflammatory cytokine IL-10 in macrophages in response to bacterial LPS, by targeting PDCD4, a negative regulator of IL-10 translation [129,144]. A study of asthma showed that miR-21 negatively regulates immune responses in dendritic cells, by controlling the production of pro-inflammatory IL-12 [161,164]. In addition, miR-21 has also been implicated in positively regulating the phenomenon of efferocytosis whereby activated macrophages ingest dying cells and prevent further inflammation [165]. MiR-21 has been previously been shown under certain contexts to act as a break in the differentiation of macrophages to an M2-like phenotype, allowing a more robust bactericidal M1 macrophage to emerge. Although the role of miR-21 in the host response to bacterial pathogens is relatively unexplored, this implies a potentially important role for miR-21 in the control of infection [162].

The aim of this chapter was to explore the significance of miR-21 expression during bacterial infection *in vivo* using the miR-21$^{-/-}$ mouse, and more specifically using primary bone-marrow-derived macrophages (BMDMs), to elucidate its role phagocytosis of invading bacteria, in particular the intracellular pathogens *L. monocytogenes* and *Salmonella enterica* subsp. Typhimurium (*S.* Typhimurium UK-1).

4.2. Results

4.2.1. miR-21 is induced by TLR4 stimulation in RAW264.7 macrophages and BMDMs

Previous studies have demonstrated that miR-21 is induced in response to LPS [129,280]. In order to confirm these reports, the macrophage like cell line RAW 264.7 was initially employed. miR-21 was induced early in the experiment, with the induction waning slightly before reaching its peak at 10-fold induction at 24 hours (Fig. 4.1A) . Subsequently, WT BMDMs were generated and treated with LPS. These cells are a very representative macrophage for experimental studies and the model of choice for this project. Upon treatment with LPS, miR-21 is induced in BMDMs peaking at 20-fold induction at 4 hours and remaining at this level through to 8 hours before dropping at 24 hours (Fig. 4.1B). This was in agreement with previous observations regarding miR-21 induction in these cell types [129].

4.2.2. miR-21 expression alters TLR-stimulated cytokine secretion in BMDMs

LPS binding to TLR4 induces multiple signalling events which lead to the transcription, translation and secretion of cytokines. As miR-21 has been demonstrated to regulate the production of these crucial immune mediators, it was decided to explore the effect of miR-21 deletion on cytokine production. With this in mind, BMDM were generated from WT and miR-21$^{-/-}$ mice and cytokines secretion measured in response to LPS (Fig. 4.2). LPS induced IL-10, IL-6 and TNF-α secretion was assessed in both WT and miR-21$^{-/-}$ BMDMs after the course 24 hours treatment. The most consistent timepoints, 1h and 24h, are presented here (Fig 4.2). Previous reports have described a role for miR-21 in allowing translation of the anti-inflammatory cytokine IL-10 via degradation of PDCD4. In keeping with this observation, IL-10 secretion was observed to be reduced in BMDMs deficient in miR-21 (Fig. 4.2A) though this difference was not statistically significant. The secretion of pro-inflammatory cytokine IL-6 was heightened in the miR-21$^{-/-}$ cells, but this effect was inconsistent and not statistically significant (Fig. 4.2B). However, there was a significant increase in the levels of TNF-α by miR-21$^{-/-}$ BMDMs relative to WT cells, which was detectable at both 1h and 24h in keeping with previously published studies (Fig. 4.2C). Other TLRs have been shown to influence miRNA expression and signal

for cytokine secretion in response to infection or damage, and so it was decided to explore the effect of stimulation of TLR1/2 and TLR3 using the synthetic ligands Pam3CSK4 and Poly (I:C) respectively (Fig. 4.3). After 24 hours treatment, IL-10 secretion was reduced in miR-21$^{-/-}$ macrophages relative to WT cells upon treatment with stimulation of both TLR1/2 and TLR3 (Fig. 4.3A). IL-6 levels were very similar in both WT and miR-21$^{-/-}$ macrophages with both agonists, aside from a slight reduction apparent in the Poly (I:C) treated miR-21$^{-/-}$ cells (Fig. 4.3B) in contrast to the previous LPS stimulation in Figure 4.2. TNF-α levels were higher in miR-21$^{-/-}$ macrophages treated with Pam3CSK4 compared to WT cells, but unchanged in response to the TLR3 agonist Poly (I:C) (Fig. 4.3C).

4.2.3. miR-21 expression alters LPS induced cytokine secretion in BMDCs.

Dendritic cells (DCs) are a vital link between the innate and adaptive immune system through their capacity to sense danger signals and present antigen to T cells. In order to sense these danger signals DCs, like macrophages, express a variety of PRRs including TLR4. As DCs have a distinct but overlapping role in the immune response to gram-negative pathogens, experiments were carried out to assess if their cytokine response was affected by miR-21 expression, as was the case in BMDMs. Bone marrow-derived DCs (BMDCs) were cultured from WT and miR-21$^{-/-}$ progenitor cells to this end. Upon LPS treatments, similar cytokine levels were obtained as to those seen in BMDMs after 24 hours stimulation (Fig. 4.4). Cells lacking miR-21 again displayed reduced IL-10 secretion relative to WT cells, and again not quite reaching statistical significance (Fig. 4.4A). IL-6 levels were no different between WT and miR-21$^{-/-}$ BMDCs and consistent with data obtained in experiments with BMDMs (Fig. 4.4B), miR-21$^{-/-}$ cells secrete significantly higher levels of TNF-α than WT cells after 24 hours treatment with LPS (Fig. 4.4C). Given the importance of DCs to the shaping of adaptive responses via T cell polarization, the Th1 polarizing cytokine IL-12 was also measured. miR-21 has previously been shown to target the mRNA of the p35 subunit of this cytokine, and indeed in BMDCs miR-21 deletion allows significant IL-12 secretion to occur relative to WT controls after 24 hours treatment with LPS (Fig. 4.5). This is consistent with previous reports demonstrating miR-21 limiting the inflammatory Th1 response in the lung [161,164].

4.2.4. miR-21 restricts LPS-induced TNF-α secretion *in vivo*.

In order to test the relevance of the previous *in vitro* observations *in vivo*, the LPS-induced sepsis model was used to test the levels of cytokine induction in mice (Fig. 4.6). WT and miR-21$^{-/-}$ mice were injected for 4 hours (Fig. 4.6A and B) or 24 hours (Fig. 4.6C and D) with 15mg/kg LPS, and circulating serum cytokines were measured. After 4 hours, IL-10 levels were similar between WT and miR-21$^{-/-}$ mice, but significantly higher levels of TNF-α were detectable in the serum of the miR-21$^{-/-}$ animals. Unsurprisingly, higher absolute levels of IL-10 and TNF-α were detectable after 24 hours, and again there was a significantly higher level of TNF-α detectable in the serum of the miR-21$^{-/-}$ mice (Fig. 4.6D).

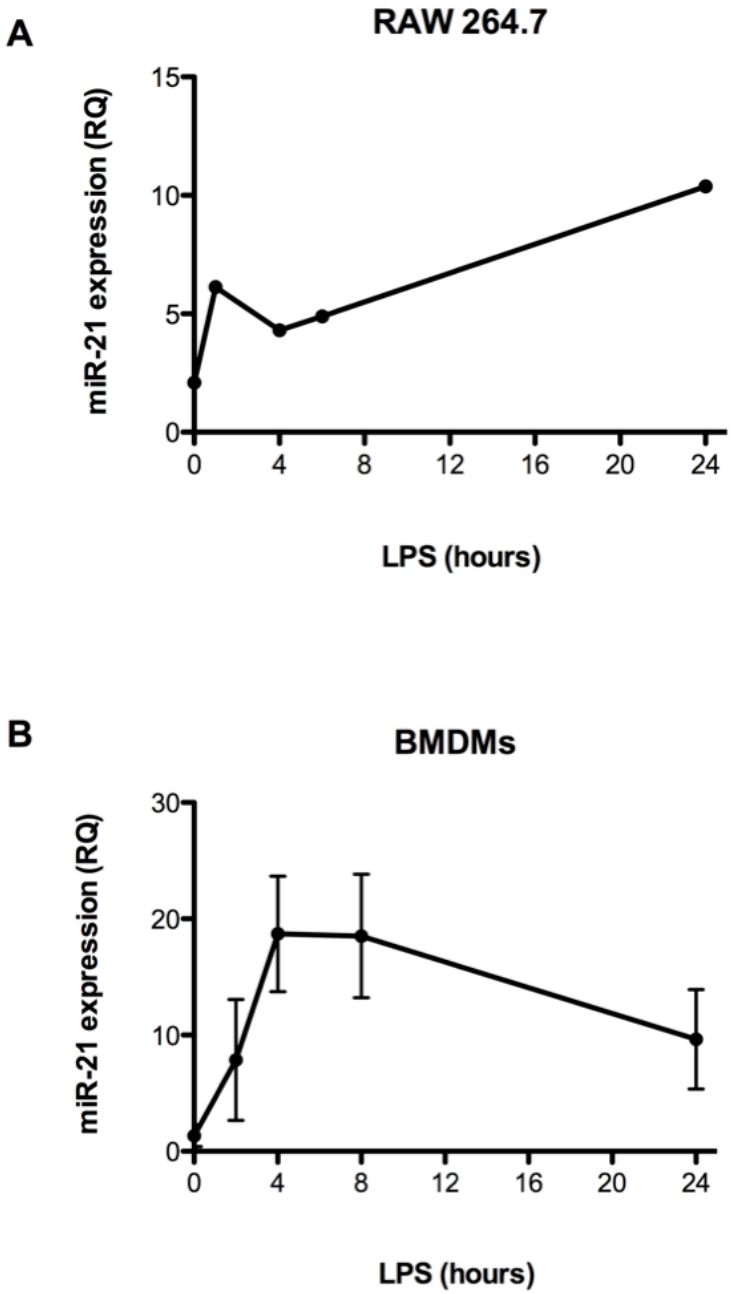

Figure 4.1 miR-21 is induced by TLR4 stimulation in RAW264.7 macrophages and BMDMs.

A) RAW 264.7 cells were plated at $5x10^5$/ml in 12 well plates and incubated overnight at 37°C in FCS-supplemented DMEM media. The following day, the media on the cells was replaced with either fresh media, or fresh media containing 100ng/ml LPS and incubated for various times. MiR-21 levels in the lysates were quantified using the ΔΔCt method relative to U6. Data presented are representative of an individual experiment. B) BMDMs were plated at $5x10^5$/ml in 12 well plates and incubated overnight at 37°C in FCS-supplemented DMEM media with 10% L929 media. The following day, the media on the cells was replaced with either fresh media or fresh media containing 100ng/ml LPS and incubated for various times. MiR-21 levels in the lysates were quantified using the ΔΔCt method relative to untreated controls using U6 as an endogenous control. Data presented are representative of an individual experiment. Data are presented as mean±SD, n=3, relative quantitation (RQ) relative to 0h control.

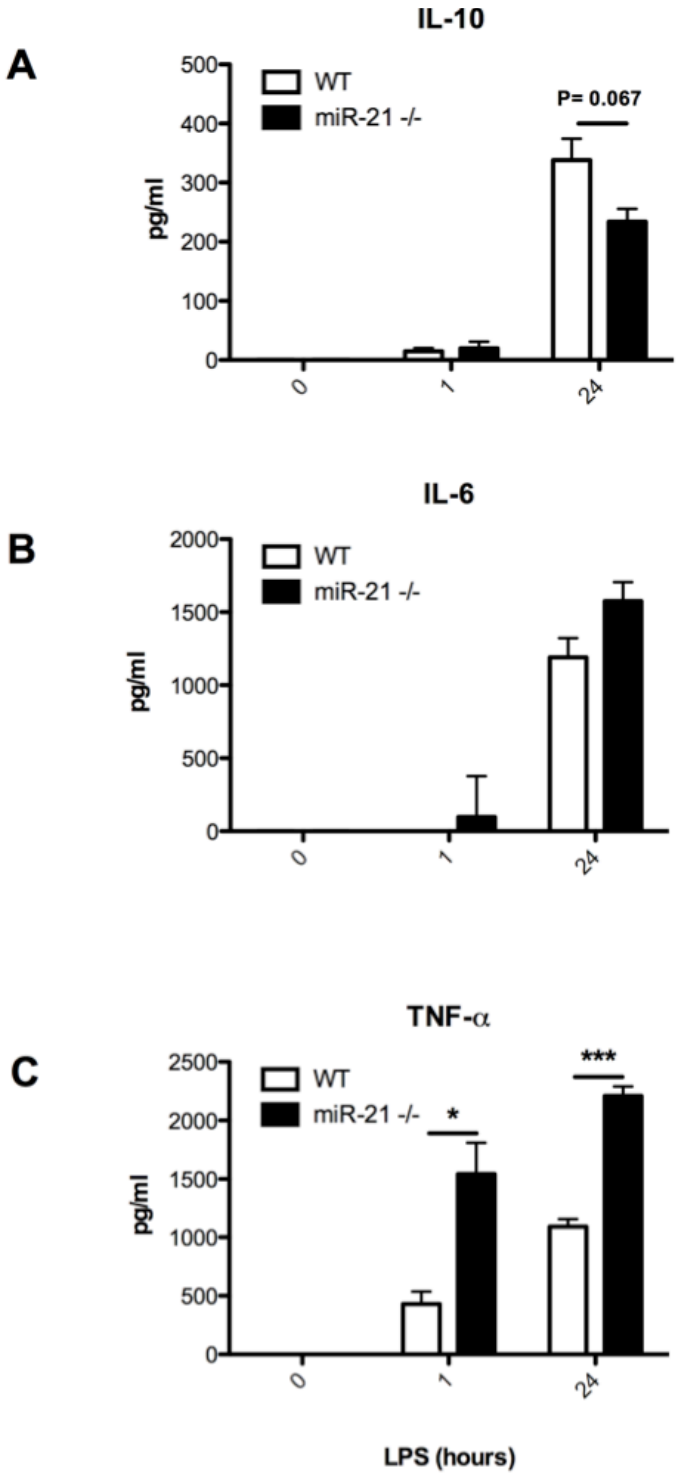

Figure 4.2 Comparison of cytokines secretion in WT versus miR-21$^{-/-}$BMDMs in response to LPS.

Wild-type (WT) or miR-21$^{-/-}$ BMDMs were plated at 5x10^5/ml in 12 well plates and incubated overnight at 37°C in FCS-supplemented DMEM media with 10% L929 media. The following day, the media on the cells was replaced with either fresh media or fresh media containing 100ng/ml LPS and incubated for various times. Supernatants were collected and analysed for the presence of IL-10 (A), IL-6 (B) and TNF-α (C) by ELISA . Data are presented as mean±SD, n=3. P values were calculated using student's T test (* $p<0.05$, ***$p<0.001$).

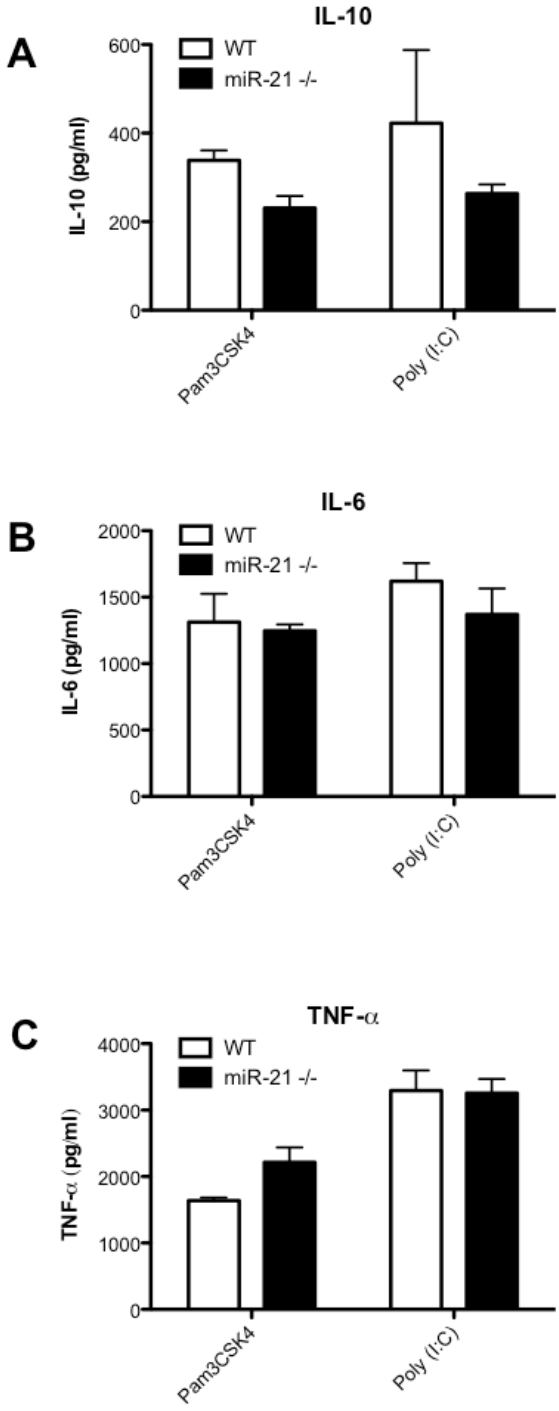

Figure 4.3 Comparison of cytokines secretion in WT versus miR-21$^{-/-}$BMDMs in response to other TLR agonists.

Wild-type (WT) or miR-21$^{-/-}$ BMDMs were plated at 5x10^5/ml in 12 well plates and incubated overnight at 37°C in FCS-supplemented DMEM media with 10% L929 media. The following day, the media on the cells was replaced with either fresh media or fresh media containing 1μg/ml Pam3CSK4 or Poly (I:C) and incubated for various times. Supernatants were collected and analysed for the presence of IL-10 (A), IL-6 (B) and TNF-α (C) by ELISA . Data are presented as mean±SD of two independent experiments.

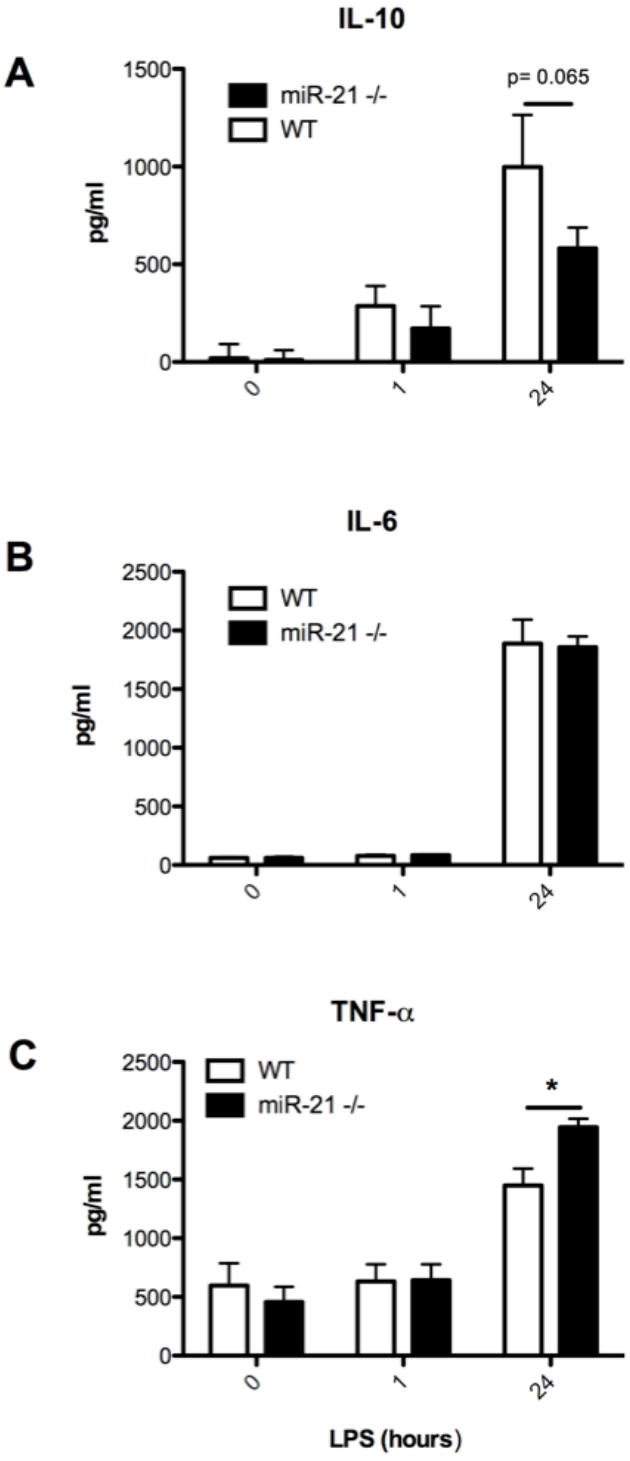

Figure 4.4 Comparison of cytokines secretion in WT versus miR-21$^{-/-}$ BMDCs in response to LPS.

Wild-type (WT) or miR-21$^{-/-}$ BMDCs were plated at 5x10^5/ml in 12 well plates and incubated overnight at 37°C in FCS-supplemented DMEM media with 20% GM-CSF enriched media. The following day, the media on the cells was replaced with either fresh media or fresh media containing 100ng/ml LPS and incubated for 1h and 24h. The concentrations of IL-10 (A), IL-6 (B), TNF-α (C) were measured by ELISA. Data is expressed as mean±SEM, n=3. P values were calculated using Student's T test such that * indicates $p<0.05$).

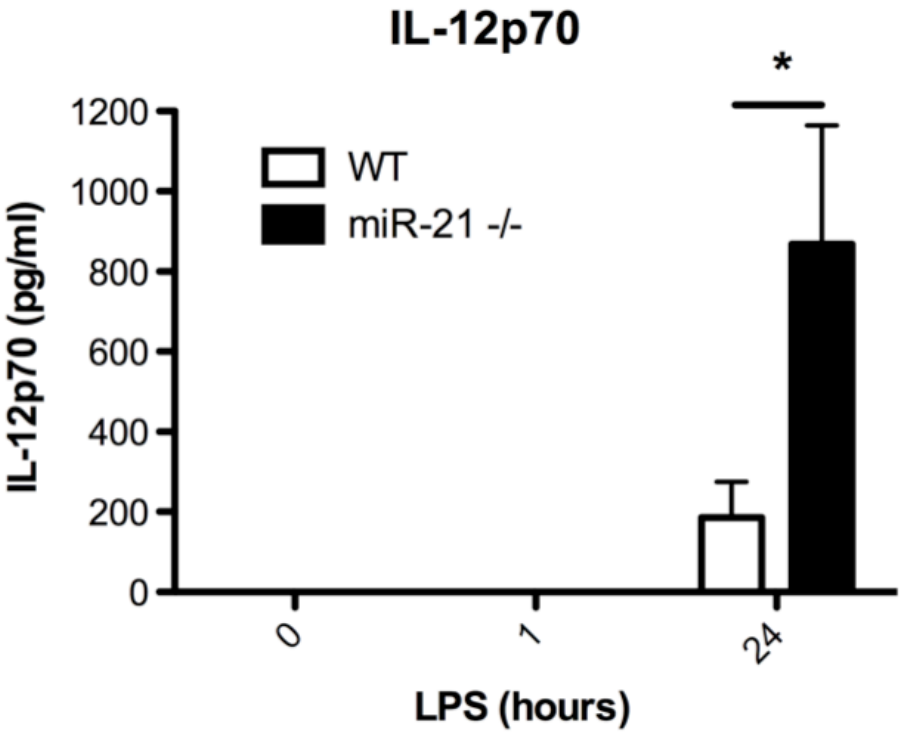

Figure 4.5 Comparison of IL-12p70 secretion in WT versus miR-21$^{-/-}$ BMDCs in response to LPS.

Wild-type (WT) or miR-21$^{-/-}$ BMDCs were plated at 5x10^5/ml in 12 well plates and incubated overnight at 37°C in FCS-supplemented DMEM media with 20% GM-CSF enriched media. The following day, the media on the cells was replaced with either fresh media or fresh media containing 100ng/ml LPS and incubated for 1h and 24h. The concentration of IL-12p70 was measured by ELISA. Data is expressed as mean±SEM, n=3. P values were calculated using Student's T test such that * indicates $p<0.05$).

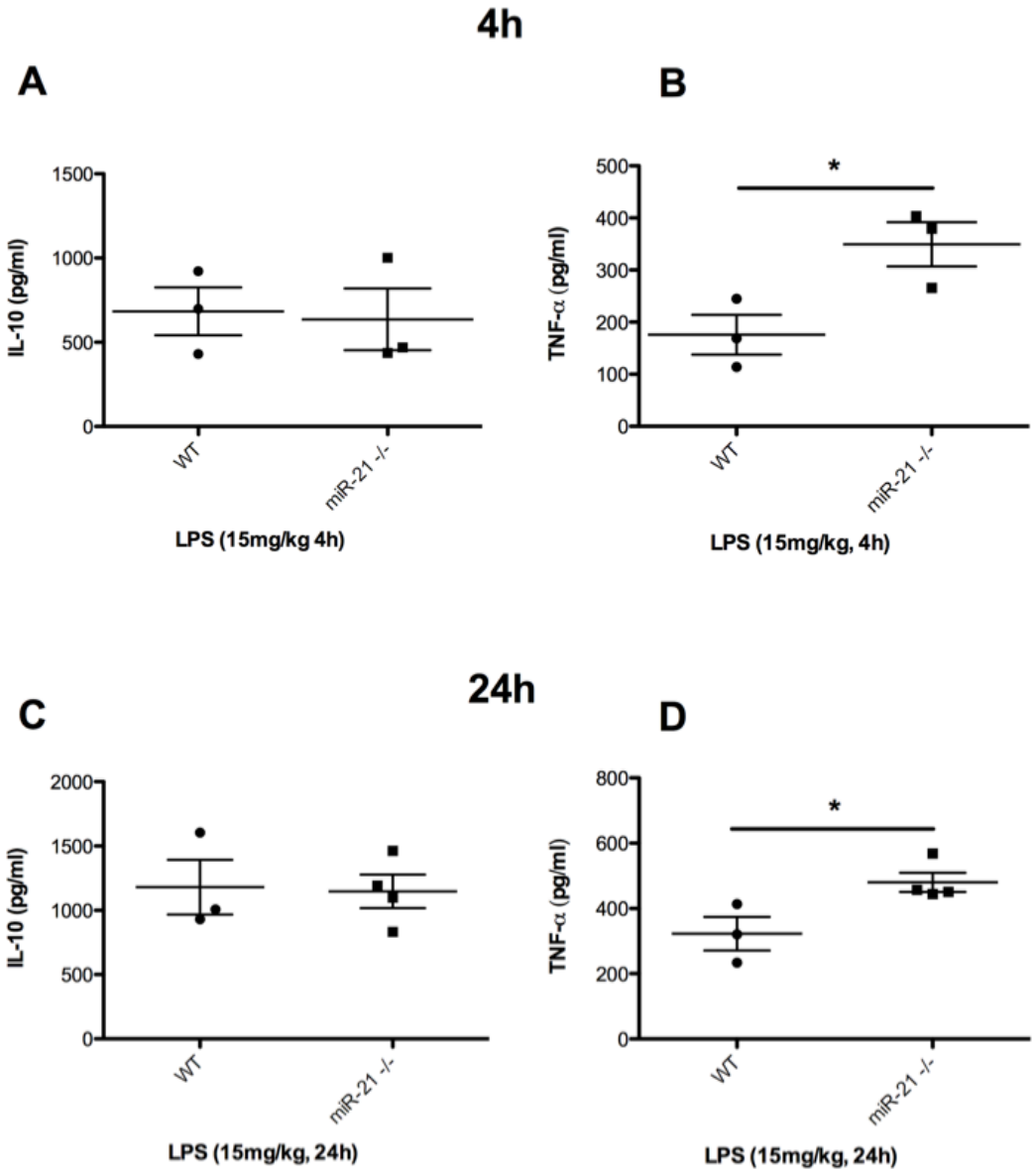

Figure 4.6 Comparison of serum cytokine response of WT versus miR-21$^{-/-}$ mice in response to intraperitoneal LPS challenge.

Wild-type (WT) and miR-21$^{-/-}$ mice were challenged with LPS 15mg/kg for 4 (A and B) or 24 (C and D) hours before being sacrificed using CO_2 and cervical dislocation. Blood was extracted by terminal bleed and centrifuged to obtain serum. The concentrations of IL-10 (A,C) and TNF-α (B,D) in the serum were measured by ELISA. Data is expressed as mean±SEM, n≥3. P values were calculated using Student's T test such that * indicates $p<0.05$).

4.2.5. miR-21 is induced in BMDMs in response to bacterial infection in a time dependent manner.

Having confirmed that miR-21 is induced upon stimulation of TLR4 with purified LPS, experiments were conducted infecting BMDMs with live gram positive and gram-negative bacteria (Fig. 4.7). *L. monocytogenes* EGDe and *S.* Typhimurium UK-1 were chosen as model organisms. Both strains induced miR-21 expression at early times [2-4 hours post-infection (p.i.)], with *Salmonella* inducing its expression 10-fold at early time points during infection before subsequently receding to levels below untreated controls 24 hours p.i.. *Listeria* induced miR-21 to a lesser extent and at a later time, but this response also proceeded to wane and return to baseline levels at 24 hours p.i.. This was in contrast to the sustained expression of miR-21 seen in LPS-treated BMDMs.

4.2.6. miR-21-deletion increases TNF-α secretion in response to *Listeria* infection

Having established that miR-21 is induced during bacterial infection, cytokine release in response to infection was assessed in WT and miR-21$^{-/-}$ BMDMs and BMDCs after 24 hours infection (Fig. 4.8). Surprisingly, no differences were observed between WT and miR-21$^{-/-}$ BMDMs in cytokine levels 24h p.i. with *Salmonella* or *Listeria*. *Listeria* induced high levels of IL-10 in contrast to *Salmonella* (Fig. 4.8A), and similar secretion levels of IL-6 were also evident for both infections (Fig. 4.8B). No TNF-α was detected 24 hours p.i. with *Salmonella*, however the consistent difference in secretion seen between WT and miR-21$^{-/-}$ BMDMs treated with LPS was evident after *Listeria* infection. These experiments were also performed in BMDCs (Fig. 4.9). Data from BMDCs were more variable, and so while there was a difference in TNF-α secretion post-*Salmonella* infection this was not deemed to be significant (Fig. 4.9C).

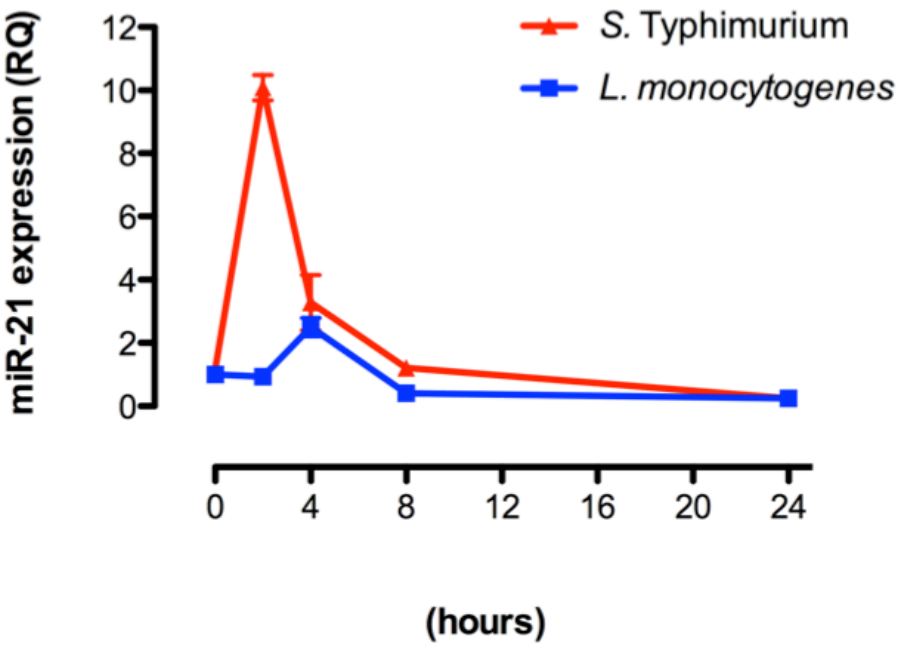

Figure 4.7 miR-21 is induced in macrophages following bacterial infection.

BMDMs were plated at $5x10^5$/ml in 12 well plates and incubated overnight at 37°C in FCS-supplemented DMEM media with 10% L929 media. The following day, the cells were washed with warm PBS and the media was replaced with antibiotic-free DMEM. The cells were then infected with *Salmonella* or *Listeria* at an MOI of 50. After 15 min, the cell monolayers were washed and the media was replaced with media containing gentamicin to kill extracellular bacteria. At the end of the infection, the cells were lysed and miR-21 expression quantified using the ΔΔCt method relative to untreated controls using U6 as an endogenous control. Data presented are representative of an individual experiment. Data are presented as mean±SD, n=3, relative quantification (RQ) relative to 0h control.

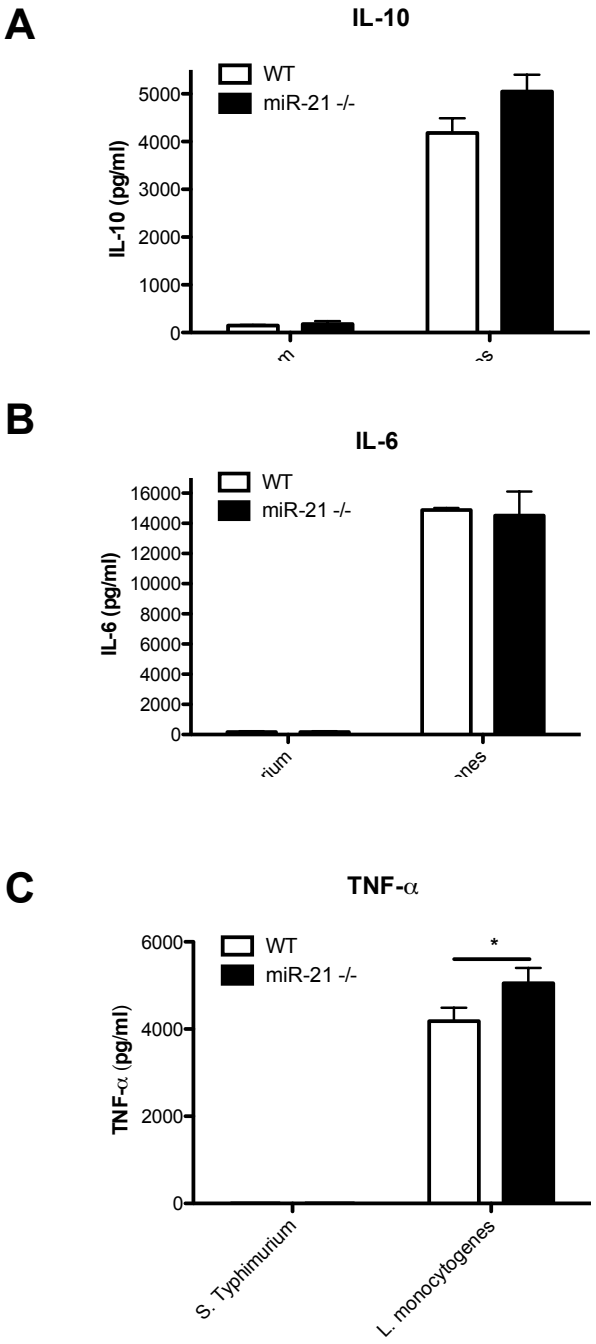

Figure 4.8 Comparison of cytokine secretion by WT versus miR-21$^{-/-}$ BMDMs in response to bacterial infection.

Wild-type (WT) or miR-21$^{-/-}$ BMDMs were plated at 5x10^5/ml in 12 well plates and incubated overnight at 37°C in FCS-supplemented DMEM media with 10% L929 media. The following day, the cells were washed with warm PBS and the media was replaced with antibiotic-free DMEM. The cells were then infected with *Salmonella* or *Listeria* at an MOI of 100. After 15 min, the cell monolayers were washed and the media was replaced with media containing gentamicin to kill extracellular bacteria. After 24h, the The concentrations of IL-10 (A), IL-6 (B), TNF-α (C) in the supernatant were measured by ELISA. Data are presented as mean±SD, n=3. P values were calculated using Student's T test such that * indicates $p<0.05$).

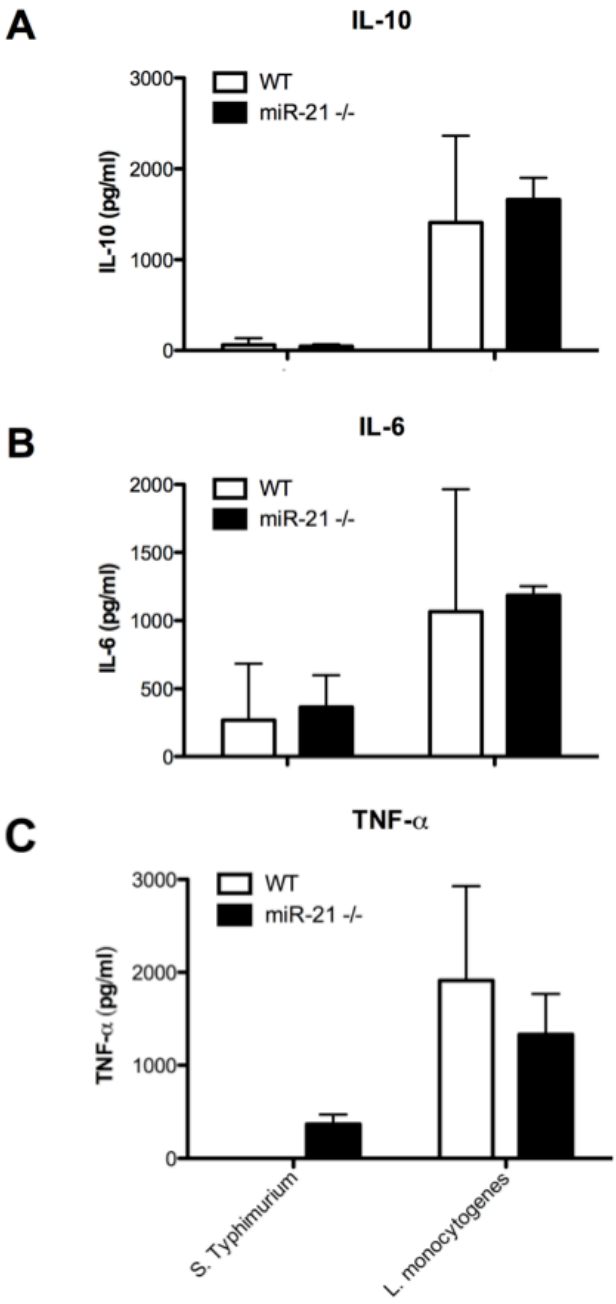

Figure 4.9 Comparison of cytokine secretion by WT versus miR-21$^{-/-}$ BMDCs in response to bacterial infection.

Wild-type (WT) or miR-21$^{-/-}$ BMDCs were plated at 5x10^5/ml in 12 well plates and incubated overnight at 37°C in FCS-supplemented DMEM media with 10% GM-CSF containing media. The following day, the cells were washed with warm PBS and the media was replaced with antibiotic-free DMEM. The cells were then infected with *Salmonella* or *Listeria* at an MOI of 100. After 15 min, the cell monolayers were washed and the media was replaced with media containing gentamicin to kill extracellular bacteria. After 24h, the concentrations of IL-10 (A), IL-6 (B), TNF-α (C) in the supernatant were measured by ELISA. Data are presented as mean±SD, n=3.

4.2.7. miR-21 controls bacterial burden post-*Listeria monocytogenes* infection

At the outset of this project, the role of miR-21 in the process of infection by intracellular pathogens was relatively unexplored. In order to address this, the two model bacteria above were used to infect WT and miR-21$^{-/-}$ BMDMs and BMDCs. The well described gentamicin protection assay was employed, whereby cells are incubated together with the pathogen for a brief period before being washed and cultured in media containing the broad spectrum antibiotic gentamicin to kill extracellular bacteria [281]. BMDMs were tested to explore their capacity to kill invading bacteria intracellularly over the course of 24 hours (Fig. 4.10). In WT BMDMs, colony forming units (CFUs) of both *Salmonella* (Fig. 4.10A) and *Listeria* (Fig. 4.10B) were reduced over the course of the experiment and found to be significantly reduced after 24 hours. To test the role of miR-21 in this system, timepoints of 30 minutes (0.5 hours) and 2 hours were chosen to represent the initial bacterial uptake and beginning of intracellular killing respectively. WT and miR-21$^{-/-}$ BMDMs and BMDCs were infected with *Salmonella* (Fig. 4.11) and uptake and intracellular killing were assayed. In BMDMs, there was no difference in LogCFU/ml at either timepoint (Fig. 4.11A and B) and the same was the case in BMDCs (Fig. 4.11C and D). The same experiments were performed using *Listeria* (Fig. 4.12) and in this case there was a marked increase in bacterial CFUs (expressed as LogCFU/ml) present in BMDMs lacking miR-21 after both 30 minutes and 2 hours (Fig. 4.12A and B). This was also observed in miR-21$^{-/-}$ BMDCs at the same timepoints (Fig. 4.12C and D). As BMDMs and BMDCs displayed similar phenotypic responses to LPS stimulation and infection, it was decided to proceed solely with BMDMs.

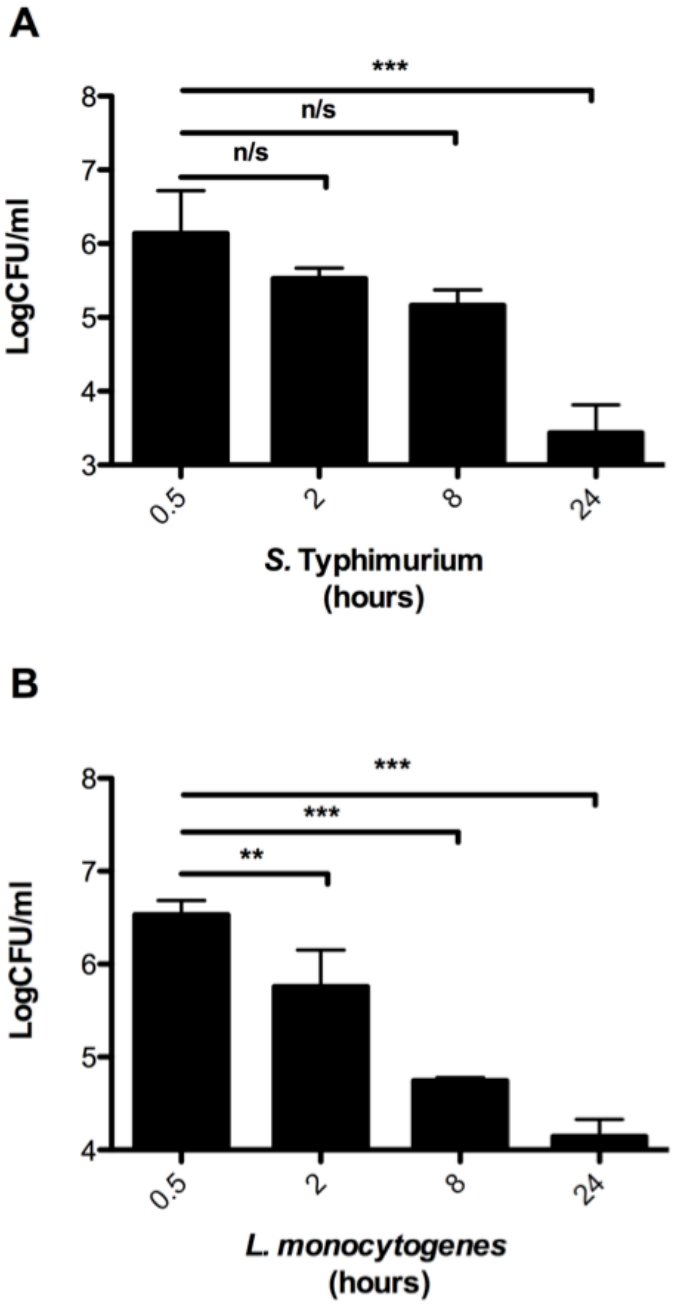

Figure 4.10 Assessment of intracellular killing capacity of BMDMs.

BMDMs were plated at $5x10^5$/ml in 12 well plates and incubated overnight at 37°C in FCS-supplemented DMEM media with 10% L929 media. The following day, the cells were washed with warm PBS and the media was replaced with antibiotic-free DMEM. The cells were then infected with *Listeria* (A) or *Salmonella* (B) at an MOI of 100. After 15 min, the cell monolayers washed and the media was replaced with media containing gentamicin to kill extracellular bacteria. At the end of each timepoint, the cells were lysed in 100µl ice cold water and scraped. The cell lysate was then serially diluted and these dilutions plated on LB agar plates. The plates were incubated at 37°C overnight and colonies formed were enumerated the following day and converted into Log CFU/ml. Data are presented as mean±SD, n=3. P values were calculated using one-way ANOVA using the Newman-Keuls post-test to compare multiple groups such that ** indicates $p<0.01$, *** indicates $p<0.001$).

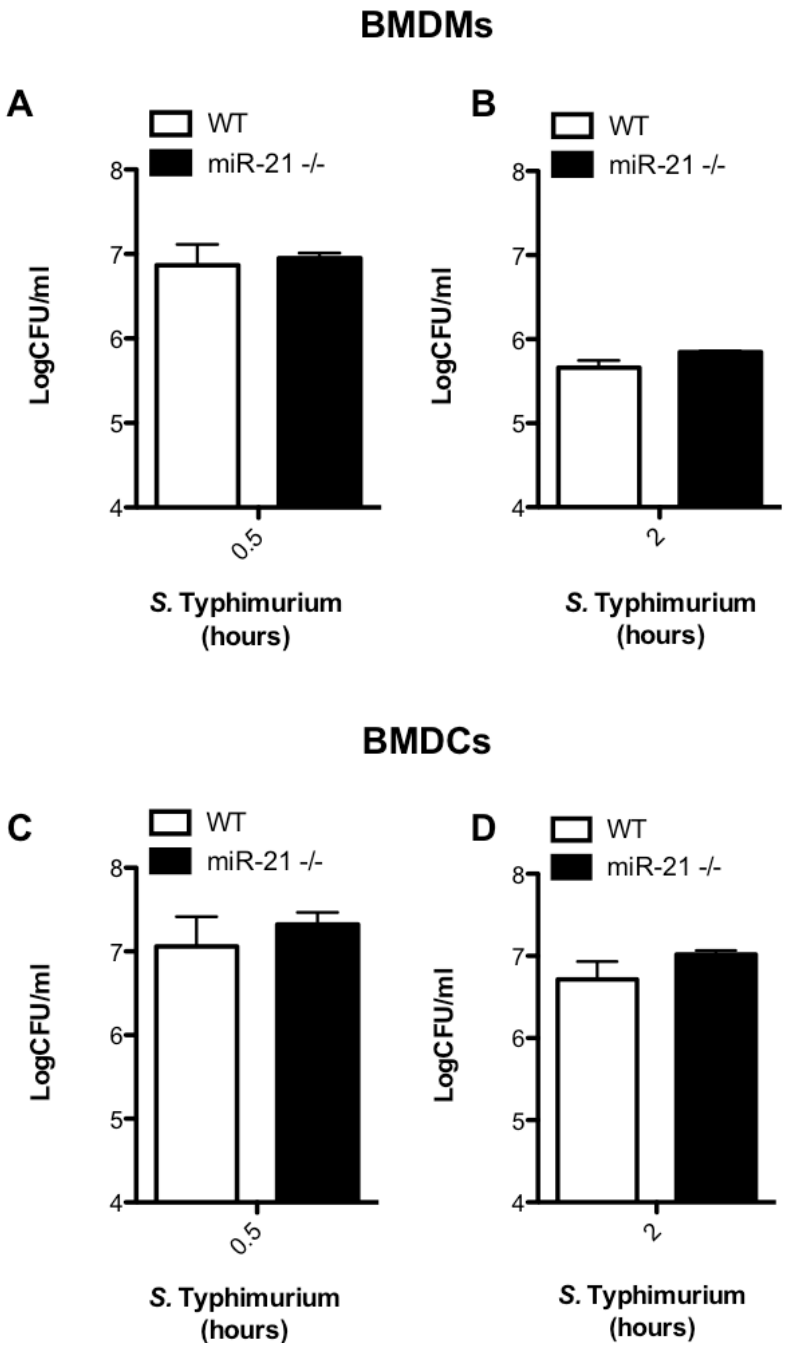

Figure 4.11 Comparison of uptake and intracellular killing capacity of WT versus miR-21$^{-/-}$ phagocytes upon *Salmonella* infection.

Wild-type (WT) or miR-21$^{-/-}$ BMDMs (A and B) and BMDCs (C and C) were plated at 5x10^5/ml in 12 well plates and incubated overnight at 37°C in FCS-supplemented DMEM media with 10% L929 media. The following day, the cells were washed with warm PBS and the media was replaced with antibiotic-free DMEM. The cells were then infected with *Salmonella* at an MOI of 100. After 15 min, the cell monolayers washed and the media was replaced with media containing gentamicin to kill extracellular bacteria. After a total of either 30 min (Uptake) or 2h (intracellular killing), the cells were lysed in 100µl ice cold water and scraped. The cell lysate was then serially diluted and these dilutions plated on LB agar plates. The plates were incubated at 37°C overnight and colonies formed were enumerated the following day and converted into Log CFU/ml. Data are presented as mean±SD, n=3.

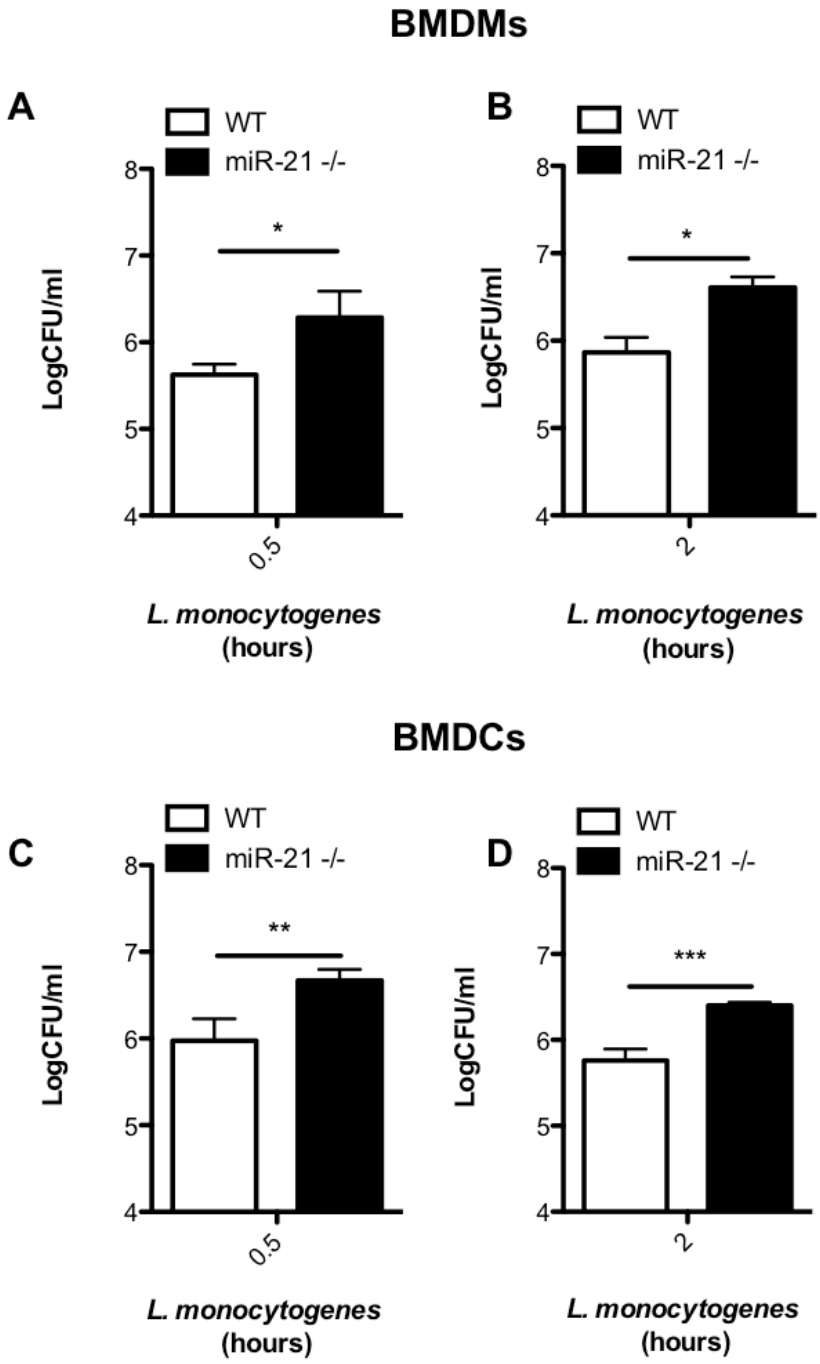

Figure 4.12 Comparison of uptake and intracellular killing capacity of WT versus miR-21$^{-/-}$ phagocytes upon *Listeria* infection.

Wild-type (WT) or miR-21$^{-/-}$ BMDMs (A and B) and BMDCs (C and D) were plated at 5x10^5/ml in 12 well plates and incubated overnight at 37°C in FCS-supplemented DMEM media with 10% L929 media or GM-CSF containing media respectively. The following day, the cells were washed with warm PBS and the media was replaced with antibiotic-free DMEM. The cells were then infected with *Listeria* at an MOI of 100. After 15 min, the cell monolayers washed and the media was replaced with media containing gentamicin to kill extracellular bacteria. After a total of either 30 min (Uptake) or 2h (intracellular killing), the cells were lysed in 100µl ice cold water and scraped. The cell lysate was then serially diluted and these dilutions plated on LB agar plates. The plates were incubated at 37°C overnight and colonies formed were enumerated the following day and converted into Log CFU/ml. Data are presented as mean±SD, n=3. P values were calculated using Student's T test such that * indicate $p<0.05$, ** indicates $p<0.01$, and *** indicates $p<0.001$).

4.2.8. Loss of miR-21 expression does not influence the basal expression of M1/M2 markers in BMDMs.

In order to explore the divergent phenotype of the miR-21$^{-/-}$ macrophage in response to *Listeria* infection, experiments were performed to establish if miR-21 expression influenced the polarity of the BMDMs generated in our system. With this in mind, the expression of a panel of M1/M2 markers was assessed basally in WT and miR-21$^{-/-}$ BMDMs by qPCR (Fig. 4.13). The data obtained in these experiments was highly variable. In the M1 panel, WT BMDMs displayed lower TNF-α and higher NOS2 expression (with no IL-12p40 being detectable in WT or miR-21$^{-/-}$ cells) (Fig. 4.13A-C). In the M2 panel, there was no difference in the levels or Arg1 of YM-1 expression, and an increase in the expression of mannose receptor (also known as CD206 or MRC) though the latter effect was extremely variable from experiment to experiment (Fig. 4.13D-F).

4.2.9. miR-21 deletion does not impact on several bacterial killing mechanisms.

Having established that miR-21 expression was important for controlling *Listeria* infection, experiments were performed to establish whether or not this was due to a reduced capacity to destroy invading bacteria. The formation of free radicals from cellular redox processes is crucial part of the intracellular host defence against invading bacteria. To examine if miR-21 had a role in the generation of these radicals, WT and miR-21$^{-/-}$ BMDMs were treated with LPS and infected with *Listeria*. Nitric oxide (NO) is a crucial mediator of defence against *Listeria* infection [282]. Levels of the NO induced are commonly estimated by measuring the breakdown product NO_2^- (nitrite) in biological samples using a Greiss reaction as an analogue of the unstable gaseous radical [283]. WT and miR-21$^{-/-}$ BMDMs were treated with LPS and *Listeria* and supernatant nitrite levels were assessed at various times (Fig. 4.14). NO was inducible at 2 and 24 hours in response to LPS (Fig. 4.14A) and furthermore the levels present in the supernatants of WT and miR-21$^{-/-}$ were found to be similar. WT and miR-21$^{-/-}$ BMDMs infected with *Listeria* displayed similar absolute levels of NO production and once again there was no difference between WT and miR-21$^{-/-}$ cells (Fig. 4.14B). The other important radical species induced in macrophages in

response to infection or TLR stimulation is radical oxygen species (ROS). The induction of ROS was assessed in response to LPS treatment and *Listeria* infection (Fig. 4.15). In response to LPS, ROS species were induced just over 2-fold compared to untreated controls after 90 minutes and almost 3-fold after 24 hours in WT macrophages. miR-21$^{-/-}$ cells exhibited a slight reduction in ROS induction after 90 mins (1.9 fold vs 2.2) but this was not significant, and at 24 hours the reverse was the case (Fig. 4.15A). Infection with *Listeria* failed to induce ROS production after 90 minutes, and induction at 24 hours was highly variable. Neither timepoint during the course of the infection pointed to a difference between the response of WT and miR-21$^{-/-}$ BMDMs (Fig. 4.15B).

4.2.10. miR-21 expression does not impact on LDH release following infection.

As it did not appear that miR-21 expression had an impact on mechanisms of bacterial killing, it was deemed important to explore the possibility that it affected macrophage survival in response to infection. WT and miR-21$^{-/-}$ BMDMs were infected with both *Listeria* and *Salmonella* and cell death was measured by lactate dehydrogenase (LDH) release. As expected, at both 4 and 24 hours *Salmonella* induced significant cell death (~60% and 80% respectively). *Listeria* also induced cell death but at a much more modest level. There was no difference in levels of cell death exhibited by WT and miR-21 $^{-/-}$ BMDMs in either infection (Fig. 4.16). This suggested that the difference in bacterial burden was not simply due to increased macrophage cell death upon loss of miR-21 expression.

4.2.11. Loss of miR-21 does not impact phagosome maturation

Uptake of bacteria by phagocytic cells leads to the formation of a phagosome which undergoes maturation and fuses with intracellular lysosome to form a phagolysosome capable of destroying the invading bacterium. The expression of several markers of phagocytic maturation were measured to assess whether the heightened bacterial burden exhibited in miR-21$^{-/-}$ phagocytes was due to an alteration of this process of maturation (Fig. 4.17). WT and miR-21$^{-/-}$ BMDMs were infected with increasing MOIs of *Listeria* and the expression of the early endosome markers EEA1 and Rab 5

as well as the late endosome marker Rab 7 was assessed by Western blot. EEA1 was difficult to detect cleanly but its expression seemed to be equivalent in WT and miR-21-deficient cells. This was also the case for the Rab5 and 7 proteins. Confocal microscopy was employed to see if the numbers of EEA1-positive phagosomes was altered in a miR-21$^{-/-}$ BMDMs upon *Listeria* infection (Fig. 4.18). Representative images show EEA1-positive puncta upon *Listeria* infection (Fig. 4.18A) which were quantified to reveal similar numbers in WT and miR-21$^{-/-}$ cells (Fig. 4.18B). To further assess if altered phagosome activity could explain the increased bacterial burden, WT and miR-21$^{-/-}$ BMDMs were infected with a mutant *Listeria* strain deficient in Listerioslysin O, a pore-forming toxin which allows escape from the phagosome. Upon infection with this ΔLLO mutant, miR-21$^{-/-}$ macrophages retained their higher burden relative to WT cells (Fig. 4.19). This suggested that the increased bacterial burden was due to an impairment in the steps between initial uptake and phagolysosome formation, as it would be expected that *Listeria* strains lacking LLO would be destroyed in a functional phagolysosome, as has been reported in the literature [284]. However as we had just ruled out differences in phagosome maturation as shown by similar levels of expression of phagosome markers, we next looked at steps in the process prior to this, specifically initial uptake of the bacteria.

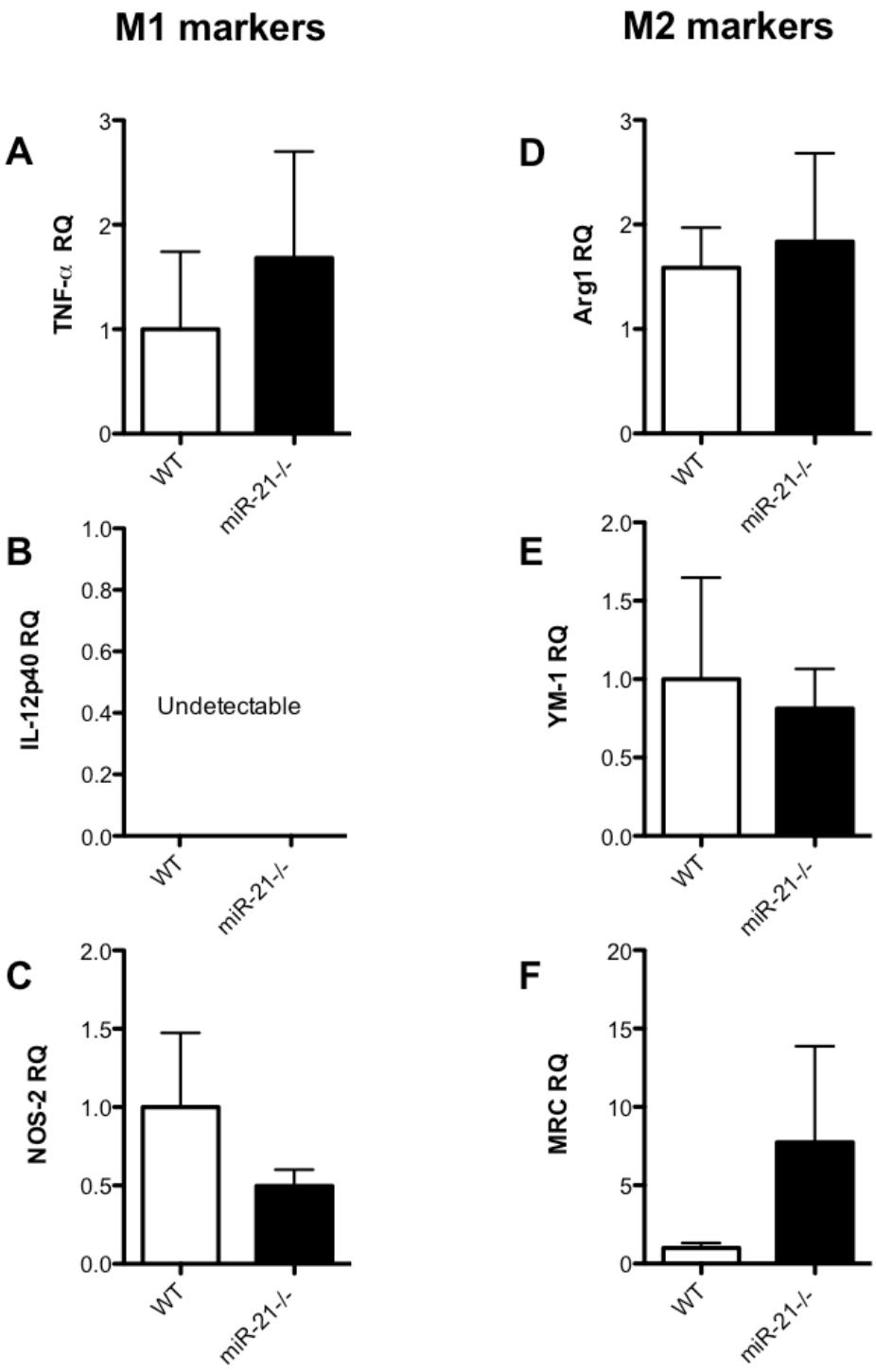

Figure 4.13 Comparing expression of M1/M2 expression markers in WT and miR-21$^{-/-}$ BMDMs.

Wild-type (WT) or miR-21$^{-/-}$ BMDMs were plated at 5x10^5/ml in 12 well plates and incubated overnight at 37°C in FCS-supplemented DMEM media with 10% L929 media. The following day, the cells were lysed and the basal expression of TNF-α (A), NOS2 (B), IL-12p40 (C), Arg1 (D) YM-1 (E) and Mannose receptor or MRC (F) were assessed by Sybr Green qPCR analysis using the ΔΔCt method relative to untreated controls using Rps13 as an endogenous control. Data are presented as mean±SD, n≥3., relative quantification (RQ) relative to WT.

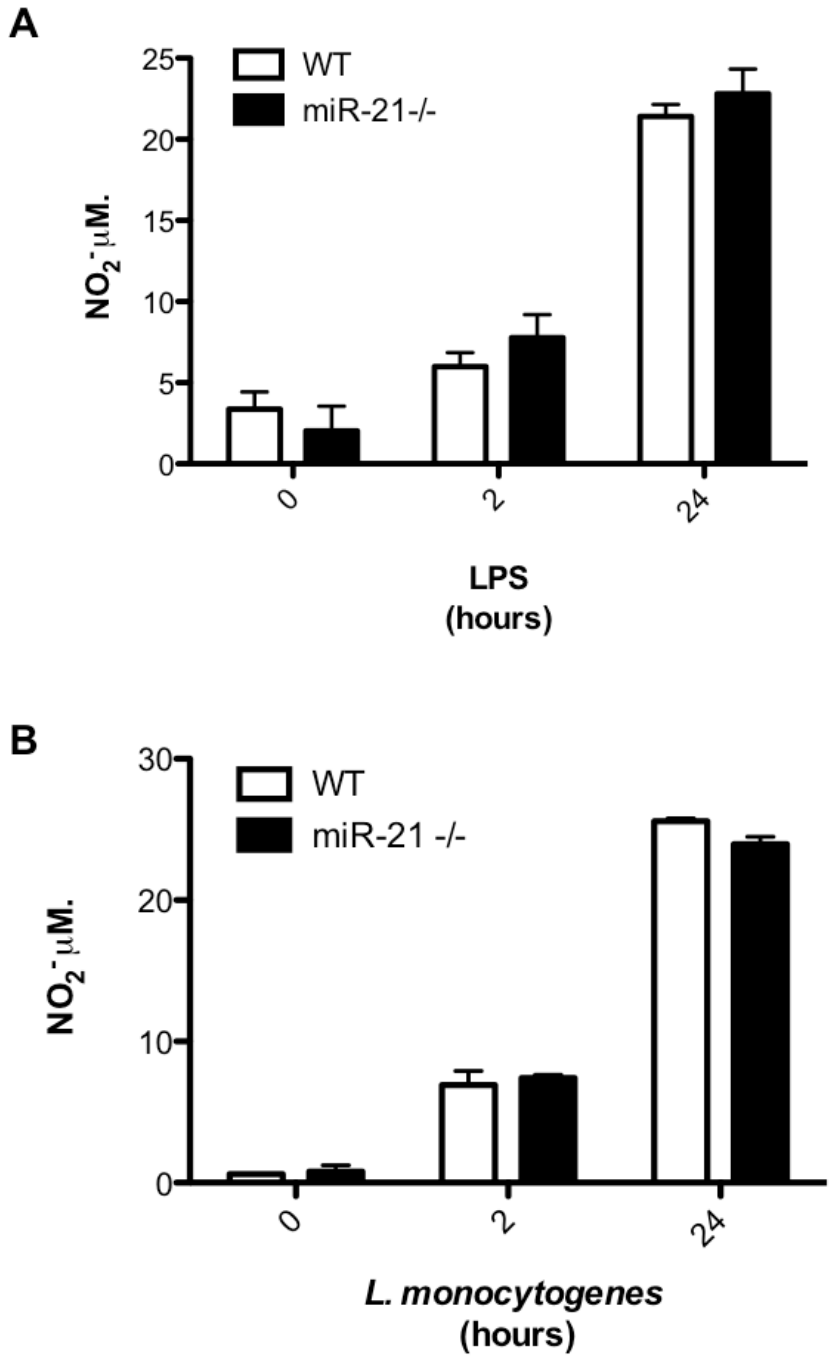

Figure 4.14 Comparing WT and miR-21$^{-/-}$ BMDM NO production.

Wild-type (WT) or miR-21$^{-/-}$ BMDMs were plated at 5x10^5/ml in 12 well plates and incubated overnight at 37°C in FCS-supplemented DMEM media with 10% L929 media. The following day, the cells were washed with warm PBS and the media was replaced media containing 100ng LPS (A) or with antibiotic-free DMEM. The cells were then infected with *Listeria* at an MOI of 100 (B). After 15 min, the cell monolayers washed and the media was replaced with media containing gentamicin to kill extracellular bacteria. At the end of the treatment, nitrite concentrations were measured by Greiss reaction. Data are presented as mean±SD, n≥3.

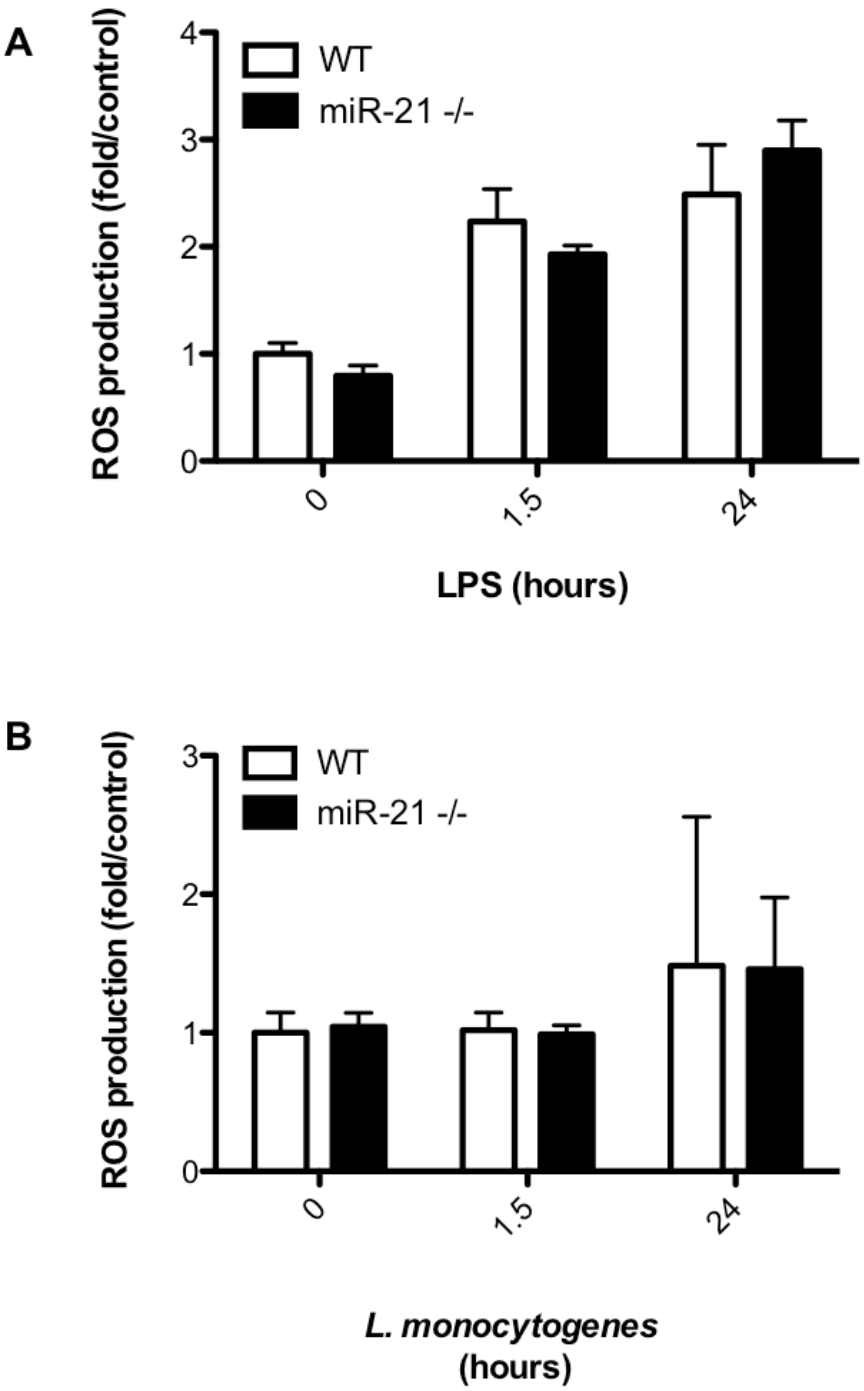

Figure 4.15 Comparing WT and miR-21$^{-/-}$ BMDM ROS production.

Wild-type (WT) or miR-21$^{-/-}$ BMDMs were plated at 5x10^5/ml in 12 well plates and incubated overnight at 37°C in FCS-supplemented DMEM media with 10% L929 media. The following day, the cells were washed with warm PBS and the media was replaced media containing 100ng LPS (A) or with antibiotic-free DMEM. The cells were then infected with *Listeria* at an MOI of 100 (B). After 15 min, the cell monolayers washed and the media was replaced with media containing gentamicin to kill extracellular bacteria. 1h before the end of each treatment, cells were stained with CellRox. ROS production was assessed by flow cytometry. Data are presented as mean±SD, n=3 relative mean florescence intensity folded over untreated WT control.

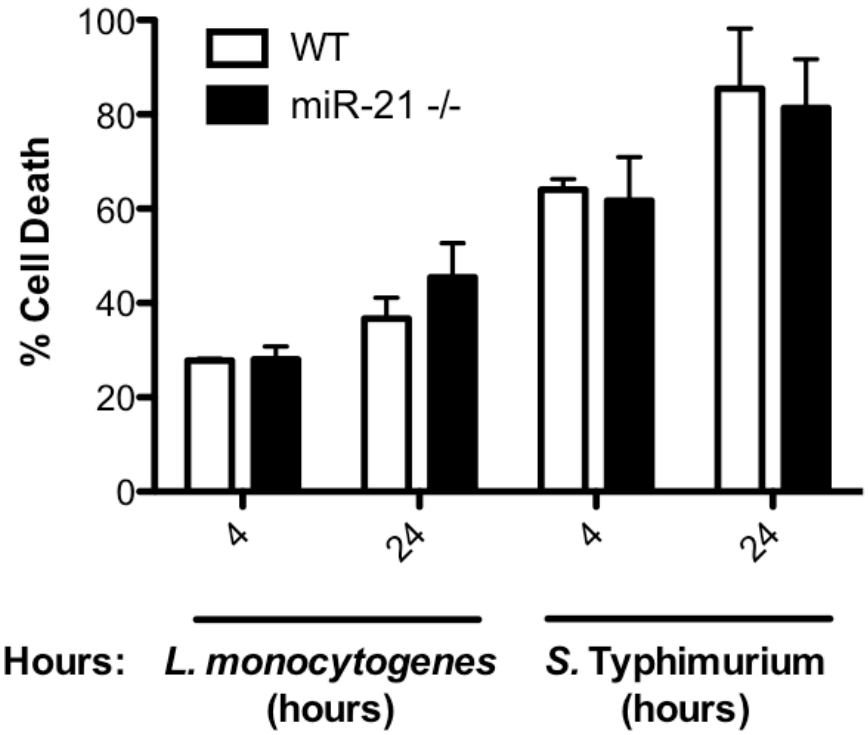

Figure 4.16 Comparing WT and miR-21$^{-/-}$ BMDM cell death in response to infection.

Wild-type (WT) or miR-21$^{-/-}$ BMDMs were plated at 5x10^5/ml in 12 well plates and incubated overnight at 37°C in FCS-supplemented DMEM media with 10% L929 media. The following day, the cells were washed with warm PBS and the media was replaced media containing antibiotic-free DMEM. The cells were then infected with *Listeria* or *Salmonella* at an MOI of 100. After 15 min, the cell monolayers washed and the media was replaced with media containing gentamicin to kill extracellular bacteria. Supernatants were taken at 4 and 24h and LDH levels were measured. Data are presented as mean±SD of percentage cell death relative to a lysed positive control, n=3.

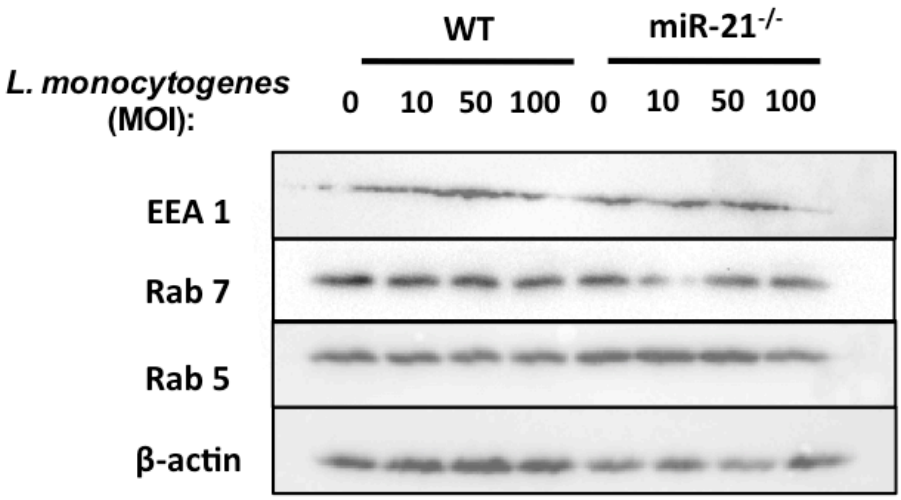

Figure 4.17 Loss of miR-21 expression does not impact phagosome maturation.

Wild-type (WT) or miR-21$^{-/-}$ BMDMs were plated at 5x10^5/ml in 12 well plates and incubated overnight at 37°C in FCS-supplemented DMEM media with 10% L929 media. The following day, the cells were washed with warm PBS and the media was replaced media containing antibiotic-free DMEM. The cells were then infected with *Listeria* at MOIs of 10, 50 and 100. After 15 min, the cell monolayers washed and the media was replaced with media containing gentamicin to kill extracellular bacteria. After an additional 15 minutes (30 min total) the cells were lysed. For protein analysis, the lysates were resolved by SDS-PAGE, transferred on to a PVDF membrane and probed for EEA1, Rab5 and Rab7 protein expression. Representative of three independent experiments.

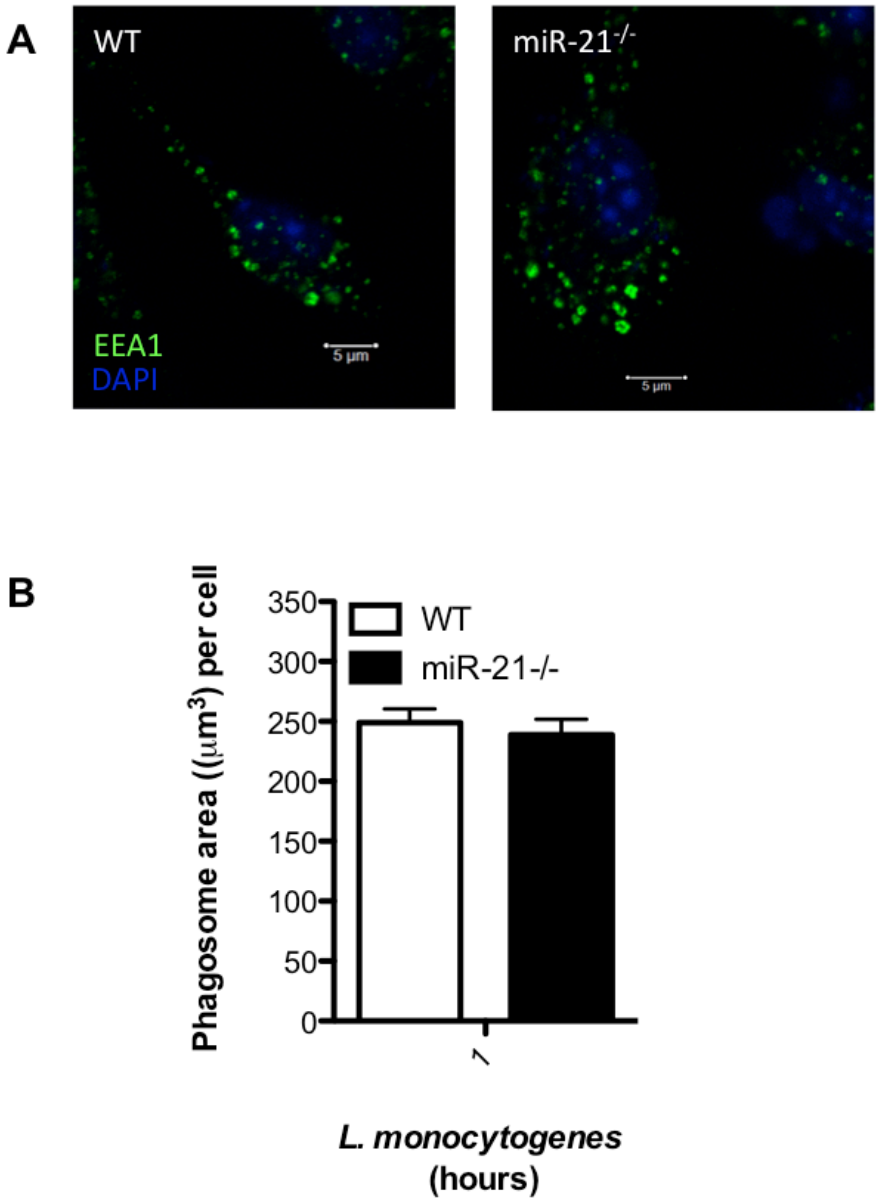

Figure 4.18 Confocal analysis of phagosome formation in WT and miR-21$^{-/-}$ BMDMs infected with *Listeria.*

Wild-type (WT) or miR-21$^{-/-}$ BMDMs were plated at 5x10^5/ml in 12 well plates and incubated overnight at 37°C in FCS-supplemented DMEM media with 10% L929 media. The following day, the cells were washed with warm PBS and the media was replaced with antibiotic-free DMEM. The cells were then infected with *Listeria* at MOI 100 for 15 mins. The cell monolayers were then washed and the media was replaced with media containing gentamicin to kill extracellular bacteria. After a total of 30 mins the cells were fixed with paraformaldehyde before immunostained for EEA1 (A). Phagosome formation was assessed using Imaris software. 5 fields were examined with a minimum of 80 cells assessed. Data are presented as mean±SD where error bars indicate the range. Representative of two independent experiments.

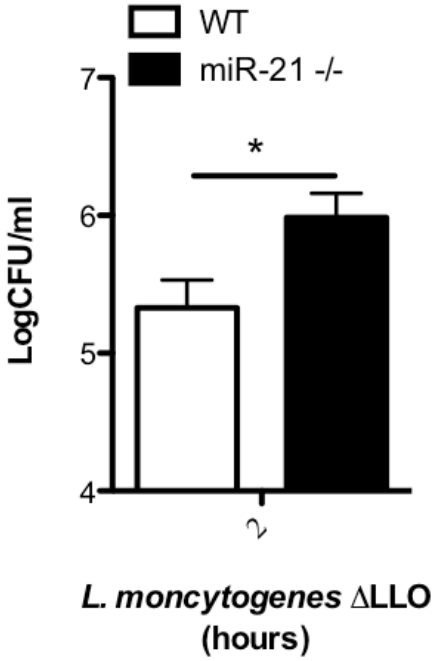

Figure 4.19 Comparison of intracellular killing capacity of WT versus miR-21$^{-/-}$ phagocytes upon infection with a listeriolysin deficient *Listeria* mutant strain.

Wild-type (WT) or miR-21$^{-/-}$ BMDMs were plated at 5x10^5/ml in 12 well plates and incubated overnight at 37°C in FCS-supplemented DMEM media with 10% L929 media. The following day, the cells were washed with warm PBS and the media was replaced with antibiotic-free DMEM. The cells were then infected with Δ*LLO Listeria* at an MOI of 100. After 15 min, the cell monolayers washed and the media was replaced with media containing gentamicin to kill extracellular bacteria. After 2h (intracellular killing), the cells were lysed in 100µl ice cold water and scraped. The cell lysate was then serially diluted and these dilutions plated on LB agar plates. The plates were incubated at 37°C overnight and colonies formed were enumerated the following day and converted into Log CFU/ml. Data are presented as mean±SD, n=3. P values were calculated using Student's T test such that * indicate $p<0.05$.

4.2.12. miR-21 regulates uptake of particles, possibly via modulation of actin.

Given that miR-21 null cells display enhanced *Listeria* burden after a very brief window of infection (30 minutes, Fig. 4.12A), it seemed reasonable that miR-21 may be involved in regulating the initial uptake process. To examine this, initially we assessed uptake of an inert particle, specifically dextran particles conjugated to FITC (FITC-dextran). WT and miR-21$^{-/-}$ BMDMs were incubated with FITC-dextran and uptake of this fluorescent particle was assessed by flow cytometry (Fig. 4.20). Uptake of these particles was significantly enhanced in miR-21$^{-/-}$ relative to WT counterparts (Fig. 4.20A). This was also apparent in heterogenous *ex vivo* peritoneal exudate cells (PECs) indicating potential for *in vivo* relevance (Fig. 4.21). To further investigate this process, WT and miR-21$^{-/-}$ BMDMs were treated with the actin inhibitor cyochalasin D to inhibit actin polymerisation before being infected with *Listeria* to see if the increased bacterial burden in miR-21$^{-/-}$ cells would then be reduced or levels returned to those of WT cells (Fig. 4.22). Interestingly, the previously demonstrated increase in burden in the miR-21$^{-/-}$ BMDMs was lost at both 30 minutes (Fig. 4.22A) and 2 hours (Fig. 4.22B). This suggested that the increased bacterial burden seen in miR-21$^{-/-}$ macrophages is indeed due to altered levels of uptake of *Listeria.*

4.2.13. miR-21 represses the regulation of actin-modulating proteins.

As the previous data suggested that miR-21 expression influences initial uptake, we investigated whether there were any predicted targets of miR-21 which are required for this part of the process. A number of miR-21 targets involved in actin regulation and phagocytosis were identified in the literature. MARCKS and RhoB were the most interesting among them, and offered an interesting point of overlap with our work investigating miR-21 in colitis, in which we found that there is increased expression of both targets in colonic tissue of miR-21$^{-/-}$ mice. Thus these are verified targets of miR-21. As such, WT and miR-21$^{-/-}$ BMDMs were probed for expression of these two modulators both basally and post-*Listeria* infection (Fig. 4.23). MARCKS and RhoB were both expressed in substantially higher levels in miR-21$^{-/-}$ BMDMs basally (Fig. 4.23A, compare lane 1 and 2) with MARCKS expression enhanced upon *Listeria* (Fig. 4.32A, lanes 3 and 4). This was assessed by

densitometry (Fig. 4.23B). Along with this observation, MARCKS expression was significantly enhanced at the mRNA level after infection in miR-21$^{-/-}$ BMDMs (Fig. 4.32C). At the mRNA level, RhoB was marginally higher basally and enhanced post infection in miR-21$^{-/-}$ cells (Fig. 4.23D).

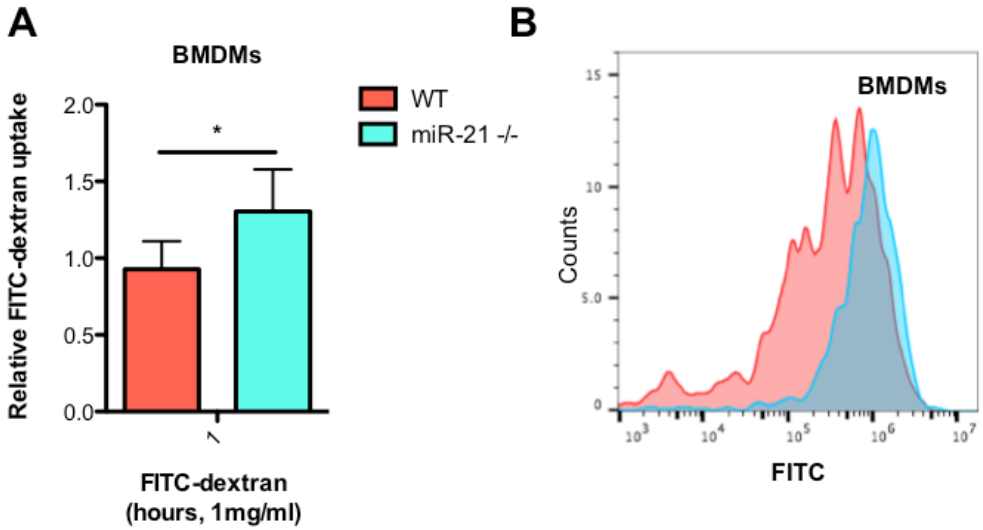

Figure 4.20 MiR-21-deficient macrophages display increased uptake of FITC-dextran.

Wild-type (WT) and miR-21$^{-/-}$ BMDMs were incubated with media containing 1mg/ml FITC-dextran for 1h at 37°C. Uptake of FITC-dextran was determined by measuring the median fluorescence intensity by flow cytometry and data expressed relative to WT (Relative FITC-dextran uptake) with a corresponding histogram representative of median florescent intensity. Data are expressed as means ± SD, n=3. P values were calculated using Student's T test such that * indicates $p<0.05$.

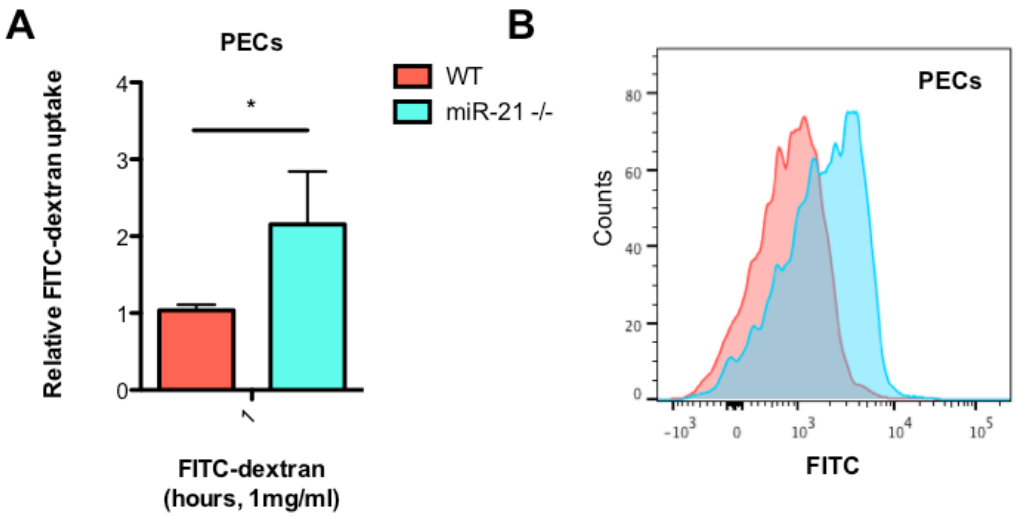

Figure 4.21 MiR-21-deficient PECs display increased uptake of FITC-dextran.

Wild-type (WT) and miR-21$^{-/-}$ PECs were incubated with media containing 1mg/ml FITC-dextran for 1h at 37°C. Uptake of FITC-dextran was determined by measuring the median fluorescence intensity by flow cytometry and data expressed relative to WT (Relative FITC-dextran uptake) with a corresponding histogram representative of median florescent intensity. Data are expressed as means ± SD, n=3. P values were calculated using Student's T test such that * indicates $p<0.05$.

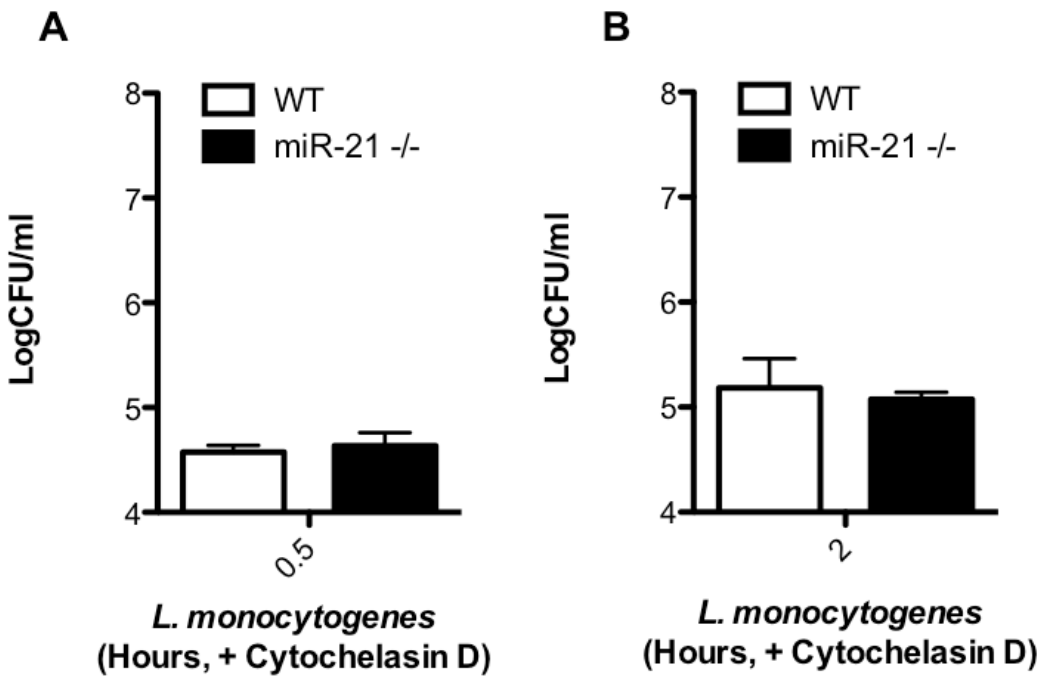

Figure 4.22 Comparison of uptake and intracellular killing capacity of cytochalasin D treated WT and miR-21$^{-/-}$ BMDMs upon *Listeria* infection.

Wild-type (WT) or miR-21$^{-/-}$ BMDMs were plated at 5x10^5/ml in 12 well plates and incubated overnight at 37°C in FCS-supplemented DMEM media with 10% L929 media. The following day, the cells were washed with warm PBS and the media was replaced with antibiotic-free DMEM. The cells were then pre-treated with 10μM cytochalasin D for 30 mins before being infected with *Listeria* at an MOI of 100. After 15 min, the cell monolayers washed and the media was replaced with media containing gentamicin to kill extracellular bacteria. After a total of either 30 min (A) or 2h (B), the cells were lysed in 100μl ice cold water and scraped. The cell lysate was then serially diluted and these dilutions plated on LB agar plates. The plates were incubated at 37°C overnight and colonies formed were enumerated the following day and converted into Log CFU/ml. Data are presented as mean±SD, n=3.

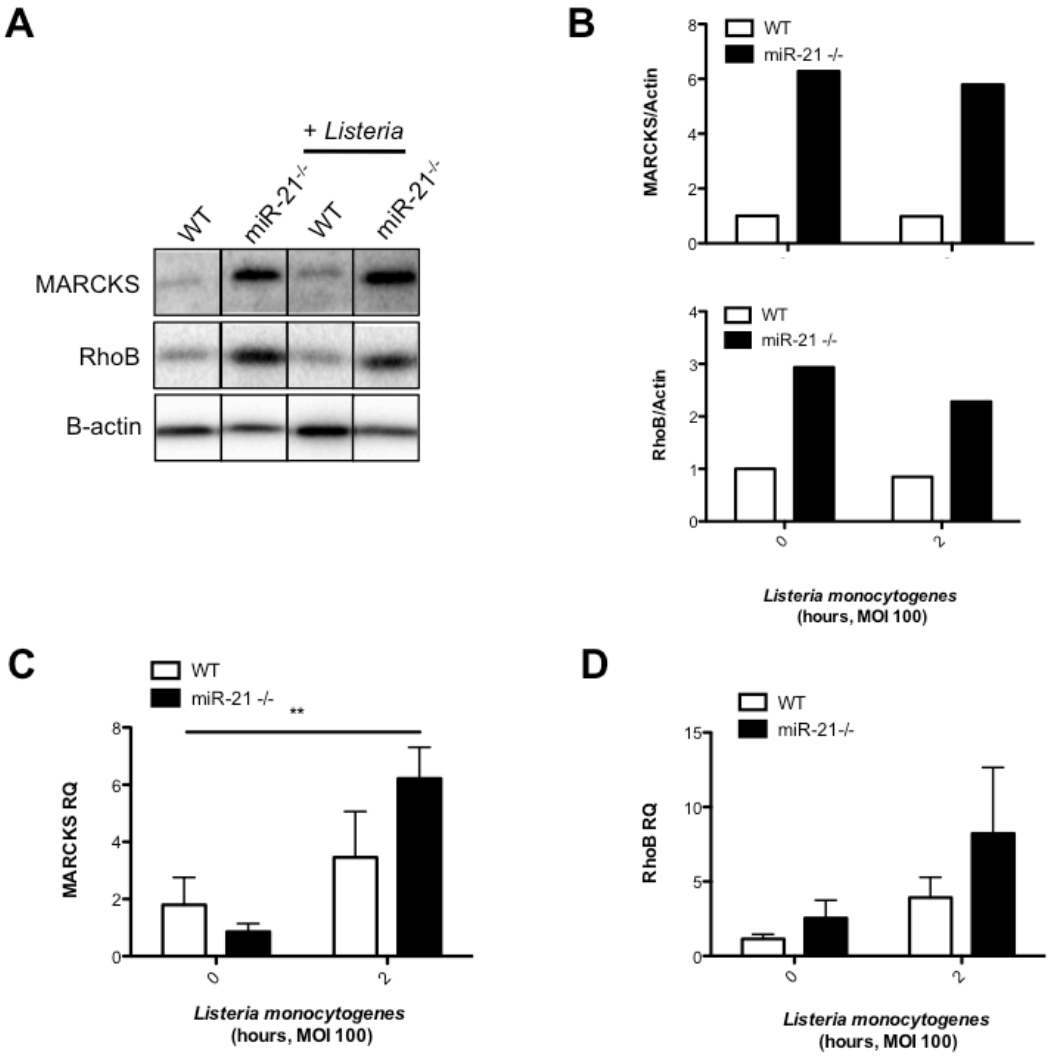

Figure 4.23 MiR-21 represses expression of the pro-phagocytic proteins MARCKS and RhoB.

(A) Immunoblot analysis of basal MARCKS and RhoB protein expression in untreated wild-type (WT) and miR-21$^{-/-}$ BMDMs. (B) Densitometry of immunoblot analysis. (C and D) BMDMs were infected with *L. monocytogenes* at an MOI 100 for 15 mins and subsequently cultured with media containing gentamycin (100ug/ml) for a further 105min. At 2h post-infection, the RNA was isolated and assayed by qRT-PCR for (C) MARCKS and (D) RhoB expression using Rps13 as an endogenous control, with WT 0h serving as relative quantification (RQ) datum point. Data are expressed as means ± SD, n=3. P values were calculated using Student's T test such that * indicate s $p<0.05$.

4.2.14. *Listeria* dissemination is increased in miR-21$^{-/-}$ mice post-intraperitoneal infection.

In addition to the *in vitro* studies above, the affect of miR-21 deletion was assessed in mice using different modes of infection. WT and miR-21 mice were infected with *Salmonella* both intraperitoneally and by oral gavage (Fig. 4.24) and bacterial dissemination was assessed by enumerating CFUs present in the spleens (Fig. 4.24A and C) and livers (Fig. 4.24B and D) of the mice at the end of the infection. There was no difference in dissemination of *Salmonella* by either route. These models were both employed in the context of *Listeria* infection (Fig. 4.25) where bacterial burden was increased in the spleens and livers of miR-21$^{-/-}$ mice compared to WT mice via the intraperitoneal route (Fig. 4.25A and B). This increase was not as apparent in mice infected via oral gavage (Fig. 4.25C and D).

Intraperitoneal *S.* Typhimurium infection

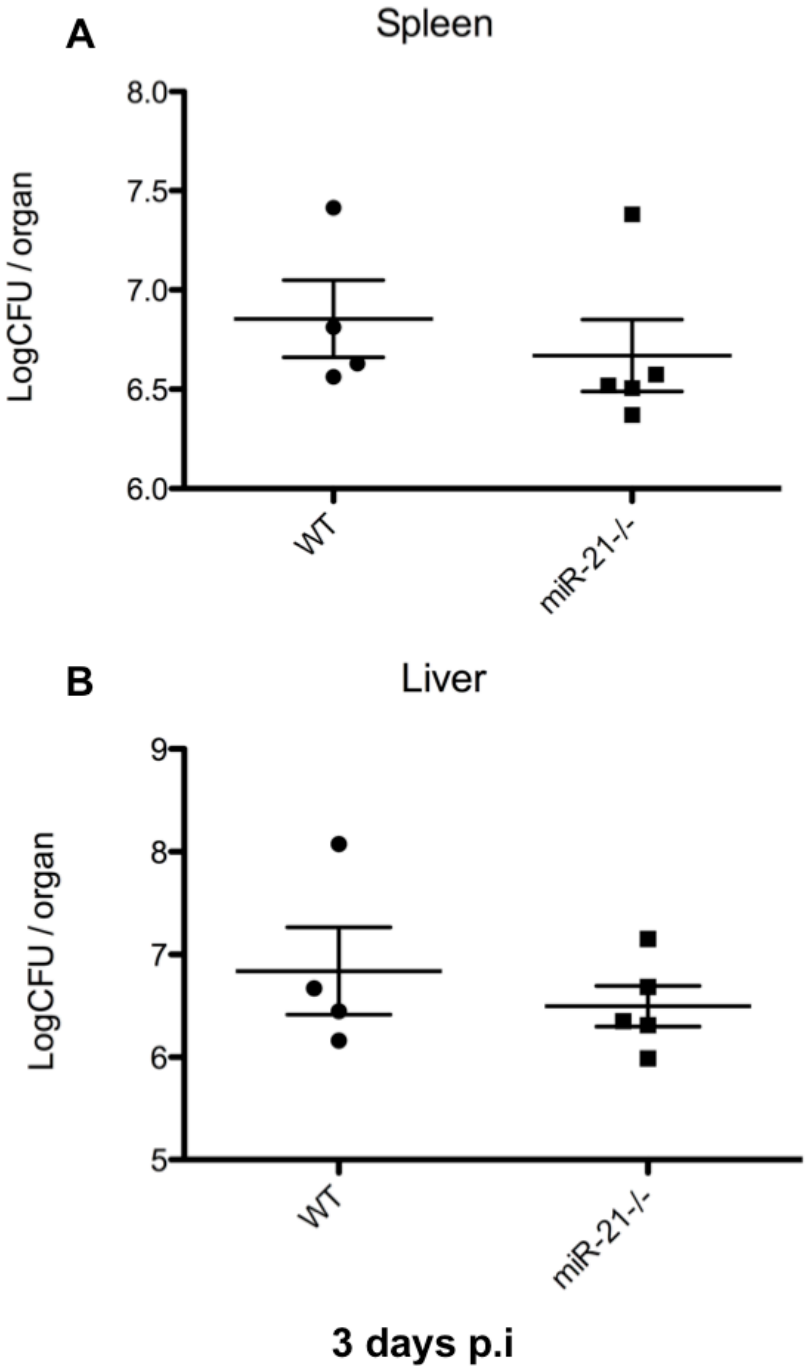

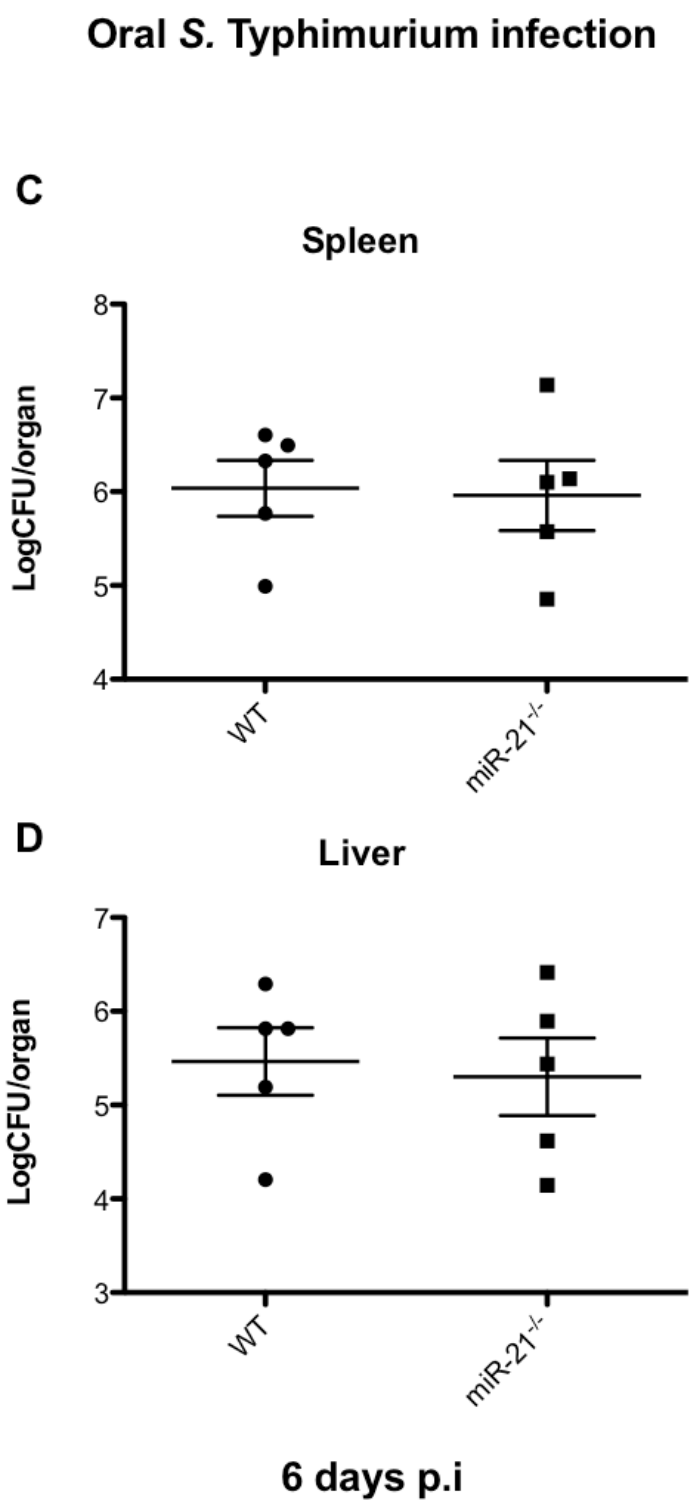
Oral S. Typhimurium infection
C
Spleen
LogCFU/organ
8
7
6
5
4
WT
miR-21-/-
D
Liver
LogCFU/organ
7
6
5
4
3
WT
miR-21-/-
6 days p.i

Figure 4.24 Comparing bacterial dissemination in WT versus miR-21$^{-/-}$ mice via intraperitoneal and oral infection with *Salmonella.*

Intraperitoneal infection: Wild-type (WT) or miR-21$^{-/-}$ mice were infected with *Salmonella* by intraperitoneal infection of 1x10^{6} CFU bacteria in 100µl PBS. The mice were monitored and sacrificed three days post-infection and their organs including spleen (A) and liver (B) were harvested. The organs were then homogenised, and dilutions of the homogenates were plated on LB agar plates which were incubated overnight at 37°C. The following day, the colonies were enumerated and converted into LogCFU/organ. Data are presented as mean±SEM, n≥4.

Oral infection: Wild-type (WT) or miR-21$^{-/-}$ mice were fasted overnight before being infected with *Salmonella* by oral gavage of 5x10^{7} CFU bacteria in 100µl PBS. The mice were monitored and sacrificed 6 days post-infection their organs including spleen (A) and liver (B) were harvested. The organs were then homogenised, and dilutions of the homogenates were plated on LB agar plates which were incubated overnight at 37°C. The following day, the colonies were enumerated and converted into LogCFU/organ. Data are presented as mean±SEM, n=5.

Intraperitoneal *L. monocytogenes* infection

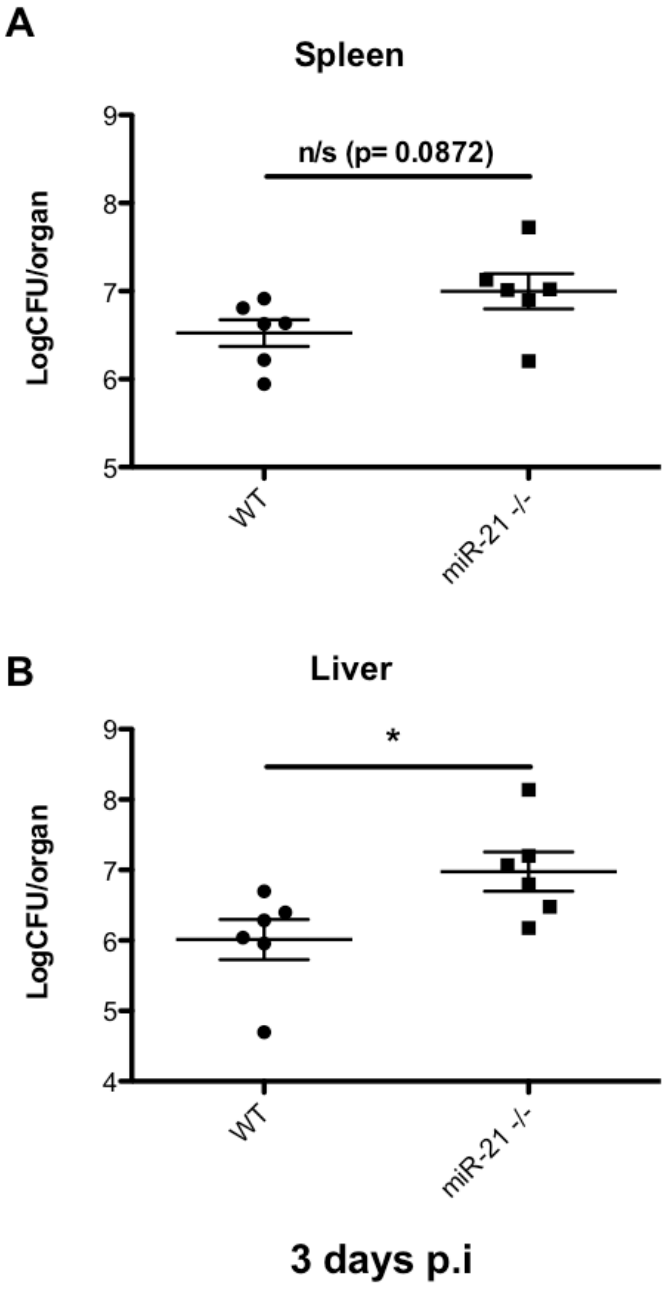

3 days p.i

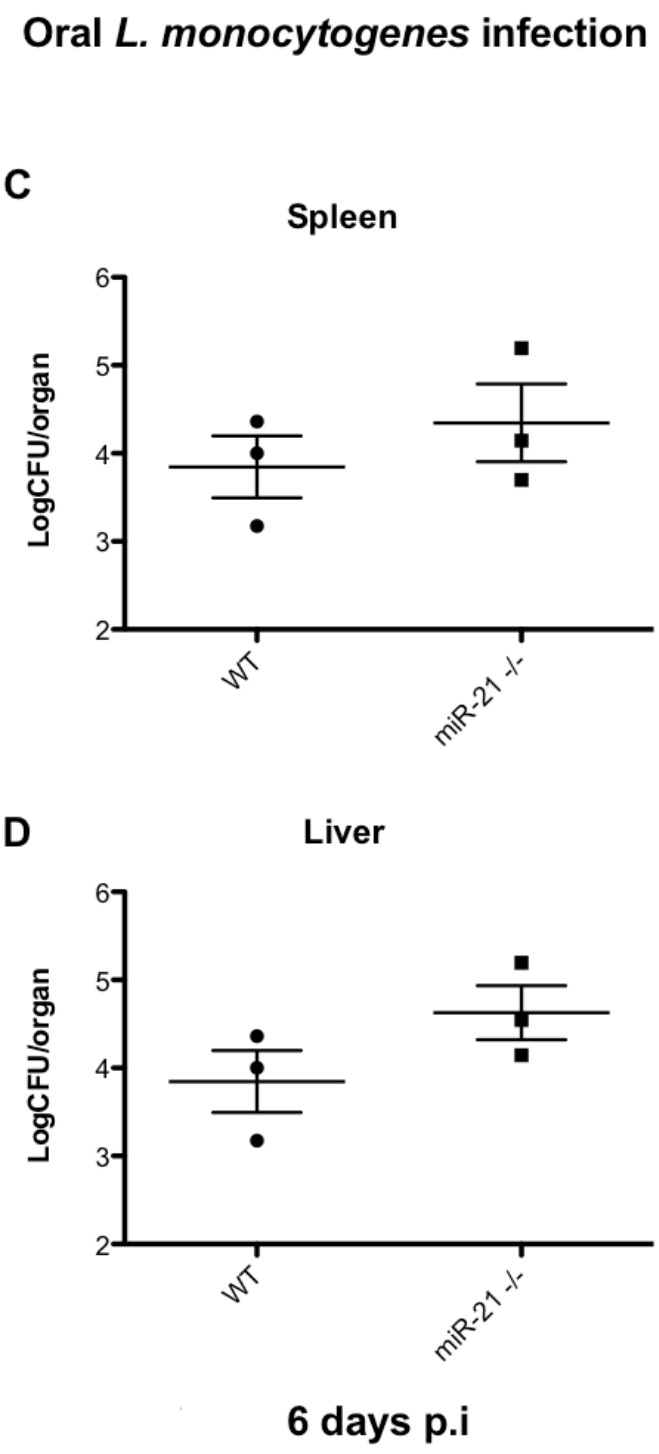
Oral L. monocytogenes infection
C
Spleen
LogCFU/organ
6
5
4
3
2
WT
miR-21 -/-
D
Liver
LogCFU/organ
6
5
4
3
2
WT
miR-21 -/-
6 days p.i

Figure 4.25 Comparing bacterial dissemination in WT versus miR-21$^{-/-}$ mice via intraperitoneal and oral infection with *Listeria.*

Intraperitoneal infection: Wild-type (WT) or miR-21$^{-/-}$ mice were infected with *Listeria* by intraperitoneal infection of 1x10^{6} CFU bacteria in 100µl PBS. The mice were monitored and sacrificed three days post-infection and their organs including spleen (A) and liver (B) were harvested. The organs were then homogenised, and dilutions of the homogenates were plated on BHI agar plates which were incubated overnight at 37°C. The following day, the colonies were enumerated and converted into LogCFU/organ. Data are presented as mean±SEM, n=6.

Oral infection: Wild-type (WT) or miR-21$^{-/-}$ mice were fasted overnight before being infected with *Listeria* by oral gavage of 5x10^{7} CFU bacteria in 100µl PBS. The mice were monitored and sacrificed 6 days post-infection their organs including spleen (A) and liver (B) were harvested. The organs were then homogenised, and dilutions of the homogenates were plated on BHI agar plates which were incubated overnight at 37°C. The following day, the colonies were enumerated and converted into LogCFU/organ. Data are presented as mean±SEM, n=3.

4.3. Discussion

This chapter set out to explore the role of miR-21 in bacterial infection and the cytokine release pertaining to these infections. A novel regulatory role for miR-21 has been demonstrated, whereby it limits this intracellular niche by inhibiting initial uptake of bacteria within macrophages, thereby reducing the severity and outcome of infection and possible resultant inflammation.

Initial experiments set out to confirm some previously established roles miR-21 plays in macrophages. The induction of miR-21 in response to the TLR agonist LPS was confirmed in two cell types: the RAW264.7 macrophage-like cell line and in BMDMs. miR-21 was more robustly induced in the latter cell type, and they were chosen as our model system of choice for a number of reasons. Chief among these reasons was the availability of the miR-21$^{-/-}$ mouse and the capacity to generate macrophages lacking miR-21 without using pharmacological inhibition. In addition, primary cells are regarded as being a more physiologically relevant cell type than immortalised cell lines which often display phenotypic and genetic idiosyncrasies specific to their line.

Having confirmed miR-21 induction in response to LPS as demonstrated in previous publications, we wished to establish the impact of miR-21-deletion on cytokine release after stimulation with the same bacterial PAMP. miR-21 has previously been shown to enhance secretion of the anti-inflammatory cytokines IL-10 via degradation of PDCD4 transcript allowing translation of the IL-10 mRNA transcript. After 24 hours stimulation with LPS, macrophages lacking miR-21 did indeed display an impaired capacity to produce IL-10 as predicted though perhaps not as dramatically as might have been anticipated. In addition to IL-10 translation, miR-21 has been shown to regulate TLR induced signalling pathways which culminate in translocation of the transcription factor NF-κB into the nucleus and transcription of various genes, generally pro-inflammatory. Included in this list of NF-κB regulated genes are the cytokines IL-6 and TNF-α. Accordingly, in response to LPS, IL-6 levels appeared to be slightly increased in the miR-21$^{-/-}$ relative to that of the WT. This would be consistent with some of the literature, however this readout was not hugely consistent

throughout these experiments. Indeed, inconsistency is often associated with this particular cytokine which, while its is generally considered to be pro-inflammatory, is in fact pleotropic as evidenced by several anti-inflammatory functions it fulfils including in the DSS model of IBD where is promotes epithelial healing [254]. miR-21 and IL-6 have been shown to be closely linked in cancer, with a pathway involving STAT3 being linked to enhancement of EMT transition. In two studies involving IL-6 induction in an inflammatory context, deletion or inhibition of miR-21 has been shown to allow increased IL-6 secretion which would agree with our observation [155,280]. Upon LPS stimulation TNF-α levels were seen to be significantly increased in cells lacking miR-21 compared to their WT counterparts, again in agreement with previous literature citing miR-21's inhibition of NF-κB [129,155]. These results indicate that miR-21 is indeed an anti-inflammatory agent in LPS treated macrophages, and are in agreement with two publications which appeared during the course of the thesis [155,280] However, macrophages sense danger and pathogens via multiple receptors and so it was deemed prudent to ascertain whether or not this cytokine secretion profile was shared upon activation of other TLRs. Accordingly, WT and miR-21 BMDMs were treated with agonists of the plasma membrane bound TLR2/1 heterodimer and endosomal TLR3. The same IL-10 secretion profile was observed following stimulation of both TLRs as before indicating the miR-21 plays a similar role in inflammation resolution in response to danger sensed by these receptors. The IL-6 response was less clear, with little difference between WT and miR-21$^{-/-}$ cells post-TLR2/1 stimulation and a reduction in the knockout following TLR3 stimulation. Given that during the course of this study IL-6 has been reported to be elevated with miR-21 deficiency this effect was unexpected, but perhaps in keeping with its nature as a pleiotropic agent [155]. The enhanced levels of TNF-α secretion evidenced in LPS treated miR-21$^{-/-}$ BMDMs were again present upon TLR2/1 stimulation but not in TLR3 stimulation. These receptors share some elements of their signalling pathways for NF-κB induction so it was anticipated that the TNF-α phenotype would be shared. TLR3 senses dsRNA which is released by damaged cells but also a hallmark of viral infection, and indeed miR-21 has been shown to be co-opted by hepatitis C (HCV) to evade anti-viral immunity by suppressing interferon signalling [285]. However, other studies have shown miR-21 to be among the least strongly induced miRNA in viral infection so perhaps its relevance in this system is limited [286,287].

Dendritic cells are key cells of both the innate and adaptive immune response, and their cytokine secretion profile is an important part of polarizing T cells for different functional outcomes. Again the availability of the miR-21 null mouse was exploited to culture BMDCs and assess their phenotypic traits in response to TLR stimulation and infection. In response to LPS, miR-21$^{-/-}$ BMDCs exhibited the same differences in IL-10 and TNF-α output as seen in the BMDMs, and IL-6 levels were no different to that of WT BMDCs. In addition, it had been previously reported that miR-21 can target the p35 subunit of IL-12, a key cytokine for polarizing naïve T cells towards a pro-inflammatory IFN-γ secreting Th1 cell, and that miR-21$^{-/-}$ DCs displayed an enhanced secretion of this cytokine with a negative impact in models of lung inflammation [161,164]. This was also the case in our experiments, and it has interesting implications regarding the IBD phenotype described in the previous chapter which will be discussed later.

The relevance of miR-21 as an anti-inflammatory mediator in TLR stimulation *in vivo* was assessed using the LPS-induced sepsis model and measuring cytokine release. Previous publications had demonstrated that PDCD4-deficient mice were resistant to LPS-induced lethality models and that this action was part due to increased IL-10 reducing inflammation [129]. Given that this pathway is part of miR-21's anti-inflammatory action, deletion of miR-21 would be predicted to reduce IL-10 and predispose these mice to increased inflammation. This hypothesis was proved to be partly correct, with miR-21$^{-/-}$ not displaying the decreased IL-10 anticipated by previous studies and our own observations but displaying and enhanced TNF-α secretion profile. This indicated that the miR-21$^{-/-}$ mice did indeed have a more inflammatory phenotype but that this was not due to a loss of IL-10 signalling. This data was in agreement with a study published by Barnett *et al* during the project, where it is demonstrated that with a higher dose of LPS (25mg/kg versus 15mg/kg used here) that miR-21$^{-/-}$ mice have a significantly impaired survival phenotype over a number of days [155]. Interestingly, they also demonstrated that this phenotype was specific to this model of sepsis, and that miR-21 expression did not have a significant bearing on the caecal ligation puncture (CLP) model where a huge variety of intestinal microbes and antigens are released in to the peritoneum to be detected by macrophages therein.

The primary aim of this project was to explore miR-21's role in bacterial infection. miR-21 has previously been reported to be induced in various immune cells following infection by several bacteria including *Helicobacter pylori* (relevant to gastric inflammation and cancer), *Salmonella* and *Mycobacterium leprae* [288-290]. This ties into other work showing its induction by TLR sensing of PAMPs, which are after all bacterial signals. However, little functional study in infection has been carried out on miR-21 specifically compared to other immunomodulatory miRNA such as miR-146a and miR-155. Two model organisms were chosen to conduct these studies: *S.* Typhimurium UK-1 and *L. monocytogenes* EGDe. These are well-characterised experimental organisms and allowed the study of both gram-negative and gram-positive infections. miR-21 was robustly induced by *Salmonella* as previously reported but this induction waned after 24 hours. A previous study reported miR-21 was still induced 2-fold at this timepoint but in a different macrophage cell line. Our observation is more in keeping with the miR-21 induction timeline seen in BMDMs with LPS, the major PAMP present as part of *Salmonella*'s cell wall. *Listeria* also induced miR-21 though to a lesser extent than the gram-negative *Salmonella*. *Listeria* has previously been shown to induce miRNA expression in a MyD88 and TLR2 dependant manner, but miR-21 expression was not reported so this is a novel observation [291]. This miR-21 induction is likely through TLR2 sensing peptidoglycan and lipoteichoic acid but *Listeria* also expresses a form of endotoxin (LPS) which may bind TLR4 [292].

To establish if this induction of miR-21 resulted in a functional difference in macrophage behaviour, BMDMs lacking miR-21 were generated to examine the impact of infection on cytokine secretion in response to infection. It was surprising that no difference in IL-10, IL-6 or TNF-α was observed between WT and miR-21$^{-/-}$ macrophages following 24h infection with *Salmonella* given the clear effects observable using purified bacterial ligands in the previous experiments. Indeed, in the case of *Salmonella* infection there was very little observable cytokine secreted at all. This may be due to issues of toxicity as *Salmonella* induce cell-death at earlier timepoints. It was anticipated that miR-21 would have an impact on TNF-α secretion in the case of *Listeria* due to the well-known role of this cytokine in the immune response to the pathogen, as well miR-21's demonstrable influence on its secretion in response to LPS [293]. Whilst there was a significant elevation in TNF-α secretion in

the miR-21$^{-/-}$ macrophages it was not as pronounced as demonstrated with LPS treatment. There was no significant difference in IL-10 or IL-6 secretion. This observation was also apparent in BMDCs, as well as a lack of observable TNF-α levels. This difference in cytokine secretion phenotype observed between purified ligands and live bacterial infection may be explained in a number of ways, chief amongst them being the many additional pathways that become activated by introducing a whole organisms rather than a single immunogenic element. For instance, *Listeria* is a potent activator of the PRR Nod2 which is important for modulating host defence mechanisms post-TLR stimulation [102,294]. These additional pathways may impact on miR-21's role in cytokine production in this context. In addition, it is worth restating that miRNA function is complex due to the multitude of mRNA transcripts each miRNA can target, and this may well be responsible for the loss of translation of phenotype here.

The most basic function of the innate immune response is the destruction of invading pathogens, and one of the most important processes used to achieve this is ingestion by phagocytosis and subsequent intracellular killing of the aforementioned invader. Several bacteria have evolved strategies to use the phagocytic process to gain entry in to the cell, before either subverting the intracellular killing process to suit their requirements or escaping it completely to replicate within the cell. Different miRNA have been implicated at various stages of these processes and so experiments were performed to establish if miR-21 might also regulate them. WT BMDMs were cultured and infected with the two chosen model organisms, both of which exhibit evolved immune evasion strategies, to determine effectiveness of intracellular killing. Bacterial loads steadily decreased over 24 hours, until very small number of CFUs were detectable at the end of the experiment, indicating that these primary macrophages are effective intracellular killers of both *Salmonella* and *Listeria*. The gentamicin protection assay was used in this experiment, and it was decided to use the standard timepoints to measure uptake and killing (namely 30 mins and 2 hours) [281]. WT and miR-21$^{-/-}$ BMDMs and BMDCs were infected with *Salmonella,* and it was clear that the deletion of miR-21 had no impact on the uptake or killing of the bacteria in either cell type. However, upon infection with *Listeria,* there was a significant difference between WT and miR-21$^{-/-}$ cells both at the very early 30 minute timepoint and after 2 hours. It was decided to focus on the *Listeria* phenotype primarily for the

remainder of the project. The increased *Listeria* burden displayed by the miR-21$^{-/-}$ cells was initially surprising for a number of reasons. Based on published studies, we had hypothesised that as miR-21 is ostensibly an anti-inflammatory mediator, phagocytic cells lacking miR-21 would likely be more pro-inflammatory and as a result more bacteriocidal. These observations led us to question the status of the miR-21$^{-/-}$ macrophage on the M1/M2 spectrum relative to WT cells. There is a conflicting existing literature regarding miR-21's role in M1/M2 polarization, with some reports suggesting that miR-21 is in fact associated with negatively regulating anti-inflammatory M2 polarization in certain contexts [144,162,295]. A panel of M1/M2 markers was assessed by qPCR, as is standard in the field, in WT and miR-21$^{-/-}$ BMDMs in their basal state. These results indicate that there is no particular skewing of macrophage polarization basally upon miR-21 deletion. The data was quite variable between experiments, and there wasn't a consistent difference across markers. For instance, in the M1 markers TNF-α expression was slightly higher in the miR-21 deficient macrophages but the opposite was seen in the case of NOS2 expression, and there was an increase in the M2 marker MRC. The studies previously published in this area showed miR-21 had an impact on active polarization with different stimuli, and this may account for the conflicting data obtained from cells in their basal state.

Upon internalization of bacteria, the phagosome matures in to a highly acidic bacteriocidal phagolysosome capable of destroying the ingested material. Part of the process of generating this bacteriocidal environment is the development of radical ions which damage the bacterial DNA and induce cell death. miR-21 has been associated with alterations in production of the free radicals NO and ROS in the context of cancer, and so it was hypothesised that a reduced capacity to produce these mediators as part of a functioning phagolysosome may explain the increased bacterial burden observed in miR-21$^{-/-}$ cells [151,153,154]. These radicals can also be released by a phagocytosing cell causing damage to surrounding tissue but also, in the case of NO, causing dilation of surrounding vasculature to allow infiltration of immune cells and subsequent inflammation to clear the encountered infection. To investigate this, WT and miR-21$^{-/-}$ BMDMS were treated with LPS or infected with *Listeria* and NO generation was estimated in the supernatants. There was a time dependant increase in NO detectable in the supernatants of macrophages treated with LPS (LPS or LPS

combined with IFN-γ being the archetypal NO inducting stimuli) but there was no observed difference in this increase between WT and miR-21$^{-/-}$ cells. NO is a particularly important mediator of host defence against *Listeria*, as demonstrated by studies which deleted the key NO producing enzymes and showed impaired bacterial clearance capacity [282,296,297]. A similar level of increase in NO was detectable after infection with *Listeria* as had been observed in response to LPS, and similarly there was no alteration to this increase upon deletion of miR-21. The other main form of free radicals employed by the immune system in response to infection are ROS which both directly damage bacteria as in a still not fully established manner as well as influencing cytokine production and host cell gene expression [298,299]. miR-21 has been demonstrated to increase ROS levels in the context of cancer, and so we hypothesised that its deletion may lead to a less bacteriocidal phagosome [151]. However, there was no difference observed in basal ROS between WT and miR-21$^{-/-}$ nor when ROS was induced by LPS treatment. *Listeria* infection failed to induce ROS after both 4 and 24 hours and this was seen to be common to both WT and miR-21$^{-/-}$ BMDMs. This lack of ROS induction was surprising given the important role it plays in mediating host defence against intracellular pathogens and that previous studies have shown it to be induced following infection [300,301]. However, these experiments were performed in different cell types and with different conditions which may account for the differing observations.

At this point it was deemed prudent to establish if the WT and miR-21$^{-/-}$ cells were undergoing different rates of cell death in response to bacterial infection. *Salmonella* is a known cause of inflammatory cell death in macrophages, activating the NLRC4 inflammasome to and induce pyroptosis [302]. *Listeria* too can induce cell death in macrophages via an intermediate mechanism that is akin to necrosis [303]. The activation of caspase 1 by *Listeria* is thought to be a macrophage defence mechanism, and so it was important to ascertain what might be occurring in our system [304]. miR-21 itself has been linked to alteration of cell survival/cell death patterns in cancer: being an oncomiR, it is often associated with prolonging cell survival through its targeting of tumour suppressors. WT and miR-21$^{-/-}$ BMDMs were infected with *Salmonella* and *Listeria* and LDH release was measured as a readout for inflammatory cell death. As expected, *Salmonella* induced rapid inflammatory cell death, with almost 90% death occurring after 24 hours. *Listeria* infection also induced some cell

death, but at much more modest levels than *Salmonella* as anticipated. There was no difference in cell death between WT and miR-21$^{-/-}$ in any condition tested, which led us to assume that altered cell survival was not responsible for the enhanced bacterial burden phenotype we encountered in the miR-21 deficient cells. LDH assays have been used to monitor *Listeria* infected cells in the past but as stated previously the primary mode of cell death is not pyroptotic but necrotic and occurs after several hours of cytosolic bacterial replication [303,305].

Satisfied that our phenotype was not caused due to altered cell viability, the question of why miR-21 seemed to control burden of *Listeria* returned to the phagosome and how miR-21 deletion might impact on its normal function. Impaired phagosome maturation is associated with increased survival of intracellular bacteria, and so we hypothesised that miR-21 may positively regulate this process and its deletion may lead to abrogated maturation [306 13 15]. Phagosome maturation is characterized by the binding of different markers to the phagosome as it transitions through early, intermediate and late stages. To assess whether or not these markers were present at similar levels in WT and miR-21$^{-/-}$ macrophages, cells were infected with various MOIs of *Listeria* and assessed by Western blot for the early endosome markers EEA1 and Rab 5 as well as the late endosome marker Rab 7. The expression of these markers was stable across all infectious levels and similar to that of the untreated controls across both WT and miR-21$^{-/-}$ cells, indicating that miR-21 does not directly or indirectly influence the expression of these effector proteins. To further establish this, phagosome formation was quantified by immunostaining EEA1 in *Listeria* infected cells measuring the puncta formation. These puncta were formed in equal measure in both WT and miR-21 cells, suggesting that the once the phagosome is formed there is no difference between the two.

Listeria expresses its own form of hemolysin called LLO. This thiol-activated cholesterol-dependent cytolysin or pore-forming toxin punctures the phagosome vacuole allowing the bacterium to escape from the intracellular killing mechanisms that become prohibitive to growth and replication, and instead reach the niche of the cytosol where is can replicate and go on to infect other cells [16,305]. By altering the capacity of *Listeria* to produce LLO, the bacteria are trapped within the phagosome to be killed by the acidification and exposure to free radicals previously described. To

confirm whether miR-21 was influencing phagosome maturations, we compared bacterial burdens of WT Listeria and the LLO mutant, to see if the inability of the mutant to escape the phagosome by *Listeria* altered the observed miR-21$^{-/-}$ increased bacterial burden phenotype. WT and miR-21$^{-/-}$ BMDMs were infected with the ΔLLO mutant strain or WT parent strain. It was observed that the phenotype persisted, with enhanced bacterial burden with the ΔLLO strain in the miR-21$^{-/-}$ cells compared to WT macrophages. This was an interesting observation which led to two possible conclusions. The first possible conclusion is that miR-21$^{-/-}$ macrophages have such an impaired killing capacity so that even when *Listeria* are unable to escape the phagosome they still survive and replicate more readily then bacteria unfortunate enough to end up in a WT cell. Although we had accumulated several lines of evidence that indicated that miR-21$^{-/-}$ macrophages had no defects in the production of common bacteriocidal mechanisms or phagosome formation. The other conclusion to be drawn was that perhaps miR-21 is acting upstream of this event and influencing the initial uptake of the bacteria and formation of the phagocytic cup which is eventually pinched off to form the early phagosome. This conclusion is initially supported by the observation of the phenotype as early as 30 minutes post-infection.

Several miRNAs have previously been demonstrated to regulate the process of phagocytosis, with examples of both pro- and anti-phagocytic actin. miR-1 for instance has been shown to negatively regulate phagocytosis in RAW263.7 macrophages by targeting elements of the clathrin pathway [307]. miR-107 is downregulated by LPS, allowing macrophage motility via cyclin dependant kinase expression to facilitate actin mobilization [308]. Other miRNA positively regulate phagocytosis, such as miR-34a [309]. We hypothesised that miR-21 might belong in the former camp of negative phagocytosis regulators.

To test this hypothesis, experiments were conducted using the commonly employed FITC-dextran uptake assay in which uptake by a population of cells is assessed using flow cytometry. miR-21$^{-/-}$ BMDMs took up significantly more FITC-dextran than their WT counterparts, indicating that miR-21 may indeed play a role in regulating the uptake of *Listeria* as hypothesised. This observation was also confirmed in PECs, a heterogenous population of phagocytic innate immune cells that act as an effective *ex vivo* of macrophage/monocyte function.

Phagocytosis and in particular initial uptake, is dependent primarily on the actin cytoskeleton, and a series of cytoskeletal rearrangements triggered following receptor activation. In order to ascertain the importance of this actin rearrangement step in the observed miR-21$^{-/-}$ phenotype, the actin filament formation inhibitor cytochalasin D was utilized. WT and miR-21$^{-/-}$ cells pre-treated with this potent mycotoxin inhibitor of actin polymerisation displayed far lower absolute numbers of invading bacteria as would be expected, but crucially the increased burden previously associated with miR-21$^{-/-}$ cells was lost. Macrophages express a variety of phagocytic receptors which bind to particles, pathogens and components of dying cells and signal for actin rearrangement to facilitate their uptake. These include FcγRs and complement receptor 3 (CR3), which bind to immunolglobulin G (IgG)-opsonised particles and complement-coated particles respectively as well as mannose receptor (CD206/MRC) which binds C type lectins [310]. A key mediator of actin rearrangements are the RhoGTPases, which have been shown to be important for the initial formation of the phagocytic cup, which engulfs the invading pathogen [277]. We identified several targets of miR-21 involved in phagocytosis and actin rearrangement including the RhoGTPase, RhoB, which has been reported to operate in coordination with Cdc42 [133,167,311-315].

Macrophages have been shown to express high levels of the myristoylated, alanine-rich, C kinase substrate (MARCKS), an actin cross-linking protein [312]. In particular, this increased MARCKS expression is found in areas of the cell where actin filaments associate with the plasma membrane, and its expression is associated with regulation of cell motility [312,316]. A study by Carballo *et al.* implicated MARCKS in the regulation of the phagocytosis ofzymosan, specifically, in the rate of initial uptake. The authors observed significant differences in the rate of zymosan uptake between MARCKS-deficient cells and WT cells, with lower rates of uptake in particular at 45min and 60min [312]. This difference disappeared at a later time point (120 minutes). MARCKS has recently been shown to be a target of miR-21 in epithelial cells, where its expression influences mucin secretion [249,317]. Given that macrophages also express MARCKS, we wondered whether miR-21 may target MARCKS thereby regulating initial uptake by phagocytes. Indeed, we observed increased expression of MARCKS in miR-21$^{-/-}$ BMDM compared to WT cells. Furthermore, we show that MARCKS is induced in miR-21$^{-/-}$ BMDM following infection with *Listeria*.

Intracellular bacteria frequently allow their engulfment by macrophages so that they can shelter from components of the host immune system. Following internalisation, intracellular pathogens utilize sophisticated strategies to avoid destruction by these cells, enabling them to overcome host cell defences and replicate successfully. They block intracellular killing by inhibiting phagosome maturation, or express effector proteins which allow them to escape into the cytosol [279]. *Listeria* is among the archetypal bacteria employing these mechanisms, expressing LLO as previously discussed. Subsequently, *Listeria* induces actin tails through expression of an actin polymerising protein, ActA that facilitate its propulsion through the cell cytosol towards the cell membrane, where it forms protrusions into neighbouring cells allowing its internalization and facilitating cell-cell [318]. As a result of these bacterial strategies, there is an even greater pressure for host measures to counteract these immune evasion mechanisms in order to clear the infection. The ability of miR-21 to reduce internalization of *Listeria* by macrophages significantly impacts the outcome of infection in mice, with miR-21$^{-/-}$ mice displaying a significantly higher bacterial burden compared to WT mice. The increased dissemination of *Listeria* to livers and spleens of mice following intraperitoneal infection is in direct agreement with our previous observation that miR-21$^{-/-}$ resident peritoneal macrophages display increased phagocytosis of particles. Interestingly, this phenotype did seem to be particular to a model where macrophage uptake was required, as it was not recapitulated in the oral gavage model of infection which entails entry through IEC adherence and invasion. The *in vivo* phenotype did however mirror the *in vitro* observation that this effect does not appear to extend to phagocytosis of *Salmonella*.

In this chapter, we confirm several previously reported aspects of miR-21 biology in relation to TLR activation and induction by infection. In addition, a novel role for miR-21 during the host response to intracellular bacterial infection has been uncovered, whereby miR-21 regulates the fundamental process of phagocytosis. By targeting MARCKS and RhoB-mediated uptake of *Listeria* by macrophages, miR-21 limits the intracellular niche of *Listeria* and significantly impedes the pathogenesis of infection.

Chapter 5
-
Final discussion and future perspectives

5. Final discussion and future perspectives

Since the initial characterization of miRNA and RNA interference, over two decades of research have yielded many insights in to the working of cells and the complex layers of regulation that govern their function. The study of miRNA in the context of immune pathways is a more recent development, however many insights have begun to emerge into their importance to the function of immune cells in health and in disease states. miR-21 has been demonstrated to be a highly important miRNA in this context, performing many roles in different cells and acting to prevent inflammation on the one hand, but promoting carcinogensis and cancer progression on the other.

This study has identified two novel functions of miR-21 in the regulation of intestinal health and disease, specifically during intestinal inflammation and infection. Firstly, we show that miR-21 is a novel regulator of the intestinal microbiota, which subsequently impacts on the development of intestinal inflammation, as shown using the murine DSS-induced colitis model. Secondly, we demonstrate a novel role for miR-21 in the regulation of macrophage phagocytosis, with induction of miR-21 during infection with the facultative intracellular pathogen *Listeria monocytogenes* appearing to limit the entry of this bacterium, denying it the opportunity to form an intracellular niche.

Our initial studies with the miR-21$^{-/-}$ mouse indicated that there is indeed a role for miR-21 in colitis as suggested by the numerous observations that its expression was elevated in colitis. As miR-21 is generally considered to be an anti-inflammatory mediator, it came as a surprise to us that the knockout mouse exhibited a protected phenotype. The hypothesis we entered in to the project with was that a deficiency in miR-21 would lead to a reduction in the levels of the archetypal anti-inflammatory cytokine IL-10 and enhanced inflammation. This was based on reports of IL-10$^{-/-}$ mice exhibiting spontaneous colitis [251]. Interestingly, we did observe the expected reduction in IL-10 but it was not followed by increased inflammation. The fact that

IL-10 therapies have yet to show efficacy in human IBD hints that perhaps it is not the crucial effector that the field anticipated [319].

Our discovery that miR-21 expression is deleterious in a murine model of DSS-induced colitis via modulation of the intestinal microbiota is a fascinating insight into a miRNA function that has only just recently begun to be explored in earnest. While several studies have been published recently which highlight the importance of miRNA to the maintenance of intestinal homeostasis, few demonstrate an influence for miRNAs over the gut microbiota. One such paper, by Biton *et al,* demonstrated the importance of total miRNAs in governing intestinal immunity using a gut specific *Dicer1* knockout mouse [235]. With this tool they demonstrated that the absence of all gut miRNAs resulted in an impaired intestinal barrier within these mice. Another crucial paper in the miRNA field was published by Liu *et al* illustrating the capacity of miRNA to influence the shape of the intestinal microbiota [256]. This paper demonstrated that secreted host miRNA have the capacity to influence gene expression in commensal microbes present in the gut lumen, regulating growth signals in bacteria such as *Fusobacteria nucleatum* and *Escherichia coli* (*E. coli*). Using an IEC-specific *Dicer1* knockout mouse, similar to the study by Biton *et al*, the authors showed that miRNA deletion led to a significant dysbiosis of the intestinal microflora corresponding to a more severe reaction to induction of colitis with DSS which could be rescued by transfer of WT feces which contained multiple host secreted miRNA.

It is likely that an additional underlying mechanism for the dysbiosis observed in the Dicer-KO mouse, is the influence of the impaired barrier function directly on the microbiota, as it is known the integrity of the intestinal barrier and the gut microbiota are intimately connected. Indeed, Biton *et al* demonstrated reduced mucin secretion in colon-specific Dicer-KO mice. Intestinal mucins are an important part of the intestinal barrier, with the mucus layer forming a physical barrier which segregates the luminal contents including pathogenic and commensal organisms from the intestinal epithelium. Mucins also provide a source of nutrition for members of the gut microbiota, aiding their colonisation within the gut environment. Biton *et al* showed that this reduced mucin secretion was specifically due to the loss of transcription factor KLF5 inhibition by miR-375 which was essential for Goblet cell development as confirmed using a miR-375 knockout mouse. This result lent credence to the idea that individual miRNA could have profound impacts on fundamental intestinal

homeostatic function as had been seen in other systems [235]. The authors went further and described immunological mechanisms for homeostatic modulation of miR-375 whereby the Th2 cytokine IL-13 induced miR-375 which in turn promoted induction of the Th2 facilitating epithelial cytokine thymic stromal lyphoprotein (TSLP). This pathway was crucial for defence against helminth parasites, indicating a powerful miRNA mediated mechanism for intestinal homeostasis.

Our own data suggests that miR-21 has a role in shaping the microbiota which is deleterious in DSS-induced colitis. This discovery is highly novel, and demonstrates the importance of the microbiota in this disease model. The precise mechanisms governing the shift towards a less colitogenic microbiota in the miR-21$^{-/-}$ mice are yet to be fully elucidated, but there are several promising targets which are likely to help shed light on this process. Chief amongst them is the putative modulation of the mucus barrier. As demonstrated here, miR-21 has the capacity to directly target MARCKS, a protein that has already been shown to influence mucin secretion and have relevance in colitis [250,317,320]. The alteration of the make-up of the mucus layer can have a substantial impact on the composition of the commensal microbiota, as resident bacteria can employ the layer as a scaffold niche as well as a souce of nutrition in the form of mucin glycans. Even non-mucolytic bacteria have been shown to preferentially colonize altered mucous layers, such as commensal *E. Coli* which expand in the mucus layer during regrowth post antibiotic treatment. With this in mind, we hypothesize that miR-21 expression may influence the composition of the mucus layer, specifically the production of Muc5AC (a known MARCKS regulated mucin) and by doing so alter the available niche for different microbial populations to flourish. This idea is supported by the identification of taxa present in higher abundances in the miR-21$^{-/-}$ microbiota which are specialised for mucin degradation for nutrient acquisition. The prime example of this demonstrated in our data is *Bifidobacteria* which are present in higher abundances at several phylogenetic levels in the miR-21$^{-/-}$ microbiota and are adapted for nutrient acquisition from mucin glycoproteins [41,321]. In order to test this hypothesis, it would be interesting to use immunohistochemistry to assess whether or not MARCKS and/or Muc5AC are alternatively expressed in miR-21$^{-/-}$ tissue. These experiments have been attempted, so far unsuccessfully, and work is ongoing

The papers by Biton *et al* and Liu *et al,* demonstrate the capacity of miRNA to regulate all aspects of intestinal health and disease: the mucus layer, the intestinal epithelium, local immunity and of course the microbiota. In the paper published by Liu *et al*, miR-21 was seen to be present in mouse feces, though they did not go on to explore any putative function in their study. Other recent studies have shown that the microbiota can be disturbed by deletion of bacterial sensors such as NLRP6 [216]. Given that miR-21 regulates bacterial sensing through modulation of TLR4 signalling we hypothesised that it might play a role in the shaping the microbiota.

Another aspect of miR-21's role in colitis which our study has confirmed is the direct negative regulation of the tight-junction regulating actin polymerisation protein RhoB. A concurrent study by Shi *et al* demonstrated that elevated RhoB expression in miR-21$^{-/-}$ gave rise to enhanced barrier integrity during colitis which contributed to the protective colitis phenotype [133,252]. Our data is in agreement with this observation. However, this further suggests an underlying mechanism for the altered microbiota present in our miR-21$^{-/-}$ mice, given the already established links between barrier integrity and the microbiota. It has been demonstrated that certain probiotic bacteria, such as *Bifidobacterium*, protect from barrier permeability in obesity driven inflammation and our observation may represent more evidence of this cross talk in occurrence [322]. It is plausible to speculate that in a healthy individual, a higher commensal proportion of *Bifidobacterium* may signal to increase barrier integrity by suppressing miR-21 and allowing RhoB to maintain a functional barrier. Conversely, a microbiota that is less diverse and lacking these beneficial regulatory microbes may allow aberrant signalling to upregulate miR-21 and allow the barrier to become compromised. Shi *et al* also noted that miR-21 expression led to higher IEC apoptosis which also contributed to the breakdown of barrier integrity. As it has been stated previously, miR-21 is an oncomiR which is associated with halting cell death and facilitating the carcinogenic endothelial to mesenchymal transiton (EMT) [139,143,148-150]. This apparent contradiction is a feature of miRNA's capacity to regulate multiple targets.

The role of miR-21 in modulating immune cell activation in this model is very interesting as previously mentioned with regards IL-10. Our study has demonstrated that miR-21 deletion leads to a decrease in IL-10 secretion both in DSS treated colons

and in primary macrophages and dendritic cell cultures. In addition, we have demonstrated that TNF-α secretion is enhanced in miR-21$^{-/-}$ macrophages, consistent with various studies which report a role for miR-21 in regulating NF-κB activity [129,155]. Furthermore, we also confirm that miR-21 negatively regulates IL-12 expression in dendritic cells, an observation which has been observed in models of lung injury, asthma and mycobacterial infection [161,164,167]. The accumulating evidence of the anti-inflammatory action of miR-21 seemed to be somewhat at odds with our observations and the observations of Shi *et al* that miR-21 deletion was protective in colitis. A further study by Wu *et al* has shown that miR-21 deletion has a divergent phenotype in different models of colitis [323]. In this paper, the miR-21 protective phenotype is confirmed once again, but the opposite phenotype is observed in the TNBS and T cell transfer models of colitis, with CD4+CD45RB^{high} T cells displaying a tendency to skew towards a Th1 phenotype which would be predicted by miR-21's suppression of the Th1 polarizing cytokine IL-12. The latter observation is interesting as Shi *et al* report reduced T cell infiltration and reduced TNF-α secretion in the DSS model of colitis.

This divergence of phenotype raises interesting questions about miR-21's role in disease. Despite its many anti-inflammatory properties, miR-21 has been shown to contribute to inflammation in a number of other diseases where its ablation has been shown to be protective, including colitis-associated colorectal cancer and psoriasis [171,253]. The authors of the study implicating miR-21 in attenuation of TNBS colitis symptoms suggest that their results indicate that miR-21 may be having different effects in the pathogenesis of IBD, which is after all a highly complex multi-factorial disease. Our findings contribute to this literature, and it would be very interesting to examine the effect of antibiotic-depletion of the microbiota on the TNBS-coiltis phenotype observed by Wu *et al*. We would argue that miR-21 plays a deleterious role in the maintenance of barrier integrity and host-microbe cross talk and that this effect may be missed in a model which so strongly polarizes T cell responses. Additional models of bacterially induced colitis may help clarify these observations, such as the *Citrobacter reodentium* induced colitis model (which unfortunately failed to elicit a response in our facilities) or the *Helicobacter hepaticus* induced colitis model. The latter is particularly interesting as *H. hepaticus* is a commensal bacteria ordinarily found in conventional mouse microflora. This model mimics microbial

dysregulation and loss of immunosupression by the addition of anti-IL-10R antibodies, and so might be a highly relevant model in light of our findings and the findings of the other groups who have published in this area.

In the second part of this thesis, we examined the influence of miR-21 expression on innate immune cell function, specifically in response to infection with the pathogenic bacteria *Salmonella* and *Listeria*. We describe a novel mechanism for miR-21 in regulating the immune response to *Listeria* infection, specifically controlling this prevalent pathogen's entry in to phagocytes where the bacteria is ideally adapted to replicate and spread to cause systemic infection which is deleterious to the host. We show that miR-21 expression significantly impacts on *Listeria's* ability to exploit this intracellular niche, and furthermore impacts the outcome of infection.

As has been described throughout this thesis, miR-21 negatively regulates signalling by TLRs, particularly TLR4, which induce miR-21 as part of a negative feedback mechanism to dampen the inflammatory signals they generate to prevent excessive inflammation. To date, much of the work demonstrating this had been performed *in vitro* using immortalised cell lines and primary cells in which miR-21 was inhibited by siRNA technology. An advantage to our study was the fact that we had access to a specifically generated miR-21 deficient mouse, allowing us to directly characterise the role of miR-21 both *in vitro* using primary cells and *in vivo* in the mouse model itself. In this way, we sought to confirm previous findings of a role for miR-21 in regulating TLR responses to bacterial ligands as well as explore other aspects of the immune response of innate immune cells important during live bacterial infection.

Our initial results in RAW 246.7 macrophages and in BMDMs confirmed that miR-21 is indeed a TLR4 inducible gene. Its induction profile was similar to previous reports in the literature, where miR-21 is induced in a time dependant manner, with its induction being slightly delayed relative to the reported induction of other miRNA by the same stimuli [129,131]. miRNA regulation is complicated when compared to ordinary Pol II transcription of protein–coding genes due to the requirement of second processing of primary transcripts in to mature active molecules. This delay in induction of miR-21 has been shown to be due to a delay in processing the mature form of the miRNA from pri-miR21 by the enzymes Drosha and Dicer, with the rate

of transcription of the pri- form outstripping this processing step in certain contexts [144,324].

Cytokines are crucial effectors of the innate and adaptive immune system, and miRNAs have been shown to be important in promoting their expression and secretion as well as, in the case of miR-21 in particular, suppressing cytokine expression when the inflammation elicited by their activity is no longer required. This miRNA-mediated effect on cytokine activity can take place intracellularly, as is the case in the suppression of TLR4 signalling by miR-155. Here, miR-155 suppresses the regulatory protein SHIP1 to allow amplification of TLR4 signalling which in turn signals to secrete more pro-inflammatory cytokines such as IL-1β, TNF-α, IL-6 etc. Another example of negative regulation in an intracellular manner comes in the form of miR-146a which is strongly induced by TLR4 stimulation, and acts to dampen the signalling from TLR4 that gives rise to its own expression, targeting downstream signalling molecules such as TRAF6 [325]. In a similar context, miR-21 has an important role in allowing translation of IL-10 to dampen down systemic inflammation following its own NF-κB-dependant induction by TLR4. Our own results were in agreement with these previous studies, with miR-21$^{-/-}$ -derived macrophages and dendritic cells secreting less IL-10 and more TNF-α upon stimulation with LPS. However, there were some time dependant differences which were notable between our findings and previous reports, in particular, the equalization of IL-10 levels at 24 hours which was not the case in our hands [155]. These observations also carried through to stimulation of TLR2 which shares several signalling pathways in common with TLR4 and is an important receptor for sensing gram-positive bacteria such as *L. monocytogenes*. These cytokines were also assessed after *in vivo* infection and miR-21 was again confirmed to be anti-inflammatory in its repression of TNF-α secretion in the serum of WT mice relative to miR-21$^{-/-}$ mice. However, IL-10 secretion was found to be unaltered perhaps indicating that its regulation is secondary to that of TNF-α in this model of sepsis. There was no consistent effect demonstrated regarding IL-6 secretion, which is interesting in a number of ways. IL-6 is a NF-κB-regulated gene and so it would be predicted to behave like TNF-α in this system. Indeed in other studies employing miR-21$^{-/-}$ cells an increase in IL-6 with TLR4 stimulation has been observed consistently [155]. miR-21 induction by IL-6 has been shown to be a key mechanism for EMT (along the so-

called IL-6/STAT3/miR-21 axis) so it was surprising that there was no reciprocal regulation lost upon miR-21 deletion [141,143,149].

More surprising than this however, was the failure of the miR-21$^{-/-}$ -dependent IL-10 and TNF-α phenotype to fully translate into models of infection. While there was an increased level of TNF-α release by miR-21$^{-/-}$ macrophages in response to *Listeria* infection, the IL-10 phenotype was not demonstrated to hold true to the previous observations. This observation is closely aligned with those in the paper previously referred to by Barnett *et al,* in which miR-21$^{-/-}$ mice display a significant increase in mortaility in an LPS sepsis model, which is not replicated using the bacterial CLP model. The authors suggest that this may be due to the time of delay of miR-21 expression in this CLP model (miR-21 is not observed until 48 hours) and that the anti-inflammatory role of miR-21 may actually be harmful in sepsis. This argument references the "2-hit" model of sepsis which states that the mortality associated with sepsis is caused not just by the initial hyperinflammatory response but by the subsequent period of immunosuppression which allows primary infections to take hold of the host or opportunistic secondary infections to occur. They also suggest that antagonising miR-21 might be therapeutically beneficial to allow a sufficiently robust immune response to clear these infections. Our observations regarding miR-21 expression post-infection are different, although they are also in a single cell culture system rather than in the whole animal. *Salmonella* and *Listeria* both induced miR-21 at early times (2-4 hours) before this faded towards 24 hours post-infection. This induction peaks earlier and fades faster than in LPS treated cells, which is interesting in the context of the different levels of regulation mentioned earlier. Furthermore, infection with live bacteria likely triggers a greater number of cellular machinery components more rapidly to process a pre-existing pool of miR-21 precursors than a single PRR signal before fading with bacterial degradation. In contrast, a more sustained PRR signal might induce more *de novo* transcription of the miR-21 gene. It would be interesting to assess induction of miR-21 after exposure to non-virulent heat killed bacteria to assess whether uptake of PAMP covered particles induces the miRNA to the same extent as a live bacterium. This would also be interesting in the context of cytokine secretion, where differences in IL-10 and TNF-α levels observed post-PRR stimulation are not recapitulated upon infection with live bacteria. Perhaps a heat-killed bacterium would not override these PRR driven differences. Our study

together with that of Barnett *et al* have demonstrated that miR-21's anti-inflammatory action through cytokine secretion may not be as straightforward as previously thought due to the complexity of signalling elicited by live pathogens.

The initial response of many innate immune cells upon detection of a foreign entity (pathogen, particle or dying cell) is to phagocytose it and destroy it. There are many downstream consequences of this process, such as the cytokine release discussed above and the presentation of antigen to the adaptive immune system in order to ensure a robust immune response. However, some pathogens have adapted to take advantage of this process and develop a niche inside phagocytic immune cells. We have discovered a novel role for miR-21 in the context of infection with the facultative intracellular pathogen *L.monocytogenes*. miR-21 limits uptake of *Listeria* within macrophages, thereby depriving this intracellular pathogen of its cellular niche from which it is protected from the external immune environment, and can happily replicate and spread to neighbouring cells, ultimately causing the systemic infection which leads to severe listeriosis.

Our initial observation that *Listeria* were present in higher numbers in miR-21$^{-/-}$ macrophages and dendritic cells was counter to our initial expectations. It was anticipated that deletion of miR-21 would result in a more bacteriocidal M1-like macrophage due to the loss of anti-inflammatory that is entailed (elevated TNF-α expression for instance). The literature on this is mixed, with reports of miR-21 acting as a brake on PGE2-induced M2 macrophage polarization contrary to the anticipated phenotype described above [162]. In addition, RAW264.7 macrophages have been reported to display an increased M1-like phenotype upon transfection with an miR-21 mimic in a study where miR-21 was suggested to be a causative agent in deleterious macrophage polarization in acute kidney injury [295]. Thus, we sought an explanation for the apparent failure of miR-21$^{-/-}$ cells to control bacterial infection in our model. Initially, WT and miR-21$^{-/-}$ BMDMs were assessed for evidence of M1/M2 differentiation, but there was little consistent data obtained from these experiments. To better understand miR-21's potential role in the phenotype, comparison of WT and miR-21$^{-/-}$ BMDMs conventionally polarized with either LPS (M1) or IL-4 (M2) would be a more appropriate experiment, and indeed this is currently being investigated by other members of the Corr lab and the Sheedy lab.

The increased bacterial burden in cells upon loss of miR-21 was not simply due to increased cell death in WT cells, a there was no observable difference in loss of cell viability upon infection with either *Listeria* or *Salmonella*, though the latter did cause far higher pyroptotic cell death as measured by LDH assay. It would be interesting to assay this effect using AnnexinV staining in order to further differentiate different forms of cell death, particularly in light of miR-21's contradictory roles in this area and the particular form of semi-necrotic cell death instigated by *Listeria*.

We next looked to the steps of the phagocytic process, initially focussing on the phagosome itself, which is crucial to successful clearance of an infection. Indeed, phagosome maturation and the bacterial killing associated with it are vital processes in innate immune cells. Defective phagosome function is associated with several disease states including chronic autoimmune polyarthritis caused by DNA escaping from ineffective macrophage phagosomes and leading to a break down in self tolerance [326]. Among the primary killing mechanisms elicited by phagocytes are induction of the free radicals ROS and NO. miR-21 has been associated with altered NO production previously and it is a key mechanism for anti-*Listeria* defence [153]. Interestingly, with regard to the first chapter of this thesis, miR-21 is positively correlated with increased macrophage infiltration and expression of the NO producing enzyme NOS2, which might imply that miR-21 deficiency would correlate with a reduction of this NO producing enzyme [327]. However we could detect no role for miR-21 in either NO or ROS induction that led us to believe this contributed to the observed increased bacterial burden in miR-21 deficient cells. The ROS assay employed was based on standard practice in the O' Neill laboratory, and it is possible that *Listeria* induced ROS induction has been missed as it has been reported that intracellular ROS production can be induced by *Listeria* as early as 20 minutes post-infection [328].

Literature implicating miRNA in the process of phagosome formation and maturation is sparse. However there are some reports of miRNA being hijacked or interfered with by invading pathogens to subsequently alter phagosome conditions. For instance, miR-17-5p was recently reported to arrest the maturation of mycobacterial phagosomes in part by targeting ULK1, subsequently reducing the ability of host cells

to kill intracellular BCG [329]. In our study, it was initially hypothesised that the increased burden of *Listeria* detected in miR-21$^{-/-}$ BMDMs and BMDCs was due to an impairment of phagosome processing. However, following investigation, we observed no difference in phagosome maturation in WT vs miR-21$^{-/-}$ BMDMs, indicating that miR-21 is not involved in this part of the process.

As described previously, miRNA have been demonstrated to regulate the process of phagocytosis, and we hypothesised that miR-21 might be a negative regulator of phagocytosis in order to limit the uptake of *Listeria*, as such denying it of the intracellular niche in which *Listeria* have adapted to replicate effectively [16]. *Listeria* has been shown to subvert the classical immune role of phagocytic cells to allow them reach peripheral organs and disseminate freely. Indeed experiments have been conducted showing that mice infected with *Listeria* display reduced dissemination to and infection of major organs (such as the spleen, liver and brain) compared to mice inoculated with macrophages that had previously been infected with *Listeria* [330]. On this basis, we further hypothesised that as miR-21 did not appear to have a role in the process of ensuring efficient bacterial killing, it may act earlier to stop *Listeria* establishing its intracellular niche. This idea is supported by our *in vivo* data, where the heavily phagocyte dependant intraperitoneal infection model was seen to lead to higher dissemination in the absence of miR-21, indicating that miR-21 controls the uptake of the bacteria by peritoneal macrophages to limit their systemic infection. Indeed our own FITC-dextran uptake assays in PECs confirm that this mechanism is likely to occur in this context.

Actin mobilization is absolutely integral to phagocytosis of particles, with actin rearrangements being required for the cytoskeletal rearrangements needed for engulfment. Following pre-treatment of BMDMs with the actin inhibitor cytochalasin D, the previous enhanced burden phenotype was lost, indicating that actin regulation is a key determinant in our system. In our investigation into how miR-21 might be regulating actin rearrangements and initial engulfment of *Listeria,* we identified several miR-21 targets predicted to regulate actin filament formation and rearrangements that are critical to formation of the phagocytic cup and subsequent engulfment. These targets were RhoB and MARCKS. MARCKS in particular has been shown to be involved in the phagocytosis of zymozan by macrophages, in

particular at early time points, so we considered it to be a leading candidate for further investigation [311]. Deletion of miR-21 allowed the expression of RhoB, Cdc42 and MARCKS to increase dramatically with *Listeria* infection. This demonstrates that miR-21 acts to control these actin mediators to limit bacterial invasion of phagocytes, as well as subsequent dissemination as was demonstrated in an *in vivo* model of infection. During *Listeria* infection, following escape from the phagosome, cytosolic *Listeria* use the bacterial factor ActA to induce actin polymerisation and formation of distinctive actin tails which propel the bacteria through the cell cytosol, eventually coming into contact with neighbouring cells[16]. It would be interesting to investigate if the dysregulated actin mobilization mechanisms in the miR-21$^{-/-}$ allow for enhanced comet tail formation and greater cell-cell spread by *Listeria*.

It was curious that these mechanisms did not translate in to a similar phenotype upon infection with *Salmonella*. Phagocytosis is a complex process with many receptors and it is possible that miR-21$^{-/-}$ cells also express a receptor which preferentially binds one bacterium or the other and causes differential signalling to be elicited downstream. Another consideration, which may explain the difference between *Listeria* and *Salmonella*, is the relative size of the bacteria which has a bearing on the nature of the phagocytic process which occurs [10]. *Salmonella* are significantly larger than *Listeria* (0.7-1.5 by 2.0-5.0 μm versus 0.4-0.5 by 0.5-2.0 μm) and this may lead to an overwhelming receptor binding by comparison to *Listeria* infection. This process is likely mediated by the C type lectin receptor MRC (CD206 or mannose receptor) which has also been demonstrated to be responsible for FITC-dextran uptake. Another possible explanation is that *Salmonella* induced cell death to such a great extent in our system that differences may have been buffered out as a result.

Overall, this work has confirmed several roles for miR-21 in different immune contexts, as well as describing two novel roles for this miRNA in homeostatic gastrointestinal regulation and gram-positive infection. The main findings are summarised in Figure 5.1. This study provides further insights in to the established immunological role of miR-21, as well as the emerging field of host miRNA-microbiota interactions. MiR-21's capacity to modulate the host response to bacteria in different contexts is interesting when one wishes to assess miR-21's potential as a therapeutic target.

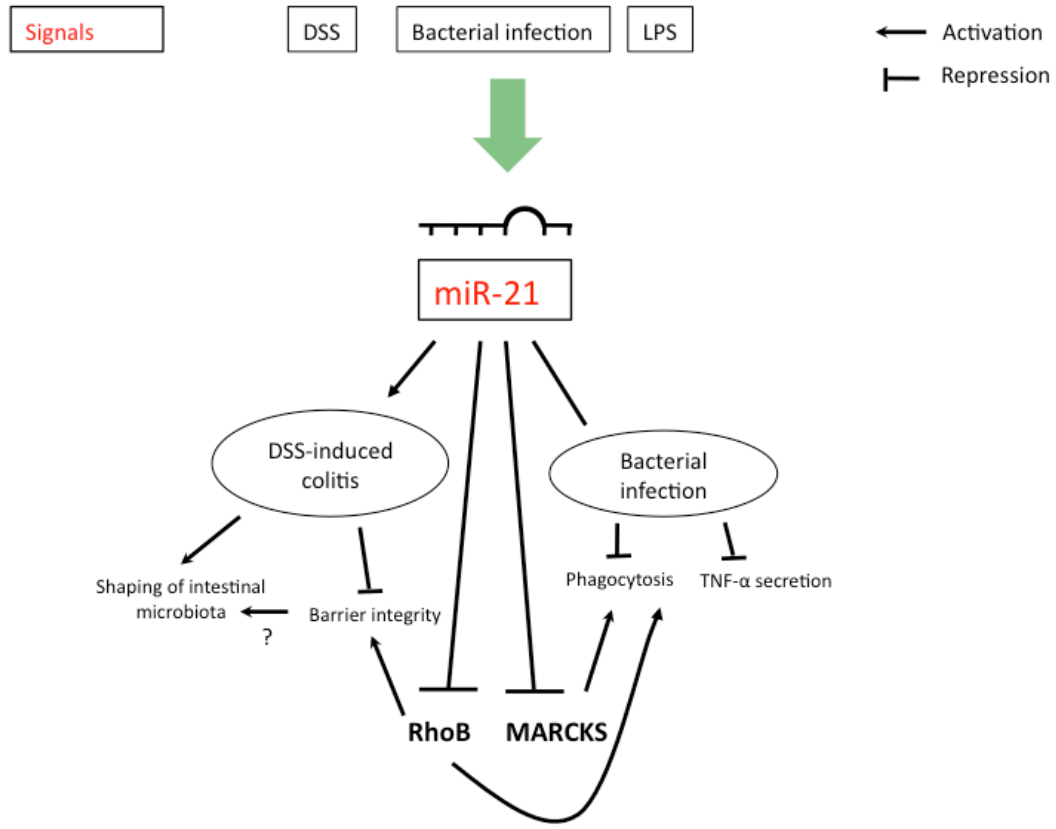

Figure 5.1 MiR-21 in infection and IBD

MiR-21 induction in response to various bacterial stimuli, and DSS treatment has a number of downstream consequences for the cells and organs in question. The reduction of RhoB in colitis by enhanced miR-21 expression has been demonstrated to lead to impaired barrier integrity and enhanced disease. This study has shown that miR-21 influences the composition of the intestinal microbiota, and that this too impacts on the disease, possibly due to the barrier integrity alteration. In addition, this study has demonstrated an anti-inflammatory role for miR-21 in bacterial infection with *Listeria*, where miR-21 suppresses phagocytosis to prevent the formation of an intracellular niche and subsequent dissemination. The suppression of pro-phagocytic actin modifying molecules RhoB and MARCKS may play a role in this effect.

There are several existing examples of studies which explore therapeutic manipulation of miR-21 in inflammatory diseases, reviewed extensively elsewhere [144]. These studies have for the most part sought to block miR-21 in the diseases in question (models of kidney disease and psoriasis for example), and the interventions have led to protection in the models employed [171,331]. The work presented in this thesis adds to the existing literature on miR-21 in inflammatory disease. The finding that miR-21 deletion protects mice in a model of IBD initially seemed to suggest that blocking miR-21 therapeutically in patients may be a successful strategy to aid in treatment of this disease. However, whilst our work and the work of other groups has demonstrated this effect with DSS-colitis, other models have shown that the reverse is true and that the anti-inflammatory roles of miR-21 are important when certain pathways in IBD are more active (such as the T and B cell response initiated by the TNBS model of acute colitis). As with all potential miRNA modulating therapeutics, this underscores the need for a through understanding of the miRNA's role in that disease and what off-target effects may occur. In this example, the use of targeted delivery may allow specific, cell-type dependant modulation of miR-21 to maximise therapeutic potential. In addition, morpholino oligonucleotide technology may present a means of limiting problem by allowing the targeting of specific miRNA:mRNA interactions (e.g. limiting miR-21 repressing RhoB expression and allowing a more intact barrier) [144].

A particularly interesting aspect of this is the microbiota modulating capacity of miR-21 which may impact of the disease. Altering the microbiota (or the more accurately the microbiota products that aid host homeostasis or lead to disease) has become a field of intense interest in recent years as our understanding of the host-microbe interface has developed. This must be borne in mind in the context of all disease models which are being targeted for therapeutic intervention, as alteration of the microbes present may enhance or limit efficacy of the treatment. It also points to further complexity in miR-21's role in homeostasis and the response to infection, as our data suggests that miR-21 negatively shape the microbiota in the context of IBD but also limits the capacity of certain GI tract pathogens to gain access to host cells and cause more severe infection. Several existing immunotherapies for inflammatory disease which block pro-inflammatory pathways (such as TNF-α) come with an increased risk of infection as a result of the immunosuppression involved, and this

may prove to be a particularly complex challenge for miRNA therapies as highlighted by the results presented here [332].

The study of potential uses for miRNA in a therapeutic context is not limited simply assessing whether or not modulating individual miRNA can be beneficial for patients. MiRNA can also reveal target mRNAs which may be involved in disease, and our work and that of others perhaps demonstrates that RhoB and MARCKS may be interesting in both IBD and in understanding *Listeria* and its modes of infection. In addition, the potential of miRNA to act as biomarkers is an established idea and their study may aid to more effective diagnoses and the ability to demarcate subtleties which can differentiate a patients disease in a precise manner. MiR-21 has been shown to be deleterious in mouse models of inflammation induced CAC and in patients with the disease [253]. Given that miR-21 is so heavily involved in cancer progression, it is interesting to consider whether it may serve as a marker for a transition from inflammatory disease to a cancer diagnoses, especially in IBD and CAC. Longitudinal studies of the miR-21 expression status in such patients would be interesting in this regard. It is possible that tumour progression may be initiated gradually through repeated cycles of miR-21 induction to begin inflammation resolution and repair in chronic diseases such as IBD.

Overall it is clear that miR-21 is a highly impactful molecule in homeostasis and disease and that control of its expression in different contexts is crucial for effective homeostasis. The results presented in this thesis add to out understanding of miR-21's role in IBD and in the innate immune response to infection by GI tract pathogens, as well as revealing an intriguing and novel role in modulating the commensal microflora of the gut which may have consequences throughout the whole organism. Elucidation of the mechanisms governing this effect may open up a range of possible miRNA:microbiota interactions with great potential for future discoveries and therapeutic interventions.

Chapter 6
-
References

6. References

1 Turner, J. R. Molecular basis of epithelial barrier regulation: from basic mechanisms to clinical application. *The American journal of pathology* **169**, 1901-1909, doi:10.2353/ajpath.2006.060681 (2006).

2 Kenneth Murphy, J. C. J., Travers P, Walport M, et al. . *Immunobiology: The Immune System in Health and Disease*. 8th edition edn, (New York: Garland Science; , 2012).

3 Benoit, M., Desnues, B. & Mege, J. L. Macrophage polarization in bacterial infections. *Journal of immunology (Baltimore, Md. : 1950)* **181**, 3733-3739 (2008).

4 Ginhoux, F. & Jung, S. Monocytes and macrophages: developmental pathways and tissue homeostasis. *Nature reviews. Immunology* **14**, 392-404, doi:10.1038/nri3671 (2014).

5 Ovchinnikov, D. A. Macrophages in the embryo and beyond: much more than just giant phagocytes. *Genesis (New York, N.Y. : 2000)* **46**, 447-462, doi:10.1002/dvg.20417 (2008).

6 Gordon, S., Pluddemann, A. & Martinez Estrada, F. Macrophage heterogeneity in tissues: phenotypic diversity and functions. *Immunological reviews* **262**, 36-55, doi:10.1111/imr.12223 (2014).

7 Martinez, F. O. & Gordon, S. The M1 and M2 paradigm of macrophage activation: time for reassessment. *F1000prime reports* **6**, 13, doi:10.12703/P6-13 (2014).

8 Tauber, A. I. Metchnikoff and the phagocytosis theory. *Nat Rev Mol Cell Biol* **4**, 897-901 (2003).

9 Takeuchi, O. & Akira, S. Pattern recognition receptors and inflammation. *Cell* **140**, 805-820, doi:10.1016/j.cell.2010.01.022 (2010).

10 Kinchen, J. M. & Ravichandran, K. S. Phagosome maturation: going through the acid test. *Nat Rev Mol Cell Biol* **9**, 781-795, doi:10.1038/nrm2515 (2008).

11 Vandivier, R. W., Henson, P. M. & Douglas, I. S. Burying the dead: the impact of failed apoptotic cell removal (efferocytosis) on chronic inflammatory lung disease. *Chest* **129**, 1673-1682, doi:10.1378/chest.129.6.1673 (2006).

12 Mao, Y. & Finnemann, S. C. Regulation of phagocytosis by Rho GTPases. *Small GTPases* **6**, 89-99, doi:10.4161/21541248.2014.989785 (2015).

13 Weiss, G. & Schaible, U. E. Macrophage defense mechanisms against intracellular bacteria. *Immunological reviews* **264**, 182-203, doi:10.1111/imr.12266 (2015).

14 Gordon, S. Phagocytosis: An Immunobiologic Process. *Immunity* **44**, 463-475, doi:10.1016/j.immuni.2016.02.026 (2016).

15 Ehrt, S. & Schnappinger, D. Mycobacterial survival strategies in the phagosome: defence against host stresses. *Cellular microbiology* **11**, 1170-1178, doi:10.1111/j.1462-5822.2009.01335.x (2009).

16 Portnoy, D. A., Auerbuch, V. & Glomski, I. J. The cell biology of Listeria monocytogenes infection: the intersection of bacterial pathogenesis and cell-mediated immunity. *J Cell Biol* **158**, 409-414, doi:10.1083/jcb.200205009 (2002).
17 Himanshu Kumar, T. K., and Shizuo Akira. Pathogen Recognition by the Innate Immune System. *International Reviews of Immunology*, 16-34 (2011).
18 Unterholzner L, K. S., Baran M, Horan KA, Jensen SB, Sharma S, Sirois CM, Jin T, Latz E, Xiao TS, Fitzgerald KA, Paludan SR, Bowie AG. IFI16 is an innate immune sensor for intracellular DNA. *Nature immunology* **11**, 997-1004 (2010).
19 Cohn, R. M. S. a. Z. A. IDENTIFICATION OF A NOVEL CELL TYPE IN PERIPHERAL LYMPHOID ORGANS OF MICEI. MORPHOLOGY, QUANTITATION, TISSUE DISTRIBUTION. *Journal of Experimental Medicine* **137**, 1142–1162 (1973).
20 Lemaitre B, N. E., Michaut L, et al. Thedorsoventral regulatory gene cassette spatzle/toll/cactus
controls the potent antifungal response in drosophila adult. *Cell*, 973–983 (1996).
21 Poltorak, A., et al. . Defective LPS signaling in C3H/HeJ and C57BL/10ScCr mice: mutations in Tlr4 gene. . *Science* **5396**, 2085-2088 (1998).
22 Anderson KV, J. G., Nüsslein-Volhard C. Establishment of dorsal-ventral polarity in the Drosophila embryo: genetic studies on the role of the Toll gene product. *Cell* **3**, 779-789 (1985).
23 Medzihitov R, P.-H. P., Janeway CR Jr. A human homologue of the Drosophila Toll protein signals activation of adaptive immunity. *Nature* **388**, 394-397 (1997).
24 Tatsushi Muta, K. T. Essential roles of CD14 and lipopolysaccharide-binding protein for activation of toll-like receptor (TLR)2 as well as TLR4: Reconstitution of TLR2- and TLR4-activation by distinguishable ligands in LPS preparations. *European Journal of Biochemistry* **268**, 4580-4589 (2001).
25 Tiina Peritz, F. Z., Theresa J Kannanayakal, Kalle Kilk, Emelía Eiríksdóttir, Ulo Langel & James Eberwine. Immunoprecipitation of mRNA-protein complexes. *Nature Protocols* **1**, 577 - 580 (2006).
26 Ausube, F. M. Are innate immune signaling pathways in plants and animals conserved? *Nature immunology* **6** 973 - 979 (2005).
27 O' Neill, L. Plant science. Innate immunity in plants goes to the PUB. *Science* **332**, :1386-1387 (2010).
28 Seong, S. Y. & Matzinger, P. Hydrophobicity: an ancient damage-associated molecular pattern that initiates innate immune responses. *Nature Reviews Immunology* **4**, 469-478, doi:10.1038/nri1372 (2004).
29 O'Neill, L. A., Golenbock, D. & Bowie, A. G. The history of Toll-like receptors - redefining innate immunity. *Nature reviews. Immunology* **13**, 453-460, doi:10.1038/nri3446 (2013).
30 Novotny AR, R. D., Assfalg V, Altmayr F, Friess HM, Emmanuel K, Holzmann B. Mixed antagonist response and sepsis severity-dependent dysbalance of pro- and anti-inflammatory responses at the onset of postoperative sepsis. *Immunobiology.* **[Epub ahead of print]** (2011).
31 Owyang S, L. J., Owyang C, Zhang M, Kao JY. Helicobacter pylori DNA's anti-inflammatory effect on experimental colitis. *Gut Microbes.* **3** (2012).

32 Tarassishin L, S. H., Lee SC. Interferon regulatory factor 3 plays an anti-inflammatory role in microglia by activating the PI3K/Akt pathway. *The Journal of Neuroinflammation.* **30**, 187 (2011).
33 O'Neill, L. A. & Dinarello, C. A. The IL-1 receptor/toll-like receptor superfamily: crucial receptors for inflammation and host defense. *Immunology today* **21**, 206-209 (2000).
34 Luke A.J. O'Neill, K. A. F. a. A. G. B. The Toll–IL-1 receptor adaptor family grows to five members. *Trends in immunology* **Vol.24 No.6 June 2003**, 286-289 (2003).
35 Puel, A. *et al.* Heritable defects of the human TLR signalling pathways. *Journal of endotoxin research* **11**, 220-224, doi:10.1179/096805105X37367 (2005).
36 Belkaid, Y. & Artis, D. Immunity at the barriers. *European journal of immunology* **43**, 3096-3097, doi:10.1002/eji.201344133 (2013).
37 Johnston, D. G. & Corr, S. C. Toll-Like Receptor Signalling and the Control of Intestinal Barrier Function. *Methods in molecular biology* **1390**, 287-300, doi:10.1007/978-1-4939-3335-8_18 (2016).
38 Helander, H. F. & Fandriks, L. Surface area of the digestive tract - revisited. *Scandinavian journal of gastroenterology* **49**, 681-689, doi:10.3109/00365521.2014.898326 (2014).
39 Hooper, L. V. & Macpherson, A. J. Immune adaptations that maintain homeostasis with the intestinal microbiota. *Nature reviews. Immunology* **10**, 159-169, doi:10.1038/nri2710 (2010).
40 Johansson, M. E. *et al.* The inner of the two Muc2 mucin-dependent mucus layers in colon is devoid of bacteria. *Proceedings of the National Academy of Sciences of the United States of America* **105**, 15064-15069, doi:10.1073/pnas.0803124105 (2008).
41 Tailford, L. E., Crost, E. H., Kavanaugh, D. & Juge, N. Mucin glycan foraging in the human gut microbiome. *Frontiers in genetics* **6**, 81, doi:10.3389/fgene.2015.00081 (2015).
42 Kim, Y. S. & Ho, S. B. Intestinal goblet cells and mucins in health and disease: recent insights and progress. *Current gastroenterology reports* **12**, 319-330, doi:10.1007/s11894-010-0131-2 (2010).
43 Peterson, L. W. & Artis, D. Intestinal epithelial cells: regulators of barrier function and immune homeostasis. *Nature reviews. Immunology* **14**, 141-153, doi:10.1038/nri3608 (2014).
44 Lavelle, E. C., Murphy, C., O'Neill, L. A. & Creagh, E. M. The role of TLRs, NLRs, and RLRs in mucosal innate immunity and homeostasis. *Mucosal immunology* **3**, 17-28, doi:10.1038/mi.2009.124 (2010).
45 Corr, S. C. *et al.* MyD88 adaptor-like (Mal) functions in the epithelial barrier and contributes to intestinal integrity via protein kinase C. *Mucosal immunology* **7**, 57-67, doi:10.1038/mi.2013.24 (2014).
46 Jung, C., Hugot, J.-P. & Barreau, F. Peyer's Patches: The Immune Sensors of the Intestine. *International Journal of Inflammation* **2010**, 823710, doi:10.4061/2010/823710 (2010).
47 Sipos, F. *et al.* The possible role of isolated lymphoid follicles in colonic mucosal repair. *Pathology oncology research : POR* **16**, 11-18, doi:10.1007/s12253-009-9181-x (2010).

48 Maloy, K. J. & Powrie, F. Intestinal homeostasis and its breakdown in inflammatory bowel disease. *Nature* **474**, 298-306, doi:10.1038/nature10208 (2011).
49 Kuhn, R., Lohler, J., Rennick, D., Rajewsky, K. & Muller, W. Interleukin-10-deficient mice develop chronic enterocolitis. *Cell* **75**, 263-274 (1993).
50 Fukata, M. *et al.* Toll-like receptor-4 is required for intestinal response to epithelial injury and limiting bacterial translocation in a murine model of acute colitis. *American journal of physiology. Gastrointestinal and liver physiology* **288**, G1055-1065, doi:10.1152/ajpgi.00328.2004 (2005).
51 Thaiss, C. A., Levy, M., Suez, J. & Elinav, E. The interplay between the innate immune system and the microbiota. *Curr Opin Immunol* **26**, 41-48, doi:10.1016/j.coi.2013.10.016 (2014).
52 Lederberg J, M. A. Ome sweet 'omics: -- A genealogical treasury of words. . *The Scientist.* **15** (2001).
53 A., v. L. An abstract of a Letter from Antonie van Leeuwenhoek, Sep. 12, 1683. About Animals in the scrurf of the Teeth. *Philosophical Transactions of the Royal Society of London.* **1684**, 568–574 (1684).
54 Dobell, C. The Discovery of the Intestinal Protozoa of Man. *Proceedings of the Royal Society of Medicine* **13**, 1-15 (1920).
55 Hattori, M. & Taylor, T. D. The Human Intestinal Microbiome: A New Frontier of Human Biology. *DNA Res* **16**, 1-12, doi:10.1093/dnares/dsn033 (2009).
56 Sender, R., Fuchs, S. & Milo, R. Revised estimates for the number of human and bacteria cells in the body. *bioRxiv* (2016).
57 Marchesi, J. R. Prokaryotic and eukaryotic diversity of the human gut. *Advances in applied microbiology* **72**, 43-62, doi:10.1016/S0065-2164(10)72002-5 (2010).
58 Reyes, A. *et al.* Viruses in the faecal microbiota of monozygotic twins and their mothers. *Nature* **466**, 334-338, doi:10.1038/nature09199 (2010).
59 Reyes, A., Semenkovich, N. P., Whiteson, K., Rohwer, F. & Gordon, J. I. Going viral: next-generation sequencing applied to phage populations in the human gut. *Nature reviews. Microbiology* **10**, 607-617, doi:10.1038/nrmicro2853 (2012).
60 Lozupone, C. A., Stombaugh, J. I., Gordon, J. I., Jansson, J. K. & Knight, R. Diversity, stability and resilience of the human gut microbiota. *Nature* **489**, 220-230, doi:10.1038/nature11550 (2012).
61 Ursell, L. K., Metcalf, J. L., Parfrey, L. W. & Knight, R. Defining the human microbiome. *Nutrition reviews* **70 Suppl 1**, S38-44, doi:10.1111/j.1753-4887.2012.00493.x (2012).
62 Faith, J. J. *et al.* The long-term stability of the human gut microbiota. *Science* **341**, 1237439, doi:10.1126/science.1237439 (2013).
63 Xiao, L. *et al.* A catalog of the mouse gut metagenome. *Nature biotechnology* **33**, 1103-1108, doi:10.1038/nbt.3353 (2015).
64 Levy, M., Kolodziejczyk, A. A., Thaiss, C. A. & Elinav, E. Dysbiosis and the immune system. *Nature reviews. Immunology* **17**, 219-232, doi:10.1038/nri.2017.7 (2017).
65 Shreiner, A. B., Kao, J. Y. & Young, V. B. The gut microbiome in health and in disease. *Current opinion in gastroenterology* **31**, 69-75, doi:10.1097/mog.0000000000000139 (2015).

66 Lynch, S. V. & Pedersen, O. The Human Intestinal Microbiome in Health and Disease. *The New England journal of medicine* **375**, 2369-2379, doi:10.1056/NEJMra1600266 (2016).
67 Human Microbiome Project, C. A framework for human microbiome research. *Nature* **486**, 215-221, doi:10.1038/nature11209 (2012).
68 Qin, J. *et al.* A human gut microbial gene catalogue established by metagenomic sequencing. *Nature* **464**, 59-65, doi:10.1038/nature08821 (2010).
69 Navas-Molina, J. A. *et al.* Advancing our understanding of the human microbiome using QIIME. *Methods in enzymology* **531**, 371-444, doi:10.1016/B978-0-12-407863-5.00019-8 (2013).
70 Blaxter, M. *et al.* Defining operational taxonomic units using DNA barcode data. *Philosophical transactions of the Royal Society of London. Series B, Biological sciences* **360**, 1935-1943, doi:10.1098/rstb.2005.1725 (2005).
71 Canfora, E. E., Jocken, J. W. & Blaak, E. E. Short-chain fatty acids in control of body weight and insulin sensitivity. *Nature reviews. Endocrinology* **11**, 577-591, doi:10.1038/nrendo.2015.128 (2015).
72 Louis, P. & Flint, H. J. Formation of propionate and butyrate by the human colonic microbiota. *Environmental microbiology* **19**, 29-41, doi:10.1111/1462-2920.13589 (2017).
73 Louis, P., Hold, G. L. & Flint, H. J. The gut microbiota, bacterial metabolites and colorectal cancer. *Nature reviews. Microbiology* **12**, 661-672, doi:10.1038/nrmicro3344 (2014).
74 Machiels, K. *et al.* A decrease of the butyrate-producing species Roseburia hominis and Faecalibacterium prausnitzii defines dysbiosis in patients with ulcerative colitis. *Gut* **63**, 1275-1283, doi:10.1136/gutjnl-2013-304833 (2014).
75 Arrieta, M. C. *et al.* Early infancy microbial and metabolic alterations affect risk of childhood asthma. *Science translational medicine* **7**, 307ra152, doi:10.1126/scitranslmed.aab2271 (2015).
76 Rios-Covian, D. *et al.* Intestinal Short Chain Fatty Acids and their Link with Diet and Human Health. *Frontiers in microbiology* **7**, 185, doi:10.3389/fmicb.2016.00185 (2016).
77 Kau, A. L., Ahern, P. P., Griffin, N. W., Goodman, A. L. & Gordon, J. I. Human nutrition, the gut microbiome and the immune system. *Nature* **474**, 327-336, doi:10.1038/nature10213 (2011).
78 Flint, H. J., Scott, K. P., Louis, P. & Duncan, S. H. The role of the gut microbiota in nutrition and health. *Nat Rev Gastro Hepat* **9**, 577-589, doi:10.1038/nrgastro.2012.156 (2012).
79 Cammarota, G., Ianiro, G. & Gasbarrini, A. Fecal microbiota transplantation for the treatment of Clostridium difficile infection: a systematic review. *Journal of clinical gastroenterology* **48**, 693-702, doi:10.1097/mcg.0000000000000046 (2014).
80 Bloomfield, S. F. *et al.* Time to abandon the hygiene hypothesis: new perspectives on allergic disease, the human microbiome, infectious disease prevention and the role of targeted hygiene. *Perspectives in public health* **136**, 213-224, doi:10.1177/1757913916650225 (2016).
81 Bry, L., Falk, P. G., Midtvedt, T. & Gordon, J. I. A model of host-microbial interactions in an open mammalian ecosystem. *Science* **273**, 1380-1383, doi:DOI 10.1126/science.273.5280.1380 (1996).

82 Meurens, F. *et al.* Commensal Bacteria and Expression of Two Major Intestinal Chemokines, TECK/CCL25 and MEC/CCL28, and Their Receptors. *PloS one* **2**, doi:ARTN e677 10.1371/journal.pone.0000677 (2007).
83 Rawls, J. F., Samuel, B. S. & Gordon, J. I. Gnotobiotic zebrafish reveal evolutionarily conserved responses to the gut microbiota. *Proc Natl Acad Sci U S A* **101**, 4596-4601, doi:10.1073/pnas.0400706101 (2004).
84 Round, J. L. & Mazmanian, S. K. The gut microbiota shapes intestinal immune responses during health and disease. *Nature reviews. Immunology* **9**, 313-323, doi:10.1038/nri2515 (2009).
85 Macpherson, A. J. & Harris, N. L. Interactions between commensal intestinal bacteria and the immune system. *Nature reviews. Immunology* **4**, 478-485, doi:10.1038/nri1373 (2004).
86 Falk, P. G., Hooper, L. V., Midtvedt, T. & Gordon, J. I. Creating and maintaining the gastrointestinal ecosystem: what we know and need to know from gnotobiology. *Microbiology and molecular biology reviews : MMBR* **62**, 1157-1170 (1998).
87 Zachar, Z. & Savage, D. C. Microbial interference and colonization of the murine gastrointestinal tract by Listeria monocytogenes. *Infection and immunity* **23**, 168-174 (1979).
88 Sprinz, H. *et al.* The response of the germfree guinea pig to oral bacterial challenge with Escherichia coli and Shigella flexneri. *The American journal of pathology* **39**, 681-695 (1961).
89 Houghteling, P. D. & Walker, W. A. Why is initial bacterial colonization of the intestine important to infants' and children's health? *Journal of pediatric gastroenterology and nutrition* **60**, 294-307, doi:10.1097/MPG.0000000000000597 (2015).
90 Abraham, C. & Medzhitov, R. Interactions between the host innate immune system and microbes in inflammatory bowel disease. *Gastroenterology* **140**, 1729-1737, doi:10.1053/j.gastro.2011.02.012 (2011).
91 Gevers, D. *et al.* The treatment-naive microbiome in new-onset Crohn's disease. *Cell host & microbe* **15**, 382-392, doi:10.1016/j.chom.2014.02.005 (2014).
92 Kim, H. J., Li, H., Collins, J. J. & Ingber, D. E. Contributions of microbiome and mechanical deformation to intestinal bacterial overgrowth and inflammation in a human gut-on-a-chip. *Proc Natl Acad Sci U S A* **113**, E7-E15, doi:10.1073/pnas.1522193112 (2016).
93 Kim, I. W. *et al.* Western-style diets induce macrophage infiltration and contribute to colitis-associated carcinogenesis. *Journal of gastroenterology and hepatology* **25**, 1785-1794, doi:10.1111/j.1440-1746.2010.06332.x (2010).
94 Vijay-Kumar, M. *et al.* Metabolic Syndrome and Altered Gut Microbiota in Mice Lacking Toll-Like Receptor 5. *Science* **328**, 228-231, doi:10.1126/science.1179721 (2010).
95 Alkanani, A. K. *et al.* Alterations in Intestinal Microbiota Correlate With Susceptibility to Type 1 Diabetes. *Diabetes* **64**, 3510-3520, doi:10.2337/db14-1847 (2015).
96 Hartstra, A. V., Bouter, K. E., Backhed, F. & Nieuwdorp, M. Insights into the role of the microbiome in obesity and type 2 diabetes. *Diabetes care* **38**, 159-165, doi:10.2337/dc14-0769 (2015).

97 Zeevi, D. *et al.* Personalized Nutrition by Prediction of Glycemic Responses. *Cell* **163**, 1079-1094, doi:10.1016/j.cell.2015.11.001 (2015).
98 Priyanka, B., Patil, R. K. & Dwarakanath, S. A review on detection methods used for foodborne pathogens. *The Indian journal of medical research* **144**, 327-338, doi:10.4103/0971-5916.198677 (2016).
99 Hamon, M., Bierne, H. & Cossart, P. Listeria monocytogenes: a multifaceted model. *Nat Rev Micro* **4**, 423-434, doi:http://www.nature.com/nrmicro/journal/v4/n6/suppinfo/nrmicro1413_S1.html (2006).
100 LaRock, D. L., Chaudhary, A. & Miller, S. I. Salmonellae interactions with host processes. *Nat Rev Micro* **13**, 191-205, doi:10.1038/nrmicro3420 http://www.nature.com/nrmicro/journal/v13/n4/abs/nrmicro3420.html#supplementary-information (2015).
101 Ramaswamy, V. *et al.* Listeria--review of epidemiology and pathogenesis. *Journal of microbiology, immunology, and infection = Wei mian yu gan ran za zhi* **40**, 4-13 (2007).
102 Corr, S. C. & O'Neill, L. A. Listeria monocytogenes infection in the face of innate immunity. *Cellular microbiology* **11**, 703-709, doi:10.1111/j.1462-5822.2009.01294.x (2009).
103 Dalebroux, Z. D. & Miller, S. I. Salmonellae PhoPQ regulation of the outer membrane to resist innate immunity. *Current opinion in microbiology* **17**, 106-113, doi:10.1016/j.mib.2013.12.005 (2014).
104 Martinez-Moya, M., de Pedro, M. A., Schwarz, H. & Garcia-del Portillo, F. Inhibition of Salmonella intracellular proliferation by non-phagocytic eucaryotic cells. *Research in microbiology* **149**, 309-318 (1998).
105 Ibarra, J. A. & Steele-Mortimer, O. Salmonella--the ultimate insider. Salmonella virulence factors that modulate intracellular survival. *Cellular microbiology* **11**, 1579-1586, doi:10.1111/j.1462-5822.2009.01368.x (2009).
106 Vazquez-Boland, J. A. *et al.* Listeria pathogenesis and molecular virulence determinants. *Clin Microbiol Rev* **14**, 584-+, doi:Doi 10.1128/Cmr.14.3.584-640.2001 (2001).
107 Ambros, V. The functions of animal microRNAs. *Nature* **431**, 350-355, doi:10.1038/nature02871 (2004).
108 Lee, R., Feinbaum, R. & Ambros, V. A short history of a short RNA. *Cell* **116**, S89-92, 81 p following S96 (2004).
109 Almeida, M. I., Reis, R. M. & Calin, G. A. MicroRNA history: Discovery, recent applications, and next frontiers. *Mutat Res-Fund Mol M* **717**, 1-8, doi:10.1016/j.mrfmmm.2011.03.009 (2011).
110 Fire, A. *et al.* Potent and specific genetic interference by double-stranded RNA in Caenorhabditis elegans. *Nature* **391**, 806-811, doi:Doi 10.1038/35888 (1998).
111 He, L. & Hannon, G. J. MicroRNAs: Small RNAs with a big role in gene regulation (vol 5, pg 522 2004). *Nat Rev Genet* **5**, 522-+, doi:10.1038/nrg1415 (2004).
112 Carthew, R. W. & Sontheimer, E. J. Origins and Mechanisms of miRNAs and siRNAs. *Cell* **136**, 642-655, doi:10.1016/j.cell.2009.01.035 (2009).
113 Zisoulis, D. G., Yeo, G. W. & Pasquinelli, A. E. Comprehensive Identification of miRNA Target Sites in Live Animals. *Micrornas in Development: Methods and Protocols* **732**, 169-185, doi:10.1007/978-1-61779-083-6_13 (2011).

114 Bartel, D. P. MicroRNAs: Genomics, biogenesis, mechanism, and function. *Cell* **116**, 281-297, doi:Doi 10.1016/S0092-8674(04)00045-5 (2004).
115 Ha, M. & Kim, V. N. Regulation of microRNA biogenesis. *Nat Rev Mol Cell Bio* **15**, 509-524, doi:10.1038/nrm3838 (2014).
116 Baltimore, D., Boldin, M. P., O'Connell, R. M., Rao, D. S. & Taganov, K. D. MicroRNAs: new regulators of immune cell development and function. *Nature immunology* **9**, 839-845, doi:10.1038/ni.f.209 (2008).
117 Borchert, G. M., Lanier, W. & Davidson, B. L. RNA polymerase III transcribes human microRNAs. *Nat Struct Mol Biol* **13**, 1097-1101, doi:10.1038/nsmb1174 (2006).
118 Winter, J., Jung, S., Keller, S., Gregory, R. I. & Diederichs, S. Many roads to maturity: microRNA biogenesis pathways and their regulation. *Nat Cell Biol* **11**, 228-234, doi:10.1038/ncb0309-228 (2009).
119 Burisch, J., Jess, T., Martinato, M. & Lakatos, P. L. The burden of inflammatory bowel disease in Europe. *Journal of Crohn's and Colitis* **7**, 322-337, doi:http://dx.doi.org/10.1016/j.crohns.2013.01.010 (2013).
120 Eulalio, A., Behm-Ansmant, I., Schweizer, D. & Izaurralde, E. P-body formation is a consequence, not the cause, of RNA-mediated gene silencing. *Mol Cell Biol* **27**, 3970-3981, doi:10.1128/Mcb.00128-07 (2007).
121 Meijer, H. A. *et al.* Translational Repression and eIF4A2 Activity Are Critical for MicroRNA-Mediated Gene Regulation. *Science* **340**, 82-85, doi:10.1126/science.1231197 (2013).
122 Djuranovic, S., Nahvi, A. & Green, R. A Parsimonious Model for Gene Regulation by miRNAs. *Science* **331**, 550-553, doi:10.1126/science.1191138 (2011).
123 Bartel, D. P. MicroRNAs: Target Recognition and Regulatory Functions. *Cell* **136**, 215-233, doi:10.1016/j.cell.2009.01.002 (2009).
124 Min, H. & Yoon, S. Got target? Computational methods for microRNA target prediction and their extension. *Experimental & molecular medicine* **42**, 233-244, doi:10.3858/emm.2010.42.4.032 (2010).
125 Witkos, T. M., Koscianska, E. & Krzyzosiak, W. J. Practical Aspects of microRNA Target Prediction. *Current molecular medicine* **11**, 93-109 (2011).
126 Chi, S. W., Zang, J. B., Mele, A. & Darnell, R. B. Argonaute HITS-CLIP decodes microRNA-mRNA interaction maps. *Nature* **460**, 479-486, doi:10.1038/nature08170 (2009).
127 Hafner, M. *et al.* Transcriptome-wide identification of RNA-binding protein and microRNA target sites by PAR-CLIP. *Cell* **141**, 129-141, doi:10.1016/j.cell.2010.03.009 (2010).
128 Lu, J. *et al.* MicroRNA expression profiles classify human cancers. *Nature* **435**, 834-838, doi:10.1038/nature03702 (2005).
129 Sheedy, F. J. *et al.* Negative regulation of TLR4 via targeting of the proinflammatory tumor suppressor PDCD4 by the microRNA miR-21. *Nature immunology* **11**, 141-147, doi:10.1038/ni.1828 (2010).
130 Quinn, S. R. & O'Neill, L. A. A trio of microRNAs that control Toll-like receptor signalling. *Int Immunol* **23**, 421-425, doi:10.1093/intimm/dxr034 (2011).
131 O'Neill, L. A., Sheedy, F. J. & McCoy, C. E. MicroRNAs: the fine-tuners of Toll-like receptor signalling. *Nature reviews. Immunology* **11**, 163-175 (2011).

132 Barrett, J. C. *et al.* Genome-wide association defines more than 30 distinct susceptibility loci for Crohn's disease. *Nature genetics* **40**, 955-962, doi:10.1038/ng.175 (2008).
133 Yang, Y. *et al.* Overexpression of miR-21 in patients with ulcerative colitis impairs intestinal epithelial barrier function through targeting the Rho GTPase RhoB. *Biochemical and biophysical research communications* **434**, 746-752, doi:10.1016/j.bbrc.2013.03.122 (2013).
134 Toldo, S. *et al.* Induction of MicroRNA-21 With Exogenous Hydrogen Sulfide Attenuates Myocardial Ischemic and Inflammatory Injury in Mice. *Circ-Cardiovasc Gene* **7**, 311-320, doi:10.1161/CIRCGENETICS.113.000381 (2014).
135 Nielsen, B. S. *et al.* miR-21 expression in cancer cells may not predict resistance to adjuvant trastuzumab in primary breast cancer. *Frontiers in Oncology* **4**, doi:10.3389/fonc.2014.00207 (2014).
136 Ma, X. L. *et al.* Prognostic Role of MicroRNA-21 in Non-small Cell Lung Cancer: a Meta-analysis. *Asian Pac J Cancer P* **13**, 2329-2334, doi:10.7314/Apjcp.2012.13.5.2329 (2012).
137 Cai, X. Z., Hagedorn, C. H. & Cullen, B. R. Human microRNAs are processed from capped, polyadenylated transcripts that can also function as mRNAs. *Rna* **10**, 1957-1966, doi:10.1261/rna.7135204 (2004).
138 Fujita, S. *et al.* miR-21 gene expression triggered by AP-1 is sustained through a double-negative feedback mechanism. *J Mol Biol* **378**, 492-504, doi:10.1016/j.jmb.2008.03.015 (2008).
139 Kumarswamy, R., Volkmann, I. & Thum, T. Regulation and function of miRNA-21 in health and disease. *Rna Biol* **8**, 706-713, doi:10.4161/rna.8.5.16154 (2011).
140 Krichevsky, A. M. & Gabriely, G. miR-21: a small multi-faceted RNA. *J Cell Mol Med* **13**, x-53, doi:10.1111/j.1582-4934.2008.00556.x (2009).
141 Loffler, D. *et al.* Interleukin-6 dependent survival of multiple myeloma cells involves the Stat3-mediated induction of microRNA-21 through a highly conserved enhancer. *Blood* **110**, 1330-1333, doi:10.1182/blood-2007-03-081133 (2007).
142 Cai, X., Hagedorn, C. H. & Cullen, B. R. Human microRNAs are processed from capped, polyadenylated transcripts that can also function as mRNAs. *Rna* **10**, 1957-1966, doi:10.1261/rna.7135204 (2004).
143 Lu, X. L. *et al.* The IL-6/STAT3 pathway via miR-21 is involved in the neoplastic and metastatic properties of arsenite-transformed human keratinocytes. *Toxicol Lett* **237**, 191-199, doi:10.1016/j.toxlet.2015.06.011 (2015).
144 Sheedy, F. J. Turning 21: induction of miR-21 as a key swith in the inflammatory response. *Front Immunol* **6**, doi:ARTN 19 10.3389/fimmu.2015.00019 (2015).
145 Davis, B. N., Hilyard, A. C., Lagna, G. & Hata, A. SMAD proteins control DROSHA-mediated microRNA maturation. *Nature* **454**, 56-U52, doi:10.1038/nature07086 (2008).
146 Zhang, Z. *et al.* Negative regulation of lncRNA GAS5 by miR-21. *Cell Death Differ* **20**, 1558-1568, doi:10.1038/cdd.2013.110 (2013).
147 Mudduluru, G. *et al.* Curcumin regulates miR-21 expression and inhibits invasion and metastasis in colorectal cancer. *Bioscience reports* **31**, 185-197, doi:10.1042/bsr20100065 (2011).

148 Bornachea, O. *et al.* EMT and induction of miR-21 mediate metastasis development in Trp53-deficient tumours. *Sci Rep-Uk* **2**, doi:Artn 43410.1038/Srep00434 (2012).
149 De Mattos-Arruda, L. *et al.* MicroRNA-21 links epithelial-to-mesenchymal transition and inflammatory signals to confer resistance to neoadjuvant trastuzumab and chemotherapy in HER2-positive breast cancer patients. *Oncotarget* **6**, 37269-37280 (2015).
150 Han, M. *et al.* MiR-21 regulates epithelial-mesenchymal transition phenotype and hypoxia-inducible factor-1alpha expression in third-sphere forming breast cancer stem cell-like cells. *Cancer science* **103**, 1058-1064, doi:10.1111/j.1349-7006.2012.02281.x (2012).
151 Jiang, Y. *et al.* The role of TGF-beta1-miR-21-ROS pathway in bystander responses induced by irradiated non-small-cell lung cancer cells. *British journal of cancer* **111**, 772-780, doi:10.1038/bjc.2014.368 (2014).
152 Zhang, X. *et al.* MicroRNA-21 modulates the levels of reactive oxygen species by targeting SOD3 and TNFalpha. *Cancer research* **72**, 4707-4713, doi:10.1158/0008-5472.CAN-12-0639 (2012).
153 Cengiz, M. *et al.* Circulating miR-21 and eNOS in subclinical atherosclerosis in patients with hypertension. *Clinical and experimental hypertension* **37**, 643-649, doi:10.3109/10641963.2015.1036064 (2015).
154 Guo, Y. *et al.* Kallistatin inhibits TGF-beta-induced endothelial-mesenchymal transition by differential regulation of microRNA-21 and eNOS expression. *Experimental cell research* **337**, 103-110, doi:10.1016/j.yexcr.2015.06.021 (2015).
155 Barnett, R. E. *et al.* Anti-inflammatory effects of miR-21 in the macrophage response to peritonitis. *J Leukoc Biol* **99**, 361-371, doi:10.1189/jlb.4A1014-489R (2016).
156 Cekaite, L., Clancy, T. & Sioud, M. Increased miR-21 expression during human monocyte differentiation into DCs. *Frontiers in bioscience (Elite edition)* **2**, 818-828 (2010).
157 Hashimi, S. T. *et al.* MicroRNA profiling identifies miR-34a and miR-21 and their target genes JAG1 and WNT1 in the coordinate regulation of dendritic cell differentiation. *Blood* **114**, 404-414, doi:10.1182/blood-2008-09-179150 (2009).
158 Carissimi, C. *et al.* miR-21 is a negative modulator of T-cell activation. *Biochimie* **107**, 319-326, doi:10.1016/j.biochi.2014.09.021 (2014).
159 Murugaiyan, G. *et al.* MicroRNA-21 promotes Th17 differentiation and mediates experimental autoimmune encephalomyelitis. *J Clin Invest* **125**, 1069-1080, doi:10.1172/Jci74347 (2015).
160 Smigielska-Czepiel, K. *et al.* Dual role of miR-21 in CD4+ T-cells: activation-induced miR-21 supports survival of memory T-cells and regulates CCR7 expression in naive T-cells. *PloS one* **8**, e76217, doi:10.1371/journal.pone.0076217 (2013).
161 Lu, T. X. *et al.* MicroRNA-21 limits in vivo immune response-mediated activation of the IL-12/IFN-gamma pathway, Th1 polarization, and the severity of delayed-type hypersensitivity. *Journal of immunology (Baltimore, Md. : 1950)* **187**, 3362-3373, doi:10.4049/jimmunol.1101235 (2011).
162 Wang, Z. *et al.* MicroRNA 21 is a homeostatic regulator of macrophage polarization and prevents prostaglandin E2-mediated M2 generation. *PloS one* **10**, e0115855, doi:10.1371/journal.pone.0115855 (2015).

163 Wu, Z. W., Lu, H. F., Sheng, J. F. & Li, L. J. Inductive microRNA-21 impairs anti-mycobacterial responses by targeting IL-12 and Bcl-2. *Febs Lett* **586**, 2459-2467, doi:10.1016/j.febslet.2012.06.004 (2012).
164 Lu, T. X., Munitz, A. & Rothenberg, M. E. MicroRNA-21 Is Up-Regulated in Allergic Airway Inflammation and Regulates IL-12p35 Expression. *Journal of Immunology* **182**, 4994-5002, doi:10.4049/jimmunol.0803560 (2009).
165 Das, A., Ganesh, K., Khanna, S., Sen, C. K. & Roy, S. Engulfment of Apoptotic Cells by Macrophages: A Role of MicroRNA-21 in the Resolution of Wound Inflammation. *Journal of Immunology* **192**, 1120-1129, doi:10.4049/jimmunol.1300613 (2014).
166 Figueiredo Neto, M. & Figueiredo, M. L. Combination of Interleukin-27 and MicroRNA for Enhancing Expression of Anti-Inflammatory and Proosteogenic Genes. *Arthritis* **2017**, 6365857, doi:10.1155/2017/6365857 (2017).
167 Choi, B. *et al.* The Relevance of miRNA-21 in HSV-Induced Inflammation in a Mouse Model. *Int J Mol Sci* **16**, 7413-7427, doi:10.3390/ijms16047413 (2015).
168 Yelamanchili, S. V. *et al.* MiR-21 in Extracellular Vesicles Leads to Neurotoxicity via TLR7 Signaling in SIV Neurological Disease. *Plos Pathog* **11**, doi:ARTN e100503210.1371/journal.ppat.1005032 (2015).
169 Garchow, B. & Kiriakidou, M. MicroRNA-21 deficiency protects from lupus-like autoimmunity in the chronic graft-versus-host disease model of systemic lupus erythematosus. *Clinical immunology* **162**, 100-106, doi:10.1016/j.clim.2015.11.010 (2016).
170 Tang, Z. M. *et al.* Clinical relevance of plasma miR-21 in new-onset systemic lupus erythematosus patients. *Journal of clinical laboratory analysis* **28**, 446-451, doi:10.1002/jcla.21708 (2014).
171 Guinea-Viniegra, J. *et al.* Targeting miR-21 to treat psoriasis. *Science translational medicine* **6**, 225re221, doi:10.1126/scitranslmed.3008089 (2014).
172 Meisgen, F. *et al.* MiR-21 is up-regulated in psoriasis and suppresses T cell apoptosis. *Journal of Investigative Dermatology* **131**, S20-S20 (2011).
173 Ma, X. *et al.* The oncogenic microRNA miR-21 promotes regulated necrosis in mice. *Nat Commun* **6**, 7151, doi:10.1038/ncomms8151 (2015).
174 Xu, W. D., Pan, H. F., Li, J. H. & Ye, D. Q. MicroRNA-21 with therapeutic potential in autoimmune diseases. *Expert opinion on therapeutic targets* **17**, 659-665, doi:10.1517/14728222.2013.773311 (2013).
175 Akira, S., Uematsu, S. & Takeuchi, O. Pathogen recognition and innate immunity. *Cell* **124**, 783-801, doi:10.1016/j.cell.2006.02.015 (2006).
176 Beutler, B. *et al.* Genetic analysis of host resistance: Toll-like receptor signaling and immunity at large. *Annual review of immunology* **24**, 353-389, doi:10.1146/annurev.immunol.24.021605.090552 (2006).
177 Artis, D. Epithelial-cell recognition of commensal bacteria and maintenance of immune homeostasis in the gut. *Nature reviews. Immunology* **8**, 411-420, doi:10.1038/nri2316 (2008).
178 Abraham, C. & Cho, J. H. Inflammatory bowel disease. *The New England journal of medicine* **361**, 2066-2078, doi:10.1056/NEJMra0804647 (2009).
179 Kostic, A. D., Xavier, R. J. & Gevers, D. The microbiome in inflammatory bowel disease: current status and the future ahead. *Gastroenterology* **146**, 1489-1499, doi:10.1053/j.gastro.2014.02.009 (2014).

180 ISGE. Gut Decisions: Leading change to improve the lives of people with Crohn's and colitis. Available online at: http://www.isge.ie/images/stories/docs/2284-IBD-Quality-Initiative-Report.pdf (2015).
181 Van Der Kraak, L., Gros, P. & Beauchemin, N. Colitis-associated colon cancer: Is it in your genes? *World Journal of Gastroenterology* **21**, 11688-11699, doi:10.3748/wjg.v21.i41.11688 (2015).
182 Kaser, A., Zeissig, S. & Blumberg, R. S. Inflammatory bowel disease. *Annual review of immunology* **28**, 573-621, doi:10.1146/annurev-immunol-030409-101225 (2010).
183 Anderson, C. A. *et al.* Meta-analysis identifies 29 additional ulcerative colitis risk loci, increasing the number of confirmed associations to 47. *Nature genetics* **43**, 246-252, doi:10.1038/ng.764 (2011).
184 Franke, A. *et al.* Genome-wide meta-analysis increases to 71 the number of confirmed Crohn's disease susceptibility loci. *Nature genetics* **42**, 1118-1125, doi:10.1038/ng.717 (2010).
185 Liu, T. C. & Stappenbeck, T. S. Genetics and Pathogenesis of Inflammatory Bowel Disease. *Annual review of pathology* **11**, 127-148, doi:10.1146/annurev-pathol-012615-044152 (2016).
186 Stittrich, A. B. *et al.* Genomic architecture of inflammatory bowel disease in five families with multiple affected individuals. *Human genome variation* **3**, 15060, doi:10.1038/hgv.2015.60 (2016).
187 Goldstein, D. B. Common genetic variation and human traits. *The New England journal of medicine* **360**, 1696-1698, doi:10.1056/NEJMp0806284 (2009).
188 Karantanos, T. & Gazouli, M. Inflammatory bowel disease: recent advances on genetics and innate immunity. *Annals of Gastroenterology : Quarterly Publication of the Hellenic Society of Gastroenterology* **24**, 164-172 (2011).
189 Abreu, M. T. Toll-like receptor signalling in the intestinal epithelium: how bacterial recognition shapes intestinal function. *Nature reviews. Immunology* **10**, 131-144, doi:10.1038/nri2707 (2010).
190 Cario, E. Toll-like receptors in inflammatory bowel diseases: a decade later. *Inflamm Bowel Dis* **16**, 1583-1597, doi:10.1002/ibd.21282 (2010).
191 Toruner, M. *et al.* Risk factors for opportunistic infections in patients with inflammatory bowel disease. *Gastroenterology* **134**, 929-936, doi:10.1053/j.gastro.2008.01.012 (2008).
192 Colombel, J. F. *et al.* Adalimumab safety in global clinical trials of patients with Crohn's disease. *Inflamm Bowel Dis* **15**, 1308-1319, doi:10.1002/ibd.20956 (2009).
193 Rivkin, A. Certolizumab pegol for the management of Crohn's disease in adults. *Clinical therapeutics* **31**, 1158-1176, doi:10.1016/j.clinthera.2009.06.015 (2009).
194 Sandborn, W. J. *et al.* Colectomy rate comparison after treatment of ulcerative colitis with placebo or infliximab. *Gastroenterology* **137**, 1250-1260; quiz 1520, doi:10.1053/j.gastro.2009.06.061 (2009).
195 Maxwell, J. R. *et al.* Differential Roles for Interleukin-23 and Interleukin-17 in Intestinal Immunoregulation. *Immunity* **43**, 739-750, doi:10.1016/j.immuni.2015.08.019 (2015).

196 Mizoguchi, A. Animal models of inflammatory bowel disease. *Progress in molecular biology and translational science* **105**, 263-320, doi:10.1016/b978-0-12-394596-9.00009-3 (2012).
197 Boismenu, R. & Chen, Y. Insights from mouse models of colitis. *J Leukoc Biol* **67**, 267-278 (2000).
198 Elson, C. O., Sartor, R. B., Tennyson, G. S. & Riddell, R. H. Experimental models of inflammatory bowel disease. *Gastroenterology* **109**, 1344-1367 (1995).
199 Dieleman, L. A. *et al.* Dextran sulfate sodium-induced colitis occurs in severe combined immunodeficient mice. *Gastroenterology* **107**, 1643-1652 (1994).
200 Perše, M. & Cerar, A. Dextran sodium sulphate colitis mouse model: Traps and tricks. *J Biomed Biotechnol* **2012**, doi:10.1155/2012/718617 (2012).
201 Araki, Y., Mukaisyo, K., Sugihara, H., Fujiyama, Y. & Hattori, T. Increased apoptosis and decreased proliferation of colonic epithelium in dextran sulfate sodium-induced colitis in mice. *Oncology reports* **24**, 869-874 (2010).
202 Morgan, M. E. *et al.* New perspective on dextran sodium sulfate colitis: antigen-specific T cell development during intestinal inflammation. *PloS one* **8**, e69936, doi:10.1371/journal.pone.0069936 (2013).
203 Egger, B. *et al.* Characterisation of acute murine dextran sodium sulphate colitis: cytokine profile and dose dependency. *Digestion* **62**, 240-248, doi:7822 (2000).
204 Okayasu, I. *et al.* A novel method in the induction of reliable experimental acute and chronic ulcerative colitis in mice. *Gastroenterology* **98**, 694-702 (1990).
205 Melgar, S. *et al.* Validation of murine dextran sulfate sodium-induced colitis using four therapeutic agents for human inflammatory bowel disease. *Int Immunopharmacol* **8**, 836-844, doi:10.1016/j.intimp.2008.01.036 (2008).
206 Allen, I. C. *et al.* The NLRP3 inflammasome functions as a negative regulator of tumorigenesis during colitis-associated cancer. *J Exp Med* **207**, 1045-1056, doi:10.1084/jem.20100050 (2010).
207 Araki, A. *et al.* MyD88-deficient mice develop severe intestinal inflammation in dextran sodium sulfate colitis. *Journal of gastroenterology* **40**, 16-23, doi:10.1007/s00535-004-1492-9 (2005).
208 Takagi, H. *et al.* Contrasting action of IL-12 and IL-18 in the development of dextran sodium sulphate colitis in mice. *Scandinavian journal of gastroenterology* **38**, 837-844 (2003).
209 Croxen, M. A. *et al.* Recent advances in understanding enteric pathogenic Escherichia coli. *Clin Microbiol Rev* **26**, 822-880, doi:10.1128/cmr.00022-13 (2013).
210 Collins, J. W. *et al.* Citrobacter rodentium: infection, inflammation and the microbiota. *Nature reviews. Microbiology* **12**, 612-623, doi:10.1038/nrmicro3315 (2014).
211 Koroleva, E. P. *et al.* Citrobacter rodentium-induced colitis: A robust model to study mucosal immune responses in the gut. *Journal of Immunological Methods* **421**, 61-72, doi:http://dx.doi.org/10.1016/j.jim.2015.02.003 (2015).
212 Eckburg, P. B. & Relman, D. A. The Role of Microbes in Crohn's Disease. *Clinical Infectious Diseases* **44**, 256-262, doi:10.1086/510385 (2007).
213 Rakoff-Nahoum, S., Paglino, J., Eslami-Varzaneh, F., Edberg, S. & Medzhitov, R. Recognition of commensal microflora by toll-like receptors is

required for intestinal homeostasis. *Cell* **118**, 229-241, doi:DOI 10.1016/j.cell.2004.07.002 (2004).
214 Slack, E. *et al.* Innate and Adaptive Immunity Cooperate Flexibly to Maintain Host-Microbiota Mutualism. *Science* **325**, 617-620, doi:10.1126/science.1172747 (2009).
215 Petnicki-Ocwieja, T. *et al.* Nod2 is required for the regulation of commensal microbiota in the intestine. *Proc Natl Acad Sci U S A* **106**, 15813-15818, doi:10.1073/pnas.0907722106 (2009).
216 Elinav, E. *et al.* NLRP6 inflammasome regulates colonic microbial ecology and risk for colitis. *Cell* **145**, 745-757, doi:10.1016/j.cell.2011.04.022 (2011).
217 Siegmund, B. Interleukin-18 in intestinal inflammation: friend and foe? *Immunity* **32**, 300-302, doi:10.1016/j.immuni.2010.03.010 (2010).
218 Broz, P. *et al.* Redundant roles for inflammasome receptors NLRP3 and NLRC4 in host defense against Salmonella. *Journal of Experimental Medicine* **207**, 1745-1755, doi:10.1084/jem.20100257 (2010).
219 Franchi, L. *et al.* NLRC4-driven production of IL-1beta discriminates between pathogenic and commensal bacteria and promotes host intestinal defense. *Nature immunology* **13**, 449-456, doi:10.1038/ni.2263 (2012).
220 Abreu, M. T. & Arditi, M. Innate immunity and toll-like receptors: clinical implications of basic science research. *The Journal of pediatrics* **144**, 421-429, doi:10.1016/j.jpeds.2004.01.057 (2004).
221 Hornef, M. W., Normark, B. H., Vandewalle, A. & Normark, S. Intracellular Recognition of Lipopolysaccharide by Toll-like Receptor 4 in Intestinal Epithelial Cells. *The Journal of Experimental Medicine* **198**, 1225-1235, doi:10.1084/jem.20022194 (2003).
222 Caramalho, I. *et al.* Regulatory T cells selectively express toll-like receptors and are activated by lipopolysaccharide. *J Exp Med* **197**, 403-411 (2003).
223 Cario, E. & Podolsky, D. K. Differential alteration in intestinal epithelial cell expression of toll-like receptor 3 (TLR3) and TLR4 in inflammatory bowel disease. *Infection and immunity* **68**, 7010-7017 (2000).
224 Hausmann, M. *et al.* Toll-like receptors 2 and 4 are up-regulated during intestinal inflammation. *Gastroenterology* **122**, 1987-2000 (2002).
225 Melgar, S. & Shanahan, F. Inflammatory bowel disease-from mechanisms to treatment strategies. *Autoimmunity* **43**, 463-477, doi:10.3109/08916931003674709 (2010).
226 Velloso, L. A., Folli, F. & Saad, M. J. TLR4 at the Crossroads of Nutrients, Gut Microbiota, and Metabolic Inflammation. *Endocrine reviews* **36**, 245-271, doi:10.1210/er.2014-1100 (2015).
227 Kim, K. A., Gu, W., Lee, I. A., Joh, E. H. & Kim, D. H. High fat diet-induced gut microbiota exacerbates inflammation and obesity in mice via the TLR4 signaling pathway. *PloS one* **7**, e47713, doi:10.1371/journal.pone.0047713 (2012).
228 Cho, J. H. *et al.* Identification of novel susceptibility loci for inflammatory bowel disease on chromosomes 1p, 3q, and 4q: Evidence for epistasis between 1p and IBD1. *Proc Natl Acad Sci U S A* **95**, 7502-7507 (1998).
229 Arbour, N. C. *et al.* TLR4 mutations are associated with endotoxin hyporesponsiveness in humans. *Nature genetics* **25**, 187-191, doi:10.1038/76048 (2000).

230 Chapman, C. G. & Pekow, J. The emerging role of miRNAs in inflammatory bowel disease: a review. *Ther Adv Gastroenter* **8**, 4-22, doi:10.1177/1756283x14547360 (2015).
231 Lu, C. *et al.* MIR106B and MIR93 prevent removal of bacteria from epithelial cells by disrupting ATG16L1-mediated autophagy. *Gastroenterology* **146**, 188-199, doi:10.1053/j.gastro.2013.09.006 (2014).
232 Zhai, Z., Wu, F., Chuang, A. Y. & Kwon, J. H. miR-106b fine tunes ATG16L1 expression and autophagic activity in intestinal epithelial HCT116 cells. *Inflamm Bowel Dis* **19**, 2295-2301, doi:10.1097/MIB.0b013e31829e71cf (2013).
233 Chen, W. X., Ren, L. H. & Shi, R. H. Implication of miRNAs for inflammatory bowel disease treatment: Systematic review. *World journal of gastrointestinal pathophysiology* **5**, 63-70, doi:10.4291/wjgp.v5.i2.63 (2014).
234 Sonkoly, E. *et al.* MiR-155 is overexpressed in patients with atopic dermatitis and modulates T-cell proliferative responses by targeting cytotoxic T lymphocyte-associated antigen 4. *The Journal of allergy and clinical immunology* **126**, 581-589 e581-520, doi:10.1016/j.jaci.2010.05.045 (2010).
235 Biton, M. *et al.* Epithelial microRNAs regulate gut mucosal immunity via epithelium-T cell crosstalk. *Nature immunology* **12**, 239-246, doi:10.1038/ni.1994 (2011).
236 Smith, P. *et al.* Infection with a helminth parasite prevents experimental colitis via a macrophage-mediated mechanism. *Journal of immunology (Baltimore, Md. : 1950)* **178**, 4557-4566 (2007).
237 Schmieder, R. & Edwards, R. Quality control and preprocessing of metagenomic datasets. *Bioinformatics (Oxford, England)* **27**, 863-864, doi:10.1093/bioinformatics/btr026 (2011).
238 Edgar, R. C. Search and clustering orders of magnitude faster than BLAST. *Bioinformatics (Oxford, England)* **26**, 2460-2461, doi:10.1093/bioinformatics/btq461 (2010).
239 Wang, Q., Garrity, G. M., Tiedje, J. M. & Cole, J. R. Naive Bayesian classifier for rapid assignment of rRNA sequences into the new bacterial taxonomy. *Applied and environmental microbiology* **73**, 5261-5267, doi:10.1128/aem.00062-07 (2007).
240 Caporaso, J. G. *et al.* QIIME allows analysis of high-throughput community sequencing data. *Nat Meth* **7**, 335-336, doi:http://www.nature.com/nmeth/journal/v7/n5/suppinfo/nmeth.f.303_S1.html (2010).
241 Clevers, H. Inflammatory bowel disease, stress, and the endoplasmic reticulum. *The New England journal of medicine* **360**, 726-727, doi:10.1056/NEJMcibr0809591 (2009).
242 Kitajima, S., Takuma, S. & Morimoto, M. Changes in colonic mucosal permeability in mouse colitis induced with dextran sulfate sodium. *Experimental animals* **48**, 137-143 (1999).
243 Bamba, S. *et al.* The severity of dextran sodium sulfate-induced colitis can differ between dextran sodium sulfate preparations of the same molecular weight range. *Dig Dis Sci* **57**, 327-334, doi:10.1007/s10620-011-1881-x (2012).
244 Perse, M. & Cerar, A. Dextran sodium sulphate colitis mouse model: traps and tricks. *J Biomed Biotechnol* **2012**, 718617, doi:10.1155/2012/718617 (2012).

245 Zijlstra, F. J., van Meeteren, M. E., Garrelds, I. M. & Meijssen, M. A. Effect of pharmacologically induced smooth muscle activation on permeability in murine colitis. *Mediators of inflammation* **12**, 21-27, doi:10.1080/0962935031000096944 (2003).
246 Grover, M. & Kashyap, P. C. Germ-free mice as a model to study effect of gut microbiota on host physiology. *Neurogastroenterology and motility : the official journal of the European Gastrointestinal Motility Society* **26**, 745-748, doi:10.1111/nmo.12366 (2014).
247 Levy, M. *et al.* Microbiota-Modulated Metabolites Shape the Intestinal Microenvironment by Regulating NLRP6 Inflammasome Signaling. *Cell* **163**, 1428-1443, doi:10.1016/j.cell.2015.10.048 (2015).
248 Mantis, N. J., Rol, N. & Corthesy, B. Secretory IgA's complex roles in immunity and mucosal homeostasis in the gut. *Mucosal immunology* **4**, 603-611, doi:10.1038/mi.2011.41 (2011).
249 Lampe, W. R., Park, J., Fang, S., Crews, A. L. & Adler, K. B. Calpain and MARCKS protein regulation of airway mucin secretion. *Pulmonary pharmacology & therapeutics* **25**, 427-431, doi:10.1016/j.pupt.2012.06.003 (2012).
250 Li, T., Li, D., Sha, J., Sun, P. & Huang, Y. MicroRNA-21 directly targets MARCKS and promotes apoptosis resistance and invasion in prostate cancer cells. *Biochemical and biophysical research communications* **383**, 280-285, doi:10.1016/j.bbrc.2009.03.077 (2009).
251 Berg, D. J. *et al.* Enterocolitis and colon cancer in interleukin-10-deficient mice are associated with aberrant cytokine production and CD4(+) TH1-like responses. *J Clin Invest* **98**, 1010-1020, doi:10.1172/jci118861 (1996).
252 Shi, C. *et al.* MicroRNA-21 knockout improve the survival rate in DSS induced fatal colitis through protecting against inflammation and tissue injury. *PloS one* **8**, e66814, doi:10.1371/journal.pone.0066814 (2013).
253 Shi, C. *et al.* Novel evidence for an oncogenic role of microRNA-21 in colitis-associated colorectal cancer. *Gut*, doi:10.1136/gutjnl-2014-308455 (2015).
254 Scheller, J., Chalaris, A., Schmidt-Arras, D. & Rose-John, S. The pro- and anti-inflammatory properties of the cytokine interleukin-6. *Biochimica et biophysica acta* **1813**, 878-888, doi:10.1016/j.bbamcr.2011.01.034 (2011).
255 Wlodarska, M. *et al.* NLRP6 inflammasome orchestrates the colonic host-microbial interface by regulating goblet cell mucus secretion. *Cell* **156**, 1045-1059, doi:10.1016/j.cell.2014.01.026 (2014).
256 Liu, S. *et al.* The Host Shapes the Gut Microbiota via Fecal MicroRNA. *Cell host & microbe* **19**, 32-43, doi:10.1016/j.chom.2015.12.005 (2016).
257 Beltzer, A. *et al.* Evaluation of Quantitative Imaging Biomarkers in the DSS Colitis Model. *Molecular imaging and biology : MIB : the official publication of the Academy of Molecular Imaging* **18**, 697-704, doi:10.1007/s11307-016-0937-x (2016).
258 Singh, N. *et al.* The murine caecal microRNA signature depends on the presence of the endogenous microbiota. *International journal of biological sciences* **8**, 171-186 (2012).
259 Papa, E. *et al.* Non-invasive mapping of the gastrointestinal microbiota identifies children with inflammatory bowel disease. *PloS one* **7**, e39242, doi:10.1371/journal.pone.0039242 (2012).

260 Macia, L. *et al.* Metabolite-sensing receptors GPR43 and GPR109A facilitate dietary fibre-induced gut homeostasis through regulation of the inflammasome. *Nat Commun* **6**, 6734, doi:10.1038/ncomms7734 (2015).
261 Bloom, S. M. *et al.* Commensal Bacteroides species induce colitis in host-genotype-specific fashion in a mouse model of inflammatory bowel disease. *Cell host & microbe* **9**, 390-403, doi:10.1016/j.chom.2011.04.009 (2011).
262 Natividad, J. M. *et al.* Ecobiotherapy Rich in Firmicutes Decreases Susceptibility to Colitis in a Humanized Gnotobiotic Mouse Model. *Inflamm Bowel Dis* **21**, 1883-1893, doi:10.1097/MIB.0000000000000422 (2015).
263 Toumi, R. *et al.* Probiotic bacteria lactobacillus and bifidobacterium attenuate inflammation in dextran sulfate sodium-induced experimental colitis in mice. *International journal of immunopathology and pharmacology* **27**, 615-627, doi:10.1177/039463201402700418 (2014).
264 Osman, N., Adawi, D., Ahrne, S., Jeppsson, B. & Molin, G. Modulation of the effect of dextran sulfate sodium-induced acute colitis by the administration of different probiotic strains of Lactobacillus and Bifidobacterium. *Dig Dis Sci* **49**, 320-327 (2004).
265 Srutkova, D. *et al.* Bifidobacterium longum CCM 7952 Promotes Epithelial Barrier Function and Prevents Acute DSS-Induced Colitis in Strictly Strain-Specific Manner. *PloS one* **10**, e0134050, doi:10.1371/journal.pone.0134050 (2015).
266 Mukhopadhya, I., Hansen, R., El-Omar, E. M. & Hold, G. L. IBD-what role do Proteobacteria play? *Nature reviews. Gastroenterology & hepatology* **9**, 219-230, doi:10.1038/nrgastro.2012.14 (2012).
267 Matsuoka, K. & Kanai, T. The gut microbiota and inflammatory bowel disease. *Seminars in immunopathology* **37**, 47-55, doi:10.1007/s00281-014-0454-4 (2015).
268 Morgan, X. C. *et al.* Dysfunction of the intestinal microbiome in inflammatory bowel disease and treatment. *Genome biology* **13**, R79, doi:10.1186/gb-2012-13-9-r79 (2012).
269 Nagy-Szakal, D. *et al.* Cellulose supplementation early in life ameliorates colitis in adult mice. *PloS one* **8**, e56685, doi:10.1371/journal.pone.0056685 (2013).
270 Hernandez-Chirlaque, C. *et al.* Germ-free and Antibiotic-treated Mice are Highly Susceptible to Epithelial Injury in DSS Colitis. *Journal of Crohn's & colitis* **10**, 1324-1335, doi:10.1093/ecco-jcc/jjw096 (2016).
271 Planer, J. D. *et al.* Development of the gut microbiota and mucosal IgA responses in twins and gnotobiotic mice. *Nature* **534**, 263-266, doi:10.1038/nature17940 (2016).
272 Okai, S. *et al.* High-affinity monoclonal IgA regulates gut microbiota and prevents colitis in mice. *Nature microbiology* **1**, 16103, doi:10.1038/nmicrobiol.2016.103 (2016).
273 Donaldson, G. P., Lee, S. M. & Mazmanian, S. K. Gut biogeography of the bacterial microbiota. *Nature reviews. Microbiology* **14**, 20-32, doi:10.1038/nrmicro3552 (2016).
274 Linden, S. K., Florin, T. H. & McGuckin, M. A. Mucin dynamics in intestinal bacterial infection. *PloS one* **3**, e3952, doi:10.1371/journal.pone.0003952 (2008).

275 Moens, E. & Veldhoen, M. Epithelial barrier biology: good fences make good neighbours. *Immunology* **135**, 1-8, doi:10.1111/j.1365-2567.2011.03506.x (2012).
276 Guttman, J. A. & Finlay, B. B. Tight junctions as targets of infectious agents. *Biochimica et biophysica acta* **1788**, 832-841, doi:10.1016/j.bbamem.2008.10.028 (2009).
277 Rougerie, P., Miskolci, V. & Cox, D. Generation of membrane structures during phagocytosis and chemotaxis of macrophages: role and regulation of the actin cytoskeleton. *Immunological reviews* **256**, 222-239, doi:10.1111/imr.12118 (2013).
278 Janeway, C. A., Jr. & Medzhitov, R. Innate immune recognition. *Annual review of immunology* **20**, 197-216, doi:10.1146/annurev.immunol.20.083001.084359 (2002).
279 Kaufmann, S. H. & Dorhoi, A. Molecular Determinants in Phagocyte-Bacteria Interactions. *Immunity* **44**, 476-491, doi:10.1016/j.immuni.2016.02.014 (2016).
280 Feng, J. *et al.* miR-21 attenuates lipopolysaccharide-induced lipid accumulation and inflammatory response: potential role in cerebrovascular disease. *Lipids in health and disease* **13**, 27, doi:10.1186/1476-511X-13-27 (2014).
281 Edwards, A. M. & Massey, R. C. Invasion of human cells by a bacterial pathogen. *Journal of visualized experiments : JoVE*, doi:10.3791/2693 (2011).
282 MacMicking, J. D. *et al.* Altered responses to bacterial infection and endotoxic shock in mice lacking inducible nitric oxide synthase. *Cell* **81**, 641-650 (1995).
283 Bryan, N. S. & Grisham, M. B. Methods to detect nitric oxide and its metabolites in biological samples. *Free radical biology & medicine* **43**, 645-657, doi:10.1016/j.freeradbiomed.2007.04.026 (2007).
284 Glomski, I. J., Decatur, A. L. & Portnoy, D. A. Listeria monocytogenes mutants that fail to compartmentalize listerolysin O activity are cytotoxic, avirulent, and unable to evade host extracellular defenses. *Infection and immunity* **71**, 6754-6765 (2003).
285 Chen, Y. *et al.* HCV-induced miR-21 contributes to evasion of host immune system by targeting MyD88 and IRAK1. *Plos Pathog* **9**, e1003248, doi:10.1371/journal.ppat.1003248 (2013).
286 Cameron, J. E. *et al.* Epstein-Barr virus growth/latency III program alters cellular microRNA expression. *Virology* **382**, 257-266, doi:10.1016/j.virol.2008.09.018 (2008).
287 Cameron, J. E. *et al.* Epstein-Barr virus latent membrane protein 1 induces cellular MicroRNA miR-146a, a modulator of lymphocyte signaling pathways. *Journal of virology* **82**, 1946-1958, doi:10.1128/JVI.02136-07 (2008).
288 Liu, P. T. *et al.* MicroRNA-21 targets the vitamin D-dependent antimicrobial pathway in leprosy. *Nature medicine* **18**, 267-273, doi:10.1038/nm.2584 (2012).
289 Zhang, Z. *et al.* miR-21 plays a pivotal role in gastric cancer pathogenesis and progression. *Lab Invest* **88**, 1358-1366, doi:10.1038/labinvest.2008.94 (2008).
290 Schulte, L. N., Eulalio, A., Mollenkopf, H.-J., Reinhardt, R. & Vogel, J. Analysis of the host microRNA response to Salmonella uncovers the control of major cytokines by the let-7 family. *The EMBO Journal* **30**, 1977-1989, doi:10.1038/emboj.2011.94 (2011).

291 Schnitger, A. K. *et al.* Listeria monocytogenes infection in macrophages induces vacuolar-dependent host miRNA response. *PloS one* **6**, e27435, doi:10.1371/journal.pone.0027435 (2011).
292 Wexler, H. & Oppenheim, J. D. Isolation, characterization, and biological properties of an endotoxin-like material from the gram-positive organism Listeria monocytogenes. *Infection and immunity* **23**, 845-857 (1979).
293 Abreu, C. *et al.* Listeria infection in patients on anti-TNF treatment: Report of two cases and review of the literature. *Journal of Crohn's and Colitis* **7**, 175-182, doi:10.1016/j.crohns.2012.04.018 (2013).
294 Kim, Y. G. *et al.* The cytosolic sensors Nod1 and Nod2 are critical for bacterial recognition and host defense after exposure to Toll-like receptor ligands. *Immunity* **28**, 246-257, doi:10.1016/j.immuni.2007.12.012 (2008).
295 Pushpakumar, S., Kundu, S., Givvimani, S. & Sen, U. Deregulation of miR-21 Contributes to Differential Macrophage Activation in Acute Kidney Injury in Aged Mice. *The FASEB Journal* **29** (2015).
296 Shiloh, M. U. *et al.* Phenotype of mice and macrophages deficient in both phagocyte oxidase and inducible nitric oxide synthase. *Immunity* **10**, 29-38 (1999).
297 Endres, R. *et al.* Listeriosis in p47(phox-/-) and TRp55-/- mice: protection despite absence of ROI and susceptibility despite presence of RNI. *Immunity* **7**, 419-432 (1997).
298 Slauch, J. M. How does the oxidative burst of macrophages kill bacteria? Still an open question. *Molecular microbiology* **80**, 580-583, doi:10.1111/j.1365-2958.2011.07612.x (2011).
299 Mills, E. L. *et al.* Succinate Dehydrogenase Supports Metabolic Repurposing of Mitochondria to Drive Inflammatory Macrophages. *Cell* **167**, 457-470 e413, doi:10.1016/j.cell.2016.08.064 (2016).
300 Drevets, D. A., Schawang, J. E., Mandava, V. K., Dillon, M. J. & Leenen, P. J. Severe Listeria monocytogenes infection induces development of monocytes with distinct phenotypic and functional features. *Journal of immunology (Baltimore, Md. : 1950)* **185**, 2432-2441, doi:10.4049/jimmunol.1000486 (2010).
301 Park, D. W., Kim, J. S., Chin, B. R. & Baek, S. H. Resveratrol inhibits inflammation induced by heat-killed Listeria monocytogenes. *Journal of medicinal food* **15**, 788-794, doi:10.1089/jmf.2012.2194 (2012).
302 Matusiak, M. *et al.* Flagellin-induced NLRC4 phosphorylation primes the inflammasome for activation by NAIP5. *Proc Natl Acad Sci U S A* **112**, 1541-1546, doi:10.1073/pnas.1417945112 (2015).
303 Barsig, J. & Kaufmann, S. H. The mechanism of cell death in Listeria monocytogenes-infected murine macrophages is distinct from apoptosis. *Infection and immunity* **65**, 4075-4081 (1997).
304 Cervantes, J., Nagata, T., Uchijima, M., Shibata, K. & Koide, Y. Intracytosolic Listeria monocytogenes induces cell death through caspase-1 activation in murine macrophages. *Cellular microbiology* **10**, 41-52, doi:10.1111/j.1462-5822.2007.01012.x (2008).
305 Glomski, I. J., Gedde, M. M., Tsang, A. W., Swanson, J. A. & Portnoy, D. A. The Listeria monocytogenes hemolysin has an acidic pH optimum to compartmentalize activity and prevent damage to infected host cells. *The Journal of Cell Biology* **156**, 1029-1038, doi:10.1083/jcb.200201081 (2002).

306 Ghigo, E. *et al.* Coxiella burnetii survival in THP-1 monocytes involves the impairment of phagosome maturation: IFN-gamma mediates its restoration and bacterial killing. *Journal of immunology (Baltimore, Md. : 1950)* **169**, 4488-4495 (2002).
307 Liu, C., Wang, J. & Zhang, X. The involvement of MiR-1-clathrin pathway in the regulation of phagocytosis. *PloS one* **9**, e98747, doi:10.1371/journal.pone.0098747 (2014).
308 Hennessy, E. J., Sheedy, F. J., Santamaria, D., Barbacid, M. & O'Neill, L. A. Toll-like receptor-4 (TLR4) down-regulates microRNA-107, increasing macrophage adhesion via cyclin-dependent kinase 6. *The Journal of biological chemistry* **286**, 25531-25539, doi:10.1074/jbc.M111.256206 (2011).
309 Zhao, Y. & Lukiw, W. J. TREM2 signaling, miRNA-34a and the extinction of phagocytosis. *Frontiers in cellular neuroscience* **7**, 131, doi:10.3389/fncel.2013.00131 (2013).
310 Kerrigan, A. M. & Brown, G. D. C-type lectins and phagocytosis. *Immunobiology* **214**, 562-575, doi:10.1016/j.imbio.2008.11.003 (2009).
311 Allen, L. H. & Aderem, A. A role for MARCKS, the alpha isozyme of protein kinase C and myosin I in zymosan phagocytosis by macrophages. *J Exp Med* **182**, 829-840 (1995).
312 Carballo, E., Pitterle, D. M., Stumpo, D. J., Sperling, R. T. & Blackshear, P. J. Phagocytic and macropinocytic activity in MARCKS-deficient macrophages and fibroblasts. *The American journal of physiology* **277**, C163-173 (1999).
313 Corradin, S., Mauel, J., Ransijn, A., Sturzinger, C. & Vergeres, G. Down-regulation of MARCKS-related protein (MRP) in macrophages infected with Leishmania. *The Journal of biological chemistry* **274**, 16782-16787 (1999).
314 Quinn, K. *et al.* Rho GTPases modulate entry of Ebola virus and vesicular stomatitis virus pseudotyped vectors. *Journal of virology* **83**, 10176-10186, doi:10.1128/jvi.00422-09 (2009).
315 Zhang, J. *et al.* Cdc42 and RhoB activation are required for mannose receptor-mediated phagocytosis by human alveolar macrophages. *Molecular biology of the cell* **16**, 824-834, doi:10.1091/mbc.E04-06-0463 (2005).
316 Myat, M. M., Anderson, S., Allen, L. A. & Aderem, A. MARCKS regulates membrane ruffling and cell spreading. *Current biology : CB* **7**, 611-614 (1997).
317 W. Randall Lampe, S. F., Qi Yin, Anne L. Crews, & Joungjoa Park, K. B. A. Mir-21 Regulation of MARCKS Protein and Mucin Secretion in Airway Epithelial Cells. *Open Journal of Respiratory Diseases*, 89-96, doi:http://dx.doi.org/10.4236/ojrd.2013.32014 (2013).
318 Williams, M. A., Schmidt, R. L. & Lenz, L. L. Early events regulating immunity and pathogenesis during Listeria monocytogenes infection. *Trends in immunology* **33**, 488-495, doi:10.1016/j.it.2012.04.007 (2012).
319 Marlow, G. J., van Gent, D. & Ferguson, L. R. Why interleukin-10 supplementation does not work in Crohn's disease patients. *World J Gastroenterol* **19**, 3931-3941, doi:10.3748/wjg.v19.i25.3931 (2013).
320 Mo, J. S. *et al.* MicroRNA 429 Regulates Mucin Gene Expression and Secretion in Murine Model of Colitis. *Journal of Crohn's & colitis* **10**, 837-849, doi:10.1093/ecco-jcc/jjw033 (2016).
321 Ruas-Madiedo, P., Gueimonde, M., Fernandez-Garcia, M., de los Reyes-Gavilan, C. G. & Margolles, A. Mucin degradation by Bifidobacterium strains

isolated from the human intestinal microbiota. *Applied and environmental microbiology* **74**, 1936-1940, doi:10.1128/AEM.02509-07 (2008).

322 Cani, P. D. *et al.* Changes in gut microbiota control inflammation in obese mice through a mechanism involving GLP-2-driven improvement of gut permeability. *Gut* **58**, 1091-1103, doi:10.1136/gut.2008.165886 (2009).

323 Wu, F. *et al.* Divergent influence of microRNA-21 deletion on murine colitis phenotypes. *Inflamm Bowel Dis* **20**, 1972-1985, doi:10.1097/mib.0000000000000201 (2014).

324 Talotta, F. *et al.* An autoregulatory loop mediated by miR-21 and PDCD4 controls the AP-1 activity in RAS transformation. *Oncogene* **28**, 73-84, doi:10.1038/onc.2008.370 (2009).

325 Saba, R., Sorensen, D. L. & Booth, S. A. MicroRNA-146a: A Dominant, Negative Regulator of the Innate Immune Response. *Front Immunol* **5**, 578, doi:10.3389/fimmu.2014.00578 (2014).

326 Kawane, K. *et al.* Chronic polyarthritis caused by mammalian DNA that escapes from degradation in macrophages. *Nature* **443**, 998-1002, doi:10.1038/nature05245 (2006).

327 Sohn, J. J. *et al.* Macrophages, nitric oxide and microRNAs are associated with DNA damage response pathway and senescence in inflammatory bowel disease. *PloS one* **7**, e44156, doi:10.1371/journal.pone.0044156 (2012).

328 Lam, G. Y. *et al.* Listeriolysin O suppresses phospholipase C-mediated activation of the microbicidal NADPH oxidase to promote Listeria monocytogenes infection. *Cell host & microbe* **10**, 627-634, doi:10.1016/j.chom.2011.11.005 (2011).

329 Duan, X. *et al.* microRNA-17-5p Modulates Bacille Calmette-Guerin Growth in RAW264.7 Cells by Targeting ULK1. *PloS one* **10**, e0138011, doi:10.1371/journal.pone.0138011 (2015).

330 Drevets, D. A. Dissemination of Listeria monocytogenes by infected phagocytes. *Infection and immunity* **67**, 3512-3517 (1999).

331 Iliopoulos, D., Jaeger, S. A., Hirsch, H. A., Bulyk, M. L. & Struhl, K. STAT3 activation of miR-21 and miR-181b-1 via PTEN and CYLD are part of the epigenetic switch linking inflammation to cancer. *Mol Cell* **39**, 493-506, doi:10.1016/j.molcel.2010.07.023 (2010).

332 Ali, T. *et al.* Clinical use of anti-TNF therapy and increased risk of infections. *Drug, healthcare and patient safety* **5**, 79-99, doi:10.2147/DHPS.S28801 (2013).

Chapter 7
-
Appendices

7. Appendices

7.1. Conference attendance

Irish Epithelial Physiology Society 9th Annual Meeting, Kilkenny, Ireland
October 27th 2016
– Oral presentation

Next Generation Immunology Conference, Weizmann Institute of Science, Rehovot, Israel
February 14-16th 2016
– Poster presentation

Irish Society for Immunology Annual Meeting, Trinity Biomedical Sciences Institute, Dublin, Ireland
September 17- 18th 2015
– Poster presentation

Toll 2015, Marbella, Spain
September 30 – October 3rd 2015
– Poster presentation

Second Joint Symposium between The Weizmann Institute of Science and Trinity College Dublin, Weizmann Institute of Science, Rehovot, Israel
June 9-11th 2015
– Oral presentation

Irish Epithelial Physiology meeting, Kilkenny, Ireland – Oral presentation

Regulators of intestinal Host-Microbe interactions

This project seeks to understand if miR-21 may be involved via host-microbiome cross-talk in the gut. Using miR-21-deficient mice, we have demonstrated that wild-type mice co-housed with miR-21$^{-/-}$ mice gain a partial protection in an acute DSS colitis model. In addition, germ-free mice recolonized with the microbiota of miR-21$^{-/-}$ mice are partially protected from DSS colitis. Using 16S rRNA sequencing, we have generated data which suggests the microflora of the the miR-21$^{-/-}$ mouse is altered in composition and that this may be due to altered barrier function and/or altered mucin secretion.
In addition, miR-21 expression is important for limiting infection of macrophages by the gram-positive pathogenic bacterim *Listeria monocytogenes*.

Next Generation Immunology Conference, Weizmann Institute of Science, Rehovot, Israel – Poster Presentation

Investigating the potential role of miR-21 in host-microbiome interactions

D.G.W. Johnston[1], E. Elinav[2], L.A.J. O'Neill[1], S.C. Corr[3]
[1]Trinity Biomedical Science Institute, Trinity College Dublin, Pearse St, Dublin 2, Ireland
[2]Dept. of Immunology, Wolfson Building, Weizmann Institute of Science, Rehovot, Israel
[3] Moyne Institute of Preventative Medicine, Trinity College Dublin, Dublin 2, Ireland

Abstract

In recent years, increasing numbers of studies have shown that the composition and localization of the host microflora is important for an organism's homeostatic function. Perturbations in microflora composition and compartmentalization can lead to altered metabolism, altered homeostasis and disease. The mechanisms which govern the interaction between host and commensal microbes are not well understood, nor are the conditions which may cause an organism's microflora to be altered.
MicroRNA-21 (miR-21) is a well-characterized microRNA which post-transcriptionally regulates the expression of many genes in response to multiple stimuli. It is widely expressed in cells and tissues that interact with commensal bacteria such as those of the gastrointestinal (GI) tract and is induced upon ligand binding of many cell surface receptors including pattern recognition receptors. MiR-21 has been shown to have a deleterious role in mouse models of colitis and colitis associated colorectal cancer, and its expression is elevated in the colons of patients with inflammatory bowel disease (IBD).
Our project seeks to understand if miR-21 may be involved via host-microbiome cross-talk in the gut. Using miR-21-deficient mice, we have demonstrated that wild-type mice co-housed with miR-21$^{-/-}$ mice gain a partial protection in an acute DSS colitis model. In addition, germ-free mice recolonized with the microbiota of miR-21$^{-/-}$ mice are partially protected from DSS colitis. Using 16S rRNA

sequencing, we have generated preliminary data which suggests miR-21 may negatively regulate the abundance of the bacteria *Rikenellaceae*, a bacteria found in low abundance in IBD cohorts compared to healthy controls. Further work is needed to confirm these effects and elucidate a possible mechanism by which miR-21 might be acting in this system.

Irish Society of Immunology Annual meeting, Dublin, Ireland

September 2015

– Poster presentation

MicroRNA-21 regulates phagocytic responses during infection with *Listeria*

Johnston, D.G.W, O'Neill, L.A. and Corr, S.C.
School of Biochemistry and Immunology, Trinity College Dublin, Ireland.

Keywords: miR21*, Listeria*, phagocytosis

microRNAs (miR) are considered fine tuners of immunity with altered expression leading to disease. miR-21 in particular, negatively regulates responses to bacterial lipopolysaccharide (LPS) via production of anti-inflammatory IL-10. We investigated the role of miR21 during infection with the food-borne pathogen *Listeria monocytogenes,* which invades through the intestinal epithelium causing the potentially fatal disease, listeriosis. *L. monocytogenes* is the fourth most common cause of meningeal infection and it predominately affects pregnant, newborn and immunocompromised individuals, with a mortality rate of 20% or higher. In addition, *L. monocytogenes* is a model organism for the study of intracellular parasitism and the associated immune response. We analysed the role of miR-21 during phagocytosis of *Listeria* by professional phagocytes. Bone marrow-derived macrophages (BMDM) and dendritic cells (BMDC) were generated from wild-type and miR-21$^{-/-}$ mice and infected with *L. monocytogenes*. miR-21$^{-/-}$ cells of each lineage display significantly increased bacterial burden early during infection however there was no difference at later timepoints. This indicates a role for miR-21 in regulating phagocytosis*,* with loss of miR-21 leading to increased uptake of bacteria. This was further confirmed by analysis of uptake of FITC-dextran beads by BMDMs and BMDCs, which was increased upon loss of miR-21. Additionally, we measured the cytokine output of different cell types in response to bacterial ligands. Most notably, miR-21$^{-/-}$ macrophages and DCs display elevated levels of phagocytosis- associated IL-12.These data suggest a novel role for miR-21 in negatively regulating phagocytosis of *L. monocytogenes* and highlight its potential as a target for amelioration of listeriosis.

Toll 2015, Marbella, Spain

– Poster presentation

MicroRNA-21 regulates phagocytic responses during infection with *Listeria*

Johnston, D.G.W, O'Neill, L.A. and Corr, S.C.
School of Biochemistry and Immunology, Trinity College Dublin, Ireland.

microRNAs (miR) are considered fine tuners of immunity with altered expression leading to disease. miR21 in particular, negatively regulates responses to bacterial lipopolysaccharide (LPS) via production of anti-inflammatory IL-10. We investigated the role of miR21 during infection with the food-borne pathogen *Listeria monocytogenes,* which invades through the intestinal epithelium causing the potentially fatal disease, listeriosis. *L. monocytogenes* is the fourth most common cause of meningeal infection and it predominately affects pregnant, newborn and immunocompromised individuals, with a mortality rate of 20% or higher. In addition, *L. monocytogenes* has long been used as a model organism for the study of intracellular parasitism and the associated immune response. We analysed the role of miR21 during phagocytosis of *Listeria* by professional phagocytes. Primary bone marrow-derived macrophages and dendritic cells were generated from wild-type and miR21-deficient mice and infected with *L. monocytogenes*. miR21-deficient cells of each lineage display significantly increased bacterial burden early during infection however there was no difference in bacterial load during late infection. This indicates a role for miR21 in regulating phagocytosis, with loss of miR21 leading to increased uptake of bacteria. This was further confirmed by analysis of uptake of FITC-dextran beads by macrophages and DC, which was increased upon loss of miR21. To further investigate this role for miR21 during infection, we analysed the cytokine profiles of WT and miR21-deficient cells to *L. monocytoegenes* and bacterial pathogen associated molecular patterns (PAMPS). Most notably, miR21-deficient macrophages and dendritic cells display a heightened response to *Listeria* infection and bacterial LPS, as shown by elevated levels of the pro-inflammatory and pro-phagocytic cytokine IL-12p70. The p35 subunit of IL-12p70 is a direct target of miR-21. These data suggest a novel role for miR-21 in negatively regulating phagocytosis of *L. monocytogenes* and highlight its potential as a therapeutic target for amelioration of listeriosis.

Second Joint Symposium between The Weizmann Institute of Science and Trinity College Dublin, Weizmann Institute of Science, Rehovot, Israel

– Oral presentation

The Role of miR-21 in Gut Homeostasis and Disease

Johnston, D.G.W, O'Neill, L.A. and Corr, S.C.
School of Biochemistry and Immunology, Trinity College Dublin, Ireland.

MicroRNA(miR)-21 is a widely expressed post-translational regulator of mRNA expression involved in regulation of several immune signaling pathways. It has been shown to be directly involved in the negative regulation of TLR4 signalling in macrophages as well as being implicated in a variety of disease states. Inflammatory bowel disease (IBD) and colorectal cancer are two such diseases that are both marked by miR-21 overexpression. Our study aims to elucidate the role of miR-21 in gastrointestinal homeostasis and disease using various disease models and *in vitro* approaches. We have confirmed that miR-21 knock-out mice are protected from DSS induced colitis compared to wild-type controls in various conditions. In addition, using co-housing and cross fostering models, we have generated preliminary data suggesting that miR-21 knock-out mice may have an altered microbiota which contributes to their protection in this disease model. We hope to further explore this idea in the Weizmann. We have observed that bone marrow derived macrophages and dendritic cells generated from miR-21 knock-out mice progenitors secrete significantly higher levels of interleukin-12p70 (IL-12p70) in response to various TLR agonists than wild type controls. As it is well known that IL-12p70 is an inducer of Th1 cells, and that Th1 cells are implicated in IBD, there is an interesting conflict in these results which we are currently exploring.

7.2. Publications

MicroRNA-21 Limits Uptake of *Listeria monocytogenes* by Macrophages to Reduce the Intracellular Niche and Control Infection

- **MicroRNA-21 Limits Uptake of *Listeria monocytogenes* by Macrophages to Reduce the Intracellular Niche and Control Infection**
  Front. Cell. Infect. Microbiol., May 2017 Johnston DGW, Kearney J, Zaslona Z, Williams MA, O' Neill LAJ and Corr SC
- **Toll-Like Receptor Signalling and the Control of Intestinal Barrier Function.** Methods Mol Biol. 2016: Johnston DGW and Corr SC
- **Pyruvate kinase M2 regulates Hif-1α activity and IL-1β induction and is a critical determinant of the warburg effect in LPS-activated macrophages.** Cell Metabolism. 2015: Palsson-McDermott EM, Curtis AM, Goel G, Lauterbach MA, Sheedy FJ, Gleeson LE, van den Bosch MW, Quinn SR, Domingo-Fernandez R, Johnston DG, Jiang JK, Israelsen WJ, Keane J, Thomas C, Clish C, Vander Heiden M, Xavier RJ, O'Neill LA.
- **MyD88 adaptor-like (Mal) regulates intestinal homeostasis and colitis-associated colorectal cancer in mice.** Am J Physiol Gastrointest Liver Physiol. 2014: Aviello G, Corr SC, Johnston DG, O'Neill LA, Fallon PG.
- **Differential role of Dok1 and Dok2 in TLR2-induced inflammatory signaling in glia.** Mol Cell Neurosci. 2013: Downer EJ, Johnston DG, Lynch MA.

frontiers in Cellular and Infection Microbiology

ORIGINAL RESEARCH
published: 23 May 2017
doi: 10.3389/fcimb.2017.00201

MicroRNA-21 Limits Uptake of *Listeria monocytogenes* by Macrophages to Reduce the Intracellular Niche and Control Infection

*Daniel G. W. Johnston[1,2], Jay Kearney[1], Zbigniew Zasłona[1], Michelle A. Williams[2], Luke A. J. O'Neill[1] and Sinéad C. Corr[2]**

[1] School of Biochemistry and Immunology, Trinity Biomedical Sciences Institute, Trinity College Dublin, Dublin, Ireland,
[2] Department of Microbiology, Moyne Institute of Preventive Medicine, School of Genetics and Microbiology, Trinity College Dublin, Dublin, Ireland

MiRNAs are important post-transcriptional regulators of gene expression. MiRNA expression is a crucial part of host responses to bacterial infection, however there is limited knowledge of their impact on the outcome of infections. We investigated the influence of miR-21 on macrophage responses during infection with *Listeria monocytogenes*, which establishes an intracellular niche within macrophages. MiR-21 is induced following infection of bone marrow-derived macrophages (BMDMs) with *Listeria*. MiR-21$^{-/-}$ macrophages display an increased bacterial burden with *Listeria* at 30 min and 2 h post-infection. This phenotype was reversed by the addition of synthetic miR-21 mimics to the system. To assess the immune response of wildtype (WT) and miR-21$^{-/-}$ macrophages, BMDMs were treated with bacterial LPS or infected with *Listeria.* There was no difference in IL-10 and IL-6 between WT and miR-21$^{-/-}$ BMDMs in response to LPS or *Listeria*. TNF-α was increased in miR-21$^{-/-}$ BMDMs stimulated with LPS or *Listeria* compared to WT macrophages. We next assessed the production of nitric oxide (NO), a key bactericidal factor in *Listeria* infection. There was no significant difference in NO production between WT and miR-21$^{-/-}$ cells, indicating that the increased bacterial burden may not be due to impaired killing. As the increased bacterial load was observed early following infection (30 min), we questioned whether this is due to differences in uptake of *Listeria* by WT and miR-21$^{-/-}$ macrophages. We show that miR-21-deficiency enhances uptake of FITC-dextran and FITC-*Escherichia coli* bioparticles by macrophages. The previously observed *Listeria* burden phenotype was ablated by pre-treatment of cells with the actin polymerization inhibitor cytochalasin-D. From analysis of miR-21 targets, we selected the pro-phagocytic regulators myristoylated alanine-rich C-kinase substrate (MARCKS) and Ras homolog gene family, member B (RhoB) for further investigation. MARCKS and RhoB are increased in miR-21$^{-/-}$ BMDMs, correlating with increased uptake of *Listeria*. Finally, intra-peritoneal infection of mice with *Listeria* led

OPEN ACCESS

Edited by:
Stephanie M. Seveau, Ohio State University at Columbus, United States

Reviewed by:
Lee-Ann H. Allen, University of Iowa, United States
Alice Lebreton, École Normale Supérieure, France

***Correspondence:**
Sinéad C. Corr
corrsc@tcd.ie

Received: *06 March 2017*
Accepted: *05 May 2017*
Published: *23 May 2017*

Citation:
Johnston DGW, Kearney J, Zasłona Z, Williams MA, O'Neill LAJ and Corr SC (2017) MicroRNA-21 Limits Uptake of Listeria monocytogenes by Macrophages to Reduce the Intracellular Niche and Control Infection. Front. Cell. Infect. Microbiol. 7:201. doi: 10.3389/fcimb.2017.00201

to increased bacterial burden in livers of miR-21$^{-/-}$ mice compared to WT mice. These findings suggest a possible role for miR-21 in regulation of phagocytosis during infection, potentially by repression of MARCKS and RhoB, thus serving to limit the availability of the intracellular niche of pathogens like *L. monocytogenes.*

Keywords: microRNA, *Listeria*, macrophage, phagocytosis, miR-21, MARCKS

INTRODUCTION

Macrophages are important effector cells of the innate immune system and represent the first line of defense against invading bacterial pathogens (Benoit et al., 2008). Professional phagocytic cells of the innate immune system, macrophages encounter and engulf invading pathogens, cellular debris and other potential deleterious substances. Their expression of pattern recognition receptors (PRRs) (Takeuchi and Akira, 2010), both on the cell membrane and in the cytosol, allows them recognize potentially harmful bacteria. Following recognition of invading bacteria, intracellular signaling pathways are initiated leading to actin polymerization and formation of the phagocytic cup which subsequently encloses around the bacterium to form the phagosome. The phagosome subsequently undergoes a series of maturation steps which involves fusion with endosomal vesicles and fission vesicles, moving through early, intermediate and late stages culminating in formation of the mature phagolysosome which has acquired the full bactericidal repertoire (Weiss and Schaible, 2015). These include ability to generate reactive nitrogen intermediates such as nitric oxide (NO) and production of reactive oxygen species (ROS). In this way, macrophages play a critical role in host responses to intracellular pathogens and the clearance of infections which significantly contribute to the high morbidity and mortality rates associated with infectious diseases worldwide. However, certain intracellular bacteria have evolved strategies which allow them to exploit these intracellular niches. *Listeria monocytogenes* is the causative agent of the group of systemic infections known as listeriosis, associated with a fatality rate of 20% or more and the third leading cause of death among food-borne bacteria (Ramaswamy et al., 2007). *Listeria*'s ability to establish itself intracellularly where it can avoid host responses, creates a more favorable environment that ensures their pathogenesis. Indeed, *L. monocytogenes* have evolved to escape from the phagolysosome through the expression of a hemolysin, LLO, and subsequently grow and replicate within the cytosol of macrophages. The ability of *Listeria* to establish an intracellular niche and evade immune surveillance typifies the struggle between infectious agents and the host immunity and is critical to the outcome of infection (Corr and O'Neill, 2009).

MiRNA have emerged as critical regulators of host immune responses. MiRNA are short, non-coding RNAs that have been shown to affect numerous cellular processes in a post-transcriptional manner (Bartel, 2004; He and Hannon, 2004; Almeida et al., 2011). The role of miRNAs in immunity has been an area of intense research in recent years, and many have been implicated in the regulation of immune cell function including the fine-tuning of PRR signaling (Baltimore et al., 2008; O'Neill et al., 2011; Quinn and O'Neill, 2011). Although, there is growing understanding that regulation of miRNA expression is a crucial part of the host response to bacterial infection, knowledge of their cellular expression in response to bacteria and the impact of this on the outcome of infections is limited. Furthermore, modulation of miRNAs has emerged as a novel strategy employed by bacterial pathogens to manipulate host cell pathways and survive within host cells. MiR-21 is one of the most highly expressed miRNAs in many mammalian cell types (Krichevsky and Gabriely, 2009). MiR-21 is induced by inflammatory stimuli in particular in myeloid cells including monocytes, macrophages and dendritic cells, however the functional outcome of this is not well characterized. However, gradually a picture has developed of miR-21 as an anti-inflammatory miRNA that serves to curb excessive responses and begin the resolution phase of inflammation. It was shown to regulate expression of the anti-inflammatory cytokine IL-10 in macrophages in response to bacterial LPS, by targeting PDCD4, a negative regulator of IL-10 translation (Sheedy et al., 2010; Sheedy, 2015). A study of asthma showed that miR-21 negatively regulates immune responses in dendritic cells, by controlling the production of pro-inflammatory IL-12 (Lu et al., 2009, 2011). In addition, miR-21 has also been implicated in positively regulating the phenomenon of efferocytosis whereby activated macrophages alter their behavior to take up dying cells and prevent further inflammation (Das et al., 2014). MiR-21 has previously been shown under certain contexts to act as a break in the differentiation of macrophages to an M2-like phenotype, allowing a more robust bactericidal M1 macrophage to emerge. Although the role of miR-21 in the host response to bacterial pathogens is relatively unexplored, this implies a potentially important role for miR-21 in the control of infection (Wang et al., 2015).

In the current study, we sought to elucidate the importance of miR-21 during infection, in particular to regulate the immune response to *L. monocytogenes.* The ability of pathogens to establish an intracellular niche is dependent in part, on their uptake by macrophages. Here we show that miR-21 is induced in response to infection of macrophages with *L.* monocytogenes to regulate the amount of phagocytosis thereby limiting the intracellular niche of this pathogen. To our knowledge, this is the first report of a role for miR-21 as a host-strategy to curb infection with *L. monocytogenes.*

MATERIALS AND METHODS

Bacterial Strains and Growth Conditions

Listeria monocytogenes EGDe (BUG1600, ATCC BAA-679) were grown in brain heart infusion (BHI, Oxoid), aerobically at

37°C shaking (200 rpm). All experiments performed using *L. monocytogenes* were performed in ClassII Biohazard facilities.

Mice

MiR-21-deficient (miR-21$^{-/-}$) mice were developed by Taconic Artemis using a Cre/*lox* approach. Briefly, miR-21 was modified by the insertion of two loxP sites that enable excision of the floxed miR-21 segment through Cre-mediated recombination. Chimeric offspring were backcrossed onto the C57BL/6J background for a total of 8 generations. Homozygous deletion of miR-21 was confirmed by PCR genotyping. Homozygous miR-21$^{-/-}$ and WT littermates were used for animal studies. Animals were maintained in ventilated cages at 21 ± 1°C, humidity 50 ± 10% and with a 12 h-light/12 h-dark light cycle under specific pathogen-free conditions, in line with Irish and European Union regulations. Food and water were available *ad libitum* throughout all of the experiments. All experiments involving use of mice or mouse tissue were subject to ethical approval by the Animal Research Ethics Committee (AREC), a Level 2 ethics committee responsible for reviewing the proposed use of animals in teaching and research at Trinity College Dublin, and were carried out in accordance with the recommendations of the Irish Health Products Regulatory Authority, the competent authority responsible for the implementation of Directive 2010/63/EU on the protection of animals used for scientific purposes in accordance with the requirements of the S.I No 543 of 2012.

Isolation of Bone Marrow-Derived Macrophages

Tibia and femur from 6 to 8 week-old C57BL/6J and genetically-matched miR-21$^{-/-}$ mice were collected in ice cold PBS. Bones were sterilized with 70% ethanol, cleaned and flushed with a 25-G needle using cold DMEM (Gibco) supplemented with 10% FCS and 1% penicillin-streptomycin (Sigma Aldrich). Following red-blood cell lysis, cells were seeded onto non-cell culture coated 10 cm dishes in complete DMEM containing 20% M-CSF containing L929 media and incubated 37°C with 5% CO_2 for 6 days. Subsequently, BMDMs were seeded at 5×10^5 cells/ml in 12-well tissue culture plates (Sarstedt) in DMEM containing 10% L929 and 10% FCS.

Isolation of Resident Peritoneal Macrophages

Resident macrophages, peritoneal exudate cells (PECs) were isolated from 6 to 8 week-old C57BL/6J and genetically-matched miR-21$^{-/-}$ mice by washing the peritoneum with 3 mL sterile PBS. The recovered cells were centrifuged at 300 g for 5 min and resuspended in complete medium. 12-well tissue culture plates were seeded at 5×10^5 cells/ml (Sarstedt) in DMEM containing 10% FCS.

Transfection of Bone Marrow-Derived Macrophages

BMDMs were seeded at 3×10^5 cells/ml in 12-well tissue culture plates (Sarstedt) in DMEM containing 10% L929 and 10% FCS. The following day cells were transfected with 20 nmoles Mission® miR-21 mimic or negative control RNA (Sigma) for 24 h using RNAiMax transfection reagent (ThermoFisherScientific).

Phagocytosis/Cellular Uptake Assays

Twenty-four hour following seeding, *L. monocytogenes* were added at MOI 100:1 for 15 min, and media subsequently replaced with DMEM containing gentamicin (100 mg/ml). At 0.5 or 2 h, monolayers washed and lysed and subsequently plated on to BHI agar plates for determination of rates of phagocytosis, expressed as Log CFU/ml (or as CFU/cell as in Supplementary Figure 1). For FITC-dextran uptake assays, BMDMs or PECs were plated at 5×10^5 cells/ml, in a 12-well tissue culture plate (Sarstedt) for 24 h. Cells were then incubated with 1 mg/ml FITC-dextran at 37°C for 1 h. Control cells were left untreated, or were treated and incubated at 4°C. At the end of the incubation, the cells were collected for assessment of FITC-dextran uptake by flow cytometry (BD Fortessa flow cytometer). For Vybrant™ Phagocytosis assays (Molecular Probes), BMDMs were plated at 5×10^5 cells/ml in a 96-well plate and incubated with FITC-*E. coli* Bioparticles® for 2 h according to the manufacturer's instructions before extracellular FITC was quenched using trypan blue and fluorescence assayed using a FLUOstar Optima microplate reader at emission ∼520 nm and excitation ∼480 nm. Cytochalasin-D was used at 10 μM for 30 min pre-treatment in some assays.

Enzyme Linked Immunosorbent Assay (ELISA)

BMDMs were treated with LPS (Alexis) at 100 ng/ml or infected with *L. monocytogenes* at MOI 100:1 for 24 h. After an initial infection with *L. monocytogenes* for 15 min, media was subsequently replaced with DMEM containing gentamicin (100 mg/ml). Murine IL-10, IL-6, and TNF-α production was detected in macrophage supernatants by ELISA according to the manufacturer's procedure (R&D Duoset). Optical density was measured at 450 nm and cytokine concentrations were determined using a standard curve, expressed as pg/ml.

Quantitative Real-Time PCR (qPCR)

Total RNA was extracted from BMDMs using a PureLink RNA extraction kit (Applied Biosystems) according to the manufacturer's instructions. Total RNA was reverse transcribed with a high-capacity cDNA archive kit (Applied Biosystems) and the cDNA was amplified using both Taqman and SYBR green-based real-time PCR on a 7,300 real-time PCR system (Applied Biosystems). Primer sequences are listed in **Table 1**. Relative quantification (RQ) of mRNA levels were determined by the $2^{-\Delta\Delta CT}$ method comparing genes of interest to endogenous controls (U6 or Rps13). MiR-21 and U6 primers and probes were obtained from Applied Biosystems.

Nitric Oxide (NO) assay

To estimate NO release in response to *L. monocytogenes*, BMDMs were infected at MOI 100:1 for 15 min, the media was then

TABLE 1 | Primers used for Sybr-Green qPCR*.

Primer pair	Forward	Reverse
MARCKS	5′-CTCCTCCTTGTCGGCGGC CGG-3′	5′-GGCCACGTAAAAGTGAAC GGC-3′
RhoB	5′-GACGGCAAGCAGGTGGA G-3′	5′-ATGGGCACATTGGGGCA G-3′
Rps13	5′-GGCCCACAAGCTCTTTCC TT-3′	5′-GACCTTCTTTTTCCCGCA GC-3′

replaced with DMEM containing gentamicin (100 mg/ml) for a further 1 h 45 min or 23 h and 45 min, and subsequently the nitrate present in the supernatants of macrophages at 2 h post-infection was measured using a Griess reaction according with the manufacturer's instructions (Promega). To estimate NO release in response to LPS, BMDMs were treated with LPS (100 ng/ml) for 2 or 24 h. Optical density was read between 520 and 550 nm and the nitrate present in each sample was quantified using a standard curve.

Immunoblotting

BMDM cell lysates were obtained following infection with *L. monocytogenes* or from untreated samples. BMDMs were infected at MOI 100:1 for 15 min, and the media was then replaced with DMEM containing gentamicin (100 mg/ml) for a further 105 min. Samples were clarified, denatured with SDS loading buffer, and boiled for 5 min. A total of 40 mg protein lysate was fractionated on 12% SDS-PAGE, transferred to polyvinylidene fluoride membranes (Millipore) and probed with primary Abs to murine MARCKS (1:2,000 dilution, ab51100, Abcam), murine RhoB (1:1,000 dilution, sc-180, Santa Cruz) or murine β-actin (1:10,000 dilution, Clone AC-74, Sigma), incubated with horseradish peroxidase-conjugated secondary antibodies (Santa Cruz Biotechnology) and visualized using WesternBright ECL HRP substrate (Advansta), BD ChemiDoc system and ImageLab software.

In vivo L. monocytogenes Infection

Mice were intra-peritoneally or orally infected with *L. monocytogenes* at 1×10^6 CFU or 5×10^7 CFU respectivly. 3 days of 6 days p.i., respectively, livers were harvested and homogenized in PBS. Serial dilutions of this homogenate were plated on to BHI agar plates for determination of dissemination levels. Levels were expressed as Log CFU/liver.

MiRNA Database Analysis

A combination of miRBase, miRWALK2.0 and TargetScan were used to identify potential miR-21 targets along with consultation of the literature.

Statistical Analysis

Numerical results are given as arithmetic means ± standard deviations. Statistical differences were analyzed by GraphPad Prism 5.0 statistical software (GraphPad Software Inc., San Diego, USA) or Student's *t*-test. *P*-values of less than 0.05 ($p \leq 0.05$) are considered statistically significant.

RESULTS

MiR-21 Is Induced during Infection of Macrophages with *Listeria* and Its Expression Influences Bacterial Burden

Previous studies have shown that miR-21 expression in macrophages is induced by stimulation with bacterial TLR agonists such as LPS (Sheedy et al., 2010). To gain insight into the role of miR-21 during infection, we infected WT and miR-21$^{-/-}$ BMDMs with the intracellular bacterial pathogen *L. monocytogenes* and assayed the bacterium's intracellular survival. Strikingly, BMDMs deficient for miR-21 had a significantly higher bacterial burden than WT macrophages after 2 h infection with high bacterial loads (**Figure 1A**). MiR-21 expression was significantly induced in WT BMDMs upon infection with *L. monocytogenes* (**Figure 1B**). The difference in bacterial burden observed after 2 h was also apparent after only 30 min infection (**Figure 1C**). In order to confirm miR-21's importance in *L. monocytogenes* infection, WT and miR-21$^{-/-}$ BMDMs were transfected with synthetic miR-21 mimics, and a significant reduction of bacterial burden was observed in WT cells, as well as a reduction of bacterial burden in the miR-21$^{-/-}$ cells toward WT levels (**Figure 1D**). These results suggest that miR-21 plays an important role during infection and aids control of *Listeria* by macrophages.

Loss of MiR-21 Alters Cytokine Expression in Response to LPS but Not *Listeria*

To assess the effect of miR-21 on the immunological response of macrophages during infection, we treated WT and miR-21$^{-/-}$ BMDMs with LPS or infected with *L. monocytogenes*, and after 24 h determined the level of cytokine secretion. Although not significant, we observed a decrease in IL-10 secretion by miR-21$^{-/-}$ cells in response to stimulation with LPS (**Figure 2A**). This is in agreement with previous studies implicating miR-21 in IL-10 regulation (Sheedy et al., 2010). Furthermore, we observed a trend toward an increase in IL-6 secretion (**Figure 2B**) and significantly increased TNF-α secretion (**Figure 2C**) in cells lacking miR-21. We next determined the effect of miR-21 expression on cytokine responses during infection of macrophages with *L. monocytogenes*. We observed an increase in IL-10 secretion, counter to previous reports involving TLR ligands, a very high level of IL-6 secretion in both WT and miR-21$^{-/-}$ cells and a significant increase in TNF-α secretion by miR-21$^{-/-}$ macrophages, though the difference was less significant than that present post LPS stimulation (**Figures 2D–F**). This suggests that miR-21's capacity to affect multiple processes may present a more complex dynamic during infection. This idea is supported by recent work by Barnett et al. who reported varying survival and cytokine secretion profiles among different sepsis models in miR-21$^{-/-}$ mice, where the more physiological cecal ligation puncture model showed no differences between WT and miR-21$^{-/-}$ mice in contrast to an LPS-induced sepsis model (Barnett et al., 2016).

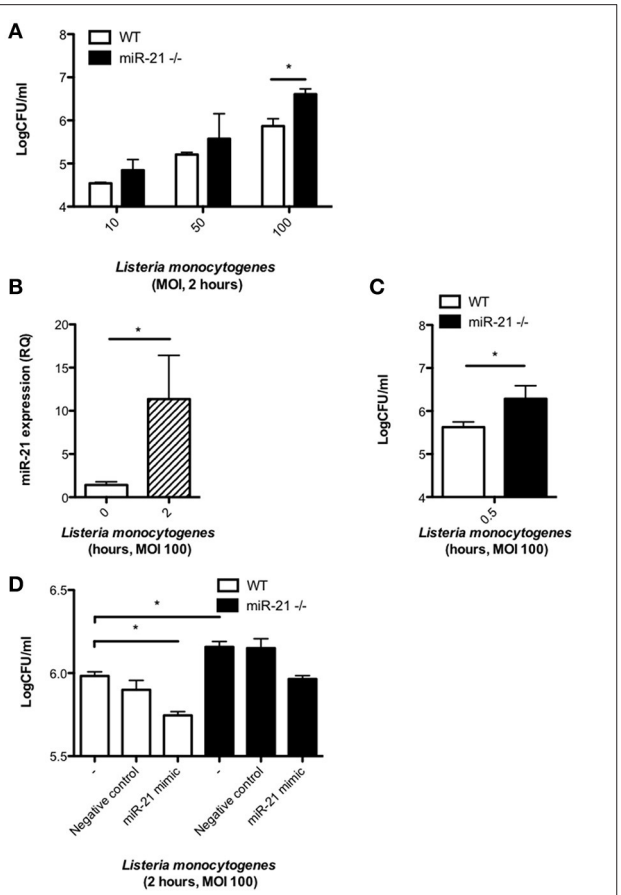

FIGURE 1 | MiR-21 is induced during *L. monocytogenes* infection of macrophages and its expression influences bacterial burden. BMDMs were infected with *L. monocytogenes* at MOIs of 10, 50, and 100 for 15 min and subsequently cultured with media containing gentamicin (100 ug/ml). **(A)** At 2 h post-infection, the number of intracellular bacteria in WT and miR-21$^{-/-}$ BMDMs was determined and expressed as Log CFU/ml. **(B)** At 2 h post-infection the RNA was isolated from WT BMDMs and mature miR-21 expression was assayed by qPCR and data expressed as relative expression from triplicate samples. **(C)** At 0.5 h the number of intracellular bacteria in WT and miR-21$^{-/-}$ BMDMs was determined and expressed as Log CFU/ml. **(D)** WT and miR-21$^{-/-}$ BMDMs were transfected with a miR-21 mimic or negative control for 24 h before subsequent *Listeria* infection. At 2 h post-infection, the number of intracellular bacteria was determined and expressed as Log CFU/ml. Data are expressed as means ± SD, $n = 3$ (except D where $n = 2$ for miR-21$^{-/-}$ BMDMs), and are representative of at least three independent experiments. *Designates a p-value < 0.05 by Students t-test.

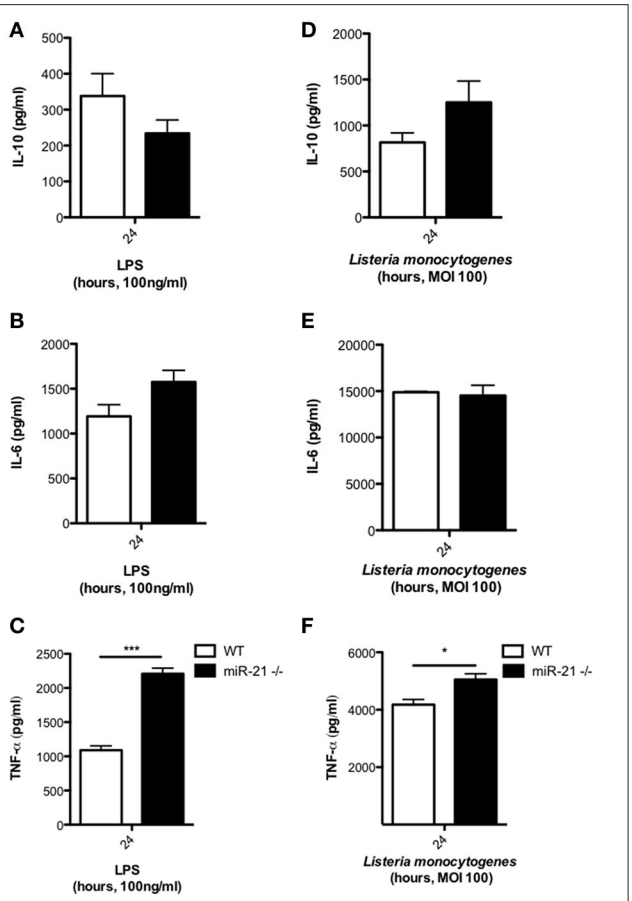

FIGURE 2 | MiR-21-deficiency alters cytokine response to LPS and *Listeria*. BMDMs were incubated with LPS at 100 ng/ml for 24 h and levels of **(A)** IL-10, **(B)** IL-6, and **(C)** TNF-α in the supernatants measured by ELISA. BMDMs were infected with *L. monocytogenes* at an MOI 100 for 15 min and subsequently cultured with media containing gentamicin (100 μg/ml) and at 24 h post-infection the levels of **(D)** IL-10, **(E)** IL-6, and **(F)** TNF-α in the supernatants measured by ELISA. Data are expressed as means ± SD, $n = 3$, and are representative of at least three independent experiments. *Designates a p-value < 0.05 and ***Designates a p-value < 0.001 by Students t-test.

Loss of MiR-21 Expression Does Not Impact Production of Bacteriocidal Nitric Oxide in Response to Infection

We next explored the possibility that miR-21 induction may regulate the antibacterial activities of macrophages. As the oxygen-free radical NO is an important factor produced within macrophages to mediate intracellular killing of phagocytosed bacteria, we assayed the effect of loss of miR-21 expression on their production in response to infection with *L. monocytogenes*. To determine if reduced production of NO was responsible for the heightened bacterial load in miR-21$^{-/-}$ BMDMs, we infected cells with *Listeria* and harvested the supernatants to measure nitrite using the Griess reaction. We saw no significant difference in NO production between WT and miR-21$^{-/-}$ macrophages (**Figure 3A**). Similarly, we saw no significant difference in the production of NO by WT and miR-21$^{-/-}$ macrophages in response to LPS (**Figure 3B**). These data led us to the conclusion that miR-21$^{-/-}$ cells are not impaired in the capacity to kill invading bacteria and that the higher burden observed in these cells is due to miR-21 regulation of an alternative part of the phagocytosis process.

MiR-21 Limits Uptake of FITC-Dextran and FITC-*E. coli* by Macrophages

Given that we observed an increased intracellular bacterial burden in miR-21$^{-/-}$ cells as early as 30 min post-infection

(**Figure 1C**), we hypothesized that miR-21 may regulate the initial engulfment of bacteria by macrophages. To determine this, we next examined the ability of resident peritoneal macrophages (PECs) (**Figure 4A**) and BMDMs (**Figure 4B**) to take up FITC-dextran. Cells were incubated with FITC-dextran for 1 h and its uptake assayed by flow cytometry. Interestingly, there was a significantly higher uptake of FITC-dextran in both PECs and BMDMs (**Figures 4A,B**) in miR-21$^{-/-}$ cells compared to WT macrophages. As dextran is not necessarily taken up by phagocytosis, we also used a commercial phagocytosis kit to assay FITC-*E. coli* particle uptake by macrophages and saw that there was a significant increase in uptake by miR-21$^{-/-}$ cells relative to WT (**Figure 4C**). Pre-treatment of cells with the actin polymerization inhibitor cytochalasin-D ablated the previously demonstrated increase in bacterial burden demonstrated post-*L. monocytogenes* infection at both 30 min and 2 h (**Figure 4D**). These results indicated that miR-21 may regulate the phagocytic process by mediation of actin polymerization.

MiR-21 Represses the Pro-Phagocytic Proteins MARCKS and RhoB

We next analyzed various databases of predicted and validated miR-21 target genes for factors which may influence initial uptake during phagocytosis. We identified myristoylated alanine-rich protein kinase C substrate (MARCKS), which has been shown in other studies to regulate actin polymerization and formation of the phagocytic cup. We observed a higher basal protein level of MARCKS in miR-21$^{-/-}$ BMDMs compared to WT macrophages (**Figures 5A,B**). Infection had no effect of the level of MARCKS protein in both WT and miR-21$^{-/-}$ macrophages (**Figures 5A,B**). There was no difference in the level of MARCKS mRNA basally between WT and miR-21$^{-/-}$ macrophages, however, infection increased the mRNA level of MARCKS in miR-21$^{-/-}$ macrophages, and this increase was significantly higher than in WT macrophages following infection (**Figure 5C**). We next analyzed another target of miR-21, *Ras* homolog gene family member B (RhoB), which has previously been reported to influence cytoskeletal changes during phagocytosis (Zhang et al., 2005; Quinn et al., 2009). We observed that the protein level of RhoB is higher basally in miR-21$^{-/-}$ BMDMs compared to WT macrophages (**Figures 5A,B**). Infection had no effect on the protein level of RhoB (**Figures 5A,B**). Although not significant, there was a trend toward increased RhoB at the mRNA level basally in miR-21$^{-/-}$ macrophages and also following infection with *L. monocytogenes* (**Figure 5D**). Taken together these data suggest that miR-21 targets MARCKS and RhoB, demonstrating that miR-21 interacts with known actin mediators. Although further work is required to show this, it may be that this represents a host strategy to limit the intracellular niche of *L. monocytogenes*.

MiR-21 Controls Intraperitoneal *Listeria* Infection *In vivo*

In order to test the hypothesis that induction of miR-21 during infection with *Listeria* is a host strategy to limit the intracellular niche of this bacterium, thereby reducing its pathogenesis and the ability of *L. monocytogenes* to establish an infection, we compared the outcome of intra-peritoneal infection of WT and miR-21$^{-/-}$ mice. We observed reduced levels of dissemination by *Listeria* to internal organs, as shown by a significant reduction in bacterial burden in the livers (**Figure 6A**) of WT mice, compared to miR-21$^{-/-}$ mice. This difference was not apparent in mice infected by oral gavage, which might indicate that the dissemination is a macrophage led phenotype (**Figure 6B**).

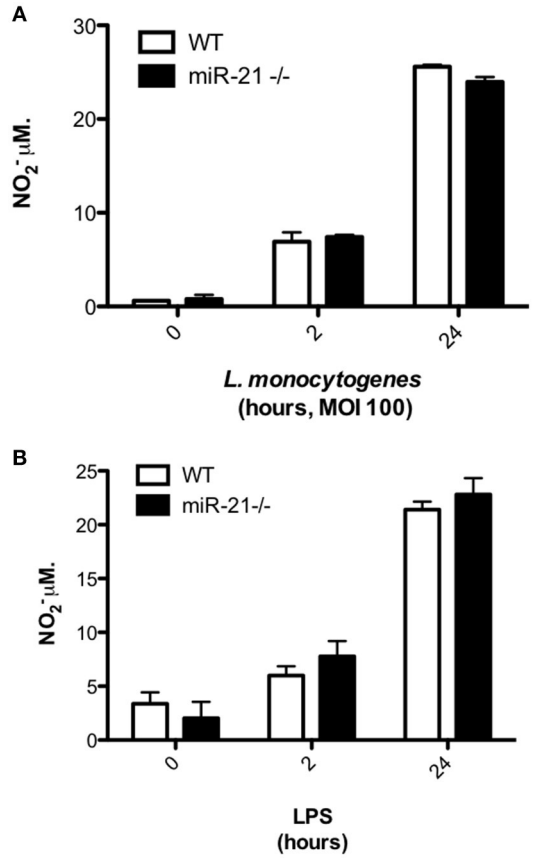

FIGURE 3 | MiR-21-deficiency does not impact on NO$^-$ production in response to infection with *Listeria*. (A) BMDMs were treated with LPS (100 ng/ml) before the supernatant was harvested and NO$^-$ production was assayed by Griess reaction. **(B)** BMDMs were infected with *L. monocytogenes* at an MOI 100 for 15 min and subsequently cultured with media containing gentamicin (100 µg/ml). At 2 and 24 h post-infection the supernatant was harvested and NO$^-$ production was assayed by Griess reaction.

DISCUSSION

Macrophages form a crucial part of our body's defense, with the ability of macrophages to engulf and digest invading pathogens, termed phagocytosis, being fundamental to the control of infection (Rougerie et al., 2013). Bacterial pathogens are sensed through the expression of PRRs on phagocytes which recognize pathogen-associated molecular patterns (PAMPS) such as bacterial lipopolysaccharide, including TLRs

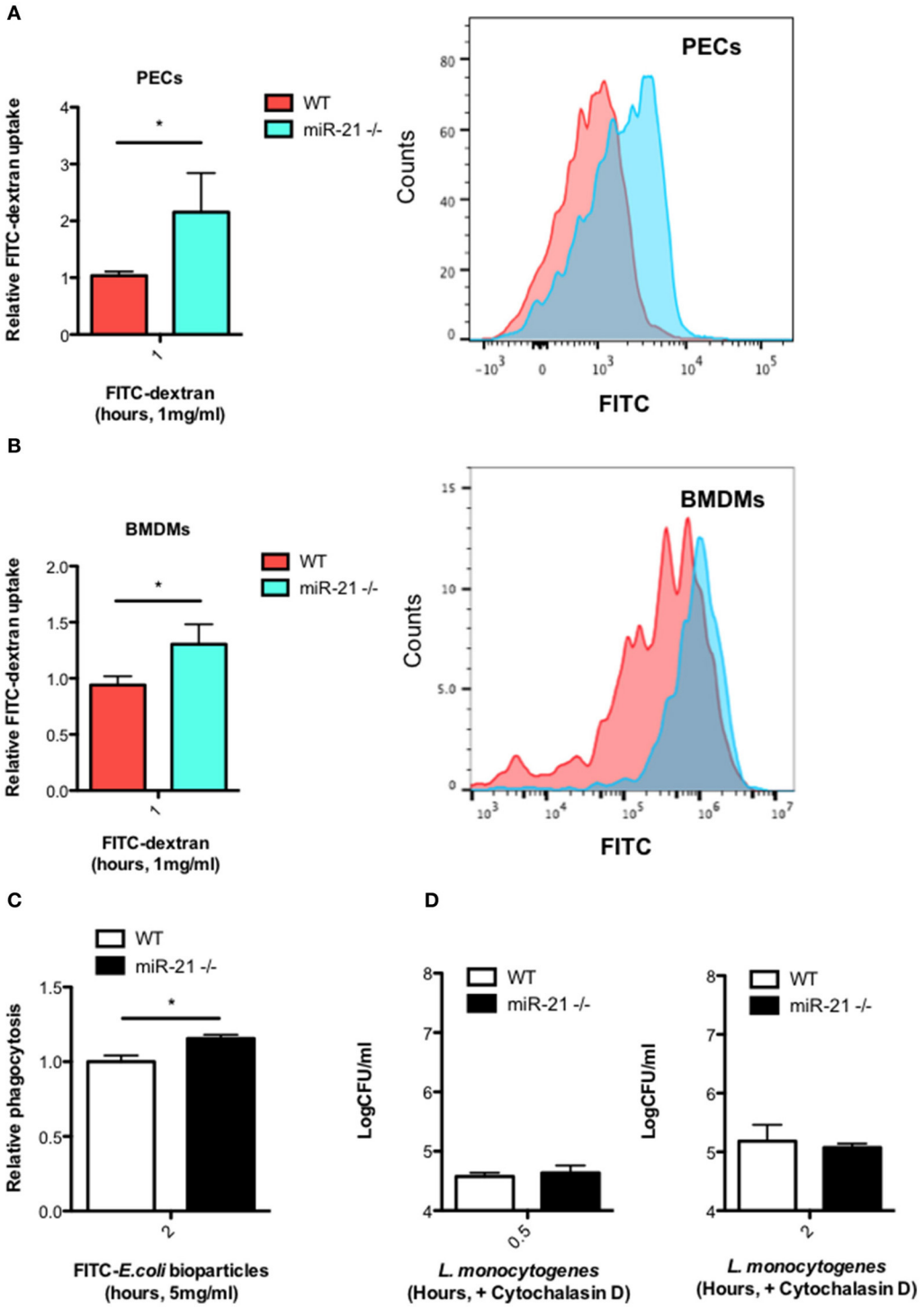

FIGURE 4 | MiR-21-deficient macrophages display increased uptake of FITC-dextran and phagocytosis of FITC-*E. coli* particles. Peritoneal exudate cells (PECs) **(A)** and BMDMs **(B)** from WT and miR-21$^{-/-}$ mice were incubated with media containing 1 mg/ml FITC-dextran for 1 h at 37°C. Uptake of FITC-dextran was determined by measuring the median fluorescence intensity by flow cytometry and data expressed relative to WT (Relative FITC-dextran uptake) with a corresponding histogram representative of median florescent intensity. **(C)** BMDMs from WT and miR-21$^{-/-}$ were incubated with FITC-K-12 *E. coli* Bioparticles for 2 h before fluorescence was determined using a microplate reader. **(D)** WT and miR-21$^{-/-}$ BMDMs were treated with cytochalasin-D for 30 min prior to *Listeria* infection. At 0.5 and 2 h post-infection, the number of intracellular bacteria was determined and expressed as Log CFU/ml. Data are expressed as means ± SD, $n = 3$ [except **(B)** where $n = 2$ for miR-21$^{-/-}$ BMDMs], and are representative of at least two independent experiments. *Designates a p-value < 0.05 by Students t-test.

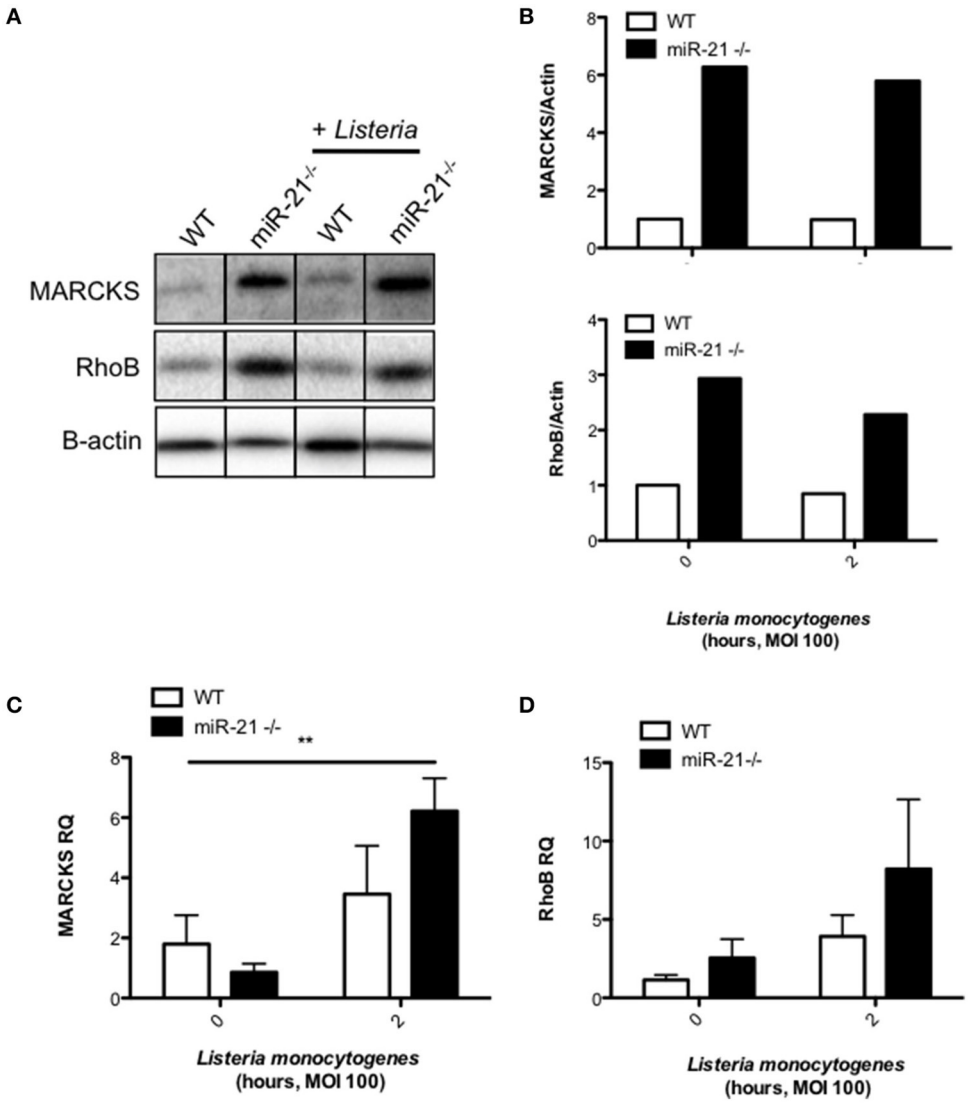

FIGURE 5 | MiR-21 represses the pro-phagocytic proteins MARCKS and RhoB. (A) BMDMs were infected with *L. monocytogenes* at an MOI 100 for 15 min and subsequently cultured with media containing gentamicin (100 μg/ml) for a further 105 min. **(A)** At 2 h post-infection, protein lysates were prepared for immunoblot analysis of basal and post-infection MARCKS and RhoB protein amounts. Protein levels were quantified by densitometry and expressed relative to the endogenous control **(B)**. RNA was isolated and assayed by qPCR for **(C)** MARCKS and **(D)** RhoB expression using Rps13 as an endogenous control. Data are expressed as means ± SD, $n \geq 5$, and are representative of at least two independent experiments. **Designates a p-value < 0.01 by Students t-test.

expressed on the phagocyte cell surface and membranes of vesicular compartments (Janeway and Medzhitov, 2002; O'Neill et al., 2013) This results in the initiation of appropriate intracellular signaling pathways that trigger active phagocytosis and also production of cytokines to alert nearby immune cells (Kaufmann and Dorhoi, 2016). Control of bacterial pathogens is an important function of phagocytes, however certain intracellular bacteria have evolved strategies which allow them to survive within macrophages and exploit this intracellular niche. This enables propagation of infection without immune detection and activation of antimicrobial responses.

In this work, we have described a novel regulatory role for miR-21, whereby it limits this intracellular niche by inhibiting initial uptake of bacteria within macrophages, thereby reducing the severity and outcome of infection. We demonstrate here, that in the absence of miR-21, macrophages exhibit an increased bacterial burden following infection with the intracellular pathogen, *L. monocytogenes*. MiR-21 was induced following infection of BMDMs with *L. monocytogenes*. MiR-21 has previously been shown to be induced in response to bacterial LPS in macrophages while it is induced in monocytes infected with *Mycobacterium leprae* (Sheedy et al., 2010; Liu et al., 2012). We were surprised to find that miR-21-deficiency

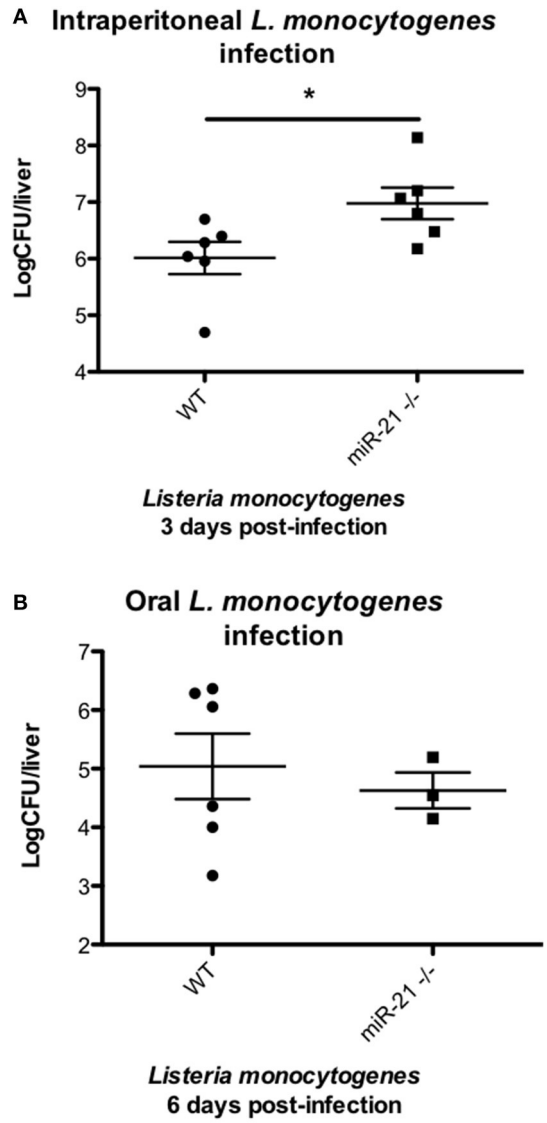

FIGURE 6 | miR-21-deficient mice are more susceptible to *Listeria* infection. (A) Mice were intra-peritoneally infected with *Listeria monocytogenes* at 1×10^6 CFU and 3 days post-infection dissemination of bacterial to livers determined and expressed as LogCFU/liver. Data are expressed as means ± SEM, $n = 6$. **(B)** Mice were fasted overnight before being orally infected with *Listeria monocytogenes* at 5×10^7 CFU and 6 days post-infection dissemination of bacterial to livers determined and expressed as LogCFU/liver. Data are expressed as means ± SEM, $n \geq 3$. *Designates a p-value < 0.05 by Students t-test.

in BMDMs led to a higher bacterial burden post-infection which translated to increased bacterial dissemination and infection in mice following i.p. infection. These results are in contrast to previous studies showing an anti-inflammatory role for miR-21 and suggesting that macrophages with high miR-21 expression are more M2 like (Sheedy, 2015). This would imply that miR-21-deficiency should correspond to a more pro-inflammatory and bactericidal phenotype. Indeed our own cytokine data supports this model, providing evidence for the miR-21 being a negative regulator of pro-inflammatory responses by inducing anti-inflammatory IL-10, as well as supporting the pre-existing studies for miR-21's negative regulation of TNF-α (Sheedy et al., 2010; Barnett et al., 2016). However, while these observations were consistent with the purified ligand LPS they were not fully consistent in an infection setting when *Listeria* were used to stimulate the macrophages, though there was still a significant increase in TNF-α secretion in the miR-21$^{-/-}$ macrophages. This failure of translation of ligand effect to physiological settings has been seen in other studies and points to a complexity in the role of the multi-target miR-21 in infectious settings (Barnett et al., 2016). In addition, the high bacterial burden present in our system may lead to an overwhelming cytokine signal, as demonstrated by the very high levels of the key *L. monocytogenes* cytokine IL-6 observed in response to infection (Dalrymple et al., 1995), which may hide potential differences.

Fusion of the phagosome with lysosomes, to form the phagolysosome is accompanied by acquisition of antibacterial mechanisms including antimicrobial peptides, proteases, an acidified environment, and the production of reactive oxygen and nitrogen species (ROS, RNS respectively), with NO (Rougerie et al., 2013). The production of NO during the oxidative burst which accompanies engulfment is a key antimicrobial mechanism of phagocytic cells, and has been shown to be important for the clearance of *L. monocytogenes* (Shiloh et al., 1999). To determine whether miR-21 may be influencing production of these antimicrobial molecules we determined production of NO in WT and miR-21$^{-/-}$ BMDM in response to *Listeria* infection. NO which is produced via the enzymatic activity of inducible nitric oxide synthase 2, has been shown to be an important mediator of immune responses to *Listeria* (MacMicking et al., 1995; Endres et al., 1997). In our study, NO was produced at similar levels in WT and miR-21$^{-/-}$ BMDM in response to both *L. monocytogenes* and LPS, indicating that the increased bacterial burden in miR-21-deficient macrophages is not due to a defect in production of RNS. It would be interesting to assess the role of ROS in this system, as miR-21 has been demonstrated to impact generation of these antibacterial mediators in cancer settings (Jiang et al., 2014; Guo et al., 2015).

As the increased bacterial burden in miR-21$^{-/-}$ cells was observed as early as 30 min post-infection, we questioned whether miR-21 may be influencing the initial engulfment and uptake of bacteria by macrophages. By assessing uptake of FITC-dextran by miR-21$^{-/-}$ and WT macrophages, we show that miR-21 influences the capacity for macrophages to take up fluid via pinocytosis or macropinocytosis. This was observed in both BMDMs and resident peritoneal macrophages. However, dextran uptake is not necessarily a phagocytic process (Pustylnikov et al., 2014) and so we sought to confirm using a phagocytosis-specific assay. We observed that miR-21$^{-/-}$ BMDMs took up significantly higher levels of FITC labeled *E. coli* particles relative to WT BMDMs using a commercially available phagocytosis-specific kit. Phagocytosis and in particular initial uptake, is dependent primarily on the actin cytoskeleton, and a series of cytoskeletal rearrangements triggered following receptor

activation. The most well characterized phagocytic receptors on macrophages include FcγRs and complement receptor 3 (CR3), which bind to immunolglobulin G (IgG)-opsonised particles and complement-coated particles respectively (Kerrigan and Brown, 2009). Key mediators of actin rearrangements are the RhoGTPases, which have been shown to be important for the initial formation of the phagocytic cup, which engulfs the invading pathogen (Rougerie et al., 2013). We identified several targets of miR-21 involved in phagocytosis and actin rearrangement including the RhoGTPase, RhoB, which has been reported to operate in coordination with Cdc42 (Allen and Aderem, 1995; Caron and Hall, 1998; Carballo et al., 1999; Corradin et al., 1999; Zhang et al., 2005; Quinn et al., 2009; Yang et al., 2013; Choi et al., 2015). We confirmed that RhoB is present in higher amounts in miR-21-deficient cells, and that it is induced to a higher degree in miR-21-deficient cells at the RNA level. Further work is required to fully elucidate the role of RhoB in this system.

Macrophages have been shown to express high levels of the myristoylated, alanine-rich, C kinase substrate (MARCKS), an actin cross-linking protein (Carballo et al., 1999). In particular, this increased MARCKS expression is found in areas of the cell where actin filaments associate with the plasma membrane, and its expression is associated with regulation of cell motility (Myat et al., 1997; Carballo et al., 1999). A study by Carballo et al. implicated MARCKS in the regulation of phagocytosis of zymosan, specifically, in the rate of initial uptake (Carballo et al., 1999). MARCKS has recently been shown to be a target of miR-21 in epithelial cells, where its expression influences mucin secretion (Vazquez-Boland et al., 2001; Li et al., 2009; Lampe et al., 2013). Given that macrophages also express MARCKS, we wondered whether miR-21 may target MARCKS thereby regulating initial uptake by phagocytes. Indeed, we observed increased protein levels of MARCKS in miR-21$^{-/-}$ BMDM compared to WT cells. Furthermore, we show that mRNA levels of MARCKS are induced in miR-21$^{-/-}$ BMDM following infection with *L. monocytogenes*. However, as with RhoB, further work is required to fully elucidate what role MARCKS might play in this system, particularly as it has been demonstrated that MARCKS and MacMARCKS deletion does not significantly impact phagocytosis *in vivo* or *in vitro* (Underhill et al., 1998).

Intracellular bacteria frequently allow their engulfment by macrophages so that they can shelter from components of the host immune system. Following internalization, intracellular pathogens utilize sophisticated strategies to avoid destruction by these cells, enabling them to overcome host cell defenses and replicate successfully. They block intracellular killing by inhibiting phagosome maturation, or express effector proteins which allow them to escape into the cytosol (Kaufmann and Dorhoi, 2016). Escape from the phagosome into the cytosol is an evasion strategy employed by *L. monocytogenes* to avoid immune detection. *L. monocytogenes* uses listeriolysin (Hly), a thiol-activated cholesterol-dependent cytolysin to form pores in the membrane of the phagosome allowing escape into the cytosol (Singh et al., 2008). Subsequently, *L. monocytogenes* induces actin tails through expression of an actin polymerizing protein, ActA that facilitate its propulsion through the cell cytosol toward the cell membrane, where it forms protrusions into neighboring cells allowing its internalization and facilitating cell-cell (Williams et al., 2012). As a result of these bacterial strategies, there is an even greater pressure for host measures to counteract these immune evasion mechanisms in order to clear the infection. The ability of miR-21 do reduce internalization of *L. monocytogenes* by macrophages significantly impacts the outcome of infection in mice, with miR-21$^{-/-}$ mice displaying a significantly higher bacterial burden compared to WT mice. The increased dissemination of *Listeria* to livers of mice following intraperitoneal infection is in direct agreement with our previous observation that miR-21$^{-/-}$ resident peritoneal macrophages display increased phagocytosis of particles. This observation appears to be macrophage-specific as oral gavage of WT and miR-21$^{-/-}$ revealed no differences in bacterial dissemination. Peritoneal macrophages have been demonstrated to act as a *L. monocytogenes* reservoir, enhancing the infectious capability of this bacterium (Drevets, 1999). In this study, we present a novel role for miR-21 during the host response to intracellular bacterial infection, whereby miR-21 regulates the fundamental process of phagocytosis. We demonstrate that miR-21 limits the actin modulating proteins RhoB and MARCKS, and suggest that this may important in explaining the observed limitation of *L. monocytogenes* infection by WT macrophages compared to miR-21$^{-/-}$ cells.

AUTHOR CONTRIBUTIONS

SC conceived ideas and oversaw the research programme. DJ carried out the research. SC and DJ analyzed data and wrote the manuscript. MW, ZZ, and JK performed experiments. LO funded creation of the miR21-deficient mice and provided mentorship during the course of the research.

FUNDING

This study was funded by a Starting Investigator Research Grant from Science Foundation Ireland (SFI) (grant number 11/SIRG/B2099) awarded to SC.

ACKNOWLEDGMENTS

The authors wish to acknowledge the technical assistance provided by the Comparative Medicine Unit in maintenance of animal colonies and B. Moran for assistance with flow cytometry.

SUPPLEMENTARY MATERIAL

The Supplementary Material for this article can be found online at: http://journal.frontiersin.org/article/10.3389/fcimb.2017.00201/full#supplementary-material

REFERENCES

Allen, L. H., and Aderem, A. (1995). A role for MARCKS, the alpha isozyme of protein kinase C and myosin I in zymosan phagocytosis by macrophages. *J. Exp. Med.* 182, 829–840.

Almeida, M. I., Reis, R. M., and Calin, G. A. (2011). MicroRNA history: discovery, recent applications, and next frontiers. *Mutat. Res. Fund. Mol. Mechan. Mutag.* 717, 1–8. doi: 10.1016/j.mrfmmm.2011.03.009

Baltimore, D., Boldin, M. P., O'Connell, R. M., Rao, D. S., and Taganov, K. D. (2008). MicroRNAs: new regulators of immune cell development and function. *Nat. Immunol.* 9, 839–845. doi: 10.1038/ni.f.209

Barnett, R. E., Conklin, D. J., Ryan, L., Keskey, R. C., Ramjee, V., Sepulveda, E. A., et al. (2016). Anti-inflammatory effects of miR-21 in the macrophage response to peritonitis. *J. Leukoc. Biol.* 99, 361–371. doi: 10.1189/jlb.4A1014-489R

Bartel, D. P. (2004). MicroRNAs: Genomics, biogenesis, mechanism, and function. *Cell* 116, 281–297. doi: 10.1016/S0092-8674(04)00045-5

Benoit, M., Desnues, B., and Mege, J. L. (2008). Macrophage polarization in bacterial infections. *J. Immunol.* 181, 3733–3739. doi: 10.4049/jimmunol.181.6.3733

Carballo, E., Pitterle, D. M., Stumpo, D. J., Sperling, R. T., and Blackshear, P. J. (1999). Phagocytic and macropinocytic activity in MARCKS-deficient macrophages and fibroblasts. *Am. J. Physiol.* 277(1 Pt 1), C163–C173.

Caron, E., and Hall, A. (1998). Identification of two distinct mechanisms of phagocytosis controlled by different Rho GTPases. *Science* 282, 1717–1721.

Choi, B., Kim, H. A., Suh, C. H., Byun, H. O., Jung, J. Y., and Sohn, S. (2015). The Relevance of miRNA-21 in HSV-Induced Inflammation in a Mouse Model. *Int. J. Mol. Sci.* 16, 7413–7427. doi: 10.3390/ijms16047413

Corr, S. C., and O'Neill, L. A. (2009). *Listeria monocytogenes* infection in the face of innate immunity. *Cell. Microbiol.* 11, 703–709. doi: 10.1111/j.1462-5822.2009.01294.x

Corradin, S., Mauel, J., Ransijn, A., Sturzinger, C., and Vergeres, G. (1999). Down-regulation of MARCKS-related protein (MRP) in macrophages infected with Leishmania. *J. Biol. Chem.* 274, 16782–16787.

Dalrymple, S. A., Lucian, L. A., Slattery, R., McNeil, T., Aud, D. M., Fuchino, S., et al. (1995). Interleukin-6-deficient mice are highly susceptible to *Listeria monocytogenes* infection: correlation with inefficient neutrophilia. *Infect. Immun.* 63, 2262–2268.

Das, A., Ganesh, K., Khanna, S., Sen, C. K., and Roy, S. (2014). Engulfment of Apoptotic cells by macrophages: a role of MicroRNA-21 in the resolution of wound inflammation. *J. Immunol.* 192, 1120–1129. doi: 10.4049/jimmunol.1300613

Drevets, D. A. (1999). Dissemination of *Listeria monocytogenes* by infected phagocytes. *Infect. Immun.* 67, 3512–3517.

Endres, R., Luz, A., Schulze, H., Neubauer, H., Futterer, A., Holland, S. M., et al. (1997). Listeriosis in $p47^{phox-/-}$ and $TRp55^{-/-}$ mice: protection despite absence of ROI and susceptibility despite presence of RNI. *Immunity* 7, 419–432.

Guo, Y., Li, P., Bledsoe, G., Yang, Z. R., Chao, L., and Chao, J. (2015). Kallistatin inhibits TGF-beta-induced endothelial-mesenchymal transition by differential regulation of microRNA-21 and eNOS expression. *Exp. Cell Res.* 337, 103–110. doi: 10.1016/j.yexcr.2015.06.021

He, L., and Hannon, G. J. (2004). MicroRNAs: small RNAs with a big role in gene regulation. *Nat. Rev. Genet.* 5, 522–531. doi: 10.1038/nrg1415

Janeway, C. A. Jr., and Medzhitov, R. (2002). Innate immune recognition. *Annu. Rev. Immunol.* 20, 197–216. doi: 10.1146/annurev.immunol.20.083001.084359

Jiang, Y., Chen, X., Tian, W., Yin, X., Wang, J., and Yang, H. (2014). The role of TGF-beta1-miR-21-ROS pathway in bystander responses induced by irradiated non-small-cell lung cancer cells. *Br. J. Cancer* 111, 772–780. doi: 10.1038/bjc.2014.368

Kaufmann, S. H., and Dorhoi, A. (2016). Molecular determinants in phagocyte-bacteria interactions. *Immunity* 44, 476–491. doi: 10.1016/j.immuni.2016.02.014

Kerrigan, A. M., and Brown, G. D. (2009). C-type lectins and phagocytosis. *Immunobiology* 214, 562–575. doi: 10.1016/j.imbio.2008.11.003

Krichevsky, A. M., and Gabriely, G. (2009). miR-21: a small multi-faceted RNA. *J. Cell. Mol. Med.* 13, 39–53. doi: 10.1111/j.1582-4934.2008.00556.x

Lampe, W. R., Fang, S., Yin, Q., Crews, A. L., Park, J., and Adler. K. B. (2013). Mir-21 regulation of MARCKS protein and mucin secretion in airway epithelial cells. *Open J. Respir. Dis.* 3, 89–96. doi: 10.4236/ojrd.2013.32014

Li, T., Li, D., Sha, J., Sun, P., and Huang, Y. (2009). MicroRNA-21 directly targets MARCKS and promotes apoptosis resistance and invasion in prostate cancer cells. *Biochem. Biophys. Res. Commun.* 383, 280–285. doi: 10.1016/j.bbrc.2009.03.077

Liu, P. T., Wheelwright, M., Teles, R., Komisopoulou, E., Edfeldt, K., Ferguson, B., et al. (2012). MicroRNA-21 targets the vitamin D-dependent antimicrobial pathway in leprosy. *Nat. Med.* 18, 267–273. doi: 10.1038/nm.2584

Lu, T. X., Hartner, J., Lim, E. J., Fabry, V., Mingler, M. K., Cole, E. T., et al. (2011). MicroRNA-21 limits *in vivo* immune response-mediated activation of the IL-12/IFN-gamma pathway, Th1 polarization, and the severity of delayed-type hypersensitivity. *J. Immunol.* 187, 3362–3373. doi: 10.4049/jimmunol.1101235

Lu, T. X., Munitz, A., and Rothenberg, M. E. (2009). MicroRNA-21 is up-regulated in allergic airway inflammation and regulates IL-12p35 expression. *J. Immunol.* 182, 4994–5002. doi: 10.4049/jimmunol.0803560

MacMicking, J. D., Nathan, C., Hom, G., Chartrain, N., Fletcher, D. S., Trumbauer, M., et al. (1995). Altered responses to bacterial infection and endotoxic shock in mice lacking inducible nitric oxide synthase. *Cell* 81, 641–650.

Myat, M. M., Anderson, S., Allen, L. A., and Aderem, A. (1997). MARCKS regulates membrane ruffling and cell spreading. *Curr. Biol.* 7, 611–614.

O'Neill, L. A., Golenbock, D., and Bowie, A. G. (2013). The history of Toll-like receptors - redefining innate immunity. *Nat. Rev. Immunol.* 13, 453–460. doi: 10.1038/nri3446

O'Neill, L. A., Sheedy, F. J., and McCoy, C. E. (2011). MicroRNAs: the fine-tuners of Toll-like receptor signalling. *Nat. Rev. Immunol.* 11, 163–175. doi: 10.1038/nri2957

Pustylnikov, S., Sagar, D., Jain, P., and Khan, Z. K. (2014). Targeting the C-type lectins-mediated host-pathogen interactions with dextran. *J. Pharm. Pharmaceut. Sci.* 17, 371–392. doi: 10.18433/J3N590

Quinn, K., Brindley, M. A., Weller, M. L., Kaludov, N., Kondratowicz, A., Hunt, C. L., et al. (2009). Rho GTPases modulate entry of Ebola virus and vesicular stomatitis virus pseudotyped vectors. *J. Virol.* 83, 10176–10186. doi: 10.1128/jvi.00422-09

Quinn, S. R., and O'Neill, L. A. (2011). A trio of microRNAs that control Toll-like receptor signalling. *Int. Immunol.* 23, 421–425. doi: 10.1093/intimm/dxr034

Ramaswamy, V., Cresence, V. M., Rejitha, J. S., Lekshmi, M. U., Dharsana, K. S., Prasad, S. P., et al. (2007). *Listeria*–review of epidemiology and pathogenesis. *J. Microbiol. Immunol. Infect.* 40, 4–13. Available online at: https://pdfs.semanticscholar.org/bb85/c7d8ed1545ed58a7b885af52e8757f87b741.pdf

Rougerie, P., Miskolci, V., and Cox, D. (2013). Generation of membrane structures during phagocytosis and chemotaxis of macrophages: role and regulation of the actin cytoskeleton. *Immunol. Rev.* 256, 222–239. doi: 10.1111/imr.12118

Sheedy, F. J. (2015). Turning 21: induction of miR-21 as a key swith in the inflammatory response. *Front. Immunol.* 6:19. doi: 10.3389/fimmu.2015.00019

Sheedy, F. J., Palsson-McDermott, E., Hennessy, E. J., Martin, C., O'Leary, J. J., Ruan, Q., et al. (2010). Negative regulation of TLR4 via targeting of the proinflammatory tumor suppressor PDCD4 by the microRNA miR-21. *Nat. Immunol.* 11, 141–147. doi: 10.1038/ni.1828

Shiloh, M. U., MacMicking, J. D., Nicholson, S., Brause, J. E., Potter, S., Marino, M., et al. (1999). Phenotype of mice and macrophages deficient in both phagocyte oxidase and inducible nitric oxide synthase. *Immunity* 10, 29–38.

Singh, R., Jamieson, A., and Cresswell, P. (2008). GILT is a critical host factor for *Listeria monocytogenes* infection. *Nature* 455, 1244–1247. doi: 10.1038/nature07344

Takeuchi, O., and Akira, S. (2010). Pattern recognition receptors and inflammation. *Cell* 140, 805–820. doi: 10.1016/j.cell.2010.01.022

Underhill, D. M., Chen, J., Allen, L. A., and Aderem, A. (1998). MacMARCKS is not essential for phagocytosis in macrophages. *J. Biol. Chem.* 273, 33619–33623.

Vazquez-Boland, J. A., Kuhn, M., Berche, P., Chakraborty, T., Dominguez-Bernal, G., Goebel, W., et al. (2001). Listeria pathogenesis and molecular virulence determinants. *Clin. Microbiol. Rev.* 14, 584–640. doi: 10.1128/Cmr0.14.3.584-640.2001

Wang, Z., Brandt, S., Medeiros, A., Wang, S., Wu, H., Dent, A., et al. (2015). MicroRNA 21 is a homeostatic regulator of macrophage polarization and

prevents prostaglandin E2-mediated M2 generation. *PLoS ONE* 10:e0115855. doi: 10.1371/journal.pone.0115855

Weiss, G., and Schaible, U. E. (2015). Macrophage defense mechanisms against intracellular bacteria. *Immunol. Rev.* 264, 182–203. doi: 10.1111/imr.12266

Williams, M. A., Schmidt, R. L., and Lenz, L. L. (2012). Early events regulating immunity and pathogenesis during *Listeria monocytogenes* infection. *Trends Immunol.* 33, 488–495. doi: 10.1016/j.it.2012.04.007

Yang, Y., Ma, Y., Shi, C., Chen, H., Zhang, H., Chen, N., et al. (2013). Overexpression of miR-21 in patients with ulcerative colitis impairs intestinal epithelial barrier function through targeting the Rho GTPase RhoB. *Biochem. Biophys. Res. Commun.* 434, 746–752. doi: 10.1016/j.bbrc.2013.03.122

Zhang, J., Zhu, J., Bu, X., Cushion, M., Kinane, T. B., Avraham, H., et al. (2005). Cdc42 and RhoB activation are required for mannose receptor-mediated phagocytosis by human alveolar macrophages. *Mol. Biol. Cell* 16, 824–834. doi: 10.1091/mbc.E04-06-0463

Conflict of Interest Statement: The authors declare that the research was conducted in the absence of any commercial or financial relationships that could be construed as a potential conflict of interest.

Chapter 18

Toll-Like Receptor Signalling and the Control of Intestinal Barrier Function

Daniel G.W. Johnston and Sinéad C. Corr

Abstract

Epithelial barrier function and innate immunity are fundamental to the pathogenesis of inflammatory and infectious disease. Along with plasma membranes, epithelial cells are the primary cellular determinant of epithelial barrier function. The mechanism by which polarized epithelia form a permeability barrier is of fundamental importance to the prevention of many infectious and inflammatory diseases. Moreover, epithelial cells express Toll-like receptors (TLRs) which upon recognition of conserved microbial factors such as lipopolysaccharide (LPS) induce epithelial responses including epithelial cell proliferation, secretion of secretory IgA into the lumen and production mucins and antimicrobial peptides, thereby promoting intestinal barrier function. Understanding gut barrier integrity and regulation of permeability is crucial to increase our understanding of the pathogenesis of intestinal disease. A variety of tests have been developed to assess this barrier, including assessing intestinal epithelial cell proliferation or death, intestinal tight junction status and the consequence of intestinal barrier integrity loss such as increased intestinal permeability and susceptibility to bacterial infection. Using a mouse model, this chapter describes some of the methods to assess the functional integrity of this epithelial barrier and the part played by a TLR signalling pathway.

Key words Defence, Permeability, Leakiness, Epithelial, Barrier, Tight junction, Infection, TLR, MAL

1 Introduction

Intestinal epithelial barrier dysfunction and leaky gut are linked to the development of infectious and inflammatory disease [1, 2]. In order to gain access to the host and cause disease, bacterial pathogens must first breach the epithelial barrier, and as such, this is the first line of defence against entry of most human pathogens. Intestinal epithelial cells express pattern recognition receptors (PRRs) including TLRs and NOD-like receptors (NLRs) which have an important role in the regulation of intestinal homeostasis and barrier integrity [3]. These PRRs recognize microbial moieties and promote intestinal homeostasis through induction of cytokines including IL-10, antimicrobial peptides including

Claire E. McCoy (ed.), *Toll-Like Receptors: Practice and Methods*, Methods in Molecular Biology, vol. 1390,
DOI 10.1007/978-1-4939-3335-8_18,

β-defensins, epidermal growth factor receptor (EGFR) ligands including amphiregulin and epiregulin which promote cell proliferation and tissue repair, and anti-apoptotic factors which promote epithelial restitution [3].

TLR signalling also fortifies a crucial component of the epithelial barrier, intercellular tight junctions (TJ) or zonula occludens [4]. TJ are important structures which regulate intestinal barrier permeability or leakiness. TJ join epithelial and endothelial cells, and thereby regulate the permeability of the intestinal epithelium [2] (Fig. 1). They are dynamic structures which are regulated by the crosstalk of many signalling pathways, allowing absorption of nutrients but limiting entry of potentially harmful pathogens, toxins and antigens [3]. TJ are multiprotein complexes composed of the transmembrane proteins occludin and claudin, and the intracellular protein zonula occudens (ZO) [5]. TJ and barrier function are regulated by multiple kinases which phosphorylate TJ proteins to determine their expression and localization and ultimately TJ formation [2, 6]. Disruption of TJ structure and increased permeability as a result of specific mutation or aberrant regulatory signals can be the cause of disease due to uncontrolled entry of bacteria or antigens. Indeed, dysregulation of epithelial barrier function

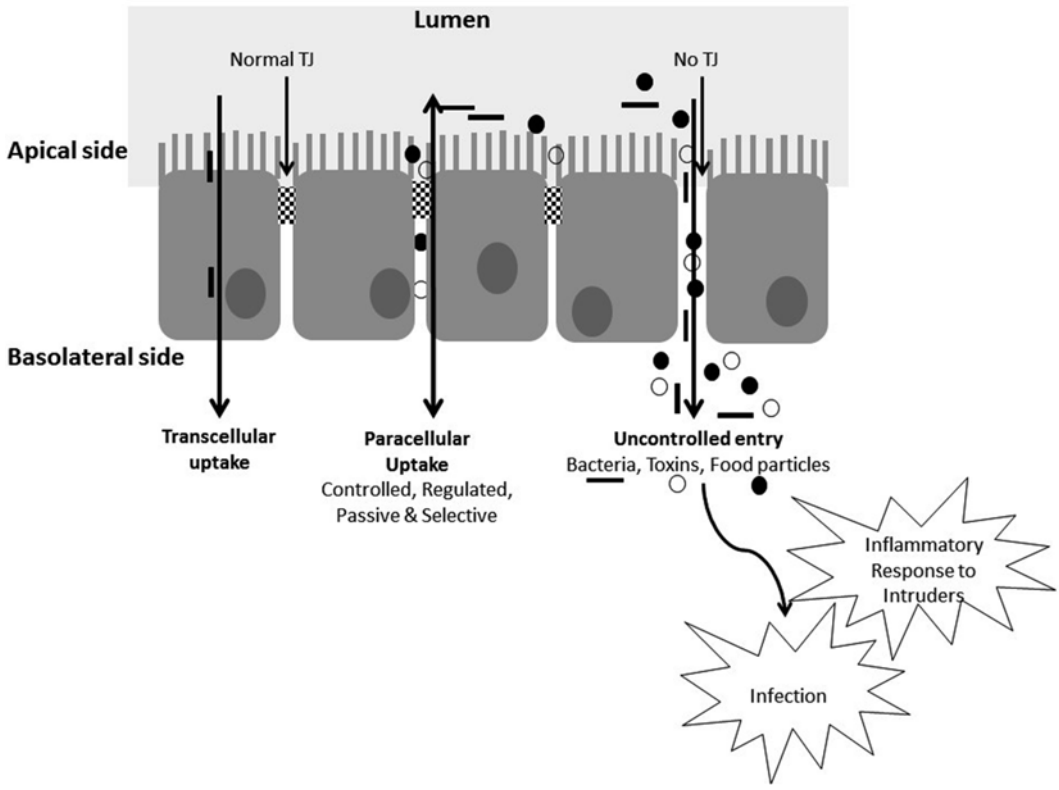

Fig. 1 Epithelial tight junctions regulate the paracellular pathway and contribute to intestinal permeability

including altered TJ formation and "leaky gut" have been associated with the pathogenesis of a variety of infectious, inflammatory and autoimmune diseases including IBD, infectious enterocolitis, rheumatoid arthritis, diabetic retinopathy and asthma [2, 3].

There is accumulating evidence of the role played by TLR signalling pathways in the regulation of intestinal epithelial barrier function. Intestinal barrier function and the role of TLR signalling can be assessed both in vitro using models of intestinal epithelium such as the Caco2 adenocarcinoma cell line or in vivo in mice in which specific components of TLR signalling pathways have been knocked out or silenced [5, 7]. Using these models, $TLR4^{-/-}$ and $MyD88^{-/-}$ mice display reduced expression of the EGF-R ligands and reduced epithelial cell proliferation. MyD88 also induces the antibacterial peptides RegIIIγ and α-defensins thereby promoting defence against infection. TLR2 has been shown to regulate TJ formation and promote barrier integrity, through induction of anti-apoptotic factors which promote epithelial cell survival and regulate ZO-1 localization. Furthermore, the TLR2/TLR4 adaptor MAL plays a critical role in maintaining barrier integrity during infection or assault, by regulating TJ formation via PKC [5].

In mice, intestinal permeability or leakiness can be determined by analysing the mucosal-blood flux of a tracer molecule such as FITC-dextran which is administered orally [5, 8]. Increased mucosa-blood flux in a knockout mouse or across an epithelial monolayer like Caco2 cultured on a transwell system suggests increased leakiness and impaired barrier function. Electrophysical measurements can also be used to assess permeability across intestinal epithelium segments or monolayers of Caco2 [5]. Reduced transepithelial electrical resistance (TEER) suggests impaired barrier function and increased permeability. Measurement of epithelial permeability is essentially a measure of how intact the interepithelial TJ are and passage through the paracellular pathway. TJ formation and structure can be investigated by analysing expression of TJ proteins by Western blot and RT-PCR, while localization can be determined by immunohistochemistry [5, 8, 9]. Expression of antimicrobial factors and EGFR ligands can also be measured in this way. As TJ formation and indeed barrier integrity can also be impaired due to loss of epithelial cells themselves, assays can be used to measure both epithelial cell proliferation and apoptosis [10]. Finally, the functional importance of an intact epithelial barrier can be shown by performing an oral infection model and determining bacterial dissemination from the intestinal epithelium, across the mucosae and to distant organs [5]. Generation of chimeric mice in which a TLR signalling component such as MAL has been knocked out specifically in epithelial cells can be used to confirm the importance of this TLR component in regulation of epithelial barrier integrity [5, 10, 11]. In this model, bone marrow from a TLR knockout donor mouse is reconstituted into a WT

recipient mouse, so that hematopoietic cells in the WT mouse now lack the signalling component being investigated. In this way, you can test the role of the TLR component in epithelial and immune cells. Using the TLR adaptor MAL as an example, this chapter describes some of these assays and their use in assessment of intestinal barrier function, specifically focusing on regulation of intestinal permeability by epithelial TJ.

2 Materials

2.1 Infection Model

1. *S.* Typhimurium UK-1.
2. Luria Bertani (LB) broth (Merck).
3. 37 °C Incubator.
4. Gavage needle.
5. 1 ml syringe.
6. Sterile phosphate buffered saline (PBS) solution.
7. Dissection kit.
8. Stomacher bags (80 m; Seward, UK).
9. Eppendorf tubes containing 900 μl sterile PBS.
10. LB agar (Merck).
11. Mice.

2.2 Intestinal Permeability

1. FITC-dextran, molecular mass 4 kDa (Sigma).
2. Gavage needle.
3. 1 ml syringe.
4. Sterile phosphate buffered saline (PBS) solution.
5. Acid-citrate dextrose.
6. Black 96-well microplate (Nunc).
7. Coloured Eppendorf tubes or similar.

2.3 Electrophysiological Measurements

1. Ussing chambers: 0.6 cm^2 aperture.
2. Superfusate (KBR Ringer's solution): 140 mM Na, 5.2 mM K, 1.2 mM Ca_2, 0.8 mM Mg_2, 120 mM Cl, 25 mM HCO_3, 2.4 mM K_2HPO_4, 0.4 mM KH_2PO_4, 10 mM glucose.
3. Voltage–current clamp (VCC) (Physiological Instruments, San Diego, CA, USA)
4. Intestinal preparation: Mouse distal colon section stripped of seromuscular layer.
5. Amiloride.
6. Secretagogues: carbachol (CCh; 100 μM basolaterally) and forskolin (FSK; 10 μM apically).

2.4 Immunohistochemistry (IHC)

1. Ileum tissue sections obtained from experimental mice: removed, placed in histology cassettes and stored in 4 % paraformaldehyde prior to dehydration.
2. Dehydration kit: Graded ethanol concentrations.
3. Paraffin wax (Eli Lilly) plus moulds (~6 mm).
4. Polysine® Slides (ThermoFisher Scientific).
5. Isocitrate buffer.
6. Blocking buffer: 1 % Fc blockers (Miltenyi Biotec) and 10 % donkey serum (Jackson ImmunoResearch Laboratories).
7. Primary Antibodies: polyclonal rabbit anti-mouse ZO-1, occludin and claudin-3 (Life Technologies). Store at 4 °C.
8. Secondary antibody: Alexa Flour 555 donkey anti-rabbit (Invitrogen).
9. Nuclear stain: 40-6-diamidino-2-phenylindole nucleic acid stain (Invitrogen).
10. DeltaVision PersonalDV Deconvolution microscopy (Applied Precision, Issaquah, WA)
11. Image J software (National Institute of Mental Health, Bethesda, MD).

2.5 RT-PCR

1. RNA isolation: Qiagen RNeasy Mini Kit (Qiagen).
2. NanoDrop spectrophotometer (ThermoFisherScientific).
3. Reverse Transcription reagents (Applied Biosystems): Multiscribe™ reverse transcriptase (RT), RNase inhibitor, dNTP (10 mM solution of 2.5 mM each of dATP, dCTP, dGTP, and dTTP), 10× RT buffer, random primers. Store all reagents at –20 °C.
4. Probes for real-time PCR (Applied Biosystems): various targets, FAM labelled; 18S endogenous control labelled with VIC to allow multiplexing. Store at –20 °C.
5. Endogenous Controls: 18S rRNA (Applied Biosystems). Store at –20 °C.
6. qPCR Mastermix: 2× TaqMan Universal PCR Mastermix (Applied Biosystems). Store at –20 °C.
7. ABI Prism 7700 Sequence Detection system (Applied Biosystems).

2.6 Western Blotting

1. Radioimmunoprecipitation assay buffer (RIPA buffer) for protein extraction: 50 mM Tris, pH 8, 150 mM NaCl, 0.1 % (w/v) SDS, 0.5 % (w/v) sodium deoxycholate and 1 % (v/v) NP-40 dissolved in dH_2O, supplemented with 5 mM EDTA and proteinase inhibitors: aprotinin, phenylmethansulfonyl and leupeptin (1:1000 dilution).

2. Micro-BCA protein quantification kit (Thermo Fisher Scientific).
3. Sample Buffer for protein denaturation: 0.125 M Tris–HCl, pH 6.8, 10 % SDS 0.02 % Bromophenol blue, 10 % glycerol, dH_2O. Add 5 % DTT prior to use as a reducing agent. Store sample buffer and DTT at –20 °C.
4. 12 % resolving gel (10 ml/gel): 3.25 ml H_2O, 4 ml 30 % Protogel, 2.55 ml 1.5 M Tris–HCl, pH 8.8, 100 µl 10 % SDS, 100 µl 10 % APS, 4 µl TEMED.
5. 5 % Stacking gel (6 ml/gel): 4.1 ml H_2O, 1 ml 30 % Protogel, 0.75 ml 1 M Tris–HCl, pH 6.8, 60 µl 10 % SDS, 60 µl 10 % APS, 6 µl TEMED (*see* **Note 1**).
6. Water-saturated Butanol: 50 % Butanol, 50 % dH_2O (*see* **Note 2**).
7. Running Buffer: 0.3 % Tris (w/v), 1.44 % Glycine (w/v), 0.1 % SDS (w/v), dH_2O (*see* **Note 3**).
8. Tris-Buffered Saline (TBS): 0.303 % Tris (w/v), 0.801 % NaCl (w/v), 0.037 % KCl, 0.0103 % $CaCL_2$ (w/v), 0.0072 % NaH_2PO_4 (w/v), dH_2O.
9. Tris-Buffered Saline Tween (TBS-Tween): 0.303 % Tris (w/v), 0.801 % NaCl (w/v), 0.037 % KCl, 0.0103 % $CaCL_2$ (w/v), 0.0072 % NaH_2PO_4 (w/v), dH_2O, 0.05 % Tween.
10. Transfer Buffer 10×: 0.303 % Tris (w/v), 1.5014 % Glycine (w/v), dH_2O. Make up to 1× with 20 % methanol and 70 % water for use in Western blotting.
11. Blocking reagent: 5 % Dried Milk in TBS-Tween (w/v), store at 4 °C for up to 4 days.
12. Primary Antibodies: Phospho-PKC (pan) and phospho-PKC antibodies from sampler kit (Cell Signalling Technologies), PKCz (H-1) (Santa Cruz Biotechnologies), anti-hemagglutinin (Covance, Princeton, NJ). Store at 4 °C.
13. Negative Control Antibodies: IgG control antibody, store at 4 °C.
14. Secondary Antibodies: Anti-rabbit heavy+light chain and anti-mouse heavy+light chain (Jackson ImmunoResearch).
15. Developing reagents: 20× LumoFlur ECL reagents (Cell Signalling Technologies) and acetate film (Fuji Film). Store at 4 °C.

2.7 Quantification of Epithelial Cell Apoptosis

1. Rabbit polyclonal anti-Ki67 antibody (Abcam).
2. 10 % Normal goat serum (DakoCytomation).
3. Mayer's haematoxylin (Sigma-Aldrich).
4. In Situ Cell Death Detection kit (Roche).
5. EnVisionTM Detection System (DakoCytomation, UK).
6. Leica® microscope (Leica® DM 3000 LED) equipped with Leica® DFC495 camera (Leica® Microsystem, Germany).

2.8 Bone Marrow Chimeras

1. Mice: CD45.1$^+$ C57Bl6, CD45.2$^+$*Mal*$^{-/-}$ (or mice lacking TLR component of interest).
2. Radiation Source.
3. Tin foil.
4. 23G needles and 10 ml syringes.
5. Sterile dissection kit.
6. Cell culture media: DMEM with 10 % FCS and penicillin/streptomycin, store at 4 °C.
7. Sterile phosphate buffered saline (PBS) solution.
8. Tuerk solution.
9. 240 V heat lamp and mouse restrainer for i.v. injection.
10. 25 G needles and 1 ml syringes.
11. Flow cytometry markers: CD45.1, CD45.2 (A20, 104; BD Biosciences).

3 Methods

3.1 Infection Model

1. S. Typhimurium culture: Use a sterile pipette tip to take a single culture from an existing plate. Place in 10 ml LB broth in a 15 ml tube and incubate overnight in a 37 °C shaker.
2. The next day, spin down the culture at $3000 \times g$ for 10 min. Resuspend with PBS and centrifuge again before finally resuspending in PBS to give a concentration of 5×10^8 CFU/ml.
3. Using a gavage needle, administer 100 μl (approximately $5 \times 10^{7)}$) of the bacterial suspension per mouse orally. Serially dilute the remainder of the bacterial suspension in sterile PBS from 10^{-1} to 10^{-7} and spread 100 μl with a spot plate technique onto LB plates. Place in a bacterial incubator overnight at 37 °C with % CO_2. Perform bacterial counts and retrospectively enumerate bacteria delivered.
4. Every other day, collect faecal samples from inoculated mice and homogenize in 1 ml sterile PBS. Serially dilute the homogenate from 10^{-1} to 10^{-7} in sterile PBS and spread with an altered spot plate technique: divide each plate into four quadrants and label each quadrant with a dilution (*see* **Note 1**). Add 20 μl to each quadrant and spread by spot plate technique. Place in a bacterial incubator overnight at 37 °C with % CO_2. The next day, perform bacterial counts.
5. At the end of the experiment, cull mice and harvest organs as follows: Remove spleens and livers aseptically, weigh and manually crush in 2 ml of PBS in a stomacher bag by rolling the bag with a 10 ml pipette (*see* **Note 2**). Serially dilute and plate onto LB agar before incubating overnight at 37 °C to enumerate bacterial dissemination into these organs.

6. Additionally, aseptically remove the large intestine and flush with sterile PBS using a 10 cm dish filled with PBS and a 10 ml syringe with a 23G needle. Separate into 1 cm samples for various analyses:
   (a) RNA isolation: place in RNA later and snap freeze at –80 °C.
   (b) Protein Isolation: snap frozen at –80 °C.
   (c) Immunohistochemistry: Place in 4 % paraformaldehyde (PFA) for subsequent dehydration and paraffinization.
   (d) Electrophysiological Measurements: snap freeze at –80 °C.

3.2 Intestinal Permeability

1. Prepare fluorescein isothiocyanate conjugated dextran (FITC-dextran) for gavage, keeping away from light using coloured Eppendorf tubes for aliquots. Make up in sterile PBS at 12 mg per mouse in 100–200 μl per mouse.
2. Administer FITC-dextran to the mice in the various experimental groups by gavage. Mice can be either uninfected or orally infected with a pathogen of choice prior to gavage.
3. Sacrifice the mice 4 h later by CO_2 asphyxiation and perform a terminal bleed. Immediately after the blood is collected in coloured Eppendorf tubes, add acid-citrate dextrose and maintain in the dark throughout the following steps.
4. Centrifuge the samples at 4 °C for 12 min at $1000 \times g$. Remove the serum using a micropipette and add to a black 96-well microplate. In addition, prepare a serial dilution of the fluorescein and add to the 96-well microplate to be used as a standard curve.
5. Assess the concentration of fluorescein in the blood samples by spectrophotofluorometry with an excitation wavelength of 485 nm and an emission wavelength of 535 nm.

3.3 Electrophysiological Measurements

1. Intestinal epithelial layer preparation: after euthanasia, dissect out the distal colon with careful sharp dissection. Then remove the seromuscular layer by scraping that side off a pre-cooled glass slide.
2. Equilibrate the Ussing chamber to ensure there is no electrical bias. Add superfusate solution to both sides of the chamber and allowing it to come to 37 °C and "zeroing" by applying an offset voltage and compensating the resistance. This is achieved using the built-in "fluid resistance compensation" on the VCC.
3. After zeroing is completed the epithelial preparation can be fixed to the pins of the Ussing chamber, which should be filled with fresh superfusate.
4. Transepithlial resistance (TER) is then measured every 5 min for 1 h and the average is taken and used to calculate basal TER and expressed in Ω/cm^2.

5. To examine Cl– secretion, add amiloride (10 μM) to the basolateral side. The secretagogues carbachol (CCh) (100 μM basolaterally) and forskolin (FSK) (10 μM apically) are then used to stimulate Ca^{2+} and cAMP-mediated Cl– secretion, respectively. Normalize results and express as ΔI_{sc} (μA/cm^2).

3.4 Immunohistochemistry (IHC)

1. Paraffin embedding: Take the ileal section from its histology cassette. Pour a small drop of wax into the plastic mould and insert the section vertically so that is resembles a column. Fill the rest of the mould with paraffin and place the labelled base of the original cassette on top. Allow to cool on a cold plate until set (~4 h).
2. Sectioning: Transfer the embedded ileum sections to the cryostat and allow 5 min equilibration time to reach cryostat temperature (–20 °C). Cut 5 μm sections and mount sections on Polysine slides. Allow sections air dry for ~30 min at room temperature.
3. Deparaffinate sections by two washes of xylene, 5 min per wash. Rehydrate the sections via exposure to a decreasing ethanol gradient: Hydrate in 2 changes of 100 % ethanol for 3 min each, 95 % and 80 % ethanol for 1 min each. Rinse in PBS.
4. Antigen retrieval: Heat a water bath containing appropriate staining dishes containing isocitrate buffer to 95 °C. Place the slides in the staining dishes for 30 min. Rinse with PBS twice with 2 min per rinse.
5. Blocking: Incubate slides in 1 % Fc blockers and 10 % donkey serum for 30 min. Wash with PBS (*see* **Note 3**).
6. Incubate with primary antibody solution (polyclonal rabbit anti-mouse ZO-1, occludin, and claudin-3) overnight at 4 °C. Wash with PBS.
7. Incubate in secondary antibody for 1 h at room temperature. Wash with PBS.
8. Counterstain with 40-6-diamidino-2-phenylindole nucleic acid stain to visualize the nuclei.
9. Collect images using a DeltaVision PersonalDV Deconvolution microscopy. Image the 5-mm tissue slices using Z-stack with 0.2 mm per section (25 sections total), using 2_2 binning during image acquisition. Image J software is used to calculate the sum of fluorescence intensity from the stack and MFI from the epithelial regions of the tissue.

3.5 RT-PCR

1. Isolate total RNA from tissue samples according to the RNeasy Mini Kit manufacturer's instructions. Assess the RNA concentration using a NanoDrop spectrophotometer and equalize to desired concentration.

2. Reverse Transcription (RT): Total RNA is reverse transcribed into cDNA with random primers to transcribe all RNA (mRNA, rRNA, tRNA). Prepare RT reaction mix as follows per 20 µl point: 2 µl 10× buffer, 1 µl dNTP, 1 µl Reverse Transcriptase, 2 µl random primers, 0.25 µl RNase inhibitor, 1.75 µl H_2O. Pipette 8 µl of this RT reaction mix into each appropriate labelled PCR reaction tube followed by 12 µl of RNA at 100 ng/ml. Cap the tubes and tap or flick gently to mix. Centrifuge the tubes briefly to force all the solution to the bottom of the tube. Transfer tubes to the thermal cycler and run the RT reaction as follows: 10 min at 25 °C, 30 min at 37 °C, 5 min at 85 °C, hold at 4 °C.
3. TaqMan real-time PCR: Prepare individual reaction mixture for each mRNA target, including appropriate endogenous controls, as follows per 10 µl reaction (each reaction should be performed in duplicate): 5 µl TaqFast, 2.5 µl H_2O, 0.5 µl 20× primer/probe (*see* **Note 4**). Vortex all target reaction mixtures and pipette 8 µl per reaction well of a MicroAmp 96-well reaction plate. Add 2 µl cDNA to the appropriate reaction mix. Cover and seal the reaction plate before centrifuging briefly to mix solution and remove air bubbles. Transfer the reaction plate to the ABI Prism 7700 Sequence Detection system (*see* **Note 5**).
4. Use the endogenous control to normalize the results, according to the comparative threshold cycle (*Ct*) method for relative quantification as described by the manufacturer. Calculate the ΔCT between the target and control values and calculate the relative expression levels with the $\Delta\Delta CT$ method.

3.6 Western Blotting

1. Take colon sections for protein extraction as mentioned in Subheading 3.1, **step 6**. Add 400 µl RIPA buffer and leave on ice for 10 min before homogenizing using either a benchtop rotor-stator homogenizer or the Qiagen TissueLyserII system. Centrifuge the resulting homogenate using a benchtop microcentrifuge at 14,000 rpm for 10 min at 4 °C.
2. Take 50 µl of the supernatant and use the Micro BCA kit to quantify the protein present according to the manufacturer's instructions. It is likely that you will need to dilute your supernatants between 1:25 and 1:100 to get them into the range of the kit standard.
3. Dilute a portion of your supernatants in PBS to allow you load a total of 20 µg protein/well in 25–30 µl. This dilution must take into account a further 1:2 dilution in sample buffer. Once the sample buffer is added, the sample is boiled for 5–10 min. Samples can be stored at −20 °C or used immediately with prepared gels as outlined in **steps 4**–**5**. Remaining supernatant can be stored at −20 °C.

4. Make up 12 % resolving gel and pour between plates sealed with plastic gasket (all thoroughly cleaned with 70 % EthOH beforehand) up to ~1 cm below base of the comb (*see* **Note 6**). Add water-saturated butanol ~1 cm over gel edge to give straight top. Allow set for 20 min.
5. Tilt gel to drain off butanol (*see* **Note 7**). Make up 5 % stacking gel (keeping components on ice throughout) and pour between plates before adding comb to generate wells. Leave to set for 15–20 min.
6. Gently remove comb and rinse wells twice with running buffer (*see* **Note 8**). Remove seal gaskets from plates. Place gels into running tank, avoiding bubbles, with wells facing in towards each other. Add running buffer to cover wire. Load sample with gel-loading tips (25–30 μl/well), empty wells should be loaded with sample buffer.
7. Run at 25 mA/gel, unlimited voltage, for 50–60 min. Ensure gel is not run for too long so that proteins do not run into dye front.
8. Remove plates and free gel by bending plate pairs apart with a spatula. Cut off stacking gel, wells, edges and top right hand corner of the gel with a razor blade or scalpel.
9. Soak gels in transfer buffer three times for 5 min after a brief wash in TBS. Prepare transfer cassettes as follows: fill open container with transfer buffer and lay back of cassettes down into the container. Add soaked sponge, then two soaked filter papers followed by the gel. Cut the filter papers to the shape of the gel, including the missing top right corner. On top of this add a methanol activated PVDF membrane very carefully before adding two more soaked filter papers. Cut the filter papers to fit the gel. Replace in cassette in original orientation, roll over with roller or 50 ml tube to remove bubbles and add the second sponge on top. Close the cassette. Avoid air bubbles throughout.
10. Add cassettes to transfer tank in correct orientation as dictated by the manufacturer. Fill chamber to top with transfer buffer after adding cooling pack to rear (Ice or Polyethylene Glycol Pack). Run transfer for 1.5 h at 200 mA, 2 h at 150 mA or overnight at 30 mA.
11. Wash membrane three times for 5 min in TBS-Tween before blocking in 5 % marvel for a minimum of 1 h (*see* **Note 9**).
12. Wash the membranes three times for 5 min in TBS-Tween. Place the membranes into 50 ml tubes containing 5 ml of antibody solution containing relevant antibodies (1:1000 dilution in 5 % Marvel). Place the tubes on a roller overnight at 4 °C.
13. The next day, wash the membranes three times for 5 min in TBS-Tween before placing them into tubes containing 5 ml of

secondary antibody solution (1:1000 in 5 % Marvel). Place the tubes on the roller for 1 h at room temperature.

14. Wash the membranes in TBS-Tween for a total of 25 min, once for 15 min and twice for 5 min.
15. Prepare ECL solution for developing blots (25 μl of reagent 1, 25 μl of reagent 2 and 450 ml dH_2O per membrane). Cut several acetate sheets on the top right corner to maintain orientation during analysis. Develop the membranes in a darkroom using ECL, acetate film, the ECL processor and a film cassette (*see* **Note 10**).

3.7 Quantification of Epithelial Cell Apoptosis

1. Immunohistochemistry: prepare paraffin-embedded sections as detailed in Subheading 3.4.
2. Deparaffinate sections by two washes of xylene, 5 min per wash. Rehydrate the sections via exposure to a decreasing ethanol gradient: Hydrate in 2 changes of 100 % ethanol for 3 min each, 95 % and 80 % ethanol for 1 min each. Rinse in PBS.
3. Block for non-specific background staining using 10 % normal goat serum. Cover the section and incubate for minimum 1 h.
4. Wash briefly in water before incubating overnight in anti-Ki67 antibody (1:1000). Following this incubation counterstain using Mayer's haematoxylin.
5. Visualize using EnVisionTM Detection System (DakoCytomation, UK).
6. Epithelial cell apoptosis is analysed by TUNEL assay using a commercial kit (In Situ Cell Death Detection kit, Roche) according to the manufacturer. Sections are imaged by a Leica® microscope (Leica® DM 3000 LED) equipped with Leica® DFC495 camera (Leica® Microsystem, Germany).

3.8 Bone Marrow Chimeras

1. Separate the wild-type (WT) and *Mal*$^{-/-}$ recipient mice (or mice lacking TLR component of interest) into the appropriate experimental groups for bone marrow transfer. Irradiate the mice with a sublethal dose of 9 Gy in two doses, 3 h apart. Allow 24 h to elapse before reconstitution with bone marrow suspension.
2. Extract bone marrow from donor mice legs as follows: Warm cell culture media and PBS. Lay out a sheet of tin foil in a biosafety cabinet. Isolate the femur and tibia bones and cut both ends. Flush the bone marrow into a 50 ml tube containing 5 ml DMEM by placing a 10 ml syringe containing cell culture media with 23G needle into the larger orifice and depressing. Pool bone marrow from all donor mice of the same strain and count using Tuerk solution. Resuspend cells in sterile PBS for reconstitution at 5×10^7 cells/ml.

3. Reconstitute the bone marrow of the recipient mice with appropriate donor cells depending on their experimental group (WT > WT, *Mal*$^{-/-}$ > WT, WT > *Mal*$^{-/-}$ and *Mal*$^{-/-}$ > *Mal*$^{-/-}$ [donor > recipient]) by injecting 1×10^7 cells/mouse via the lateral tail veins. Begin by incubating the individual cage beneath a heat lamp for ~5 min. Prepare 1 ml syringes with 200 μl of cell suspension and top with 25G needles. Take each mouse and insert into the restrainer, ensuring the mouse is held securely. Wipe the tail with ethanol to sterilize and help make the veins visible. Insert the needle, bevel up, half way down the tail and inject the cell suspension.
4. After 6 weeks reconstitution can be assessed by flow cytometry of blood for markers CD45.1 vs. CD45.2.
5. Following generation of chimeras, oral infection of mice can be repeated to determine the role of Mal or other TLR components in epithelial cells and thus epithelial barrier integrity.

4 Notes

1. This spot plating technique is used for efficacy and also to reduce amount of agar plates required. Alternatively, perform bacterial enumeration using traditional spread plating technique of 100 μl per agar plate, one dilution per plate.
2. This method of homogenizing organs is used for speed, as you do not need to sterilize a hand-held homogenizer in-between each sample, as one sterile stomacher bag is used per sample.
3. Use a wax pen to encircle the section on the slide. This will keep the block/antibody solutions on the slide for a more consistent incubation.
4. If you wish to multiplex using multiple channels (e.g. FAM and VIC) replace 0.5 μl H_2O with 0.5 μl primer/probe.
5. Plates can be prepared to be run in advance and stored temporarily at 4 °C.
6. Mix H_2O, Protogel, Tris and SDS first and then add APS and TEMED.
7. Add butanol to vessel and add water on top. Shake vigorously until mixture becomes milky. Allow separation and use upper layer, store at room temperature.
8. Final pH should be 8.3 but do not use a pH meter as SDS will damage electrode.
9. This step is very flexible: the membrane can be blocked overnight if necessary.

10. It is best to prepare several acetates ahead of time to ensure you get a clear exposure. Writing the approximate exposure time on the acetate will allow you know what to expect for repeat experiments with the antibodies in use.

References

1. Turner JR (2009) Intestinal mucosal barrier function in health and disease. Nat Rev Immunol 9:799–809
2. Harhaj NS, Antonetti DA (2004) Regulation of tight junctions and loss of barrier function in pathophysiology. Int J Biochem Cell Biol 36:1206–1237
3. Fasano A, Shea-Donohue T (2005) Mechanisms of disease: the role of intestinal barrier function in the pathogenesis of gastrointestinal autoimmune diseases. Nat Clin Pract Gastroenterol Hepatol 2:416–422
4. Balkovetz DF, Katz J (2003) Bacterial invasion by a paracellular route: divide and conquer. Microbes Infect 5:613–619
5. Corr SC, Palsson-McDermott EM, Grishina I et al (2014) *MyD88* adaptor-like (Mal) functions in the epithelial barrier and contributes to intestinal integrity via protein kinase C. Mucosal Immunol 7(1):57–67
6. Gonzalez-Mariscal L, Tapia R, Chamorro D (2008) Crosstalk of tight junction components with signaling pathways. Biochim Biophys Acta 1778:729–756
7. Guo S, Al-Sadi R, Said HM et al (2013) Lipopolysaccharide causes an increase in intestinal tight junction permeability in vitro and in vivo by inducing enterocyte membrane expression and localization of TLR-4 and CD14. Am J Pathol 182(2):375–387
8. Alenghat T, Osborne LC, Saenz SA et al (2013) Histone deacetylase 3 coordinates commensal-bacteria-dependent intestinal homeostasis. Nature 504:153–157
9. Cario E, Gerken G, Podolsky DK (2004) Toll-like receptor 2 enhances ZO-1 associated intestinal epithelial barrier integrity via protein kinase C. Gastroenterology 127(1):224–238
10. Aviello G, Corr SC, Johnston DGW et al (2014) MyD88 adaptor-like (Mal) regulates intestinal homeostasis and colitis-associated colorectal cancer in mice. Am J Physiol 306(9):G769–G778
11. Brandl K, Sun L, Neppl C (2010) MyD88 signaling in nonhematopoietic cells protects mice against induced colitis by regulating specific EGF receptor ligands. Proc Natl Acad Sci 107(46):19967–19972